Alma Mater Studiorum – Università di Bologna

DOTTORATO DI RICERCA

Biologia Funzionale dei Sistemi Cellulari e Molecolari

Settore Disciplinare: BIO/19 – Microbiologia Generale

Ciclo XXII

Monossigenasi coinvolte nel metabolismo di *n*-alcani in *Rhodococcus* sp. BCP1: caratterizzazione molecolare e espressione del gene *alkB*

(Monooxygenases involved in the *n*-alkanes metabolism by *Rhodococcus* sp. BCP1: molecular characterization and expression of a*lkB* gene)

Submitted by Dott.ssa Martina Cappelletti

PhD Coordinator:

Prof. Vincenzo Scarlato

Tutor:

Prof. Davide Zannoni

Alma Mater Studiorum – Università di Bologna

DOTTORATO DI RICERCA

Biologia Funzionale dei Sistemi Cellulari e Molecolari

Settore Disciplinare: BIO/19 – Microbiologia Generale

Ciclo XXII

Monossigenasi coinvolte nel metabolismo di *n*-alcani in *Rhodococcus* sp. BCP1: caratterizzazione molecolare e espressione del gene *alkB*

(Monooxygenases involved in the *n*-alkanes metabolism by *Rhodococcus* sp. BCP1: molecular characterization and expression of a*lkB* gene)

Submitted by Dott.ssa Martina Cappelletti

PhD Coordinator: *Tutor:*

Prof. Vincenzo Scarlato   **Prof. Davide Zannoni**

Key words: alkane 1-monooxygenase (AlkB), n-alkanes, Rhodococcus

Academic year 2008/2009

To my Parents
with love and gratitude

Hunc igitur terrorem animi tenebrasque necessest

non radii solis neque lucida tela diei

discutiant, sed naturae species ratioque

(Titus Lucretius Carus, De rerum natura, I, 146-148)

Table of Contents

List of Abbreviations

A	adenine
aa	amino acid
Amp	ampicillin
BD	bi-distilled
BLAST	basic local alignment search tool
BSA	bovin serum albumin
C	cytosine
ºC	degree Celsius
DEPC	Diethyl pyrocarbonate
DNA	deoxyribonucleic acid
DNase	deoxyribonuclease
dNTP	deoxy nucleoside triphosphate
DTT	1,4-dithio-DL-threitol
E.coli	Escherichia coli
e.g.	for example (abbreviation of Latin: *exempli gratia*)
e.i.	that is (abbreviation of Latin: *id est*)
et al.	and others (Latin: *et alteri*)
EDTA	ethylenediamine tetraacetate
FAD	flavin adenine dinucleotide
G	guanine
HEPES	(4-(2-Hydroxyethyl) piperazine-1-ethanesulfonic acid
kb	kilo base pairs
kDa	kilo dalton
LC/MS/MS	Liquid chromatography- quadrupole mass spectrometry
min	minutes
µg	microgram
µL	microliter
MM	minimal medium
MMenr	minimal medium enriched
n	"normal"; e.g. concerning the homologous line of alkanes
NAD	nicotinamide adenin dinucleotide
NADP	nicotinamide adenin dinucleotide phosphate
nm	nanometers

OD	optical density
ONPG	2-Nitrophenyl-β-D-galactopyranoside
Orf	open reading frame
PalkB	promoter region of *alkB* gene
pH	negative decade logarithm of the proton concentration
pI	isoelectric point
PCR	polymerase chain reaction
PMSF	phenylmethylsulfonyl fluoride
RNA	ribonucleic acid
RNase	ribonuclease
rpm	rotations per minute
16S-rRNA	16S ribosomal RNA
T	thymine
Tc	tetracycline
TCA cycle	tricarboxylic acid cycle
TE	tris-EDTA buffer
Tris	tris(hydroxymethyl) aminomethane
v/v	volume per volume
w/v	weight per volume
X-Gal	5-bromo-4-chloro-3-indolyl-β-D-galactoside

Chapter 1 - General Introduction

1.1 Preface

The quality of life on Earth is tightly related with the overall quality of the environment [1]. During the last century it was commonly believed that the abundance of land and resources were unlimited and it was rarely acknowledged that the production, use, and disposal of hazardous substances had environmental and health effects [1-3]. Owing to this, human activity has deliberately or inadvertently released into waters and soil a variety of toxic compounds as refrigerants, paints, solvents, herbicides and pesticides that can cause considerable environmental pollution and human health problems as a result of their persistence, toxicity, and transformation into hazardous metabolites [4, 5]. Very soon, however, it became clear how the carelessness and negligence in handling the industrial wastes and gas emissions had caused dramatic effect on the nature and on human health [1]. Nowadays, the concern about the global warming and the climate changing induced the government regulatory agencies to establish procedures for assessing the environmental impact and health hazards of chemicals and for controlling/limiting their utilization. International efforts have been applied to remedy many contaminated sites all over the world, either as a response to the risk of adverse health or environmental effects caused by contamination or to enable the site to be redeveloped for use [5]. In response to public and government concern and because of the intriguing research problems presented, environmental scientists, biologists and chemists have been giving increased attention to identifying and determining the behavior and fate of organic compounds in natural ecosystems [5].

Bioremediation procedures offer an economical and effective possibility to degrade or render innocuous toxic pollutants using natural biological activity [1]. By definition, *bioremediation* implies the use of living organisms, primarily microorganisms, to degrade the

environmental contaminants into less toxic forms. It uses naturally occurring (native) bacteria or newly introduced microorganisms to degrade or detoxify substances hazardous to human health and/or environment [6, 7]. The microbial degradation of a contaminant typically occurs because microorganisms can benefit from the use of the contaminant compound as an electron donor and carbon source to support growth. The redox reactions result in the flow of electrons from the substrate to a terminal electron acceptor (e.g. an oxidant such as O_2) and the release of energy that is used to support cell synthesis [8, 9]. In the absence of O_2, a large number of alternative terminal electron acceptors (NO_3^-, Fe^{3+}, $Fe(OH)_3$, SO_4^{2-}) can be utilized to support anoxic respiration. For example, chlorinated compounds can serve as electron acceptor in a process known as *halorespiration*. During this type of metabolism (called *reductive dehalogenation*), the use of chlorinated compounds, as electron acceptors, is linked to anoxic decomposition of simple organic substrates (e.g. lactic acid) [10]. Alternatively, microorganisms can fortuitously transform chlorinated compounds while they are degrading non-halogenated primary substrates. In this case, enzymes, expressed to degrade the primary substrate, display activity with the chlorinated compound. This type of metabolism is referred to as *cometabolism* [11]. By definition, cometabolism describes the microbial transformation of co-substrates that do not support cell-replication [12]. A special type of cometabolism involves the oxidation of chlorinated solvents by oxygenases, which is known as cooxidation [13].

Since contaminant compounds are transformed by living organisms through reactions that take place as a part of their metabolic processes, environmental biotechnology focuses on the development of techniques to optimize environmental parameters to allow these metabolic pathways to proceed faster and, therefore, to improve the bio-degradation [1]. As a result, the removal of the contaminated soil can be necessary to let the biodegradation proceed in controlled sites (such as bioreactors). These *ex situ* approaches provide optimal conditions

2

and constant monitoring unlike the *in situ* bioremediation approaches that do not require neither the transfer of the contaminants or its extraction from the polluted area [1]. Additionally, *biostimulation* or *bioaugmentation* can improve the efficiency of these bioremediation processes. *Biostimulation* provides the addition of nutrients, oxygen or other electron donors and acceptors to increase the population or activity of naturally occurring microorganisms available for bioremediation. *Bioaugmentation* is the addition of single microorganisms or microbial communities that can biotransform or biodegrade contaminants [3]. It is, indeed, more usual that the remediation of contaminated area is obtained by inoculating microbial communities instead of a single microorganism culture. Microbial consortia are composed by different bacterial species that cooperate so that each strain carries out one single step of the entire bio-degradation process.

1.2 Hydrocarbons in the environment

Hydrocarbons are energy-rich organic compounds consisting of carbon and hydrogen atoms and they can be saturated (only single C-H bounds) or unsaturated (one ore more double or triple C-H bounds). Alkanes are saturated hydrocarbons with the general formula C_nH_{2n+2}; they can be linear (*n*-alkanes), cyclic (cyclo-alkanes) or branched (iso-alkanes). Those naming short-chain length alkanes (methane C_1, ethane C_2, propane C_3 and butane C_4) are gasses at room temperature, while longer chain-length alkanes (>pentane C_5) are liquid or (>octadecane C_{18}) solid (the sub-index indicates the number of carbon atoms of the alkane molecule).

Although these compounds are naturally present in the environment due to biological and geochemical processes [14-17], the larger amount of hydrocarbon that ends up in nature has anthropogenic origins [18, 19]. Annually, around 35 million metric tons of petroleum enters the sea [20]. The major part of this oil is not released by large tanker accidents, which constitute 'only' one million metric tons per annum, but comes from municipal and industrial

wastes and runoffs, leaks in pipelines and storage tanks and discharge of dirty ballast and bilge waters [21]. Oil input to the sea from natural sources, principally seepages, only accounts for 0.5 million tons annually [20-22]. The consequences of hydrocarbon release include; (a) global warming by low molecular weight gaseous hydrocarbons such as methane [23], (b) contamination of ocean and surface waters by liquid hydrocarbons ($>C_5$), which locally harm plant and animal life, dissolving the lipid portion of the cytoplasmic membrane thus allowing the cell content to escape [19, 20], (c) contamination of drinking water by liquid hydrocarbons ($>C_5$), leading to liver and kidney damages in humans [24, 25]. For these reasons, several studies were initiated in the '70s on the fate of petroleum in various ecosystems. To date, the expansion of petroleum studies into new frontiers, such as deep offshore waters and ice-dominated Arctic environments, and the apparently inevitable spillages, which occur during routine operations as a consequence of accidents, have maintained a high research interest in this field [7, 26, 27].

1.3 Biodegradation of alkanes

As alkanes are apolar and chemically inert compounds with low water solubility, they are recalcitrant to abiotic decay. However, microorganisms capable of utilizing these compounds as only energy source can be found almost everywhere, even in non-contaminated sites [28, 29].

Table 1.1 Microorganisms that aerobically degrade aliphatic hydrocarbons. A (+) indicates that information on the genetics of alkane degradation is available for strains belonging to the genus. (Information from [30])

BACTERIA	YEASTS	FUNGI	ALGAE
Achromobacter	Candida (+)	Aspergillus	Prototheca
Acinetobacter (+)	Cryptococcus	Cladosporium	
Alcanivorax (+)	Debaryomyces (+)	Corallosporium	
Alcaligenes	Hansenula	Cunninghamella	
Bacillus	Pichia	Dendryphiella	
Brevibacterium	Rhodotorula	Fusarium	
Burkholderia (+)	Saccharomyces	Gliocladium	
Corynebacterium	Sporobolomyces	Lilworthia	
Flavobacterium	Torulopsis	Penicillium	
Mycobacterium (+)	Trichosporon	Varicospora	
Nocardia	Yarrowia (+)	Verticillium	
Pseudomonas (+)			
Rhodococcus (+)			
Sphingomonas			
Streptomyces			

Aliphatic hydrocarbons pose a variety of challenges to degradative microorganisms due to their physico-chemical properties (Table 1.2) [31]. The physical state of the compounds at physiological temperatures may be gaseous, liquid or solid. It is generally true to state that the gaseous and liquid compounds are the most readily degraded but liquids of lower molecular weight may prove to be inhibitory to microorganisms by virtue of their solvent effect [7, 31, 32]. However, the most significant challenges that aliphatic hydrocarbons impose with respect to their bio-utilization take account of the energy required to activate them and their extremely limited solubility. As the solubility of aliphatic compounds rapidly decreases with increasing molecular weight, the degrader microorganisms had developed a variety of specific adaptations in order to be able to utilize the majority of potential hydrocarbon substrates [31].

Table 1.2 Physical properties of selected aliphatic hydrocarbons. (Modified from [31])

Compound	C atoms	Mol.wt (gr mol^{-1})	m.p. (°C)	b.p. (°C)	Solubility (mg L^{-1}) (at 20°C)
Methane	1	16.04	-182.5	-161.6	35
Ethane	2	30.1	-172	-88.6	63.7
n-Propane	3	44.09	−187.6	-42.1	70
n-Butane	4	58.12	-138.4	-0.5	61
n-Hexane	6	86.2	-94.3	68.7	13
n-Decane	10	128.3	-28	174.0	0.05
n-hexadecane	16	226.4	18.0	287.0	5.2×10^{-2}
n-Eicosane	20	282.6	36.7	343.0	3.1×10^{-7}
n-Triacontane	30	422.8	66	450	1.3×10^{-11}
2-methylpentane (isohexane)	6	86.2	-154.0	60.3	13.8
2,2,4-trimethylpentane	8	114.2	-1072	127.0	2.4
4-methyloctane	9	128.3	n/a	142.0	0.12
1-hexene	6	84.2	-139.8	63.5	50.0
Trans-2-hexene	7	98.2	-109.5	98.0	15.0
1-octene	8	112.2	-121.3	121.0	2.7

1.3.1 Uptake of hydrocarbons

The limited solubility in water hampers the uptake of alkanes by microorganisms. The mechanisms through which the alkanes enter the cell are still mostly unknown. However it is clear that the mechanism may differ depending on the bacterial species considered, the molecular weight of the alkane and the physico-chemical characteristics of the environment [33]. In case of medium- and long-chain-length *n*-alkanes, two mechanisms for accessing these substrates are generally considered for bacteria: (1) interfacial accession by direct contact of the cell with the hydrocarbon droplets and (2) biosurfactant-mediated accession by cell contact with emulsified hydrocarbons [34-37]. The Gram-positive eubacteria belonging to the actinomycete genera *Corynebacterium*, *Mycobacterium*, *Nocardia* and *Rhodococcus* (the CMNR group) have cell wall containing long aliphatic chains of mycolic acids that facilitate

6

the uptake of hydrophobic substrates into the cells. The ability of these bacteria to degrade *n*-alkanes is also supported by the production of surfactants. These compounds, mainly trehalose-containing glycolipids, facilitate the adhesion of cells to hydrophobic phases, decrease the interfacial tension between phases and disperse hydrophobic compounds [38-40]. Furthermore, the presence of various substrates in the growth medium induces changes in the fatty acid composition of the membrane lipids of CMNR group bacteria. This can alter the fluidity of the cell envelope [40] and the adaptability of membrane composition to the media proved to be an efficient way to resist to toxic compounds [41].

Surfactants produced by microorganisms probably have also other roles, such as facilitating cell motility on solid surfaces [42, 43], or the adhesion/detachment to surfaces or biofilms [44, 45].

1.3.2 Hydrocarbon bio-activation as first step in alkanes metabolism

The understanding of the metabolic processes and bacterial responses involved in the oxidation of hydrocarbons is essential in order to find effective strategies for their biotransformation to non-toxic compounds [46]. Additionally, during the last decade, the possibilities of utilization of enzymes able to degrade hydrocarbons for the industrial production of chemicals and pharmaceutical products as epoxides, high value fatty acids and wax esters [31] opened new frontiers. As a consequence, the research efforts are focusing on developing and applying molecular techniques in order to identify the gene/proteins involved in the activation of alkanes and to study the regulatory mechanisms leading to their oxidation; this approach will expand our understanding on petroleum degrading-bacteria metabolism and will aid in developing new industrial catalyst.

1.3.3 Anaerobic degradation of alkanes

Over the last ten years several microorganisms, mostly belonging to the β- and δ-

subclasses of proteobacteria, have been described being able to use *n*-alkanes (except for methane) as carbon source in the absence of O_2 [47]. These microorganisms use nitrate or sulfate as electron acceptors [48]. Although the growth rate is significantly slower than that of aerobic alkane degraders, the anaerobic degradation of alkanes plays an important role in the recycling of hydrocarbons in the environment [49]. These strains normally use a narrow range of alkanes as substrate. For example, the strain BuS5 is a sulfate-reducing bacterium, belonging to the *Desulfosarcina/Desulfococcus* cluster, that assimilates only propane and butane [50]. *Azoarcus* sp. HxN1 is a denitrifying bacteria and uses C_6–C_8 *n*-alkanes, while *Desulfobacterium* Hdx3 metabolizes C_{12}–C_{20} alkanes [47]. To date, the metabolic pathways, that have been studied, follow two general strategies. One involves the activation of the alkane at subterminal position by addition of a fumarate molecule to the alkane, producing an alkyl-succinate derivative. This reaction is believed to occur through generation of an organic radical intermediate, most likely a glycyl radical [51]. The reaction product is subsequently linked to the CoA and converted into an acyl-CoA that can be further metabolized by β-oxidation. In the second reaction mechanism that has been described only for propane, the fumarate molecule is added to one of the terminal carbon atoms of the alkane [49, 50].

1.3.4 Aerobic degradation of alkanes

Aerobic alkane degraders use O_2 as a reactant for the activation of the alkane molecules. While oxidation of fatty alcohols and fatty acids is common among microorganisms, activation of the alkane molecules requires oxygenase activity that overcomes the low chemical reactivity of the hydrocarbons by generating reactive oxygen species. These enzymes are much less widespread and can belong to different families.

Oxidation of methane is performed by methanotrophs that can use methane as carbon and energy source. These bacteria oxidize methane by means of a methane monooxygenase that can be soluble (iron-dependent) or particulate (copper-dependent). Oxidation of methane

8

produces methanol that is subsequently transformed to formaldehyde by methanol dehydrogenase and then to formic acid. Approximately 50% of the formaldehyde produced is assimilated into cell carbon for biosynthesis of multicarbon compounds via the ribulose monophosphate pathway (RuMP) or via serine pathway and the remainder is oxidized to CO_2 [52, 53].

In the case of *n*-alkanes containing two or more carbon atoms, aerobic degradation usually starts by the oxidation of a terminal methyl group to render a primary alcohol that is further oxidized to the corresponding aldehyde, and finally converted into fatty acid. Fatty acids are conjugated to CoA and further processed by β-oxidation to generate acetyl-CoA, which can enter the TCA cycle to yield carbon dioxide and energy [26, 31, 33, 54-56] (Fig. 1.1). In some cases, both ends of the alkane molecule are oxidized through ω-hydroxylation of fatty acids at the terminal methyl group (the ω position), rendering an ω-hydroxy fatty acid that is further converted into a dicarboxylic acid and processed by β-oxidation [31, 57] (Fig. 1.1). Sub-terminal oxidation of *n*-alkanes has also been described (Fig. 1.1) [58-60]. A secondary alcohol is produced that is converted to the corresponding ketone, and then oxidized by a Baeyer–Villiger monooxygenase to form an ester. The ester is hydrolyzed by an esterase, generating an alcohol and a fatty acid. Both terminal and sub-terminal oxidation can coexist in some microorganisms (Fig. 1.1)[31].
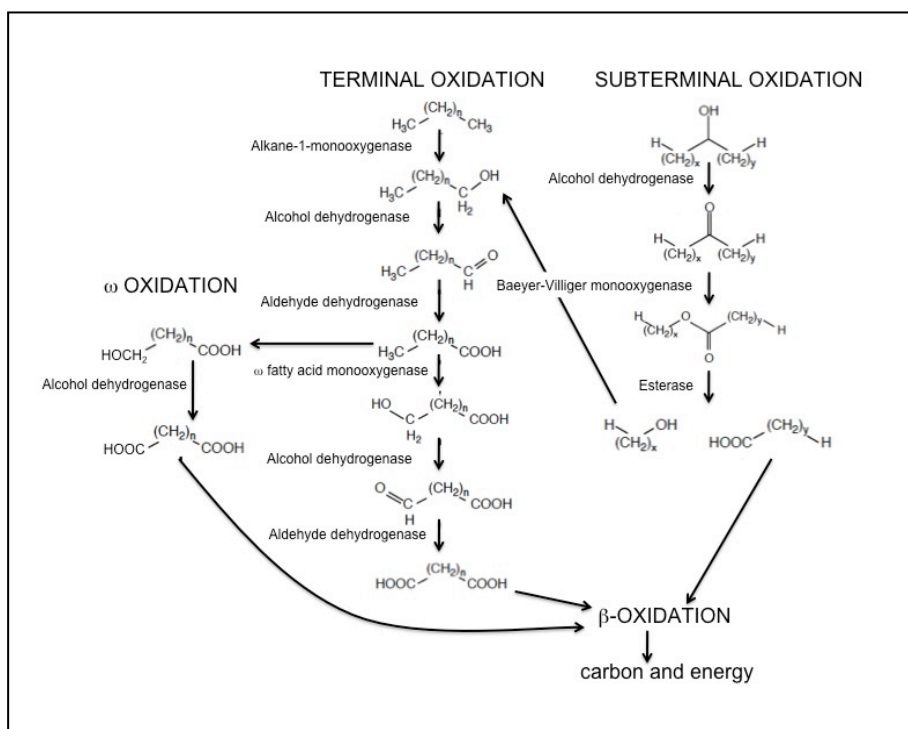
Figure 1.1 Pathways for the degradation of alkanes by terminal, sub- and bi-terminal oxidation. (Modified from [30, 31])

Alternatively, the fatty acids, deriving from the *n*-alkanes consecutive oxidations, are incorporated into the phospholipids of membrane. As result, the phospholipids composition will reflect the chain-length on which the strain was grown: odd-chain length alkanes will yield more odd-chain fatty acid moieties in the phospholipids, while even-chain-length alkanes yield a higher amount of even-chain fatty acid moieties. The ratio between saturated and unsaturated fatty acid moieties in the phospholipids shifts more towards saturated fatty acids when *n*-alkanes are used as carbon source [56, 61].

The different families of monooxygenase performing this first oxidation are summarized in the Table 1.3 The association between alkane-degrading abilities and monooxygenase can be summarized as follows:

• strains degrading short-chain *n*-alkanes express hydroxylases related to the soluble methane monooxygenases; they oxidize *n*-alkanes C_2-C_4 [62, 63];

• strains degrading medium-chain *n*-alkanes (C_5–C_{11}), or long-chain alkanes (> C_{12})

10

contain integral membrane non-haem iron monooxygenases (AlkB) or enzymes that belong

to the family of soluble cytochrome P450;

- some strains assimilating n-alkanes with more than 18 carbon atoms can contain alkane

hydroxylases unrelated to the former ones [30, 64].

Table 1.3 Enzyme classes involved in the oxidation of alkanes are listed. Some of them are described in details. in the next paragraphs (Modified from [30])

Enzyme class	Composition and cofactor	n-alkanes range	Presence in:	References
sMMO (soluble methane monooxygenase)	α2β2γ2 hydroxylase: bi-nuclear iron reductase: [2Fe–2S], FAD, NADH regulatory subunit	C_1-C_8 alkanes	*Methylococcus, Methylosinus, Methylocystis, Methylomonas, Methylocella*	McDonald et al. (2006)
pMMO (particulate methane monooxygenase)	α3β3γ3 hydroxylase; trimer composed of PmoA, PmoB, PmoC: mononuclear copper and bi-nuclear copper in PmoB	C_1-C_5 n-alkanes	*Methylococcus, Methylosinus, Methylocystis, Methylobacter, Methylomonas, Methylomicrobium, etc.*	McDonald et al. (2006)
Butane monooxygenase (similar to sMMO)	a2b2g2 hydroxylase: bi-nuclear iron Reductase: [2Fe-2S], FAD, NADH Regulatory subunit	C_2-C_8 n-alkanes	*Pseudomonas butanovora*	Hammamura, 1999; Sluis, 2002
Butane monooxygenase (similar to pMMO)	Two polypeptides: copper, iron quinone oxidoreductase: FAD, NADH	Probably C_4-C_{10} n-alkanes	Short-chain alkane oxidizers, *Nocardioides* sp. CF8	Hammamura, 2001
Propane monooxygenase (similar to BMO/sMMO)	Hydroxylase: large and small subunits with bi-nuclear iron Oxidoreductase Coupling protein	C_2-C_4	Gordonia sp. TY5 Rhodococcus jostii RHA1	Kotani et al, 2003; Sharp, 2007
AlkB-related alkane hydroxylase	Membrane hydroxylase: bi-nuclear iron Rubredoxin: iron Rubredoxin reductase: FAD, NADH	C_5-C_{16} n-alkanes	*Acinetobacter, Alcanivorax, Burkholderia, Mycobacterium, Pseudomonas, Rhodococcus, etc.*	Van Beilen 2003
Bacterial P450 (CYP153, class I)	P450 oxygenase: P450 heme Ferredoxin: iron-sulfur Ferredoxin reductase: FAD, NADH	C_4-C_{16} n-alkanes	*R. rhodochrous* 7E1C *Acinetobacter* sp. EB104	van Beilen et al. (2006)
Eukariotic P450 (CYP52, class II)	Microsomal oxygenase: P450 heme Reductase: FAD, FMN, NADPH	C_{10}-C_{16} n-alkanes	*Candida maltosa, Candida tropicalis, Yarrowia lipolytica*	Iida et al. (2000)
Dioxygenase	Homodimer: copper, FAD	C_{10}-C_{30} n-alkanes	*Acinetobacter* sp. M-1	Maeng et al. (1996)
Unknown	54 kDa peptide essential for butane oxidation	C_4-C_{10} n-alkanes	*Pseudomonas indica* IMT37	Padda, 2001

It is important to emphasize how expanding knowledge about alkane hydroxylation

systems blur the boundaries of the hydroxylase classification into enzymes oxidizing gaseous

alkanes and enzymes oxidizing liquid alkanes [65]. For instance, AlkB-like monooxygenase

typically oxidizes liquid alkanes but, lately, few members of this family of enzymes were

described to be also induced by propane [66, 67]. This underlines the diversity that can exist

amongst members of the same hydroxylase family and indicates how increasing understanding of this important type of enzymes improves the knowledge about the variability of the oxygenase catalytic activity applicable to bioremediation strategies.

It is worth emphasizing the existing variability in the hydrocarbon degradation abilities and pathways amongst aerobic alkane-utilizing species. Various alkane-degrading bacteria have a very versatile metabolism, so that they can use as carbon source many other compounds in addition to alkanes [68, 69]. On the other hand, hydrocarbonoclastic bacteria are highly specialized in degrading hydrocarbons. For example, *Alcanivorax borkumensis* is a marine bacterium that can assimilate a broad range of linear and branched alkanes, but which is unable to metabolize aromatic hydrocarbons, sugars, amino acids, fatty acids and most other common carbon sources [70, 71]. Other hydrocarbonoclastic bacteria belong to the genera *Thalassolituus* [71], *Oleiphilus* [72] and *Oleispira* [73]. For these unusual metabolic capabilities that allow them to utilize preferentially alkanes as growth substrate, these bacteria are considered to play a key role in the removal of hydrocarbons from polluted environments [69, 74]. The recently reported genome sequence of *Alcanivorax borkumensis* SK2 [70] and the proteomic analysis of its cytoplasmic and membrane proteins after the growth on *n*-hexadecane showed the presence of multiple alkane hydroxylase systems belonging to different families [75] involved in the primary oxidation of a broad range of alkanes.

A review of the molecular genetics and regulations of the categories of bacterial monooxygenases involved in the *n*-alkanes metabolism reported in literature is summarized below.

1.3.4.1 Methane monooxygenases

Methane is a powerful greenhouse gas, and its atmospheric concentration has been steadily increasing over the past 300 years [76]. There are two major ways in which methane is removed from the environment: aerobic oxidation by a specialized group of bacteria and

12

anaerobic oxidation by a specialized group of archaea. The former is important for keeping methane concentrations balanced in freshwater sediments and soils, whereas the latter is the major process in anoxic marine environments. While the biochemistry of aerobic methane oxidation is relatively well understood, following intensive research efforts with a number of model organisms, the biochemistry of anaerobic methane oxidation is not yet fully understood and no anaerobic methane-oxidizer has been isolated in pure culture so far [76].

Methanotrophs are a unique group of Gram-negative bacteria, comprising 13 genera within the α and γ Proteobacteria, that aerobically utilize methane as sole carbon and energy source [77-79]. As previously mentioned, the ability of methanotrophs to oxidize methane is conferred by a methane monooxygenase (MMO) enzyme that converts methane in methanol [80].

There are two types of MMO systems, a soluble, cytoplasmic complex (sMMO) and a membrane-bound particulate system (pMMO) [52]. All but one genus (*Methylocella*) of known metanotrophs produce the membrane-bound (or particulate) copper-containing methane monooxygenase (pMMO) and a few of them express also the iron-containing soluble methane monooxygenase (sMMO) [81-83]. In strains containing both pMMO and sMMO, Cu-containing monooxygenase is preferentially expressed and sMMO is only expressed under conditions of low copper availability [49, 81-84]. The reciprocal relationship between the differential expression of either sMMO or pMMO is commonly referred to as the "copper switch" mechanism whose processes are still unknown [84-87]. The two systems differ in molecular structure, metal ion composition, and substrate specificity [53, 84, 88, 89]. Whereas pMMO is more selective toward alkanes and alkenes that have five carbons or less ($< C_5$), substrates for sMMO include broader range of alkanes and also alkenes, aromatics, and halogenated hydrocarbons [90, 91]. Most studies of MMO have focused on enzymes from two organisms, *Methylococcus capsulatus* (Bath) and *Methylosinus trichosporium* OB3b [84].

1.3.4.1.1 Soluble methane monooxygenase - sMMO

The biochemistry, structure, and mechanism of the soluble monooxygenase (sMMO) are well understood and have been reviewed frequently over the last decade [89, 92-97]. The soluble methane monooxygenase is the best-characterized representative of the soluble di-iron monooxygenase family (SDIMOs). The sMMO comprises three components: a hydroxylase (MMOH) which houses the active site, a reductase (MMOR) that shuttles electrons from NADH to the hydroxylase, and a regulatory protein (MMOB) that has several regulatory activities and is required for enzymatic activity [89]. MMOB seems to work as effector of electron transfer in the catalytic mechanism [98, 99]. The hydroxylase consists of three polypeptides arranged as a $\alpha_2\beta_2\gamma_2$ dimer (Fig. 1.2) [100] and it contains a non-heme carboxylate-bridged di-nuclear iron centre responsible for methane hydroxylation [100-103]. The sMMO hydroxylation was proposed to operate with a concerted mechanism, in which after the binding of substrate, the di-iron active site is reduced through electron transfers from the reductase subunit while the consecutive scission of the two atoms of oxygen occurs in the correspondence of the formation of two still unclear structural intermediates of the active site [96, 104, 105].
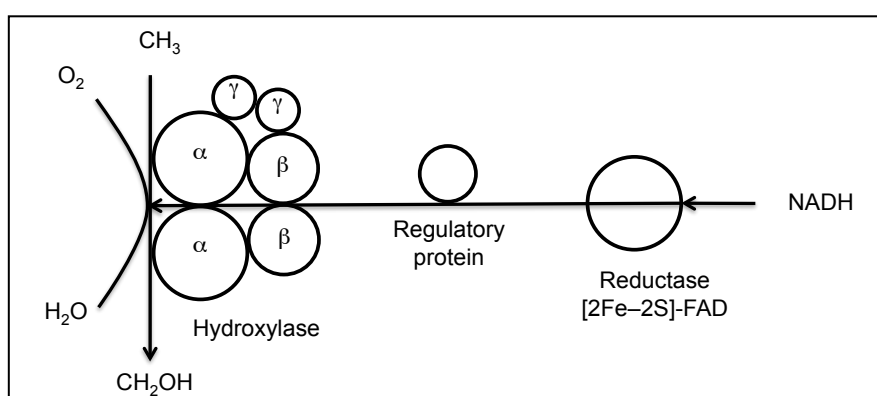
Figure 1.2 The sMMO enzyme from *Methylosinus trichosporium* OB3b (Modified from [99])

The genes coding for sMMO are clustered in the *mmoXYBZDC* operon (Fig. 1.3) [106, 107]. The *mmoX*, *mmoY*, and *mmoZ* genes encode the α, β, and γ subunits of MMOH, respectively. MMOR is encoded by *mmoC* and MMOB is encoded by *mmoB*. The function of

14

the *mmoD* (also known as *orfY*) gene product is unknown, but this protein may play a role in assembly of the MMOH di-iron active site [108].
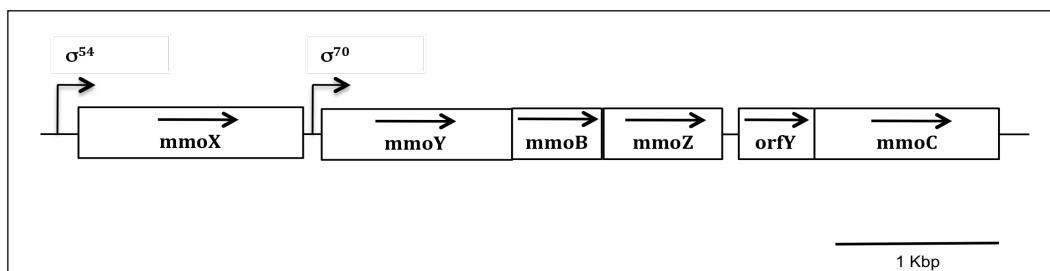
Figure 1.3 The soluble methane monooxygenase gene cluster from *M. trichosporium* OB3b (Modified from [99])

The genes encoding sMMO occur only once in the genome of both *M. trichosporium* OB3b and *M. capsulatus* (Bath). In both the metanotrophs they are clustered in the same order and also the codon usage is similar [99, 109].

The *mmo* genes in *Methylococcus capsulatus* (Bath) seem to be co-transcribed from a single σ^{54} promoter element upstream of *mmoX* [110]. On the contrary, in *Methylosinus trichosporium* OB3b, *Methylocystis sp. M* and *Methylomonas sp*. KSWIII both the putative σ^{54} promoters upstream of *mmoX* and an additional putative σ^{70} promoter in the *mmoY-mmoX* intergenic region may be involved in the transcription of *mmo* genes [52, 86, 110-112].

1.3.4.1.2 Particulate methane monooxygenase - pMMO

The particulate methane monooxygenase (pMMO) is much more prevalent than sMMO, but is less understood because of the difficulties in working with an integral membrane protein. Despite this limitation, many efforts have been putting to improve the knowledge of pMMO. This enzyme would be more effective than sMMO for in situ bioremediation processes for two reasons, namely: a) only few methanotrophs produce sMMO [80], and b) sMMO expression is repressed at the high levels of copper found in polluted environments [84, 113]. pMMO is composed of three subunits, α, β and γ, also known as PmoA, PmoB and PmoC, respectively [53, 114], and it is considered to contain

copper in the active site [53, 115]. The hydroxylase is a trimer composed of three copies of each subunit in a $\alpha_3\beta_3\gamma_3$ polypeptide arrangement; each $\alpha\beta\gamma$ protomer houses three metal centers.

The genes for pMMO (*pmo*) are organized in the *pmoCAB* operon (Fig. 1.4) in which *pmoB*, *pmoA*, and *pmoC* encode β, α and γ subunits, respectively [116]. By contrast to the genes encoding the sMMO, *pmoCAB* operon is present in multiple copies in the *M. capsulatus* (Bath) genome with two complete copies of the complete operon and a third copy of *pmoC*, named *pmoC3*, whose sequence diverges from the other two pmoC in the operons [117]. Gene disruption experiments indicated that both *pmoCAB* gene copies are functional and both are necessary for maximal pMMO activity. *pmoC3* also seems to play an important role in growth on methane, but distinct from the functions of the other two *pmoC* genes [53, 117]. Proteins analogous to the MMOR and MMOB proteins in sMMO have not been identified for the pMMO system.
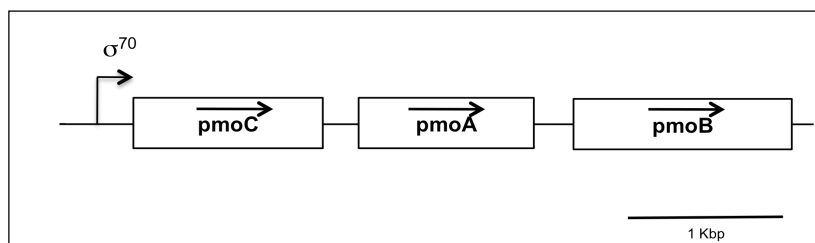
Figure 1.4 The particulate methane monooxygenase gene cluster from *M. capsulatus (Bath)*. Direction of transcription of each *orf* is indicated by arrows. (Modified from [117])

1.3.4.2 SDIMO - Short-alkanes oxidizing monooxygenases

Gaseous *n*-alkanes ranging from C_2 to C_5 are recognized as components of non-methane hydrocarbons, and their increased concentrations in the atmosphere threaten to destabilize ecosystems through a variety of mechanisms [118, 119]. Although these gases are produced as natural intermediates of bacterial, plant, and mammalian metabolism, the main sources of pollution is represented by natural oil seepages and oil spills [20, 119]. From a biotechnological perspective, gaseous alkanes are inexpensive carbon sources for microbial

16

cultivation, and the enzymes participating in the oxidation pathway promise to be versatile biocatalysts [119].

Most of the short-chain oxidizing monooxygenases described in literature belong to a group of bacterial oxygenases called soluble di-iron monooxygenases (SDIMO). The SDIMO family includes soluble methane monooxygenases (sMMO) along with toluene monooxygenases, phenol hydroxylases, alkene monooxygenases, and tetrahydrofuran monooxygenase (ThmABCD) from *Pseudonocardia* K1 [120]. The association of these sub-groups in one single family is justified on the basis of the phylogenetic analyses of the enzyme subunits and on the basis of the genes arrangement in the respective operons [120, 121].

SDIMOs are multi-component enzyme systems [78] that catalyze the initial oxidation of hydrocarbons in phylogenetically and physiologically diverse bacteria, such as *Proteobacteria* that grow on aromatic compounds or methane, and *Actinobacteria* that grow on low-molecular-weight alkanes and alkenes [121]. All these enzymes, including the soluble methane monooxygenases, contain one hydroxylase subunit with the conserved non-heme di-iron active site responsible for the activation of O_2 and the oxidation of substrate. Electrons are transferred from NADH to the hydroxylase by the reductase subunit via an enzyme bound FAD. The third component of the enzyme is a coupling protein that reduces the O_2 to H_2O_2 and increases the rates of substrate turnover [25, 122, 123]. Some members of the SDIMOs also contain a fourth subunit comprised of a short polypeptide with a bound Rieske center believed to be involved in electron transfer to the hydroxylase [120, 124-127].

Although a number of bacteria have been isolated that are capable of growth on light *n*-alkanes (ethane, propane and butane), their metabolic pathways have received little attention compared to those of methane and liquid *n*-alkanes [55, 128]. The ability to grow on gaseous *n*-alkanes has been found in some *Pseudomonas* strains [129] and many strains belonging to

the order *Actynomycetales*, such as those of the genera *Corynebacterium*, *Nocardia*, *Mycobacterium*, *Rhodococcus* [55, 66, 128, 130]; these genera possess highly hydrophobic cell surface and express numerous oxygenase enzymes which might generally facilitate their growth and predominance in *n*-alkane enrichments [55].

1.3.4.2.1 Butane monooxygenase (BMO) in Pseudomonas butanovora

The best-studied gaseous alkane metabolism is expressed in the Gram-negative bacterium *Pseudomonas butanovora* that has been widely studied for the ability to grow on C_2–C_9 alkanes as well as on a number of alcohols and organic acids [129]. The alkane degradation occurs by sequential oxidations of the terminal methyl group of the hydrocarbon [128]. The first enzyme of the pathway, termed butane monooxygenase (BMO), belongs to the SDIMO family and it shows high similarity to the sMMO [63, 131]. Despite this similarity, two striking differences between BMO and sMMO are: (i) BMO oxidizes methane very slowly [132]. (ii) BMO oxidizes butane to 1-butanol while sMMO oxidizes butane to 1- and 2-butanol [63]. The pathway of butane metabolism by this bacterium was studied by including inhibitors in the biochemical assays; these inhibiting molecules competed for the enzyme(s) that further metabolize each putative butane degradation intermediates preventing the consumption of these metabolites. The accumulated intermediates were revealed and quantified by gas chromatography [128]. The results showed that the major pathway of *n*-butane consumption proceeds through the terminal oxidation of butane to 1-butanol that is subsequently oxidized to butyraldehyde and butyrate (Fig. 1.5). Further metabolism probably proceeds via β-oxidation [128]. Gene disruption experiments demonstrated the involvement of two primary alcohol dehydrogenases (BOH and BDH) in the *n*-butane utilization [133]. Gene expression experiments reported that both the alcohol DHs were induced by the growth on *n*-butane or 1-butanol and only BOH expression was also induced by 2-butanol. This accounts for the ability of *Ps. butanovora* to grow on 2-butanol and to oxidize it to butanone,

18

even though no sub-terminal oxidation of the butane (producing 2-butanol from butane) was detected in the biochemical experiments. (Fig. 1.5) [128, 134].
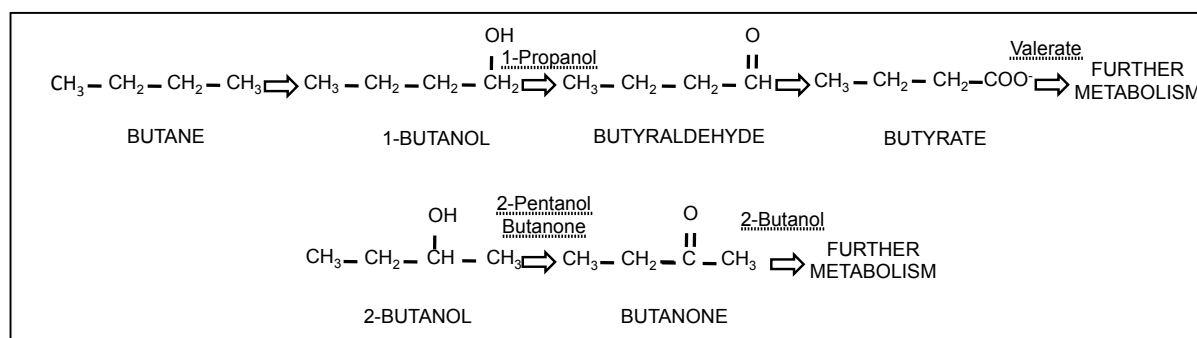
Figure 1.5 Scheme of *n*-butane and 2-butanol metabolism by butane-grown 'P. butanovora'. The upper pathway follows from the terminal oxidation of butane. The lower pathway shows the oxidation of 2-butanol, although no subterminal oxidation of butane was detected. Inhibitors of each transformation are indicated above the arrows. (Modified from [128])

The six structural genes cluster, *bmoXYBZDC*, coding for the sBMO of *Ps. butanovora* have been cloned and sequenced by Sluis *et al.* [131]. The soluble BMOH component contains three subunits (α, β and γ) encoded by *bmoX*, *bmoY* and *bmoZ*, respectively. By analogy with other hydroxylase components, BMOH is likely to have $\alpha_2\beta_2\gamma_2$ quaternary structure where the α-subunit contains the di-iron active site of sMMO [89, 131, 135, 136]. BMOB is the butane monooxygenase regulatory protein, similar in sequence to the regulatory protein required for the enzymatic activity of sMMO. BMOR is the reductase component and is encoded by *bmoC*. Its protein sequence analysis reveals the presence of a [2Fe-2S] binding domain (ferredoxin domain), additionally, a second domain contains motifs for NADH-binding and flavin-binding sites. The similarity between the sBMO and the sMMO is less for the reductases than the other components, however several structural features are conserved [131]. Because the *bmoD* gene product is similar in amino acid sequence to *mmoD* (*orfY*), BmoD is suggested to be involved in the assembly of the sBMO hydroxylase diiron centre [108].
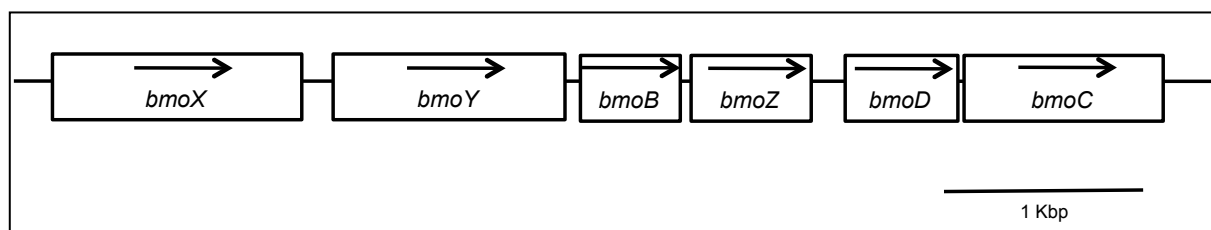
Figure 1.6 Genetic loci of the butane monooxygenase genes in *P. butanovora*. The transcription direction of each *orf* is indicated by arrows. (Modified from [131])

Induction of the alkane monooxygenase in *P. butanovora* is well studied. Alkane monooxygenase is not expressed during growth of *P. butanovora* on organic acids, but is induced during growth on C_2-C_5 *n*-alkanes [137-139] and during the growth on alcohols and aldehydes that result from the oxidation of C_2-C_9 *n*-alkanes [25, 137, 140, 141]. The BMO structural genes are transcribed as a single polycistronic mRNA and the transcription of the cluster is controlled by a σ^{54} promoter [131], identical to the consensus sequence of *mmo* genes in *Methylosinus trichosporium* OB3b, *Methylocystis sp. M*, and *Methylomonas sp. KSWIII* [52, 86, 131]

The analysis of the *bmo* genes operon revealed the presence of a gene (*bmoR)* located upstream of the BMO operon encoding a peptide (BmoR) similar to σ^{54}-transcriptional regulators. BmoR is suggested to be necessary for the exponential growth on C_6–C_8 *n*-alkanes [139]. Another gene (*bmoG*) at the 3'-end of the BMO operon encodes a peptide (BmoG) similar to GroEL chaperonins. BmoG is proposed to assist the proper assembly of BMO [139]. *orf*1 encodes a transcriptional regulator of the GntR family. *istA* and *istB* genes were identified as an operon encoding a putative transposase based on the sequence similarity [139].
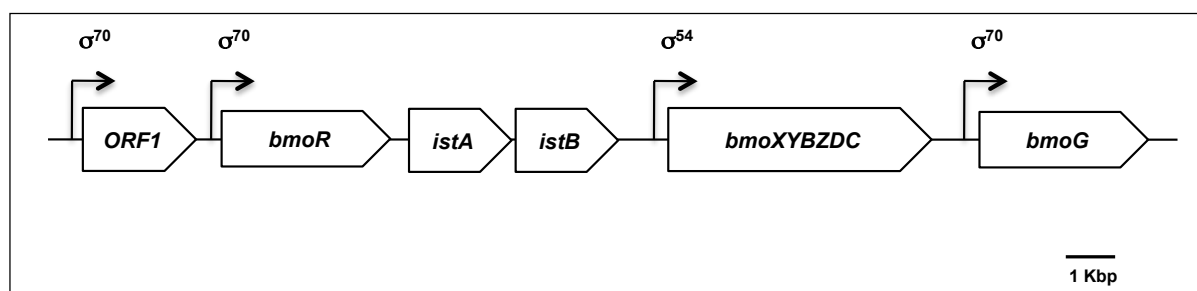
Figure 1.7 The BMO operon (*bmoXYBZDC*) and adjacent genes with putative promoters indicated by arrows. (Modified from [138])

In a variety of other microorganisms short chain alkane monooxygenase enzymes were described to be induced during growth on alkanes, but not during growth on non-alkane substrates [62, 66, 137].

1.3.4.2.2 Propane monooxygenases (PrMO) in Actinobacteria

Until recently it was difficult [55] to obtain stable preparations of gaseous *n*-alkane monooxygenases from Gram-positive strains. However, a soluble diiron-containing propane monooxygenase (PrMO) from *Gordonia* TY-5 has recently been purified [142]. The TY-5 PrMO confers to this Gram-positive strain the ability to use propane as only carbon and energy source. Similarly to *bmo* genes and *mmo* genes, the *prmABCD* gene cluster is polycistronically transcribed and it codes for three components, a hydroxylase (large and small subunits), an oxidoreductase (PrmB) and a coupling protein (PrmD) [119]. It has been defined narrow-substrate-range propane monooxygenase because, by contrast to most of gaseous *n*-alkanes monooxygeanses, it cannot oxidize gaseous *n*-alkanes other than propane. Among the components of Prm, the putative large and small subunits of the hydroxylase (encoded by *prmA* and *prmC*, respectively) show a relatively higher sequence similarity to those of sBMO, while sequences of the other components show lower similarities. In addition to this, similarly to sMMO, it oxidizes propane only at the sub-terminal position, generating 2-propanol [119]. This secondary alcohol is oxidized to acetone, which is further transformed into methylacetate and, finally, into acetic acid and methanol [60]. The secondary alcohol

21

dehydrogenase, which catalyzes the second step in the propane catabolic pathway, is transcribed by *adh1* that maps close to the *prm* genes [119].
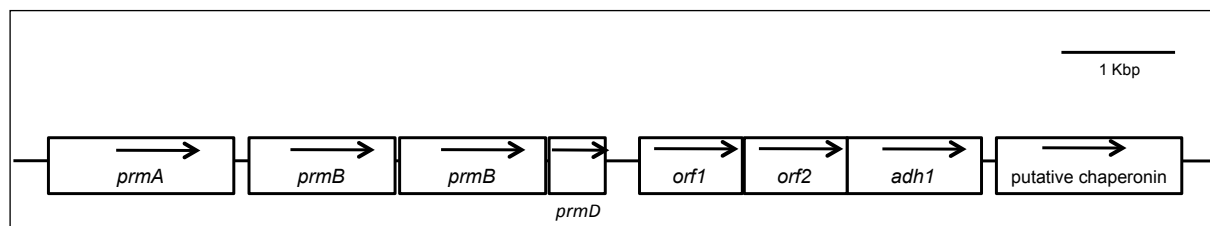
Figure 1.8 The 9.2-kb gene region of *Gordonia* sp. strain TY-5. Genetic organization of the gene cluster and restriction map. The orientation of the identified genes is indicated by arrows. (Modified from [118])

The *prm* gene cluster of *Gordonia* sp. TY5 appears to be conserved in other actinobacteria. The eight genes represented in Fig. 1.8 have homologs in *Rhodococcus jostii* RHA1 [65] and in *Mycobacterium smegmatis* (GenBank accession no. NC008596). The order of the genes is identical in the three organisms, and the encoded proteins of TY5 are 64% to 93% identical to their homologs in the other two organisms. *Rhodococcus* RHA1 *prm* genes have been further described as genes up-regulated in propane-grown cells by microarray analysis [65]. The PrMO in RHA1 has been also reported to be involved in the co-metabolic removal of xenobiotic *N*-nitrosodimethylamine (NMDA). This ability is present in RHA1 cells grown on pyruvate, soy broth and LB medium but the removal efficiency is much improved after growth on propane [65].

Furthermore, a proteomic analysis was conducted by LeBlanc [143] in order to identify the genetic basis of the strategies used by RHA1 to survive desiccation treatment. Interestingly, this analysis showed an up-regulation of *prmA* gene under this condition, thereby a correlation between desiccation-induced cell stress and induction of the *prm* genes was hypothesized [143]. The reason for this up-regulation is not clear yet; however, it can be speculated that other genes in the operon, such as *groEL* encoding a chaperone protein, may be part of a general stress response and the activation of the entire cluster in stressed biomass could increase the activity towards low-concentration environmental contaminants, such as

22

NMDA [65]

Similar propane monooxygenases have been found in other propane-utilizing species *Mycobacterium* sp. TY-6 and *Pseudonocardia* sp. TY-7 [59]. While strain TY-6 oxidizes propane at the terminal position, in strain TY-7 both terminal and sub-terminal oxidation was observed.
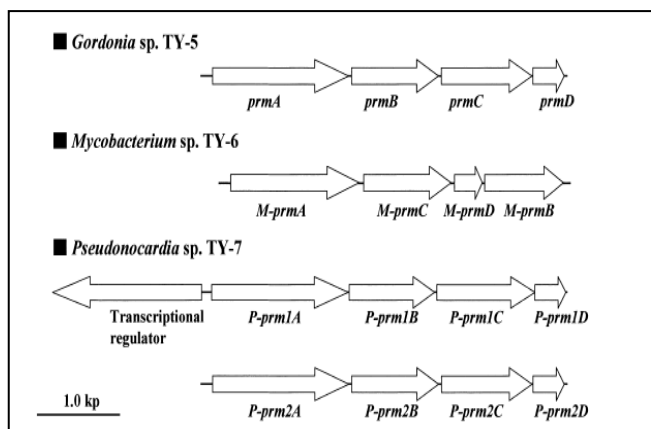
Figure 1.9 Schematic representation of propane monooxygenase gene (*prm*) clusters in *Gordonia* sp. TY-5, *Mycobacterium* sp. TY-6 and *Pseudonocardia* sp. TY-7. [58]

FIG. 3. Proposed propane oxidation pathways in *Gordonia* sp. TY-5, *Mycobacterium* sp. TY-6 and *Pseudonocardia* sp. TY-7.
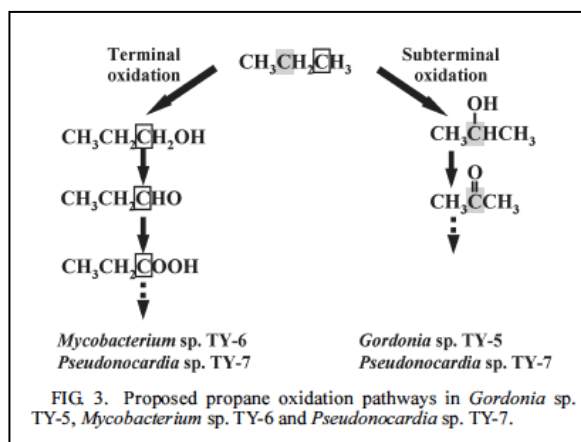
Figure 1.10 Proposed propane oxidation pathways in *Gordonia* sp. TY-5, *Mycobacterium* sp. TY-6 and *Pseudonocardia* sp. TY-7. [58]

Additonally, the BMOs of *Mycobacterium vaccae* JOB5 and *Nocardioides* CF8 have been analyzed from a physiological point of view. While the former one showed properties similar to sMMO [144], the *Nocardioides* CF8 BMO was shown to be a copper-containing enzyme similar to pMMO [62, 145]. Allylthiourea (ATU) is an inhibitor of copper-containing monooxygenases catalysis since it is a copper-selective chelator that binds reversibly the

23

copper atoms that are present in the prostethic group of the enzyme [66, 146]. ATU sensitivity assays suggested the CF8 BMO being the third example of copper-containing monooxygenases in addition to pMMO and ammonia monooxygeanse (AMO) [62].

Recently, a gene encoding a 54-kDa polypeptide was shown to be involved in butane oxidation in *Pseudomonas* sp. IMT37. The sequence was neither similar to alkane hydroxylases (liquid alkanes) nor to methane monooxygenase, and furthermore did not have significant similarity to any entries in the protein sequence databases [147]. The disruption of the gene caused *Ps*. IMT39 to loose the ability to grow on butane and on C_5-C_{10} *n*-alkanes but not the ability to grow on the corresponding alcohol, demonstrating its role in the initial step of the metabolism of these alkanes [147].

1.3.4.2.3 Significance of SDIMO hydroxylases in bioremediation

During the last decade SDIMOs members have been studied for the applicability in bioremediation and biocatalysis. Indeed, the broad substrate range [148] allows them to oxidize a variety of halogenated-alkanes, alkenes and aromatics with favourable kinetic parameters [13] and (in some cases) stereo-selectivity [149]. All SDIMO groups so far examined include enzymes capable of co-metabolically oxidizing halogenated pollutants such as trichloroethene (TCE) and vinyl chloride (VC) [150-153]. Some members showed also the ability to co-metabolize methyl *tert*-butyl ether (MTBE) [67]. Potential applications in bioremediation and biocatalysis are a strong incentive to study the details of cometabolic oxidations by alkane hydroxylase systems. Studies of alkane hydroxylase gene diversity, coupled with information on substrate range, induction, enzyme kinetics and host properties, should help to optimize the biodegradative activity of indigenous hydrocarbon degrading strains and promote fundamental research on the activation of oxygen for bio-catalytic applications [30, 154].

1.3.4.3. The AlkB family of alkane hydroxylases

1.3.4.3.1 The membrane-bound protein non-heme iron oxygenases

The family of AlkB is included in the super-family of membrane-bound non-heme iron oxygenases comprising structurally similar enzymes such as xylene monooxygenases and related enzymes, fatty acid desaturases and epoxidases, decarbonylases and methyl oxydase [155]. This family of oxygenases is able to introduce one atom of oxygen into hydrophobic substrate using one atom of oxygen originating from molecular oxygen. The other oxygen atom is reduced to water using two electrons from NAD(P)H. The electrons are transferred from the NAD(P)H to the monooxygenase by either ferredoxin and ferredoxin reductase or cytochrome b5 in the case of fatty acid desaturases [156] rubredoxin and rubredoxin reductase in the case of alkane hydroxylases (AlkB) [157, 158] or a ferredoxin-ferredoxin reductase fusion protein for xylene monooxygenases [22, 159-161]. Three, four or six membrane-spanning elements can be identified in all primary amino acid sequences of proteins belonging to this super-family, with varying numbers of amino acids between each trans-membrane helix [162, 163]. All members of this family also contain eight highly conserved histidine residues that are likely involved in iron coordination. They are grouped in three sequence motifs ($HX_{3-4}H$, $HX_{2-3}HH$, $HX_{2-3}HH$) and are essential for the function of these enzymes [162]. Additionally, all the integral-membrane non-heme iron proteins contain a non-heme diiron cluster that is of the same type present in the soluble non-heme iron proteins (SDIMO) [22, 164].

The members of the AlkB family allow a wide range of *Proteobacteria* and *Actinomycetales* to grow on *n*-alkanes with carbon chain lengths typically included between C_5 and C_{16}. The definite *n*-alkanes specificity of AlkB is consistent with most of the data that has been collected regarding the AlkB hydroxylases activity. For example, *Nocardioides* CF8 can grow on C_2-C_{16} and the *alkB* gene was described to be only active on alkanes larger than

C_6 [66], while the degradation of alkanes $< C_5$ was attributable to a copper-containing monooxygenase. Nevertheless, in the last two years, some AlkB hydroxylases have been reported to be induced by gaseous alkanes (C_2-C_4). *Mycobacterium austroafricanum* can grow on C_2-C_{16} and the *alkB* gene expression, involved in *tert*-butyl alcohol (TBA) co-metabolism, was induced not only after growth on *n*-hexane and *n*-hexadecane but also after growth on propane ([67]. The involvement of AlkB-type hydroxylase in gaseous alkanes metabolism has been also reported in *Pseudomonas putida* GPo1 [165]. These new discoveries about AlkB activity open new frontiers of applications for this family members and will allow the continuation of AlkB hydroxylases as the central focus of alkane oxidation research.

1.3.4.3.2 AlkB in Pseudomonas putida GPo1

Even though several studies have shown that the *alkB* genes are widespread in nature [166], only the *Pseudomonas putida* GPo1 alkane hydroxylase system [167] has been studied in detail with respect to enzymology, genetics, as well as potential applications [28, 167, 168]. The alkane hydroxylase system of GPo1 consists of three components: a particulate hydroxylase (AlkB), which is the catalytic component localized in the cytoplasmic membrane, and two soluble proteins, rubredoxin (AlkG) and rubredoxin reductase (AlkT) (Fig. 1.11).

AlkT is a FAD-containing NADH-dependent reductase that channels electrons from NADH, via its cofactor FAD, to the rubredoxin, which transfers electrons to the active site of the alkane hydroxylase [30] (Fig. 1.11).

AlkG is an electron transfer protein that contains one or more active centers consisting of a single iron atom with four cysteine sulfur atoms serving as the ligands in a tetrahedral structure. The AlkG of *P. putida* GPo1 is unusual because it contains two rubredoxin domains, AlkG1 and AlkG2, connected by a linker, while rubredoxins from other microorganisms have only one of these domains (Fig. 1.11) [49]. Several rubredoxins from

26

alkane-degrading bacteria have been cloned and analysed in complementation assays for their ability to substitute *P. putida* GPo1 AlkG. They clustered into two groups: AlkG1-type rubredoxins cannot transfer electrons to the alkane hydroxylase in GPo1, while AlkG2-type enzymes can do so and can substitute for AlkG [169]. AlkG1-type rubredoxins probably have other as yet unknown roles. Indeed, rubredoxin/rubredoxin reductase systems are also present in organisms that are unable to degrade alkanes, where they serve other functions.
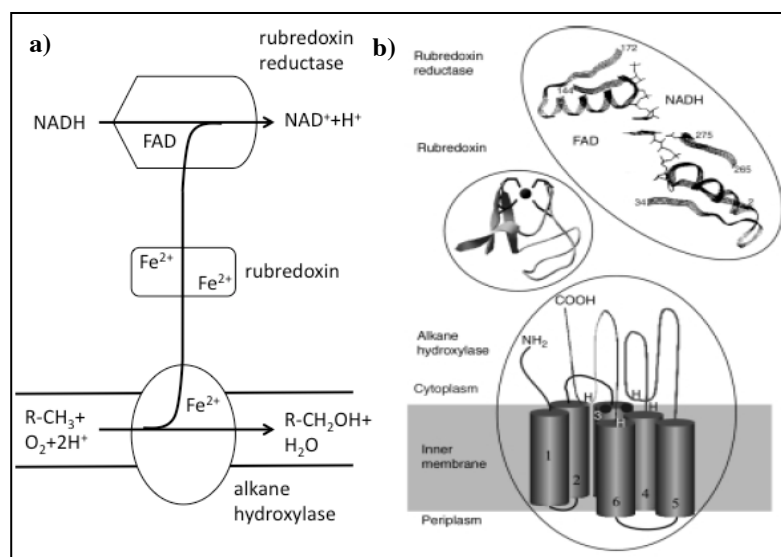
Figure 1.11 Structure of membrane-bound the alkane hydroxylase system. Fig 11a shows the passage of the electrons amongst the three components of the AlkB system. (Modified [30]). Fig 11b shows the structural properties of the three components of AlkB monooxygenase (Modified [30])

P. putida GPo1 is able to oxidize linear alkanes ranging from *n*-pentane to *n*-dodecane by virtue of the AlkB hydroxylase system [170] and can oxidize also butane and propane, even though the degradation rate is much slower [165]. In addition to the hydroxylation of aliphatic and alicyclic, the AlkB system has been shown to catalyze: oxidation of terminal alcohols to the corresponding aldehydes; demethylation of branched methyl ethers; sulfoxidation of thioethers, and epoxidation of terminal olefins [171-173]. Methane, ethane, or alkanes longer than C_{13} are not oxidized.

Although the crystal structure of AlkB is not available, the hydroxylase has been suggested to contain a deep hydrophobic pocket formed by six transmembrane α-helices and

a catalytic site that faces the cytoplasm (Fig. 1.12). The alkane molecule should slide into this pocket until the terminal methyl group is correctly positioned relative to the active site composed of four His residues that chelate two iron atoms [162, 174, 175]. The di-iron cluster allows the O_2-dependent activation of the alkane through a substrate radical intermediate [164, 176]. One of the O_2 atoms is transferred to the terminal methyl group of the alkane, rendering an alcohol, while the other one is reduced to H_2O by electrons transferred by the rubredoxin. Oxidation is regio- and stereo-specific [177]. Amino acids with bulky side-chains protruding into the hydrophobic pocket can impose a limit to the size of the alkane molecule that can slide into the pocket and still allow a proper alignment of the terminal methyl group with the catalytic His residues. Substitution of these amino acids by residues with less bulky side-chains allows larger alkanes to fit in place into the hydrophobic pocket. In particular, an increase in the *n*-alkane chain length accepted by AlkB was reported upon the substitution of a tryptophan residue with a smaller amino acid, such as serine, in the enzyme's center [178] (Fig. 1.12).
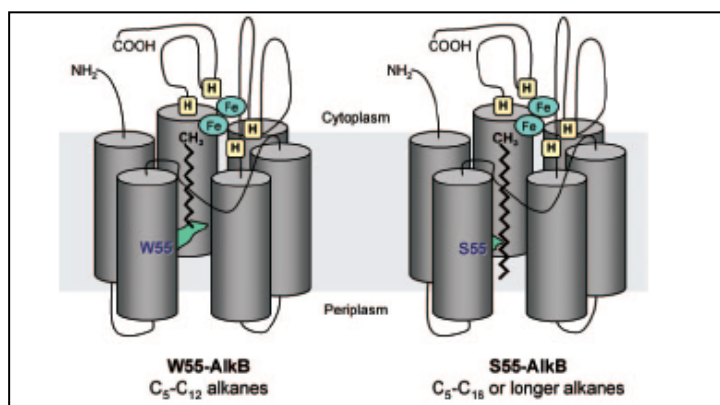
Figure 1.12 Model for the AlkB alkane hydroxylase. The residue W55 that extends its bulky arm towards the hydrophobic pocket is shown (left). This hampers the proper insertion of alkanes longer than C_{13}. The replacement of W55 by a serine residue (S55) (right) allows longer alkanes to enter. Sizes are not to scale. [178]

The alkane hydroxylase system in *Ps. putida* GPo1 is encoded by the large broad host-range OCT-plasmid [167, 170], along with all the other genes involved in the conversion of alkanes to CoA-activated fatty acids. Two gene clusters can be distinguished: *alkBFGHJKL*

28

and *alkST*. The two *alk* regions are located back-to-back on the OCT-plasmid. *alkB*, *alkF* and *alkG* codes for the membrane-bound non-heme iron alkane monooxygenase components, while the other genes, comprised in the first cluster, code for protein involved in the oxidation following the alkane-activation performed by AlkB. AlkST cluster encode the rubredoxin reductase (AlkT) and the positive regulator for the *alkBFGHJKL* operon, AlkS, that is activated by the presence of *n*-alkanes. The Fig. 1.13 shows the involvement of each protein in the alkane metabolism in *Ps. putida* GPo1.
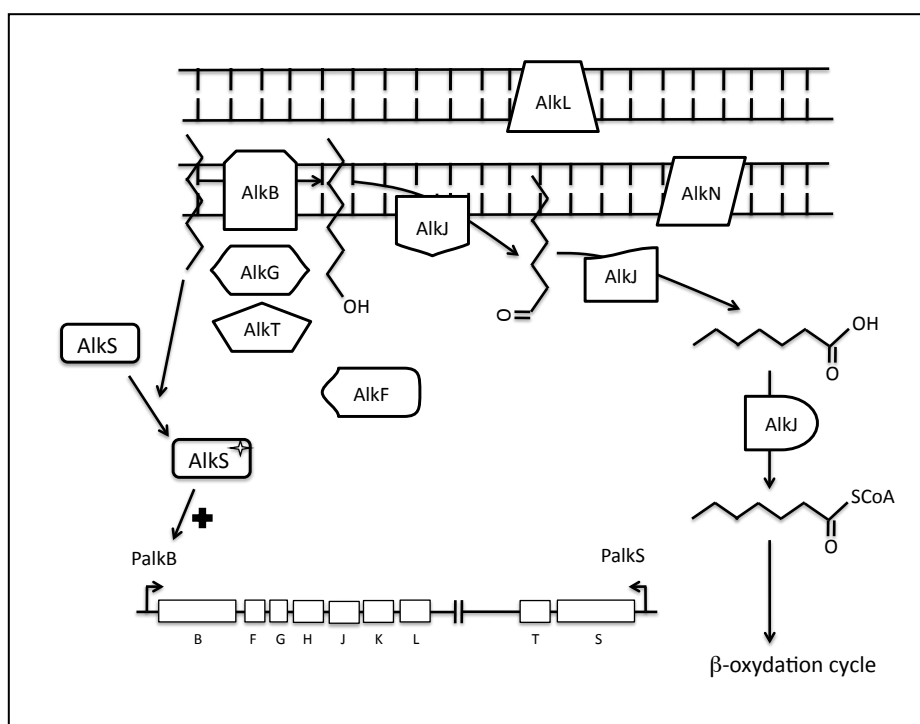
Figure 1.13 Metabolic pathway of alkane degradation, role and cellular localization of Alk proteins and regulation of the *alk* genes. (Modified from [167])

1.3.4.3.3 AlkB-type hydroxylases in other bacteria

Enzyme systems related to the *P. putida* GPo1 alkane hydroxylase were cloned from bacterial strains belonging to several different genera [179-183]. More than 60 AlkB homologues are known to date; they have been found in both Gram-positive and Gram-negative microorganisms and show high sequence diversity [179, 180, 182, 184-187]. While the *P. putida* GPo1 system acts on alkanes ranging from *n*-pentane to *n*-dodecane (C_5-C_{12})

[28, 188], most related membrane-bound alkane hydroxylases affect alkanes containing more than 10 carbon atoms [179, 189]. Alkane-degraders other than *Ps*. GPo1 were studied in much less detail (except for the methanotrophs); furthermore, even though hydrocarbon utilization is very common amongst strains belonging to the *Corynebacterium-*, *Mycobacterium-*, *Nocardia-* and *Rhodococcus-* (CMNR) complex, only a few CMNR strains were studied in some detail [30, 190, 191]. Additional membrane-bound alkane hydroxylases, acting on C_{12} and longer *n*-alkanes, were found in *Acinetobacter* sp. ADP1, *Acinetobacter* sp. strain M-1 and *A. calcoaceticus* EB104 and showed to be quite distantly related to the *P. putida* GPo1 AlkB [30, 180, 181, 183]. The genome sequence of *Mycobacterium tuberculosis* H37Rv [192] was also found to encode an AlkB-homolog, which was functional by heterologous expression [179]. The comparison of the *alkB* sequences shows a significant sequence divergence, but the four histidine-containing motifs are well conserved along with the alkane hydroxylases membrane folding with the 6 hydrophobic stretches that are likely to span the cytoplasmic membrane [30, 162]. Based on amino acid sequences conserved between the *P. oleovorans* GPo1 and the *Acinetobacter* sp. ADP1 alkane hydroxylases, highly degenerate primers were developed by Smits *et al* [180] that resulted to amplify internal gene fragments of *alkB* homologs from Gram-negative as well as Gram-positive strains [66, 179, 182, 193]. By using these primers, in order to detect the presence of GPo1 homologs AlkB-systems, many strains (especially *Rhodococcus* and *P. aeruginosa* strains) were shown to possess multiple—quite divergent—alkane hydroxylases [163, 194, 195].

1.3.4.3.4 Diversity of the alkB members and organization of the alkB gene cluster

In most of the cases, it is difficult to find a clear linkage between the diversity of the *alkB* genes and the phylogenetic lines of the corresponding *alkB* gene expressing bacteria. For instance, significant divergence degree exists amongst the AlkB homologs produced by fluorescent pseudomonads and also amongst the four AlkB-homologs expressed by the same

30

organim, such as the 4 AlkB-homologues in *R. erythropolis* NRRL B-16531 [195]. In part, the failing link between phylogenetic lineage and AlkB-diversity is due to horizontal gene transfer. For example, the *P. putida* GPo1 *alk*-genes are located on a large broad host-range plasmid named OCT [196] while the closely related *P. putida* P1 alk-genes are located on a class I transposon [30, 167]. These types of gene location promote the transfer of the AlkB gene amongst phylogenetically different bacteria.

Additionally, the organization of genes involved in alkane oxidation varies strongly among the different alkane degrading bacteria (Fig. 1.14) [30]. In most strains, genes involved in alkane degradation seem to be distributed over the genome. While most rubredoxin genes are located immediately downstream of the alkane hydroxylase genes, none of the rubredoxin reductase genes map close to an alkane hydroxylase, except for *R. erythropolis* [195]. This might be because they are also involved in other pathways and require different type of regulations. Furthermore, when several alkane hydroxylase systems coexist in a single strain, they are normally located at different sites in the chromosome and the regulators that control the expression of alkane-degradation genes may or may not map adjacent to the genes they regulate [30, 197].
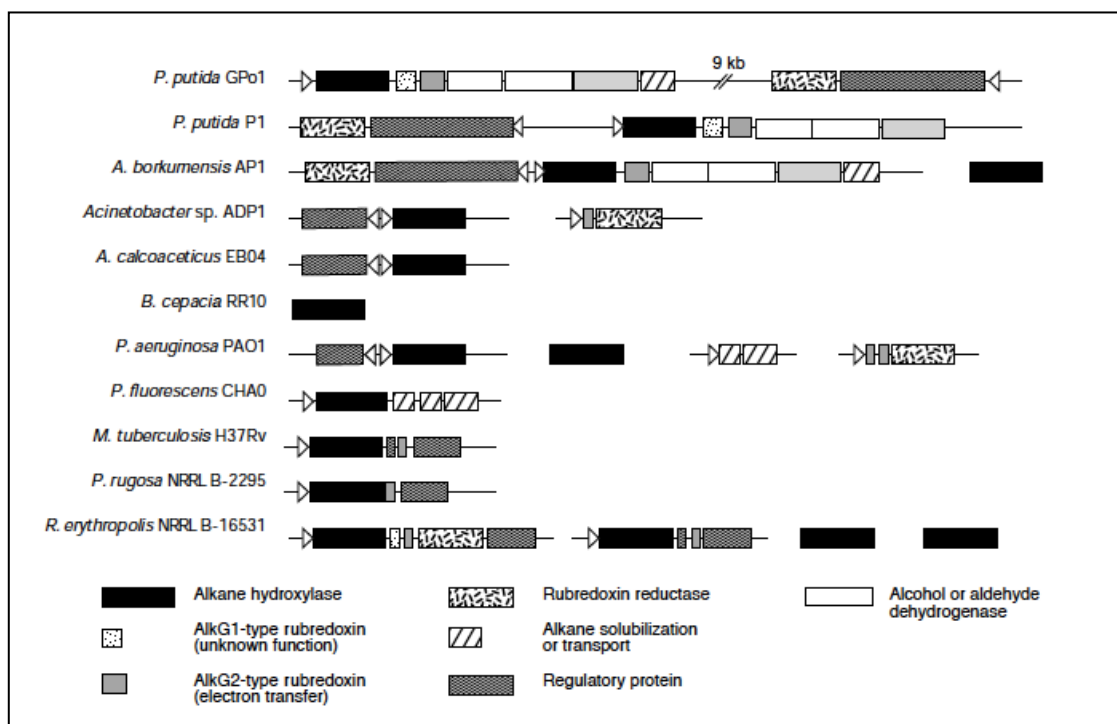
Figure 1.14 Organization of *alk* genes in different microorganisms. The function of the encoded proteins is indicated below. If the *orfs* are linked by a line, the sequence is contiguous. If the *orfs* are not linked by a line, the genes are located elsewhere on the chromosome. The triangle indicates the direction of transcription. (Van Beilen, 2003)

1.3.4.4. Cytochrome P450 alkane hydroxylases

Cytochrome P450, heme-iron hydroxylases, are ubiquitous in nature and they can be grouped in more than 100 families on the basis of sequence similarity [198]. While several eukaryotic cytochrome P450s have a broad substrate spectrum and oxidize many xenobiotics and steroids, microbial cytochrome P450s can have more narrow substrate specificity [199].

Among eukaryotes, yeasts are well-known for their ability to grow on alkanes by virtue of their membrane-bound microsomal P450s belonging CYP52 family [200-203] and they may have an important role in the biodegradation of alkanes in some oil-contaminated sites [204]. By contrast, only limited evidence showed the presence of P450 cytochromes involved in *n*-alkane metabolism in bacteria [30]. In 2001, a cytochrome P450 belonging to a new family (CYP153A1) was reported to be involved in *n*-hexane oxidation in *Acinetobacter* sp. EB104 [205]. In contrast to the eukaryotic membrane-bound P450 systems, the CYP153 appeared to occur as a soluble protein [206] like other bacterial P450s involved in other

32

metabolic pathways. This purified P450 exhibited *n*-alkane-oxidizing activity in the presence of ferredoxin and ferredoxin reductase isolated from the same bacterium [207] and it seemed to be induced by a variety of hydrocarbons [205, 207]. Subsequently, highly degenerate primers were designed based on conserved sequence motifs in CYP153A1 and two CYP153 homologs (CYP153A2 and CYP153A4) found in bacterial genome sequences available in the database. These primers were used to clone the *Mycobacterium* sp. strain HXN-1500 *CYP153A6* gene and flanking regions [200]. The cytochrome P450 from *Mycobacterium* sp. HXN-1500 was purified and showed the ability to hydroxylate C_6–C_{11} alkanes to 1-alkanols with high affinity and regio-selectivity [200]. Furthermore, the same primers were used to carry out a search for *CYP153* genes in alkane-degrading strains that possessed AlkB-like hydroxylases only acting on long-chain length alkanes, even though these strains were also able to grow well on the medium-chain hydrocarbons [208]. Many of these strains (*mycobacteria*, *rhodococci*, and *Proteobacteria*) contained cytochrome P450 enzymes belonging to the CYP153 family that showed oxidation activity on medium-chain length alkanes (C_5-C_{10}). Thereby, it was suggested that the two different types of alkane hydroxylases (AlkB and P450) had different subsets of alkanes (medium- or long-chain lenght) in these strains. The only exception was *A. borkumensis* AP1 and SK2 that possessed AlkB and CYP153 enzymes both acting on medium chain length alkanes. To date none P450s have been isolated that activate short-chain gaseous alkanes [208].

1.3.4.5. Alkane hydroxylases for long-chain n-alkanes

Several bacterial strains can assimilate alkanes larger than C_{20} and they usually contain several alkane hydroxylases. Those active on C_{10}–C_{20} alkanes are usually related to *P. putida* GPo1 AlkB or to *Acinetobacter* sp. EB104 cytochrome P450. However, the enzymes that oxidize alkanes larger than C_{20} seem to be totally different. For example, *Acinetobacter* sp. M1, which can grow on C_{13}–C_{44} alkanes, contains a soluble, Cu^{2+}-dependent alkane

hydroxylase that is active on C_{10}–C_{30} alkanes; it has been proposed to be a dioxygenase that generates *n*-alkyl hydroperoxides to render the corresponding aldehydes [183, 209]. A different *Acinetobacter* strain, DSM 17874, has been found to contain a flavin-binding monooxygenase, named AlmA, which oxidizes C_{20} to $> C_{32}$ alkanes [210]. Genes homologous to *almA* have been identified in several other long-chain *n*-alkane-degrading strains, including *Acinetobacter* sp. M1 and *A. borkumensis* SK2. A different long-chain alkane hydroxylase, named LadA, has been characterized in *Geobacillus thermodenitrificans* NG80-2 [211]. It oxidizes C_{15}–C_{36} alkanes, generating primary alcohols. Its crystal structure has shown that it is a two-component flavin-dependent oxygenase belonging to the bacterial luciferase family of proteins [212]. Several bacterial strains can degrade $> C_{20}$ alkanes using enzyme systems that have still not been characterized and that may include new proteins unrelated to those currently known [49].

1.3.4.6. Regulation of the alkanes degradation pathways

Little is known about the mechanisms that regulate the expression of the genes involved in the initial oxidation of alkanes. To date, the data collected suggest that the metabolic genes are expressed only in the presence of the appropriate alkanes or/and according to the environmental or physiological conditions. These mechanisms have been described mostly in *Pseudomonas*, *Alcanivorax* and *Burkholderia* [49].

LuxR/MalT, AraC/XylS and GntR are some of the regulators that have been found to be involved in the induction of alkane-degrading genes. One of the most intriguing question concerns how the alkanes, which are apolar molecules that tend to accumulate into the cytoplasmic membrane, interact with the transcriptional regulators that are normally cytoplasmatic [49]. One mechanism has been hypothized for the *Alkanivorax borkumensis* AlkS transcriptional regulator that is believed to activate the expression of the gene coding for the AlkB1 alkane hydroxylase and of downstream genes in response to *n*-alkanes [70, 213]. In

34

a proteomic study this regulator appeared to be associated with the membrane fraction, rather than to the cytoplasmic fraction [75]. Most probably, even though AlkS does not show the orthodox features of a membrane protein, it might have affinity for the inner side of the cytoplasmic membrane, where it can bind the alkane and subsequently move to bind regulatory sites on the DNA [49].

Three examples of mechanisms involved in the modulation of alkane-degrading genes are described below: differential regulation, product repression and catabolite repression [49].

1.3.4.6.1 Differential regulation of multiple alkane hydroxylases

While only *P. putida* GPo1 and a few other bacterial strains contain one alkane hydroxylase, in general, multiple alkane-degradation systems are present. *Nocardioides* sp. strain CF8 can produce two distinct monooxygenases for oxidation of alkanes: a copper-containing monooxygenase, acting on C_4-C_{10} *n*-alkanes, and an integral-membrane, binuclear-iron monooxygenase, induced by *n*-alkanes above C_6 [66]. Two *Rhodococcus* strains (NRRL B-16531 and Q15), which have been isolated from different geographical locations, contain at least four alkane hydroxylase gene homologues (*alkB1*, *alkB2*, *alkB3* and *alkB4*) [195]; however, the functional difference between these multiple *alkB* genes is not clear yet. *Pseudomonas aeruginosa* strain PAO1 contains two alkane hydroxylases, AlkB1 and AlkB2, whose substrate range also overlaps significantly, because AlkB1 oxidizes C_{16}–C_{24} *n*-alkanes while AlkB2 is active on C_{12}–C_{20} *n*-alkanes [179]. In *Nocardioides* sp. strain CF8 the differential expression is suggested to be directed by the chain-length of the alkanes usable as subtrates of growth. Similarly, *Acinetobacter* sp. strain M-1 contains two AlkB-related alkane hydroxylases, named AlkMa and AlkMb, which have high sequence similarity to the sequence of alkane hydroxylase (alkM) of *Acinetobacter* sp. strain ADP1. The chain length of the *n*-alkanes in the growth medium regulates their differential expression: *alkMa* expression is induced by solid alkanes (>C_{22}), and is controlled by the AlkRa regulator, while *alkMb*

expression is preferentially induced by liquid alkanes (C_{16} to C_{22}) and is regulated by AlkRb [183].

Different is the case of *Pseudomonas aeruginosa* strain RR1 where the differential expression depends on the growth phase of the cell, rather than on the substrate profile. The two RR1 alkane hydroxylases, AlkB1 and AlkB2 are induced by C_{10}–C_{22} alkanes, although the expression of *alkB1* gene is almost twice as efficient as that of *alkB2* gene. The *alkB2* gene is induced preferentially during the early exponential phase of growth, while *alkB1* is induced in the late-exponential phase of growth. The expression of both genes declines in stationary phase. The regulators responsible for this differential regulation have not been identified [49, 214].

Three or more alkane oxidation systems were found in hydrocarbonoclastic bacteria and in species having a versatile metabolism. *A. borkumensis* has two AlkB-like alkane hydroxylases, three genes coding for cytochromes P450 involved in alkane oxidation [70, 213, 215], uncharacterized genes involved in oxidation of branched alkanes and phytane [70], and a gene similar to *Acinetobacter sp.* DSM 17874 *almA*, which oxidizes alkanes of very long chain length [210]. Expression of all these alkane oxidation genes should be differentially induced according to the substrate present under each circumstance, although the regulators involved and/or the signals involved are poorly characterized [49].

The substrate range of the *A. borkumensis* AlkB-like alkane hydroxylases partially overlaps. AlkB1 oxidizes C_5–C_{12} *n*-alkanes, while AlkB2 is active on C_8–C_{16} *n*-alkanes [213]. They probably share the auxiliary proteins rubredoxin and rubredoxin reductase, as they are encoded by genes that map separately from *alkB1* and *alkB2*. The expression of both *alkB1* and *alkB2* is very low when cells grow using pyruvate as the carbon source, but is strongly induced when C_{10}–C_{16} alkanes are metabolized; expression decreases considerably upon entry into stationary phase [70, 75, 213]. A gene coding for a protein showing similarity to the *P.*

36

putida GPo1 AlkS transcriptional activator maps adjacent to *alkB1*. Contrary to what was observed in *P. putida* GPo1, the transcription of *A. borkumensis alkS* seemed to be constitutive [213]. Indeed, proteomic analysis detected a constitutive production of AlkS in *A. borkumensis* pyruvate-grown cells, even though AlkS levels were higher in *n*-hexadecane-grown cells [75]. In *P. putida* GPo1 a binding site for AlkS is present immediately upstream the -35 region of the *alkS* promoter, resulting in an auto-amplification of the regulator in the presence of alkanes [213, 216-218]. On the contrary, in *A. borkumensis* an AlkS binding site was not identified upstream of the *PalkS* promoter, according to the lack of inducibility of AlkS. However, the promoter for the *A. borkumensis alkB1* gene contains an AlkS-binding site and it was proved that the heterologous expression of *P. putida* GPo1 AlkS in *A. borkumensis* could activate the *alkB1* gene transcription [213]. Therefore, *A. borkumensis* AlkS was suggested to activate the expression of the *alkB1* hydroxylase in response to alkanes. However, AlkS is unlikely to regulate the expression of *alkB2* [213]. A gene coding for a transcriptional regulator of the GntR family is located just upstream of *alkB2*, although its role has not been reported [70].

The three *A. borkumensis* genes coding for cytochromes P450 of the CYP153 family are highly homologues within each others and are believed to participate in alkane degradation [70]. Proteomic profiling analyses revealed that P450-1 and/or P450-2 (they cannot be distinguished by this technique) have higher expression level in hexadecane-grown cells than in pyruvate-grown cells [75]. As P450-1 is probably co-transcribed with other adjacent genes that are up-regulated by hexadecane, it is likely that expression of P450-1 is induced by *n*-hexadecane. A gene coding for a transcriptional regulator of the AraC family maps close to P450-1, but its role has not been reported [49, 70].

1.3.4.6.2 Product repression mechanism

The 'product repression' mechanism defines the inhibition of metabolic genes

37

when the concentration of the alkane-degradation products increases over a certain threshold.

In *P. butanovora* the σ^{54}-dependent transcriptional regulator BmoR activates the expression of the genes coding for BMO. The BmoR is activated by the production of alcohols and aldehydes derived from the alkanes oxidized by BMO, while the alkanes are not recognized as effectors (Fig. 1.15) [139]. On the contrary, propionate, the final product of propane oxidation, represses the BMO operon transcription [137] and directly inhibits the BMO activity [219]. This inhibitory effect persists until propionate catabolism is activated. Propionate catabolism is inactive during growth on butane, but is induced by propionate or upon growth on propane or pentane [137].
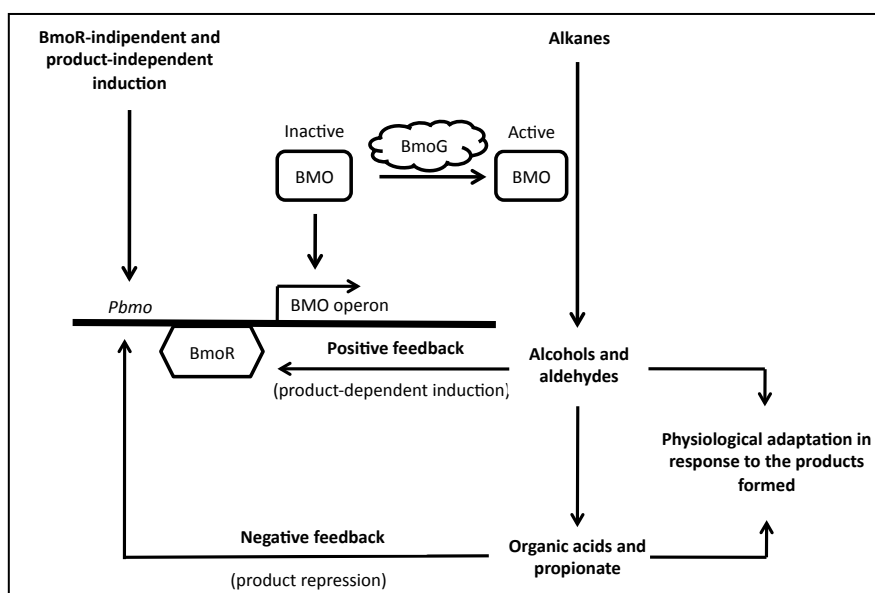
Figure 1.15 Model describing the regulation of BMO expression and activity. (Kurth, 2008)

Few other examples of product repression in pathways for medium-chain-length alkanes have been reported but none of them have been deeply described [137, 181, 214, 220].

These regulatory mechanisms may be a way to coordinate the production of fatty alcohols and fatty acids from alkanes, since these hydrocarbons compounds tend to accumulate in the cell membrane, increasing the levels of trans-unsaturated fatty acids and modifying the composition of the membrane with deleterious consequences to cell physiology

[221, 222].

1.3.4.6.3 Catabolite repression control

The catabolite repression mechanism in bacterial species with a versatile metabolism provides a hierarchical assimilation of the individual carbon sources, in order to promote the use of some compounds over other non-preferred substrates and, thereby, to optimize carbon metabolism and energy generation in response to different signals. Usually, as the hydrocarbons are known to impose a stress on cell physiology and because of their low solubility, they are typically non-preferred growth substrates. Catabolite repression acts probably to promote the bacterial fitness in their natural environments, inhibiting the expression of *n*-alkane-degradation pathways in the presence of more suitable carbon sources [49, 182].

Catabolite repression has been studied in detail for the alkane-degradation pathway encoded by *alkBFGHJKL* operon in *P. putida* GPo1 that encodes all genes required for the assimilation of C_3–C_{13} *n*-alkanes (§ 1.3.4.3.2). In the absence of alkanes, AlkS is expressed from promoter PalkS1 and since AlkS acts as a repressor of its own promoter, it allows for low expression levels. In the presence of C_5-C_{10} alkanes, AlkS activates expression of its own gene from *PalkS2*, in order to achieve AlkS levels that are high enough to activate the expression of the *alkBFGHJKL* operon from the *PalkB* promoter [166, 216, 217, 223, 224]. *Pseudomonas putida* GPo1 grows optimally on C_5–C_{10} alkanes, but can use C_3–C_4 and C_{11}–C_{13} alkanes as well, although growth is much slower and shows a long lag time [154, 165], probably because these alkanes are poor inducers of the AlkS positive loop [224]. Activation of the two promoters, *PalkS2* and *PalkB*, by alkanes is strongly repressed by catabolic repression when cells grow exponentially in rich LB medium or minimal salt medium with amino acids as alternative carbon source [217, 225, 226]. Growth in a minimal medium containing some organic acids as a carbon sources (lactate or succinate) generates a milder

catabolic repression effect [225]. Repression in rich medium abruptly disappears as cells enter the stationary phase of growth, which suggests the existence of elements that assure low-level expression of promoters *PalkB* and *PalkS2* during exponential growth [49].
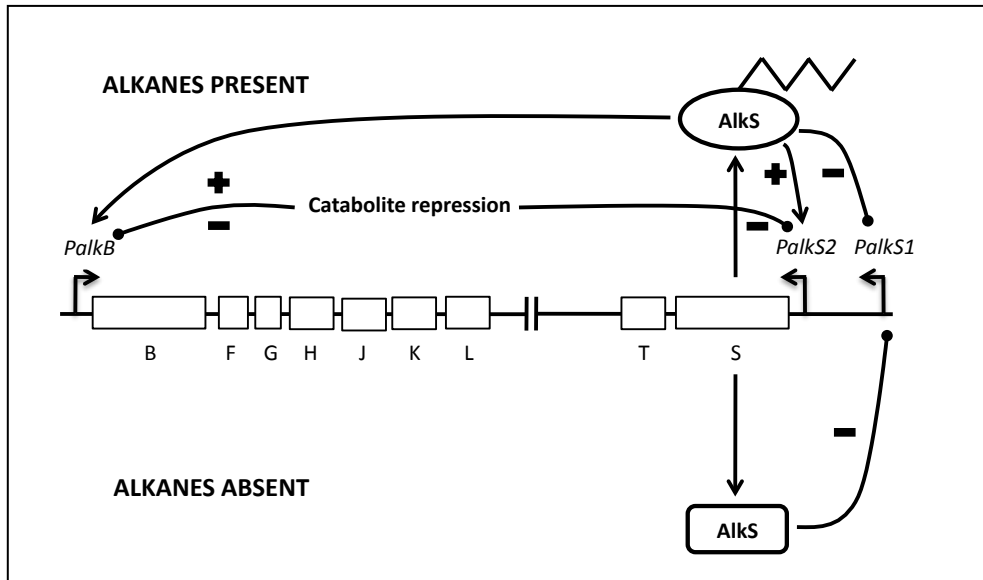
Figure 1.16 *P. putida* **GPo1 alkane degradation pathway. AlkS protein regulates the two clusters,** *alkBFGHJKL* **and** *alkST***. In the absence of alkanes (bottom part), AlkS is expressed from promoter** *PalkS1***; AlkS acts as a repressor of this promoter, allowing for low expression levels. In the presence of alkanes (upper part), AlkS activates expression from the** *PalkB* **and** *PalkS2* **promoters, generating a positive amplification loop on** *alkS* **expression. Activation of these two promoters by alkanes is strongly repressed by catabolic repression when cells grow exponentially in rich LB medium.**

When cells are grown in the LB complete medium, the catabolite repression of the alkane-degradation genes depends on the additive effects of two global regulation systems. One of them relies on the global regulatory protein Crc [218], while the other one apparently receives information from the cytochrome *o* ubiquinol oxidase (Cyo), a component of the electron transport chain [227, 228]. However, in cells grown in a minimal salts medium containing succinate as the carbon source, the role of Crc is minor and the inhibitory effect derives mainly from the Cyo terminal oxidase [218, 227].

In a complete medium, the inhibition process generates a strong decrease in the levels of the AlkS transcriptional activator that is produced in limiting amounts even under inducing conditions [218]. Keeping AlkS levels below those required for maximal induction of the

40

pathway simultaneously inhibits transcription of the *alkST* and *alkBFGHJKL* operons. Crc is an RNA-binding protein that interacts with the 5′-end of *alkS* mRNA, inhibiting its translation [229, 230]. Decreasing translation of *alkS* indirectly reduces *alkS* transcription because AlkS is less produced and cannot activate the expression of its own gene from promoter *PalkS2*. The levels and activity of Crc vary depending on growth conditions [231] and it has also been reported to inhibit the expression of many other catabolic pathways for several non-preferred compounds in *Pseudomonads* [230, 232-237].

The inhibition of the expression of the *n*-alkane-degradation pathway exerted by Cyo is still unclear. The aerobic respiratory chains of both *Escherichia coli* and *P. putida* include a number of membrane-bound dehydrogenases that transfer electrons to ubiquinone, reducing it to ubiquinol. This can then be oxidized by either of two respiratory ubiquinol oxidases: the cytochrome *o* complex or the cytochrome d complex [228]. When cells grow exponentially with a large supply of oxygen, cytochrome *o* oxidase (Cyo) accommodates most of the electron flow. The expression of the Cyo terminal oxidase varies according to oxygen levels and the carbon source being used. With regard to the correlation with the alkane-degradation pathway, it has been shown that that inactivation of cytochrome *o* ubiquinol oxidase partially reduces the catabolic repression that occurs at the *PalkB* and *PalkS2* promoters when cells grow exponentially in rich LB medium or in a defined medium with succinate or lactate as the carbon source [228, 238]. These results suggest that catabolic repression of the *P. putida* GPo1 alkane degradation pathway is linked to the activity of the electron transport chain and/or to the redox state of the cell. Therefore, it has been underlined how the link between a component of the electron transport chain and catabolic repression opens new ways to understand this global regulation process [228, 238, 239].

Other catabolite repression mechanisms have been described in *P. butanovora,* so that the induction of butane utilization is repressed when cells are exposed to lactate and *n*-butane.

The combination of *n*-butane and succinate partially represses butane metabolism, while the combination of *n*-butane and citrate has little effect [138]. This is similar to what is observed in *P. putida*, in which the induction of alkane utilization was repressed when lactate was present, it was poorly induced when succinate present and efficiently induced when citrate was present [225, 240-242].

Additionally, catabolite repression negatively modulates the transcription of *alkB* gene in *Burkholderia cepacia RR10*. However, the repression exerted on the *B. cepacia alkB* gene is significantly stronger than that observed in other alkane degradation pathways, infact all the organic acids tested (citrate, fumarate, lactate, pyruvate, succinate, glutamate, acetate), as well as glucose, fructose, lactose, and arabinose, strongly repressed expression of the *PalkB* promoter in the presence of the *n*-alkane, both in the exponential and stationary phases of growth [220]. The clear differences with P. *putida* GPo1 catabolite repression effector may be due to metabolic and/or mechanistic differences in the catabolic repression strategies of these two bacterial species [220].

1.3.4.7 Converting excess carbon into storage materials

Storage of neutral lipids like triacylglycerols, wax esters, and steryl esters is common in plants, animals, fungi, and bacteria [33, 243, 244].

Interestingly, the conversion of part of the carbon into storage compounds occurs in many bacteria when the carbon source is in excess relative to nitrogen. The storage materials produced are triacylglycerols, wax esters, poly-(hydroxybutyrate) or poly-(3-hydroxyalkanoates) that are accumulated as lipid bodies or as granules [244, 245]. These compounds can later serve as endogenous carbon and energy sources during starvation periods. Formation of storage lipids is frequent among hydrocarbon-utilizing marine bacteria. *Alcanivorax* strains, for example, can accumulate triacylglycerols and wax esters when growing at the expense of pyruvate or *n*-alkanes [246]. *n*-Octane-grown *Pseudomonas putida*

42

GPo1 can form intracellular inclusions of poly-β-hydroxyoctanoate [247], while *Acinetobacter* sp. M-1 forms wax esters from hexadecane [248, 249].

1.4 The genus *Rhodococcus*

Rhodococci are Gram-positive, non-sporulating, aerobic bacteria. They are classified into the suprageneric actinomycetes group known as mycolate-containing nocardioform, also including the genera *Mycobacterium*, *Nocardia* and *Corynebacterium* [38]. The *Rhodococcus* genus comprises of genetically and physiologically diverse bacteria, which have been isolated from various habitats, from sea level [39] to Alpine soils [68], from deep sea [250] to coastal sediments [251] and from Arctic to Antarctic samples [252, 253]; furthermore, some *Rhodococcus* strains are pathogenic: *R. fascians* causes the formation of leaf gall in many plants and *R. equi* is an important equine pathogen with the ability to infect other domestic animals [254].

Rhodococcus genus members have been described in literature to possess many peculiar properties:

- the peculiar cell wall, containing long aliphatic chains of mycolic acids, facilitates the uptake of hydrophobic substrates into the cells. The presence of various substrates in the growth medium induces changes in the fatty acid composition of the membrane lipids and can thus alter the fluidity of the cell envelope. The ability to modulate the fatty acid composition in the cell envelope is probably important to the resistance of *Rhodococcus* cells to many toxic compounds [40].

- the ability to produce surfactants supports the potential to metabolize hydrophobic substrates. Surfactants (e.g. trehalose-containing glycolipids) facilitate the adhesion of cells to hydrophobic phases in two-phase systems, decrease the interfacial tension between phases and disperse hydrophobic compounds [38-40];

- the capacity to form biofilms on carriers suitable for biotechnological purposes further enhances the tolerance of their cells to toxic and hydrophobic compounds [255];

- the ability to persist in stress conditions such as starvation [41] or after desiccation treatments [143];

- the capacity to degrade pollutants in many cases without being affected by the presence of more easily degradable carbon sources [39, 41].

- the high frequency of recombination described in some *Rhodococcus* strains contributes to the flexibility of their genomes and to the ability to acquire new genes (by horizontal gene transfer) and consequently, new enzymatic activities [256]. The large genomes of *Rhodococcus* strains (e.g. *Rhodococcus jostii* RHA1; 9.7 Mb) provide a redundancy of catabolic pathways [257], moreover *Rhodococci* typically contain megaplasmids carrying a large number of catabolic genes [257].

- the wide range of *Rhodococcus* metabolic activities includes antibiotic and amino acid productions [258, 259], degradation of alkanes and aromatic hydrocarbons, biotransformation of steroids and a number of xenobiotic compounds [41], lignin degradation [260], chemolithoautotrophic growth in the presence of hydrogen and carbon dioxide [261], and production of biosurfactants [262, 263].

Summarizing, since *Rhodococcus* strains are equipped by a large number of enzymatic activities, unique cell wall structure and suitable biotechnological properties, they are considered to have great potential to be employed for biotransformation and biodegradation of many organic compounds in environmental remediation and in the pharmaceutical and chemical industries [39, 256, 264].

However, the most of the genetic systems and regulatory mechanisms of genes and proteins, required for these degradation/biosynthetic pathways in *Rhodococcus*, is still far from understood. The progress in *Rhodococcus* genetics and biochemistry has been limited by

44

the following characteristics of the genus bacteria:

- the high rhodococcal genetic diversity creates obstacles for finding molecular tools generally applicable to *Rhodococcus* genus members [265, 266].

- the recalcitrance of *Rhodococcus* strains cell walls hampers both the nucleic acids extraction and the introduction of exogenous DNA [256];

- the pleomorphism whereby many strains grow as short rods, cocci or branched multinucleated filaments [267, 268] can lead to problems in the segregation of mutants [256];

- the genomic instability may create problems with illegitimate integration upon electroporation of *Rhodococcus* cells with exogenous DNA [256];

- the high GC content genome creates problem in PCR amplification and DNA-DNA/ RNA-DNA hybridization techniques;

- the presence of effective endogenous restriction systems that recognize unmethylated sites in exogenous DNA can causing the cleavage and the subsequent degradation of the newly introduced DNA with the consequence of low 'fertility' of some *Rhodococcus* strains in intergenic matings and/or transformation [269, 270];

- the peculiar genetical codon usage by which the start codon of gene translation is often a GTG triplet instead of the typical ATG triplet and by which stop and start codons of consecutive genes clustered in operons often overlaps. These genetic aspects can hamper the heterologous expression of rhodococcal proteins in *E.coli* or *Pseudomonas* strains that are the typical host for protein functional experiments because of the broad knowledge about their protein expression mechanisms and the significant amount of expression vectors that exist for these genera.

Because of these limitations, despite the importance that many potentially valuable *Rhodococcus* strains would have to be well characterized, the genetic analysis of *Rhodococcus* has for long time hindered by the lack of efficient molecular tools [271]. During

the last decade, the following efforts have been directed towards the development of genetics strategies for the manipulation of *Rhodococcus* members: the construction of *E.coli-Rhodococcus* shuttle vectors [272-274], the development of transposome systems to create random transposon libraries [271, 275, 276] and unmarked mutagenesis deletion systems with SacB as counter selection to generate mutants as result of two consecutive DNA single cross-over events [277-279]. Additionally, the following approaches have been recently applied in *Rhodococcus* strains: transcriptomic and proteomic techniques [280-282], analyses of regulator-operator interactions [283, 284], studies of transcription using reporters [284-287], development of systems for the overexpression of genes involved in key catabolic pathways and enzymes [288-291]. Lastly, the first complete *Rhodococcus* genome sequences have come available, revealing very large genome sizes, partly owing to the presence of (multiple) large (linear) plasmids. The three *Rhodococcus* strains whose genomes have recently become available on database are *Rhodococcus jostii* RHA1 [257], *Rhodococcus opacus* B-4 [292] and *Rhodococcus erythropolis* PR4 [293] while the genome project on *Rhodococcus erythropolis* SK121 [294] is still in process. The analysis of these genome sequences will undoubtedly improve insights in the basis of rhodococcal catabolic complexity and diversity, and genomic organization.

In conclusion, further efforts to improve *Rhodococcus* genomic knowledge and to develop new and more efficient tools for genetic engineering of this genus are needed to significantly advance the genetic analysis of *Rhodococcus* strains. Breakthroughs in *Rhodococcus* genetics and molecular biology will support attempts to construct *Rhodococcus* strains with suitable properties for environmental and biotechnological applications [264].

1.4.1 Alkane metabolism in *Rhodococcus* strains

Thanks to their ability to degrade a wide range of organic compounds [256], their hydrophobic cell surfaces, their production of biosurfactants, and their ubiquity and

46

robustness in the environment [295], *Rhodococcus* along with other closely related high-GC, mycolic acid-containing actinomycetes, (*Mycobacterium*, *Corynebacterium*, *Gordona*, and *Nocardia*) are increasingly recognized as ideal candidates for the biodegradation of hydrocarbons and for the biocatalysis finalized to produce fine chemicals and pharmaceuticals by using their alkane hydroxylase systems [223, 296, 297].

Several *Rhodococcus* strains have been isolated from oil-contaminated sites and they have been studied for the ability to grow on aliphatic, aromatic and branched hydrocarbons. The wide variety amongst *Rhodococcus* genus members can be observed in the different ability of *Rhodococcus* strains to grow and metabolize a broad range of aliphatic hydrocarbons.

To date, the metabolism and the genetics associated with the *Rhodococcus* ability to grow on short-, medium- and long-chain *n*-alkanes [295, 298, 299] have been mostly described in the literature for the following purposes:

- identification of alkanes bio-degradative genes of *Rhodococcus* strains in microbial communities from contaminated soil in different geographical areas such as deep sea environments [300-302] or arctic soils [187, 303];

- study of kinetic parameters and efficiency of the hydrocarbons degradation or xenobiotic cometabolism by *Rhodococcus* spp. [304, 305];

- analysis of changes in hydrophobicity of *Rhodococcus* membranes or biosurfactants production after the exposure to hydrocarbons [299, 306-308];

- study of metabolic pathway of *n*-hexane degrading- and propane degrading-*Rhodococcus* strains [55, 309, 310].

On the contrary, few reports have been described hydroxylase genes involved in the *n*-alkane metabolism in *Rhodococcus* at a molecular level. To date, the alkane hydroxylases system genetically described in *Rhodococcus* species are:

- *alkB* genes of *Rhodococcus* strains NRRL B-16531 and Q15 [297]. Four alkane monooxygenase systems (*alkB1*, *alkB2*, *alkB3* and *alkB4*) were found in two closely related *Rhodococcus* spp. that showed low DNA sequence identity to the alkane monooxygenase genes of most of the known Gram-negative bacteria. The organization of both *alkB1* and *alkB2* gene clusters was head-to-tail in an operon-like structure, and several ORFs had overlapping stop and start codons, suggesting the translational coupling of the correspondent proteins. These rhodococcal *alkB1* gene clusters were the first bacterial alkane hydroxylase gene clusters identified mapping all three the components of an alkane hydroxylase system (alkane hydroxylase, rubredoxin and rubredoxin reductase) in a single operon-like structure. Both the *alkB1* and *alkB2* gene clusters encoded two rubredoxins but, similarly to *alkBFGHJKL* operon in *P. putida* GPo1, only the second rubredoxins (RubA2 and RubA4; Fig. 1.17) in each *alkB* gene cluster was the functional electron transfer component. Since *alkB3* and *alkB4* genes did not show physical association with any rubredoxin or rubredoxin reductase genes, it was supposed that the rubredoxins and rubredoxin reductase encoded in the *alkB1* and *alkB2* gene clusters could also serve as electron transfer components for AlkB3 and AlkB4. Interestingly, two putative TetR-type transcription regulation genes were found in the cloned *alkB1* and *alkB2* gene regions, similarly to other actinomycetes regions including *alkB* genes (*alkU1* in Fig. 1.17). As this type of transcriptional regulator did not resemble previously identified *alk* gene regulatory proteins, it was speculated that this might constitute a new class of regulatory proteins involved in alkane degradation. Furthermore, unlike the *Ps.* GPo1 *alkB* system, neither of the *alkB1* or *alkB2* gene clusters contained alcohol dehydrogenase or aldehyde dehydrogenase genes.
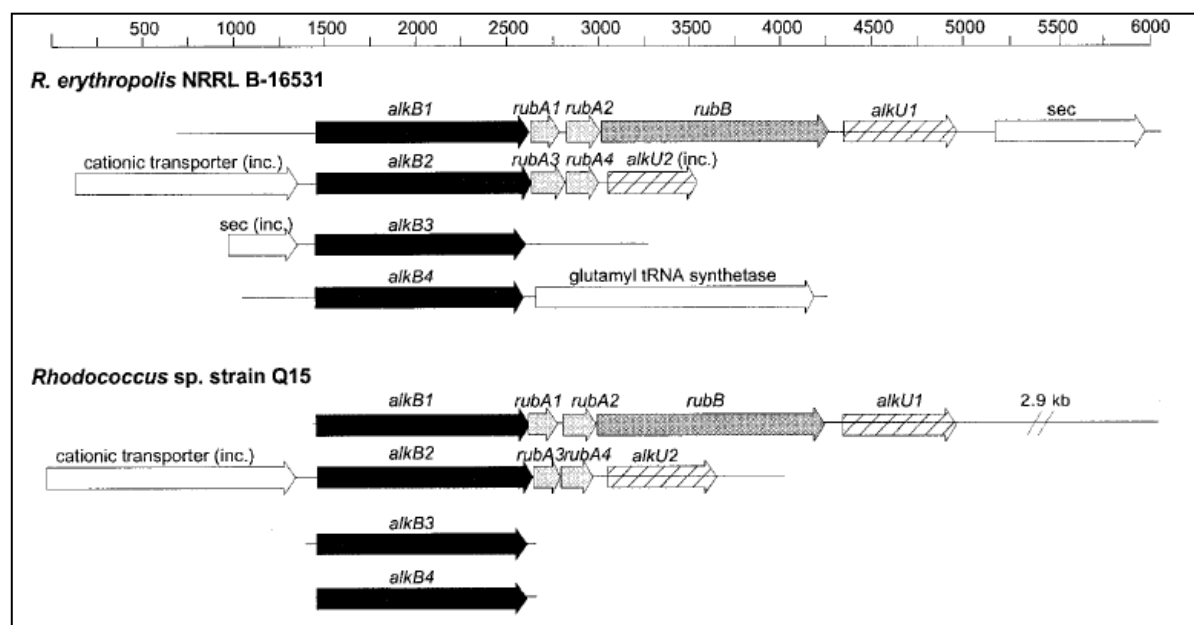
Figure 1.17 Cloned *alk* gene fragments from *Rhodococcus* strains NRRLB-16531 and Q15. Similar shading patterns of the arrows represent similar functions. The directions of the arrows indicate the directions of transcription. inc.=incomplete ORF [297].

- *alkB* genes of *Rhodococcus opacus* B-4; two *alkB* genes, *alkB1* and *alkB2*, were cloned and sequenced from the genomic DNA of *R. opacus* B-4, subsequently, they have been heterologously expressed in *E .coli* and their *n*-alkane inducing expression was studied in organic solvent. For this purpose, the promoters of both the *alkB* genes were cloned upstream of a green fluorescent protein (GFP) reporter gene and the GFP fluorescence production was followed after exposing the cells to different chain length hydrocarbons. As results, only *alkB1* gene expression seemed to be induced by the growth on *n*-alkanes and its expression level was also good in anhydrous solvent. This result is considered to have practical significance for the development of new bioconversion processes using water-immiscible chemicals [311].

- *alkB* genes in *Rhodococcus* sp. strain TMP2; five *alkB* gene homologues were found in TMP2 which showed the closest homologies to the corresponding *alkB* genes of *R. erythropolis* NRRL B-16531 and Q15, only the *alkB5* gene was a novel member. RT-PCR analysis was used to compare the transcript levels of these *alkB* genes during the incubation

49

with *n*-alkanes. The results indicated that *alkB3–5* genes were expressed constitutively, while only the expression of *alkB1* and *alkB2* was induced by the presence of *n*-alkanes. Interestingly, both the genes were also induced by the branched alkane pristine [312].

- *prm* genes of *Rhodococcus jostii* RHA1; the *prm* genes have been detailed described in § 3.4.2.2.. They were reported to be induced by the presence of propane and had great similarity in sequence and organization with those expressed by *Gordonia* sp. TY-5 [65].

As described before, *n*-alkane-degrading cytochromes P450 (CYP153) have been identified in *Rhodococcus* spp. by Van Beilen *et al.* [208]; however, they have not been further described.

In conclusion, despite the well described ability of degradation and adaptation of *Rhodococcus* spp. to oil-contaminated environments, the genes and proteins involved in alkanes degradation are still poorly described at genetic level. Further molecular characterization of hydroxylase genes in these strains will expand the understanding on the mechanisms that control the expression of the alkane-degrading systems, establishing environmental and nutritional parameters to be supplied in bioremediation of biocatalysis processes.

1.4.2 *Rhodoccus* sp. BCP1

As a result of the collaborative work between the laboratory of General Microbiology (Dept of Biology, University of Bologna) and the Environmental Engineering Lab (Dept of Chemical Engineering, Mining and Environmental Technologies (DICMA), University of Bologna), a *Rhodococcus* strain was isolated as the prevailing microorganism of a *n*-butane-grown biomass that showed the ability to carry out aerobic cometabolic degradation of chloroform (CF). The cometabolic process was monitored for 250 days in batch slurry reactors. When some of the reactors, that showed less efficiency in CF degradation, were bioaugmented with this new *Rhodococcus* strain, the CF depletion rates dramatically

50

increased and degradation lag-time was shortend. These results suggested the key role played by *Rhodococcus* strain in the butane-chloroform cometabolism [313].

The *Rhodococcus* strain 16S rRNA was sequenced and the phylogenetic relationship of this new species was assessed based on the comparison of its 16SrDNA sequence with the 'near-full-length' 16S rRNA sequences (≥1200 bases) annotated in the Rybosomal Data Project (http://rdp.cme.msu.edu; [314]). Neighbour-joining tree was constructed using Geneious pro 4.7.6 software [315].
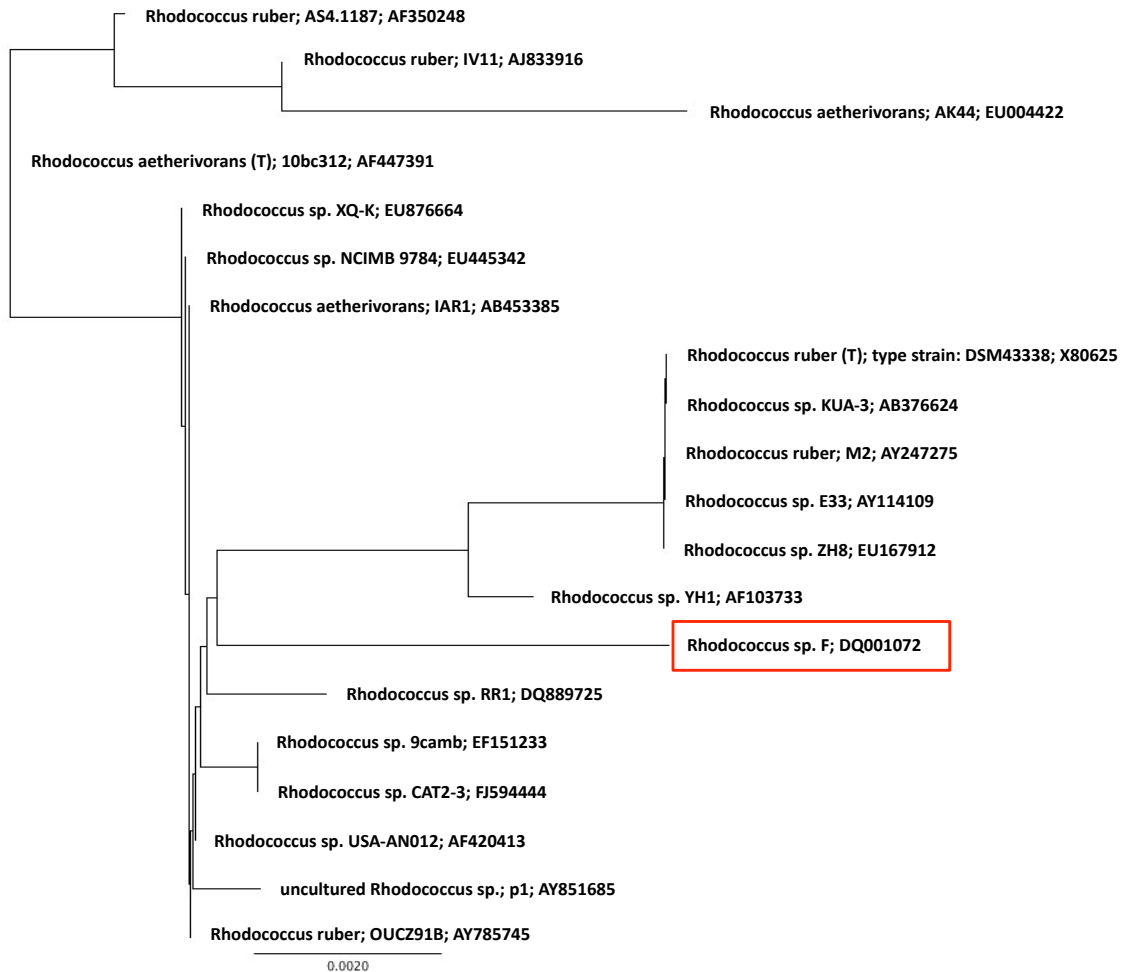
Figure 1.18 Phylogenetic analysis of strain BCP1 and related species by the Neighbor Joining method based on 16S rRNA gene sequences. The scale bars represent 0.002 substitutions/site. The accession numbers are indicated.

This *Rhodococcus* resulted to be closely related to *Rh. aetherovorans* and *Rh. ruber* species and it was named *Rhodococcus* sp. BCP1 (GenBank Accession No. DQ001072).

Further degradation experiments were conducted using pure cultures of BCP1 biomass in resting cells. Namely, the cells were grown in *n*-butane and, then, they were exposed to different concentrations of short-chain halogenated hydrocarbons, omitting *n*-butane to the media, in order to calculate the kinetic parameters relative to degradation processes conducted by BCP1 cells. The results showed BCP1 being able to degrade chloroform concentrations up to 119 mM (14.2 mg l^{-1}) (Fig. 1.19) without any sign of substrate toxicity. BCP1 also proved to be able to transform VC and 1,1,2-TCEA with rates comparable to those reported in literature. However, it couldn't degrade 1,2-trans-dichloroethylene (t-DCEY).
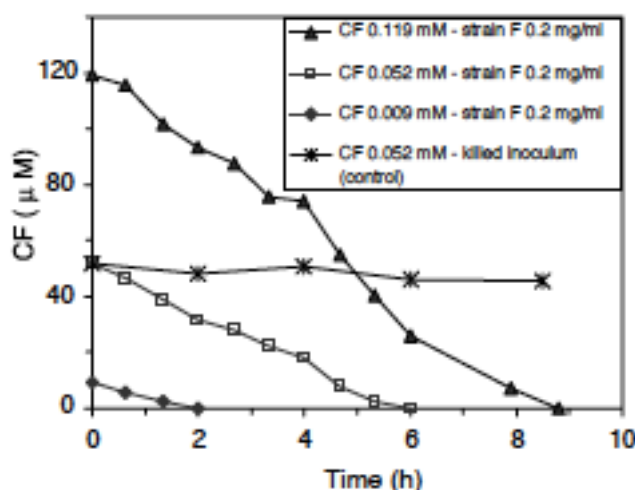
Figure 1.19 Chlorofom depletion by resting cells of butane-grown strain BCP1

The chlorofom degradation data were interpreted by means of a model called 'cometabolism with competitive inhibition' [304], which was indicated by several authors as the most appropriate model for the aerobic cometabolism of chlorinated solvents [13, 316, 317]. The competitive inhibition model postulates the concurrent transformation of the two substrates *n*-butane and chloroform. Namely, when both butane, as primary substrate, and chloroform, the cometabolic substrate, are added to the bioreactors at the same time, the

degradation of the contaminant is retarded due to the physical competition of the two compounds for the active site of the enzymes involved in the degradation. The depletion of the cometabolic substrates starts when the primary substrates decreases to below determined threshold [304].

Subsequently, since most of the cometabolic degradation of halogenated compounds activated by *n*-alkanes were mediated by monooxygenase activity, biochemical assays were performed using both the inhibitor of copper-containing monooxygenases, the allylthiourea (ATU), and the general inactivator of monooxygenases, the acetylene. Only the acetylene pre-incubated BCP1 biomass showed the loss of ability to use butane as growth substrate, while the ATU incubation did not affect the degradation. Similarly, chlorofom degradation ability was lost after the exposure of butane-grown biomass to acetylene, but not after the exposure to ATU. These results suggested that the chloroform transformation and the butane degradation were both dependent on a monooxygenase activity [304]. Moreover, since only a low inhibition of both butane utilization and chloroform degradation were observed in the presence of allylthiourea (ATU), the butane-monooxygenase of BCP1 was suggested not to contain copper as catalytic cofactor. Consequently, a Fe-containing alkane monooxygenase was considered to be probably involved in the *n*-butane and CF metabolisms. This alkane monooxygenase will be identified and molecularly described in this present Thesis work.

Chapter 2 - General Materials and Methods

2.1 Bacterial strains, media and growth conditions

Table 2.1. Bacterial strains, plasmids and primers for general purposes.

Bacterial strains	Relevant genotype or characteristics	Reference
Escherichia coli DH5α	*supE*44 *hsdR*17 *recA*1 *endA*1 *gyrA*96 *thi*-1 *relA*1	[318]
Escherichia coli LE392	*supF supE hsdR galK trpR metB lacY tonA*	[319]
Rhodococcus sp. BCP1	Ability to grow on *n*-alkanes and co-metabolize low chlorinated solvents	[304]
Rhodococcus sp. BCP1 pTP$_{alkB}$LacZ	Derived from *Rhodococcus* sp. BCP1. Contains the promoter probe vector plasmid pTipP$_{alkB}$LacZ described below	This work

Plasmids	Relevant genotype or characteristics	Reference
pUC18	Amp^r, cloning vector	[320]
pLFR5	Tc^r, conjugative plasmid and cosmid vector	[321]
pTipQT2	Amp^r (*E.coli*) Tc^r (*Rhodococcus*), *PtipA repAB* (pRE2895)	[322]
pTipP$_{alkB}$LacZ	Derived from pTipQT2. Promoter probe vector containing *PalkB-alkB* (117 bp)-*lacZ* (3000 bp) in the MCS	This work

Primers	Sequence (5'-3')	Reference
M13 For	CGCCAGGGTTTTCCCAGTCACGAC	Sigma
M13 Rev	TCACACAGGAAACAGCTATGAC	Sigma

Liquid cultures of all bacterial strains were grown in agitation at 150 rpm at the optimum temperature (i.e. *E. coli* at 37 °C while *Rhodococcus* sp. BCP1 at 30 °C). The compositions of the media used in this study are reported in Table 2.2.

Table 2.2 Composition of media

Complex media		
Luria-Bertani Broth (LB)	Tryptone	10 gr/L
(pH 7)	Yeast Extract	5 gr/L
	NaCl	10 gr/L
	H_2O	to volume
Tryptic Soy Broth (TSB)	Pancreatic Digest of Casein	17 gr/L
(pH 7.2)	Enzymatic Digest of Soybean Meal	3 gr/L
	NaCl	5 gr/L
	Dipotassium Phosphate	2.5 gr/L
	Dextrose	2.5 gr/L
	H_2O	to volume
MB 3.5% Glycine	Yeast extract	5 gr/L
(pH 7.2)	Bacto tryptone	15 gr/L
	Bacto soytone	5 gr/L
	NaCl	5 gr/L
	Glycine	35 gr/L
Defined media		
Minimal medium (MM)	MM (pH 7.2) (100X) – in BD water	
(pH 7.2)	K_2HPO_4	155 gr/L
	$NaH_2PO_4 \bullet H_2O$	73.9 gr/L
	$(NH_4)_2SO_4$	10.52 gr/L
	$NaNO_3$	76.5 gr/L
	$MgSO_4$ stock solution (1000X) – in BD water	
	$MgSO_4 \bullet 7H_2O$	60.2 gr/L
	$CaCl_2$ stock solution (1000X) – in BD water	
	$CaCl_2$	14.7 gr/L
	Microelements stock solution (1000X) – in BD water	

Table 2. *Continued*	$FeSO_4•7H_2O$	6.283 gr/L
	$MnCl_2•4H_2O$	0.3 gr/L
	$ZnSO_4•7H_2O$	0.147 gr/L
	H_3BO_3	0.061 gr/L
	$Na_2MoO_4•H_2O$	0.109 gr/L
	$NiCl_2•2H_2O$	0.024 gr/L
	$CuCl_2•2H_2O$	0.017 gr/L
	$CoCl_2•6H_2O$	0.024 gr/L
	Yeast extract stock solution (10000X) – in BD water	
	Yeast extract	5gr/L

The stock solutions were prepared and separately autoclaved. Only the MM solution was diluted every time to a final concentration of 1X and, after adjusting the pH, it was autoclaved at 121ºC for 20 minutes. Subsequently, the 1X MM solution was mixed with volumes of stock solutions of $MgSO_4$, $CaCl_2$, Microelements and Yeast extract in order to have a final concentration of 1X.

For growth on solid media, agar was added at the final concentration of 15 g/l. Antibiotic stock solutions were prepared as reported in Table 2.3. The solutions were stored at -20 °C in 1 ml aliquots until use.

Table 2.3. Antibiotic solutions and concentrations used for selective growth

Antibiotic stock solution	Concentration	
	E.coli	*Rhodococcus*
Ampicillin, 50 mg/ml, water solution,	50 µg/ml	-
Kanamycin, 50 mg/ml, water solution,	25 µg/ml	-
Tetracycline, 20 mg/ml, 70 % ethanol in water	20 µg/ml	10 or 5 µg/ml

2.2 Extraction of genomic DNA from *Rhodococcus* sp. BCP1

The genomic DNA was isolated from BCP1 cells using the protocol here described. A

100 mL culture grown on LB media to an OD_{600}=1.0 was centrifuged at 7000 rpm at 4°C for 10 minutes and washed with 1 mL of phosphate buffer (10mM, pH=7.2). The cell pellet was resuspended in 800 μL of acetone before being treated in a potter homogenizer for 30 minutes. After harvesting and washing the acetone-homogenized cells, they were resuspended in 800 μL of TE (20 mM Tris, 10 mM EDTA pH 8.0) containing lysozyme at the concentration of 30 mg/mL. Before being incubated 1 hour at 37°C, mutanolysin (final concentration of 100U/mL) and proteinase K (final concentration of 1mg/mL) were also added to the solution. At the end of the incubation, 150 μL of a 10% SDS solution were added and the suspension was mixed and incubated in a water bath at 65°C for 5 min. The solution was, then, transferred in a 2-mL microcentrifuge tube containing 0.5 mL of nitric acid pre-washed quartz beads (0.2-0.8 mm-diameter, MERCK KGaA, Germany) and the cells were broken by vigorous agitation for a total of 120 s (beat three times for 40 s with 1-min interval). The homogenized suspension was centrifuged at 13000 rpm for 5 min at 4 °C, and the aqueous phase above the beads was collected. One volume of a phenol-chloroformisoamyl alcohol 25:24:1 v/v mixture was added and the sample was vortexed for 30 seconds. The water phase containing the genomic DNA was separated from the organic phase and cell debris by centrifugation at 13000 rpm at 4 °C for 5 minutes. The extraction was repeated twice and phenol traces were removed by adding 1 volume of a 24:1 v/v mixture of chloroform-isoamyl alcohol. The aqueous phase was recovered after centrifugation at 13000rpm at 4°C for 5 minutes and 0.1 volumes of 3 M sodium acetate (pH 4.8) and 0.7 volumes of isopropanol were added. Extracts were incubated for 10 min at room temperature and then they were centrifuged for 30 min at 4°C at 13000 rpm. The DNA pellet was washed with ice-cold EtOH 70% and finally it was dried out. The resuspended genomic DNA was stored at -20°C and the aliquot to use in each experiment was previously treated with RNase at 37°C for 30 minutes.

2.3 RNA isolation from *Rhodococcus* sp. BCP1

2.3.1 Exposition to the substrates

The total RNA was extracted from 100 mL of late exponential phase (OD_{600}=0.6-0.7) cultures of *Rhodococcus* sp. BCP1 grown at 30°C on minimal medium (MM) enriched with yeast extract, caseo amnoacids, peptone (0,5 gr/L each) and succinate 1% (w/v). The cells were, subsequently, harvested by centrifugation at 7000 rpm for 10 min at 4ºC and washed with phosphate buffer (10mM; pH 7.2). The pellet, obtained from each 100 mL of initial culture, was resuspended in 30 mL of MM and divided into two 119-mL bottles that were subsequently sealed with rubber stoppers. After the substrate/s to be analysed were added to each pair of bottles, the cultures were incubated for 4 hours on minimal medium (MM) at 30°C under shaken at 150 rpm. After the incubation, 0.125 volumes of ice-cold EtOH/Phenol stop solution (5 % water-saturated phenol (pH<7.0) in ethanol) were added to each bottle kept on ice to stop the degradation of the mRNA. The cells were then harvested and one pellet from each bottle was finally frozen at -80°C for storage and later use.

2.3.2 RNA isolation procedure

The protocol for the RNA isolation was based on the 'Protocol for the isolation of total RNA from *E. coli* for microarray with several modifications. Moreover all steps were performed swiftly to minimise RNA degradation and RNase free or DEPC treated solutions, RNase free microfuge tubes and RNase free filter pipette tips were used. (http://derisilab.ucsf.edu/data/microarray/pdfs/Total_RNA_from_Ecoli.pdf)

Each frozen pellet was thawed on ice and then treated with acetone homogenization, enzymatic and mechanical lysis, as described for the genomic DNA extraction (§ 2.2). After the beads disruption step, the surnatants from the two samples deriving from the same treatment were collected together in one 2 mL-tube. 100 μL of 3M NaOAc, pH 5.2 was added and after the solution was mixed by inversion, an equal volume (around 1 mL) of water-

saturated phenol (pH<7.0) was also added. The sample was inverted 10 times and incubated at 65ºC for 6 min with inversions every 40 seconds. Subsequently, the solution was spinned at 14000 rpm for 10 min at 4ºC and the aqueous layer was collected to a fresh 2 mL-tube containing an equal volume of chloroform. After inversion of the sample, it was spinned at 14000 rpm for 5 minutes at 4ºC. The aqueous layer was divided into two 1.5 mL microfuge tubes and 1/10 of 3M NaOAc pH 5.2 and 2 volumes of cold 100% EtOH were added. The samples were incubated at -80ºC over night and the day after they were centrifuged at 14000 for 30 minutes at 4ºC. The pellets were then washed with 1 mL of 80% cold ethanol solution and they were air dried for 10 minutes under the fume hood.

The total RNA was treated twice with 5U of RNase-free DNase (QIAGEN) for 30 min at 30°C and then cleaned using the RNeasy kit (QIAGEN) before being used for primer extension and RT-PCR experiments.

2.4 DNA manipulations and genetic techniques

All restriction digests, ligations, cloning and DNA electrophoresis, were performed using standard techniques [320]. Taq polymerase, the Klenow fragment of DNA polymerase, restriction endonucleases and T4 DNA ligase were used as specified by the vendors (Roche or Promega, Milan, Italy). The plasmid pUC18 was routinely used the cloning vector and recombinant plasmids were introduced into *E. coli* DH5α by transformation of chemically competent cells, prepared according to the CaCl$_2$ method [320].

To detect the presence of insert DNA, X-Gal was added to agar media at a final concentration of 40 µg/ml. X-Gal stock solutions were prepared at a final concentration of 40 mg/ml in N-N-dimethylformamide and stored as 1 ml aliquots at - 20 °C protected from light. Kits for plasmid mini- and midi-preps, PCR purification and DNA gel extraction were obtained from QIAGEN (Milan, Italy) and used according to the manufacturer's instructions.

2.5 Southern blot analysis

Southern blot analyses were performed according to standard procedures [320]. Approximately 1 µg of digested genomic DNA or 500 ng of digested plasmid DNA were run on 1 % agarose gels and transferred onto nylon membrane (HybondTM-N+, GE Healthcare). Hybridization was carried out overnight with radioactive-labelled probes at 65 °C. Hybridization solution for Southern blot assays contained 10 mg/ml blocking reagent (Boehringer), 0.1 % SDS, SSC 5X (added from 20X SSC stock solution: 3 M NaCl, 0.3 M sodium citrate). For labelling reactions, approximately 100 ng of probe DNA were labelled with 5 µl of [α-^{32}P]dCTP (50 µCi) (GE Healthcare, Milan, Italy) using the Ready-To-Go^{TM} DNA Labelling Beads kit (GE Healthcare, Milan, Italy) according to the manufacturer's instructions.

2.6 DNA sequencing and sequence analysis

Genomic DNA fragments of interest were cloned in the pUC18 cloning vector and positive plasmids were sent for sequencing to the BMR-genomics service of the University of Padova (Padova, Italy). Samples were prepared according to the recommended procedures (www.bmr-genomics.it). M13 Forward and Reverse primers (Table 2.1) were used for sequencing the extremities of DNA fragments cloned into the pUC18 vector from the M13 promoter. Sequence identities were determined by DNA homology searches using the BLAST program to search both NCBI and TIGR databases.

2.7 Construction of Rhodococcus sp. BCP1 genomic library

The construction of a representative genomic library of *Rh*. sp. BCP1 was carried out with the Packagene® Lambda DNA Packaging System (Promega) according to the manufacturer's instructions and using the plasmid pLFR5 as a lambda vector (Table 2.1). *E. coli* LE392 was used as the host strain (Table 2.1). BCP1 genomic DNA was partially

digested with *Sau3AI* restriction endonuclease and then fractionated by a 40 % - 10 % sucrose gradient centrifugation procedure. DNA fragments that were ~ 30 kb long were purified by adding 2.5 volumes of ethanol and incubating at – 20 °C overnight to facilitate DNA precipitation. DNA fragments were washed twice with 70 % ethanol, dried and then cloned in the pLFR5 *BamHI* site. Cosmid packaging was carried out with the Packagene® Lambda DNA Packaging System (Promega) according to the manufacturer's instructions. Library clones were selected on LB plates containing tetracycline (10 μg/ml). Cosmids containing DNA sequences of interest were extracted using the Midi-prep kit (QIAGEN).

2.8 Electroporation of *Rhodococcus* sp. BCP1 (based on [323])

DAY 1

A 10-mL culture of *Rhodococcus* sp. BCP1 was inoculated in TSB.

DAY 2

1 mL of the overnight culture of *Rh*. BCP1 was transferred to 100 mL MB 3.5% Glycine supplemented with 1.8% sucrose and 0.01% isonicotic acid hydrazide (isoniazid) in a 500-mL flask. The culture was then incubated overnight at 30ºC with shaking (200 rpm).

DAY 3

When the OD_{600} was approximately 0.4-0.5 (after around 17 hours) sterile lysozyme solution was added to a final concentration of 0.5 mg/mL to the culture that was incubating for 1.5 hours at 30ºC with shaking. Subsequently, the cells were collected by centrifugation for 10 minutes at 6000 rpm at 4ºC. The cells were then washed twice with 25 mL ice-cold EPB1 (20 mM Hepes pH 7.2, 5% glycerol) and once with 10 mL ice-cold EPB2 (5mM Hepes pH7.2, 15% glycerol). The cells were harvested by spin at 8000 rpm for 10 minutes at 4ºC and after discarding the surnatant, they were resuspended in 2-3 mL EPB2. 300 μL-aliquots from the suspension were transfered into microcentrifuge tubes on ice and immediately used for the electroporation.

1 μg of DNA of interest was added to the 300μL aliquot to be electroporated. The mix was incubated on ice 5-10 minutes before being transferred in 0.2 cm-cuvettes (Biorad) and being subjected to electroporation with the following parameters: 2.5 kV, 25 μF and 400 Ω. After incubation on ice for 1 minute, 500 μL of TSB was added to each electroporated suspensions that were kept at room temperature until they were transferred into 25 mL-tube and diluted with TSB till a final volume of 5 mL. The cells were then recovered for 5-6 hours under shaking at 200 rpm at 30ºC before being spread onto plates with TSB supplemented with tetracycline (10 μg/mL).

CHAPTER 3. Growth on *n*-alkanes by *Rhodococcus* sp. BCP1: physiology and metabolic analysis

3.1 Introduction

The soil bacterium *Rhodococcus* sp. BCP1 has been described by Frascari *et al.* [304] for its ability to grow on *n*-alkanes ranging from C_2 to C_7 and for co-metabolizing low-chlorinated solvents under aerobic conditions. By contrast, *Rh.* sp. BCP1 could not grow on methane (C_1) as a unique carbon source, a property being restricted to methanotrophs (Chapter 1, §.1.3.4.1).

As described in Chapter 1 § 1.4.2, an iron containing monooxygenase was proposed to be involved in the butane/chloroform cometabolism of *Rhodococcus* sp. BCP1 because of the irreversible inhibition performed by acetylene on the degradation of both butane and chloroform. Monooxygenases bind and activate molecular oxygen catalyzing the insertion of one oxygen atom in the substrate. *n*-Alkanes were reported to be oxidized by alkane monooxygenases to alcohols, the hydroxylation reaction occurring at the terminal position of the *n*-alkane, i.e. the OH group is added to the terminal carbon of the aliphatic carbon chain, or at sub-terminal position, i.e. the OH group is added to a carbon just besides the terminal one. It is generally thought that the alcohol produced by the *n*-alkane oxidation undergoes several oxidation steps before being completely mineralized by entering the fatty acid β-oxidation cycle (Fig.3.1).

Fig 3.1 Putative metabolic pathway of *n*-alkanes under aerobic conditions in microbial cells.
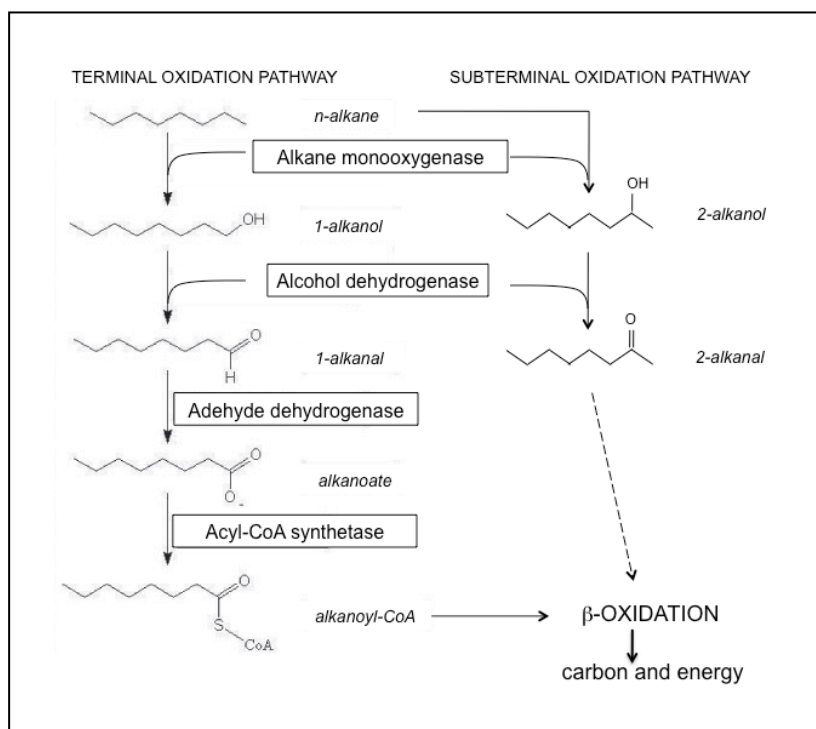
Rhodococcus sp. BCP1 had already been described to grow on most of the putative intermediates of butane and propane degradation pathway shown in Fig. 3.1, such as 1- and 2-propanol, 1- and 2-butanol, *tert*-butanol, propionic acid (propionate), butyric acid (butyrate), valeric acid (valerate), and propanone (acetone) [304].

In the first section of this thesis work, assays were conducted aiming to correlate the ability of *Rhodococcus* sp. BCP1 to grow on short-chain *n*-alkanes through the activity of a (molecular undefined) monooxygenase.

By revealing the oxidation products accumulated by BCP1 resting-cell (non-proliferating) biomass exposed to gaseous hydrocarbon substrates (butane, C_4, and propane, C_3), we aimed to confirm that these *n*-alkanes taken up by the cells were metabolized by oxidation activity. Thus, the type of alcohols produced when gaseous *n*-alkanes are oxidized by BCP1, that would also indicate the details of further degradation steps, were investigated.

Moreover, the respiratory rates of BCP1 cells grown on different substrates were examined through the use of a Clark-type oxygen electrode. To demonstrate that the

expression of the oxidizing enzymes involved in the *n*-alkanes metabolism was inducible, oxygen consumption rates were measured in *n*-butane- (C_4, gaseous alkane), *n*-hexane- (C_6, liquid alkane) and succinate-grown BCP1 exposed to different substrates. Additionally, the oxygen uptake activity induced by growth on gaseous *n*-alkane (butane) was compared with the oxygen consumption response induced on liquid *n*-alkane (*n*-hexane).

Finally, since BCP1 has already been described for its growth on C_2-C_7 *n*-alkanes, we further investigated the BCP1 *n*-alkanes metabolism by performing growth assays of BCP1 on *n*-alkanes having medium- and long-chain aliphatic hydrocarbons.

3.2 Materials and methods

3.2.1 Growth of *Rhodococcus* sp. BCP1 cultures for metabolic assays

Rhodococcus sp. BCP1 biomass to be used in the alcohols production and oxygen uptake activity experiments was developed as follows. Eight 119-mL bottles containing 50 mL of MM were prepared for each substrate. Each bottle was inoculated with 100 mL of a two day grown pre-cultured flask. After the bottles were sealed with butyl rubber stoppers and aluminium crimp seals, the substrates were injected by syringe with the following concentration: *n*-propane (150 mM), *n*-butane (150 mM), *n*-hexane (0.1% v/v) or succinate (1% w/v). The cultures were incubated for 72 hours at 30ºC under shaking at 150 rpm to early stationary phase.

3.2.2 Measurement of cell activities in whole cell experiments and analytical techniques

The accumulation of alcohols was measured in 13.9 mL serum vials capped with butyl rubber stoppers and aluminium crimp seals. The reaction mixture consisted of the substrate (2 mL of butane or propane, added as an overpressure to the headspace), 1 mL of competitor (5 mM), and O_2-saturated phosphate buffer to a total volume of 2 mL. After 30 minutes of equilibration of this reaction mixture at 30ºC, the assay was initiated by the addition of the

66

concentrated cell suspension (500 μL) in each sample vial, while no inoculum was provided in the negative control samples. The vials were shaken at 150 rpm during the reactions. For inactivation assays, the concentrated cell suspensions were added to the reaction mixture after being incubated for 30 minutes at 30°C with constant shaking in sealed 13.9-ml serum vials containing phosphate buffer (1.4 ml) (pH 7.2) and 5% (vol/gas-phase vol) acetylene. Liquid samples (4 μL) were removed after 15, 30, 45 and 60 minutes and the production of the short-chain aliphatic alcohols was determined by gas chromatograph (HP 5890) equipped with a flame ionization detector and a column Supelcowax-10, 30 m with 0.53 mm inner diameter. The gas chromatograph was run at column temperature of 45 ºC for 5 minutes to 200 ºC at 40 ºC/min and detector temperature of 300 ºC. Helium was used as the carrier gas at a flow rate of 15 ml/min. Identities of products were determined by comparison of retention times and peak shapes to those of authentic compounds. Experiments were repeated at least three times.

<u>O_2 consumption</u> of BCP1 cells grown on *n*-butane-, *n*-hexane- and succinate induced by the presence of various compounds was measured with a Clark-style O_2 electrode inserted into a 1.9 mL chamber sealed with a capillary inlet through which additions were made. Clark-electrode reveals the potential variations inside the reaction chamber that are directly proportional to the variation of oxygen concentration in the cell suspension. The depletion of oxygen in the presence of biomass will indirectly measure the bacterial respiration stimulated by the addition of a substrate into the reaction chamber. After the BCP1 biomass was grown in each condition under investigation (see below), it was harvested and washed twice with 25 mM phosphate buffer (pH 7.2) to remove the remaining substrate. The cells were then resuspended in 25 mM phosphate buffer (pH 7.2) and shaked at 30 ºC for five hours to lower the endogenous respiration. For endogenous respiration we intend the oxygen consumption activity present in the cells after the 72-hours growth in the bottles due to the accumulation of metabolites still present in the cells because not completely mineralized yet. The biomass was

diluted with air-saturated buffer in order to have a final OD_{600}=0.04. 1 mL of this suspension was used for protein quantification by method of Lowry [324] using bovine serum albumine (BSA) as a standard. 1.9 mL of cell suspension grown on each substrate was introduced in the electrode chamber where the contents were stirred with a magnetic stir bar. The 1.9 mL cell suspension that had to be exposed to the gases were injected inside 13.9 mL sealed bottles where butane or acetylene were supplied at final concentrations of 150 mM or 5% (v/v), respectively. The reactions were carried out at room temperature (20-22 °C). The liquid substrates were introduced in the electrode chamber at concentration of 0.1% (v/v) by direct addiction with a Hamilton syringe. Oxygen consumption values were determined for BCP1 cells grown on n-butane (150 mM), n-hexane (0.1% v/v), 1-butanol (0.1% v/v), butyric aldehyde (0.1% v/v) and succinate (0.1% v/v) after the addition to the reaction chamber of n-butane, n-hexane, 1-butanol, 2-butanol, butyric aldehyde and butyric acid. The values were corrected for endogenous respiration. In the inhibitory assay, an aliquot of suspension from each condition of growth was incubated with 600 μL (5% v/v) of acetylene for 30 minutes before being introduced in the electrode chamber and being exposed to the substrates. The O_2 consumption rate was measured as notches per minute. The rate has been transformed in nmol of oxygen consumed considering that each notch corresponds to 4.20 nmol of oxygen depleted from the buffer in the chamber. The O_2 consumed nmols were normalized to mg of protein contained in 1.9 mL of cell suspension in each experiment. Every experiment was conducted in triplicate.

3.2.3 Growth assays on medium and long chain n-alkanes

The ability of *Rhodococcus* sp. BCP1 to grow using n-alkanes as only carbon sources was examined in solid and liquid cultures. Solid cultures were prepared by streaking LB-grown BCP1 biomass onto mineral medium (MM) plates supplemented with n-alkanes as following described. The liquid n-alkanes (C_{12}-C_{16}) were added as vapour putting a filter soaked with the

68

n-alkane on the lid of the Petri dish, which was sealed with parafilm. Solid *n*-alkanes were added as a fine powder directly to the MM before solidifying. The powders were produced by grinding solid *n*-alkanes in a mortar. The plates were incubated at 30 ºC.

Liquid cultures of BCP1 were prepared inoculating 100 mL of a two-days grown BCP1 pre-culture in 50 mL MM in Erlenmeyer 250 mL-flasks that were incubated for one week at 30ºC on a rotary shaker at 150 rpm. *n*-Alkanes were added either as final concentration of 0.05% v/v (liquid *n*-alkanes) or as final concentration of 0.1% w/v (solid *n*-alkanes). The growth was measured as dry weight using 0.22μm-filters to collect the biomass in a Millipore filtering device.

3.3 Results

3.3.1 Correlation of a Monooxygenase activity to the ability of *Rhodococcus* sp. BCP1 to grow on short-chain *n*-alkanes hydrocarbons

3.3.1.1 Gaseous *n*-alkanes oxidation in *Rhodococcus* BCP1

To characterize the type of oxidation performed by the monooxygenase involved in the gaseous *n*-alkanes metabolism, we analysed, at first, the surnatant of *n*-butane-grown BCP1 resting cells before and after the exposure to butane. None of the predicted products of either terminal oxidation of butane (1-butanol) or subterminal oxidation (2-butanol) were detected in cultures of *n*-butane-grown *Rhodococcus* sp. BCP1; likewise, neither 1- nor 2-butanol was detected in resting cell suspensions during consumption of butane. These results suggested that the butane oxidation products were very quickly utilized as substrates by the enzymes involved in the downstream metabolic pathway; thus, inhibitors of this latter metabolic steps were required to cause accumulation of butanols to be seen by gaschromatography [128]. For this purpose, exceeding amounts of 1- and 2-propanol as structural analogues of the butane oxidation products were used and the production of butanols was examined at different times by gas chromatography using a column which was specific for short-chain alcohols (§ 3.2.2).

When 5 mM of 1-propanol and 162 μM of *n*-butane were both added to a suspension of butane-grown *Rhodococcus* BCP1 cells (1.5 mg cell protein) in a 13,9 ml vial, 1-butanol (retention time 6.4 minutes) was detected as the product of butane oxidation after 15 minutes of butane incubation. The greatest amount of 1-butanol produced was revealed after 30 minutes and, then, it decreased in the spectra collected at 45 and 60 minutes, (Fig. 3.2), most likely because the inhibition exerted by 1-propanol on the alcohol dehydrogenases involved in the downstream oxidation steps was not sufficiently efficient. The decrease of the 1-propanol peak (retention time: 3.2 minutes) in the time course of the experiment confirms the catalytic activity of these enzymes causing the depletion of the competitor over time. In the negative control (sample supplied with with *n*-butane and 1-propanol with no biomass present) no signal corresponding to 1-butanol was revealed (Fig 3.2).
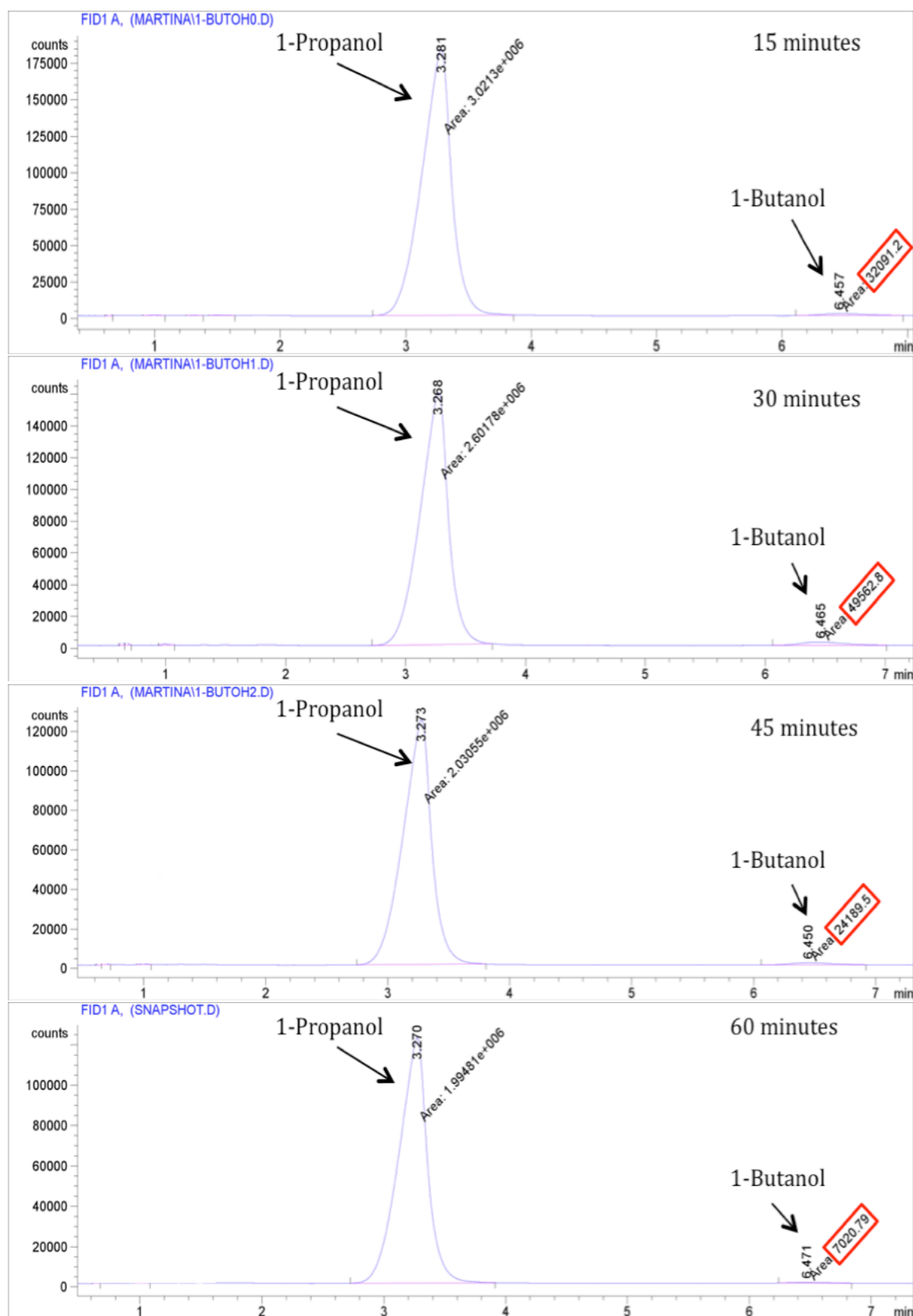
Figure 3.2. - Gas chromatographic spectra collected after different incubation times (15, 30 45 and 60 minutes) with butane, showing the production of 1-butanol. 1-Propanol is used in excess as competitor of the 1-butanol metabolic pathway. The peaks identities are indicated by arrows.

To prove that the transformation of butane into 1-butanol was due to the activity of a monooxygenase, in a subsequent experiment, the butane-grown BCP1 biomass was pre-treated with acetylene (5% v/v, 30 minutes), previously described as inhibitor of this type of enzyme [128]. After this exposure, the BCP1 biomass was incubated in the presence of *n*-butane and an excess of 1-propanol. As shown in Fig. 3.3, acetylene resulted to inhibit the production of 1-butanol detected after 30 minutes. By comparing the area of the butanol peak in experiments in the presence or absence of acetylene, the inhibition exerted by acetylene on *n*-butane oxidation was shown to decrease more than 50% of the amount of butanol produced.
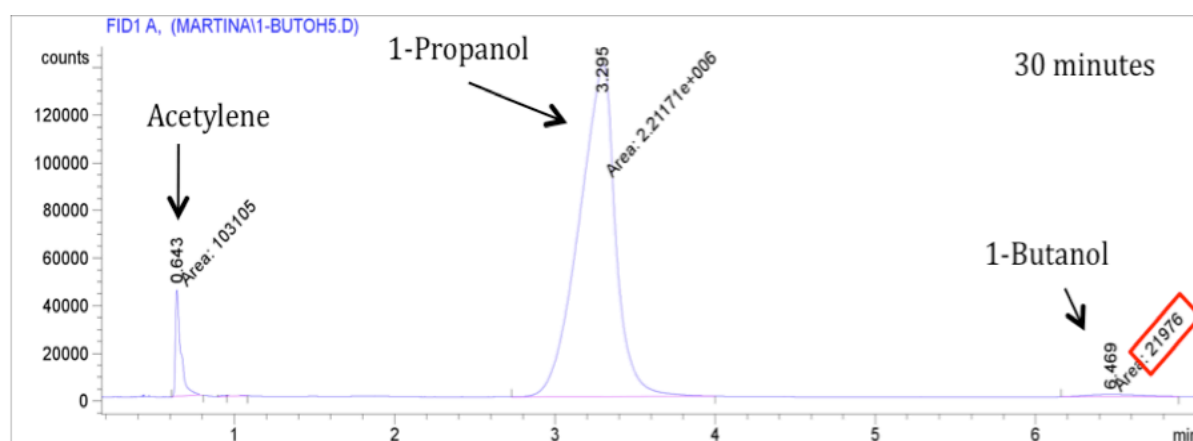
Figure 3.3. - Gas chromatographic spectrum collected after 30 minutes of incubation with butane of BCP1 biomass pre-treated with acetylene (5% v/v) in the presence of 1-propanol as competitor. The peaks identities are indicated by arrows.

To determine whether or not butane undergoes the sub-terminal oxidation pathway in BCP1 cells, 2-propanol was used as structural analogue and competitor for detecting 2-butanol production. When 5 mM of 2-propanol were added to butane-grown biomass there was no evident 2-butanol production (retention time: 2.45 minutes) for all the time course of the experiment (Fig 3.4).
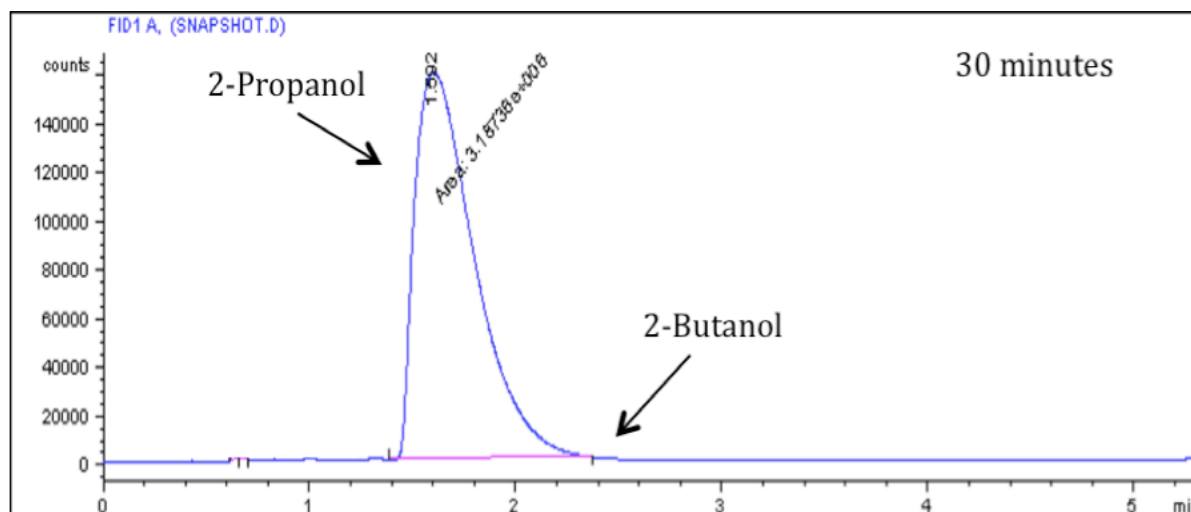
Figure 3.4 - Gas chromatographic spectrum collected after 30 minutes of exposition of the BCP1 biomass to butane in the presence of 2-propanol as competitor. The peaks identities are indicated by arrows.

Subsequently, 1- and 2-butanol were used aiming to reveal propane oxidation products metabolism. Propane-grown resting cells were exposed to 162 μM of *n*-propane in the presence of 5mM of 1- or 2-butanol as competitors. After 15 minutes, a peak corresponding to 1-propanol was detectable when BCP1 cells were exposed to both *n*-propane and 1-butanol (Fig. 3.5).
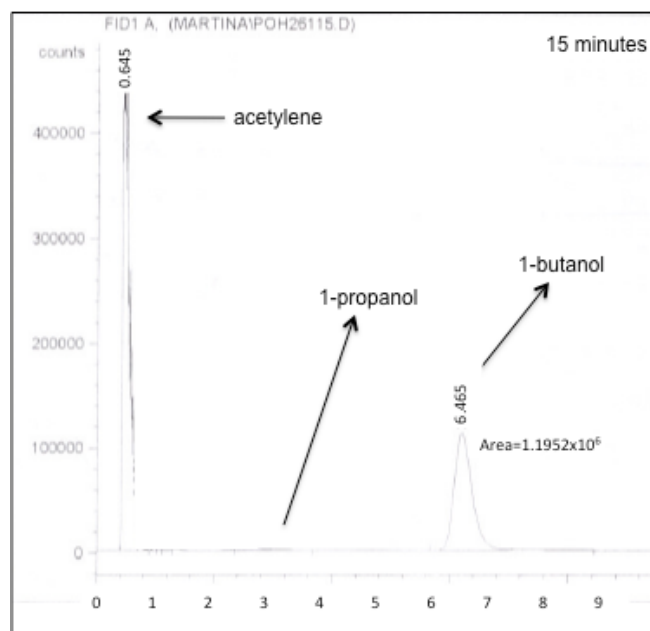
Figure 3.5 Gas chromatographic spectrum collected after 15 minutes of exposition of the BCP1 biomass to propane in the presence of 1-butanol as competitor. The peaks identities are indicated by arrows.

This latter result confirmed that a terminal oxidation process was involved in the gaseous *n*-alkanes metabolism as already revealed in the experiment to detect the butane oxidation products. The subsequent experiment, using acetylene pre-treated BCP1 cells, did not show 1-propanol production confirming the involvement of a monooxygenase in the first oxidizing step of short-chain gaseous *n*-alkanes (Fig. 3.6).
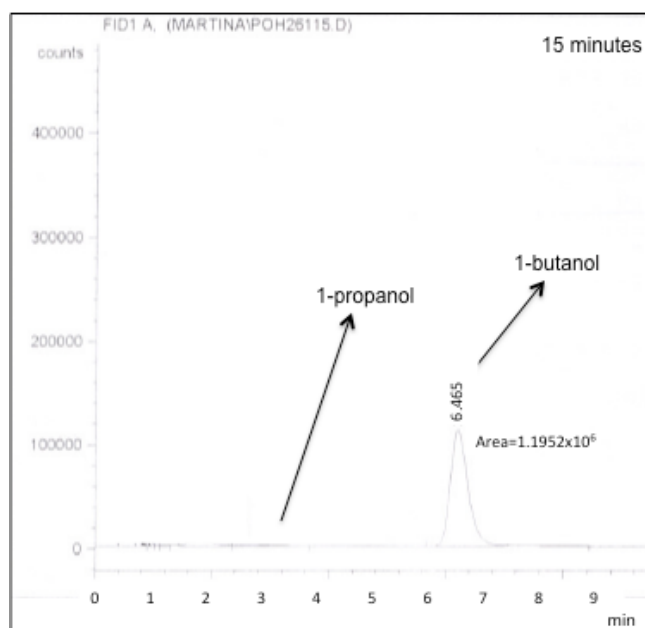
Figure 3.6 Gas chromatographic spectrum collected after 15 minutes of exposition of the acetylene pre-treated BCP1 biomass to propane in the presence of 1-butanol as competitor. The peaks identities are indicated by arrows.

Interestingly, in the presence of 2-butanol as competitor, a small peak corresponding to 2-propanol was detected after 15 minutes of exposure to *n*-propane, as shown in Fig. 3.7. This result indicates that at least a small fraction of propane undergoes a sub-terminal oxidation process.
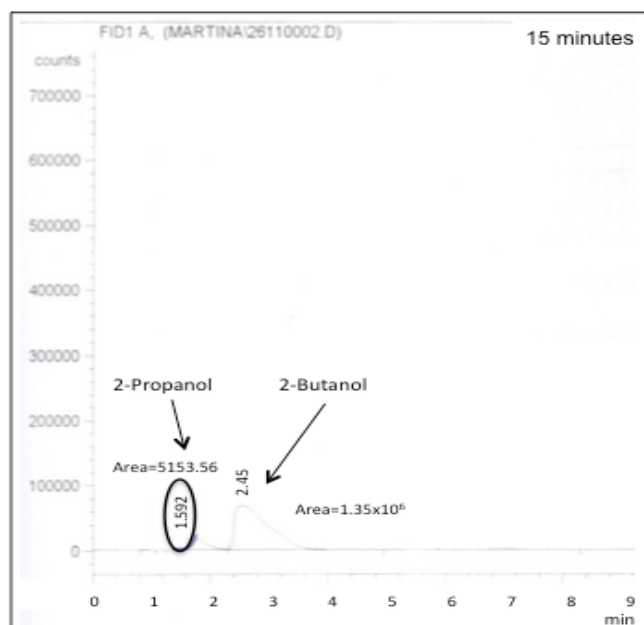
Figure 3.7 Gas chromatography spectrum collected after 15 minutes of exposition of the BCP1 biomass to propane in the presence of 2-butanol as competitor. The peaks identities are indicated by arrows.

3.3.1.2 Substrate-dependent oxygen uptake activity

Substrate-dependent oxygen uptake was determined for *n*-butane- (gaseous alkane), *n*-hexane- (liquid alkane), 1-butanol- (butane metabolism intermediate), butyric aldehyde- (butane metabolism intermediate) and succinate- (control) grown BCP1 cells. Succinate-grown cells showed basal *n*-alkane oxidation ability and this oxidation value was compared with those obtained from the *n*-alkanes- and metabolic intermediates-grown cells.

The butane metabolism intermediates that have been tested as BCP1 oxygen uptake measured by a Clark-type electrode are reported in Fig. 3.8 (marked in red).
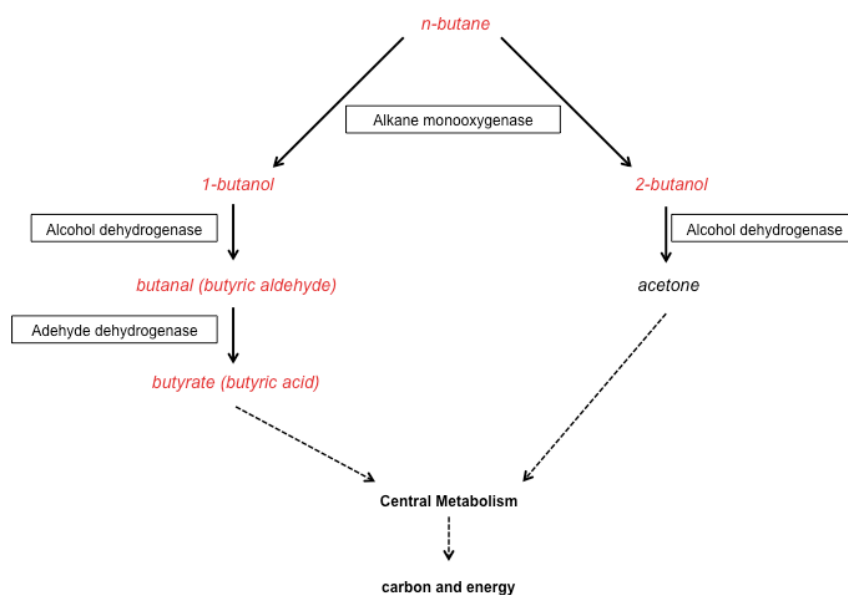
Fig. 3.8 Simplified pathway describing the putative degradation steps involved in *n*-butane metabolism. In red are indicated the metabolites used in the Clark-electrode assay

Fig. 3.9 shows a typical respiration curve associated to butane-grown biomass before and after the addition of *n*-hexane to the chamber. The oxygen uptake rate is calculated as notches per minute, where each notch corresponds to 4.20 nmol of consumed oxygen (at 25 °C). Since the respiration curve tends to reach a plateau by time, we considered only the tangent line to the first part of the respiration curve and we based on this the actual oxygen uptake per minute.
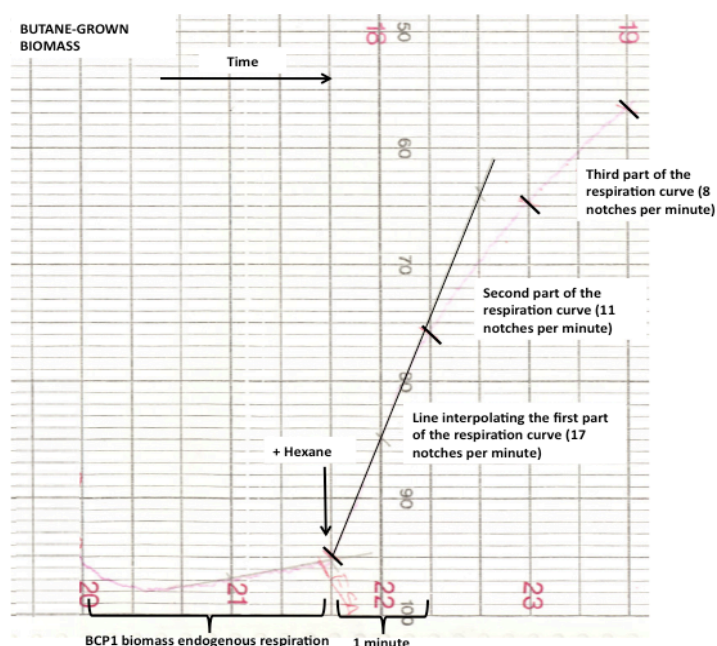
Fig. 3.9 Example of respiration curve obtained with a Clark-type oxygen electrode using butane-grown BCP1 biomass. The addition of the *n*-hexane in the electrode chamber is indicated by the arrow. The other main features of the curve are indicated in figure.

At first, we measured the oxygen consumption activity associated with the respiration of *n*-butane-, *n*-hexane and succinate-grown BCP1 biomasses stimulated by the addition of *n*-butane, *n*-hexane to the reaction chamber.
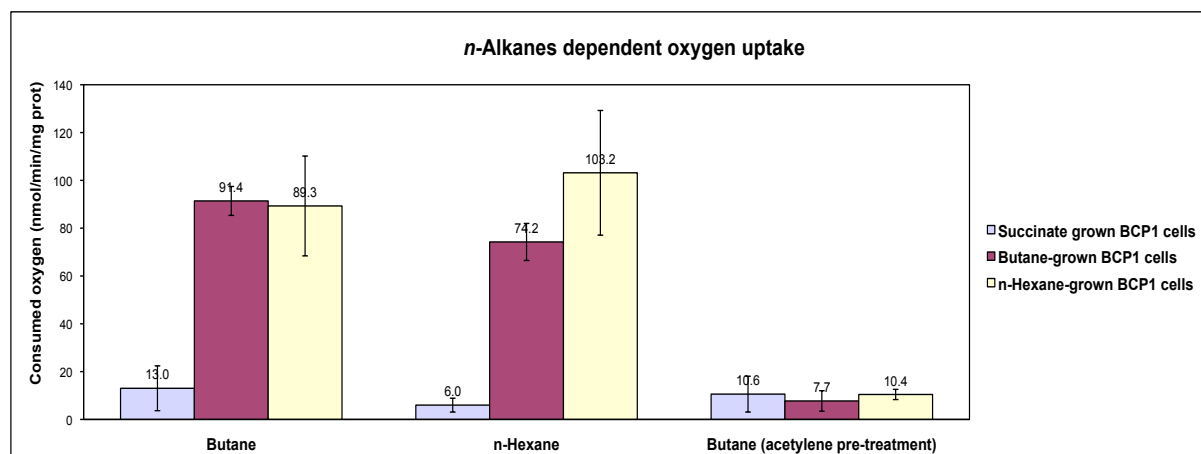
Fig. 3.10 Rates of O_2 consumption by *n*-butane-, *n*-hexane and succinate-grown *Rh*. BCP1 in the presence of *n*-alkanes

Figure 3.10 indicates that the oxygen consumption is stimulated by the addition of *n*-butane and *n*-hexane with both the *n*-alkanes-grown cells. Although the oxygen uptake mechanism, induced by growth on each type of hydrocarbon (*n*-butane and *n*-hexane) is likely

to be different, it is apparent that BCP1 biomass can oxidize both the hydrocarbons.

The oxygen uptake of BCP1 cells pre-treated with the acetylene as inactivator of monooxygenases [62, 325, 326] was also analysed using the same assay. Compared to the untreated cells, the oxygen consumption rate induced by the addition of butane decreased approximately of 70-75% when butane-grown BCP1 cells were pre-incubated for 30 minutes with the inactivator.

Subsequently, in order to investigate the inducibility of enzymes that are involved in the oxidation steps that follow the monooxygenase reaction, we tested the capacity of *n*-butane-, *n*-hexane- and succinate-grown cells to oxidize the potential intermediates of *n*-butane metabolism (1- and 2-butanol, butyric aldehyde and butyric acid).
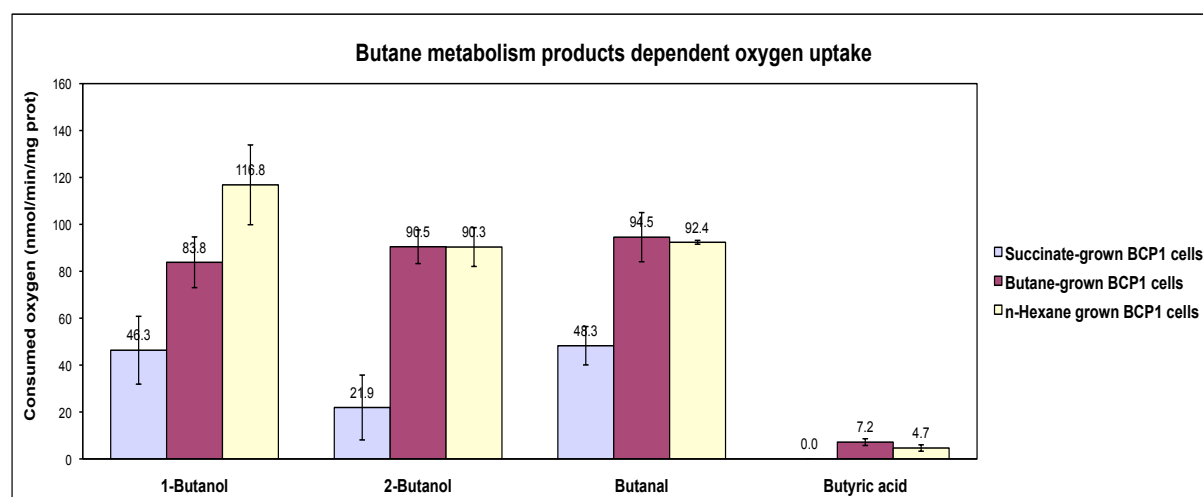
Fig. 3.11 Rates of O_2 consumption by *n*-butane-, *n*-hexane and succinate-grown *Rh*. BCP1 in the presence of the putative intermediates of the *n*-butane oxidation pathway.

Since 1-butanol, 2-butanol and butanal (butyric aldehyde) was shown to stimulate the oxygen uptake activity in succinate-grown cells, the enzymes required for the metabolic reactions downstream of the monooxygenase reaction were suggested to be constitutively expressed (Fig. 3.11). However, there appeared to be an increase in the levels of activity after the growth on both the *n*-alkane. The low level of butyric acid oxidation by *n*-butane- and *n*-hexane-grown cells might be due to the lack of an uptake system for this substrate [327] (Fig.

3.11).

The oxygen uptake activity of BCP1 biomass grown on 1-butanol and on butyric aldehyde (putative intermediates of *n*-butane metabolic pathway, see Fig.3.8) was also investigated. The response of both these type of biomasses in terms of respiratory activity was measured upon addition of *n*-hexane, *n*-butane, 1 and 2-butanol, and butyric aldehyde.
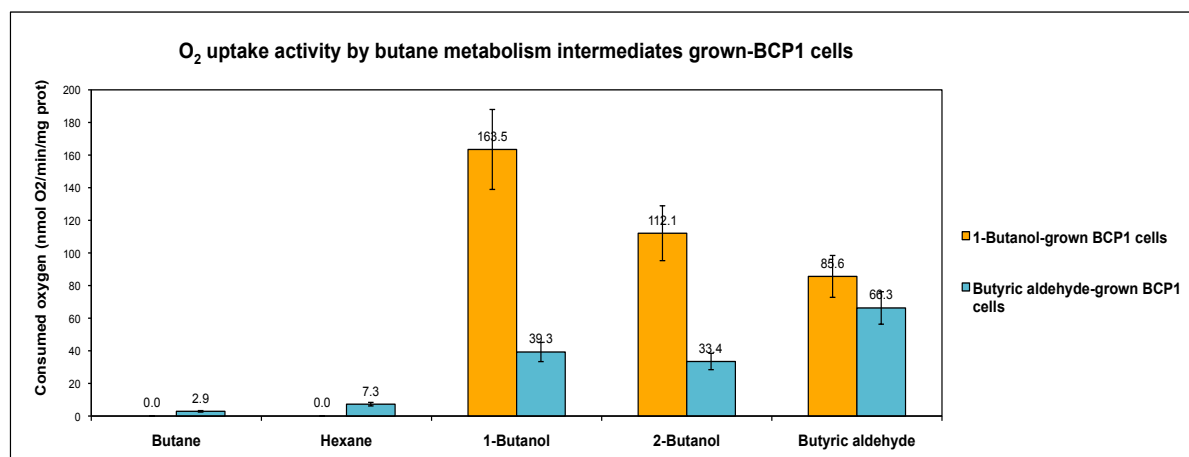
Fig. 3.12 Rates of O_2 consumption by 1-butanol- and butyric aldehyde-grown *Rh*. BCP1 in the presence of *n*-alkanes and putative intermediates of the *n*-butane oxidation pathway.

As shown in Fig. 3.12, the ability to oxidize aliphatic *n*-alkanes was absent in both 1-butanol- and butyric aldehyde-grown biomasses since the addition of either *n*-butane or *n*-hexane did not induce a significant oxygen consumption activity. This latter in 1-butanol-grown cells was stimulated by the addition of either 1-butanol or 2-butanol and, at a lower level, by the addition of butyric aldehyde. The oxygen uptake of the butyric aldehyde-grown biomass was stimulated only by the addition of the same aldehyde or by the addition of either 1- or 2- butanol.

The following table (Table 3.1) summarizes the oxygen consumption values collected in the repiration assays by using the Clark-type electrode.

Table. 3.1 Ability of *Rh*. sp. BCP1 to oxidize *n*-alkanes (*n*-butane and *n*-hexane) and potential intermediates of *n*-butane metabolism after batch growth on succinate, *n*-butane, *n*-hexane, 1-butanol and butanal.

Rates are expressed as nmol oxygen consumed min^{-1}(mg dry weight cells)$^{-1}$

Assay Substrates

Growth Substrates

	SUCCINATE	BUTANE	*n*-HEXANE	1-BUTANOL	BUTANAL
butane	13±9.37	91.40±6.05	89.3±20.89	0	2.9
n-hexane	6±2.89	74.2±7.75	103.2±26.07	0	7.3
1-butanol	46.35±16.03	83.83±11.23	116.64±24.62	168.53±24.87	39.35±6.94
2-butanol	21.92±15.64	90.45±9.56	90.34±10.27	112.13±10.54	33.47±5.97
butanal	48.25±10.30	94.45±12.43	92.37±2.57	85.64±9.69	66.38±10.75
butyric acid	0	7.16±2.36	4.65±1.65	ND	ND
butane (acetylene)	10.60±2.14	7.73±4.29	10.60±7.49	ND	ND

3.3.2 Growth of BCP1 on medium- and long-chain *n*-alkanes

In previous studies, *Rhodococcus* sp. BCP1 has been characterized for its ability to grow on gaseous (C_2-C_4) and liquid *n*-alkanes (C_5-C_7) [304]. In this study we analyzed the growth of BCP1 on MM plates and in liquid MM cultures supplemented with *n*-alkanes of carbon chains length > C_8. BCP1 grew well on MM plates supplemented with *n*-alkanes ranging in length from C_{12} to C_{17} and did not grow on plates supplemented with C_8, C_9, C_{10} and C_{11}. The growth of BCP1 on MM plates supplied with C_{18}-C_{28} *n*-alkanes was difficult to be determined due to the insolubility of solid *n*-alkanes that could not even be supplied as vapour phase. However, a certain ability to grow was indicated by the tendency of BCP1 cells to grow around the solid *n*-alkanes agglomerates formed after the solidification of the medium (Fig. 3.13. four pictures at the bottom).

Table 3.2 BCP1 growth results on liquid and solid MM supplemented with medium- and long-chain *n*-alkanes as only carbon sources.

Tested *n*-alkane	Solid medium growth	Liquid medium growth
Octane (C$_8$)	-	-
Nonane (C$_9$)	-	-
Decane (C$_{10}$)	-	-
Undecane (C$_{11}$)	-	-
Dodecane (C$_{12}$)	+	*
Tridecane (C$_{13}$)	+	*
Tetradecane (C$_{14}$)	+ +	*
Hexadecane (C$_{16}$)	+	*
Heptadecane (C$_{17}$)	+	*
Octadecane (C$_{18}$)	+	*
Eicosane (C$_{20}$)	+ °	*
Docosane (C$_{22}$)	+ °	*
Tetracosane (C$_{24}$)	+ °	*
Octacosane (C$_{28}$)	+ °	*

\- or + indicates negative or positive growth results, respectively.
* indicates the growth in flocs
° indicates the limited or unclear growth that has been shown on solid *n*-alkanes under solid MM growth conditions
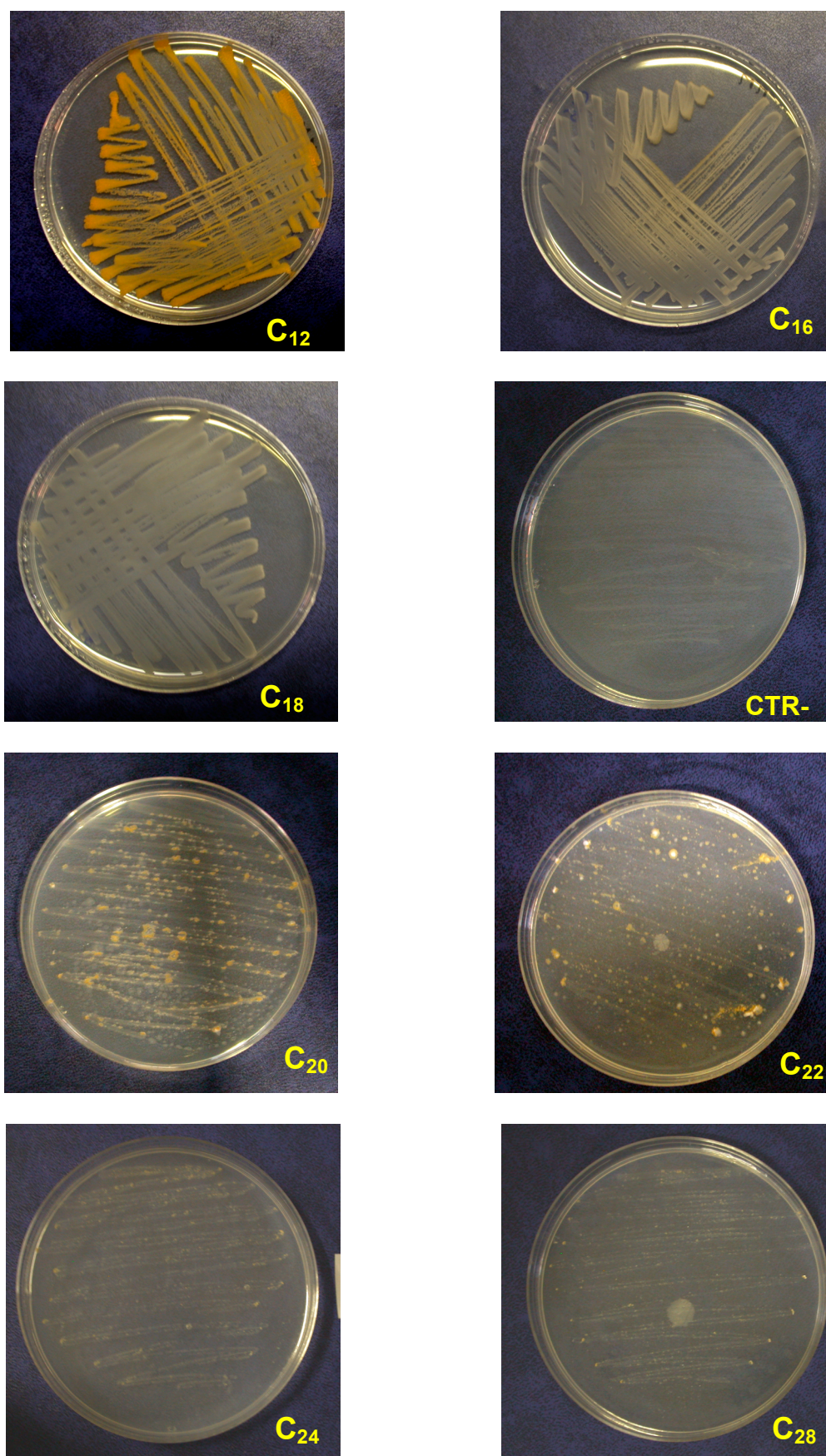
Fig. 3.13 Growth of *Rhodococcus* sp. BCP1 on minimal medium (MM) supplemented with medium-and long-chain *n*-alkanes as only carbon sources (C_{12}-C_{17} are supplied as vapor phase while C_{18}-C_{28} have been solubilized in acetone before being added to the MM).

Therefore, the ability to grow on the C_{18}-C_{28} *n*-alkanes was assayed in liquid MM. They were supplied at a concentration of 0.1% (w/v). Since BCP1 showed the tendency to produce flocks, which prevented the determination of growth on hydrocarbons by cell culture turbidity, the growth was measured as dry weight of the biomass obtained from 0.22μm-pores filtered cultures grown for 1 week.
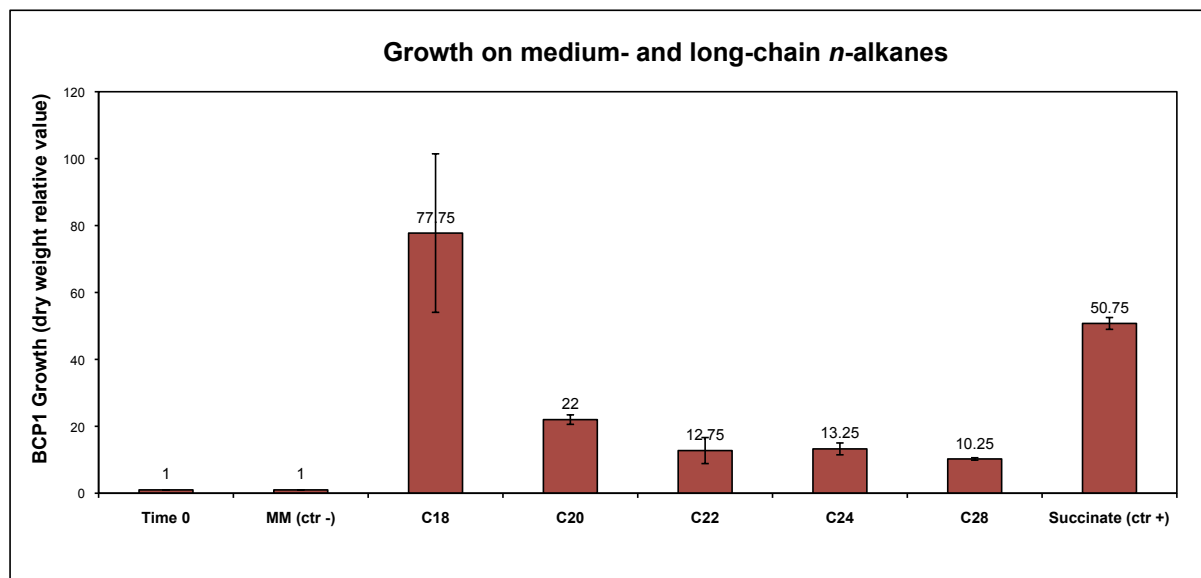
Fig. 3.14 Growth of *Rhodococcus* sp. BCP1 on minimal medium (MM) supplemented with solid *n*-alkanes as only carbon sources (C_{18}-C_{28}). The growth was measured in mg of dry weight.

BCP1 cells were shown to grow in liquid MM supplemented with all these *n*-alkanes as demonstrated by an increase in dry weight of the biomass collected by filtration, in comparison to the one collected on minimal medium with no carbon source (Fig. 3.14). However, the decrease of the BCP1 dry weight according to increasing of the carbon chain length of the solid *n*-alkanes indicated that the BCP1 ability to grow on solid *n*-alkanes was inversely proportional to the number of carbons of the solid *n*-alkane chain.

BCP1 was also shown to grow in liquid MM supplemented with C_{12}-C_{17} *n*-alkanes confirming the results obtained with the solid medium plates. These *n*-alkanes appeared to be toxic at 0.1% (v/v) and were supplied at 0.05% (v/v). However, the cells tended to grow in flocks in the same way as previously shown on solid *n*-alkanes. Interestingly, when the liquid

cultures were grown above a layer of solid MM in which these n-alkanes were entrapped, the physical separation between the BCP1 cells and the hydrocarbons seemed to enhance the formation of homogeneous grown cultures with a large proportion of bacteria dispersed in the aqueous medium.

BCP1 liquid cultures supplemented with n-alkanes ranging from C_8 to C_{11} did not show increase in either turbidity or dry weight under every conditions of growth. These results indicate the inability of the strain to grow on these n-alkanes.

Summarising, BCP1 shows a broad spectrum in the utilization of n-alkanes including n-alkanes ranging C_2 to C_7, as previously reported [304], and C_{12} to C_{22} (as shown here). However, the spectrum of n-alkanes that can be used as carbon source is not continuous from C_2 (ethane) to C_{28} (octosane) but there is a gap from C_8 to C_{11}. Although these n-alkanes might be toxic to BCP1 growth by damaging the bacterial cytoplasmic membrane, more studies are required to establish their actual molecular mechanism of toxicity.

3.4 Discussion

The concentration of gaseous n-alkanes ranging from C_2 to C_5 is dramatically increasing in the atmosphere destabilizing ecosystems through a variety of mechanisms [118, 119]. Although these gases are produced as natural intermediates of bacterial, plant, and mammalian metabolisms, the main sources of pollution is represented by natural oil seepages and oil spills [20, 119].

From a biotechnological perspective, short-chain n-alkanes are inexpensive carbon sources for microbial cultivation, and the enzymes participating in the oxidation pathway promise to be versatile biocatalysts in industrial and environmental applications [119].

Although a number of bacteria have been isolated that are capable of growth on light n-alkanes (ethane, propane and butane), their metabolic pathways have received little attention

compared to those of methane and liquid *n*-alkanes [55, 128].

Rhodococcus sp. BCP1 was isolated for the ability to grow on gaseous *n*-alkane as inducing condition for low chlorinated solvent co-metabolism [304, 313]; thus, we first focused our attention on the BCP1 utilization of short-chain *n*-alkanes (propane, butane, hexane). Since this study mainly examined the first alkane-specific oxidation step, we performed two metabolic assays to dissect the possible role of a monooxygenase in allowing BCP1 able to grow on short chain *n*-alkanes.

The first question to be solved was whether or not the oxidation of short-chain *n*-alkanes by BCP1 occurred either at the terminal or sub-terminal carbons, or both. Indeed, the site of oxidation determines the products, which in turn, influence the pathways required to metabolize these products. Through the use of gas chromatography applied to BCP1 resting cells exposed to butane or propane, the oxidation products attributable to monooxygenase catalysis were detected. The utilization of inhibitors in the assay was necessary to let the cells to accumulate the oxidation products that otherwise would have been immediately metabolized, as already described by [128]. The competitors that have been used are structural analogous of the putative oxidation products to be detected. When structural analogous are provided in excess they can saturate the enzymes activity downstream of the first oxidation step catalyzed by the alkane monooxygenase. As a result, the BCP1 cells did show the production of 1-butanol as *n*-butane oxidation product and 1-propanol as *n*-propane oxidation product. However, a small fraction of sub-terminal oxidation product was detected when the cells were exposed to *n*-propane in the presence of 2-butanol as competitor, i.e. 2-propanol was produced. By contrast 2-butanol was not detectable by using 2-propanol as inhibitor in butane-grown cells. These results suggested that short-chain *n*-alkanes are oxidized primarily through terminal oxidation. However, the detection of a small amount of 2-propanol after 15 minutes of propane exposure, suggests that a little fraction of the sub-

terminal oxidizing reaction occurs. This last consideration is even more corroborated by the ability of *Rhodococcus* BCP1 to grow on 2-butanol, 2-propanol and on butanone and acetone that are putative products of downstream metabolic pathway of 2-butanol and 2-propanol, respectively. The ability of *Rh*. BCP1 to grow on all these potential intermediates of *n*-butane and propane metabolism would suggest that this bacterial species has the metabolic capacity to utilize either the terminal or the sub-terminal pathway of gaseous *n*-alkanes metabolism. The difficulty to detect 2-butanol formation besides 1-butanol in the butane exposure experiments using 1- and 2-propanol as competitors, respectively, can be due either to a weaker capacity of 2-propanol (respect the 2-butanol) to inhibit the oxidation steps downstream of the 2-butanol production, or to different stereochemical features of the oxidative reaction performed by the monooxygenase towards the two gaseous *n*-alkanes. A different stereochemistry would explain the production of both the two isomers of the alcohol produced from the propane oxidation (1- and 2-propanol) and the production of only one isomer of the alcohol produced from the *n*-butane oxidation (1-butanol).

Respiration of BCP1 biomass grown on a gaseous alkane (*n*-butane), a liquid alkane (*n*-hexane) or succinate upon addition of different substrates was measured by a Clark-type oxygen electrode. The endogenous oxygen uptake rate increases after the addition of substrates that could be oxidized because of the presence of enzymes that have been expressed during the cells growth. The results of these determinations indicated that the oxygen uptake was stimulated (as compared to the endogenous oxygen uptake value) after the addition of *n*-alkanes (*n*-butane or *n*-hexane) only in *n*-alkanes grown BCP1 biomass. By contrast, succinate-grown BCP1 biomass, as well as *n*-butane metabolic intermediates grown-BCP1 biomass (1-butanol and butyric aldehyde), did not show oxidation activity on both *n*-alkanes. These findings suggested that the alkanes oxidizing enzymes are inducible. Interestingly, butane-grown biomass showed a respiration rate stimulated by the addition of *n*-

hexane that was comparable with that stimulated by the addition of *n*-butane. In the same way the *n*-hexane-grown biomass revealed and oxygen consumption which was *n*-butane-dependent with similar values to the *n*-hexane-dependent activity. This suggested either the involvement of the same oxygenase pattern in the metabolism of both the *n*-alkanes (one gaseous and one liquid) or the ability of each oxygenase induced by the growth on one *n*-alkane to oxidize the other one using a range of substrates broader than the range of inducers. From another point of view, the ability of succinate-grown cells to oxidize some potential intermediates of *n*-butane metabolism (1- and 2-butanol, butyric aldehyde) suggested that the enzymes required for their metabolism are constitutively expressed. However, there appeared to be an increase in the levels of oxygen uptake activity when 1-butanol grown-biomass was considered, suggesting a certain level of inducibility of the enzymes acting downstream of the monooxygenase. An increase in the level of oxygen consumption, induced by the presence of *n*-butane metabolic intermediates, was also detected on BCP1 cells grown on both *n*-hexane and *n*-butane. This result suggested that not only the growth on *n*-butane but also the growth on *n*-hexane induces enzymes that can oxidize butane metabolic intermediates, possibly indicating the involvement of a common enzyme apparatus in the metabolism of both the alkanes or a broad specificity of substrate in the *n*-hexane induced enzymes that can recognize and oxidize *n*-butane products. As expected, the oxygen consumption rate by butyric aldehyde-grown biomass was stimulated not only by the addition of the same aldehyde but also by the addition of 1- and 2-butanol whose oxidizing enzymes are supposed to act upstream of the aldehyde dehydrogenase that is believed to catalyze the oxidation of butyric aldehyde (Fig. 3.8). The oxygen uptake activity of the butyric aldehyde-grown BCP1 biomass induced by butanols can be explained by the fact that other alcohol dehydrogenases can be involved in the oxidation steps downstream of the aldehyde dehydrogenase an they are able to recognize and oxidize butanols. The low level of butyrate oxidation may be due to the lack of

an uptake system for this substrate [328].

The inhibitory effect that the acetylene exerts on the monooxygenase/s, involved in the *n*-alkanes first oxidation step, has been confirmed by both gas chromatography and respiratory assays. The inhibitory values were concordant with those reported in literature [62].

In order to extend the range of *n*-alkanes used as growth substrates by BCP1, we performed growth assays on minimal medium (MM) plates and liquid MM in flasks supplemented with *n*-alkanes of aliphatic chain length bigger than C_8 (octane). The results showed that BCP1 is able not only to grow on *n*-alkanes from C_2 to C_7 but also to utilize as carbon sources *n*-alkanes ranging from C_{12} to C_{28}. However, the dry weight values obtained from the liquid cultures after one week of growth on *n*-alkanes from C_{18} to C_{28} showed that the BCP1 ability to grow on solid *n*-alkanes decreased in parallel with the carbon chain length. This behaviour has been described also for other alkane degrading bacteria [213]. Interestingly, *n*-alkanes ranging from C_8 to C_{11} could not be used as carbon sources. The impossibility for BCP1 to grow in liquid medium in the presence of one of these *n*-alkanes together with *n*-hexane, suggested a toxicity factor putatively correlated with the carbon chain length that can cause problems in membrane structure and physiology properties [329]. The inability of alkane-degrading *Rhodococcus* strains to grow on certain range of *n*-alkanes has also been described by Sameshima *et al.* [311] in *Rhodococcus opacus* B4. B4 cells could not utilize *n*-pentane (C_5) and *n*-hexane (C_6) because of the short-chain length *n*-alkane toxicity [311]. Another example regards a propane utilizer, *R. rhodochrous* PNKbl, that was isolated by Woods and Murrell [330] and it was shown to be unable to grow on short-chain *n*-alkanes ranging from C_1 to C_8. Indeed, most of the toxic effects described in literature seemed to be exerted by liquid short chain *n*-alkanes (C_5, C_6 up to C_{10}) [331-333]; conversely, BCP1 can grow on C_5, C_6 and C_7 *n*-alkanes and toxicity is linked to *n*-alkanes from C_8 to C_{11}. The fact

that the range of toxic *n*-alkanes can be different amongst hydrocarbon-degrading *Rhodococcus* strains suggests an extreme variety of physiological features amongst the members of this genus.

3.5 Summary

Here we've shown that monooxygenase activity plays a crucial role in the degradation of short-chain *n*-alkanes in *Rhodococcus* sp. BCP1. The type of oxidation performed by this monooxygenase and the oxidation values associated with its activity have been described. The ability of *Rh*. sp. BCP1 to grow on medium- and long-chain *n*-alkanes have been investigated emphasizing the potential application of this bacterial strain in industrial and environmental applications associated with the utilization of monoxygenase activity in biosynthetic processes and with the broad *n*-alkanes degradation ability of BCP1 applicable for oil-polluted areas bioremediation purposes.

CHAPTER 4. Molecular characterization of 10.5 kb DNA region containing the *alkB* gene and the flanking regions from *Rhodococcus* sp. BCP1

4.1 Introduction

As the genome of *Rhodococcus* sp. BCP1 is unknown, both identification and isolation of the genes responsible for *n*-alkane monooxygenase activity is compelling.

Monooxygenation may be catalyzed by hydroxylases belonging to different families: SDIMO family (Chapter 1§ 1.3.4.2), AlkB family (Chapter 1 § 1.3.4.3) or P450 cytochrome family (Chapter 1 § 1.3.4.4). The alkane hydroxylase of *Pseudomonas putida* GPo1 is the most extensively characterized monooxygenase belonging to the AlkB family. Besides this, other AlkB systems have been isolated in both Gram-negative and Gram-positive bacteria even though most of them are still not well characterized. AlkB proteins and associated genes showed high sequence diversity, great variability in substrate specificity and wide difference in the organization of the genes encoding the AlkB components (Chapter 1 § 1.3.4.3). Moreover, although *P. putida* GPo1 and some other strains contain only one AlkB hydroxylase, in many other alkane-degrading strains multiple hydroxylases are present. For example two *Rhodococcus* strains (NRRL B-16531 and Q15) have been shown to contain at least four alkane hydroxylase gene homologues (*alkB1*, *alkB2*, *alkB3* and *alkB4*).

In several bacteria expressing multiple AlkB monooxygenases, the redundancy seems to be due by the different chain length of the alkanes that each AlkB can oxidize but in most of the cases the presence of multiple AlkB is still not understood.

Since *Rhodococcus* sp. BCP1 has previously been shown to grow on a broad range of *n*-alkanes (Chapter 3), our goal was to find out the presence of gene/s coding for alkane hydroxylases belonging to the AlkB family whose members are known to have a wide range of substrates. The general strategy applied for the isolation of homologues of these genes from

BCP1 genomic DNA can be summarized as following (Fig 4.1).
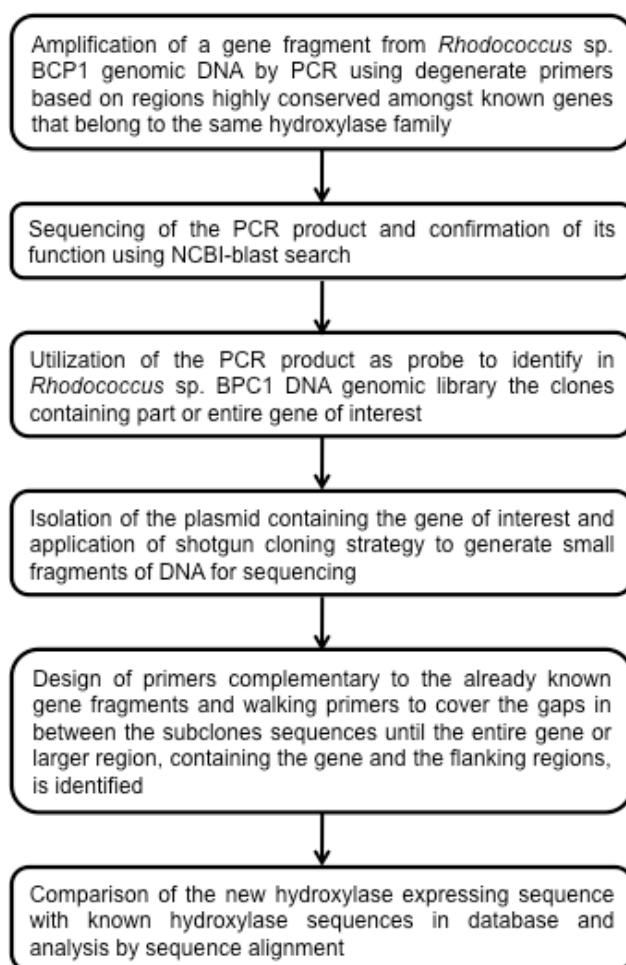
Fig. 4.1 Strategy for the identification of a new *alkB* gene in *Rhodococcus* sp. BCP1

We decided to use degenerate oligonucleotide primers designed by Smits *et al.* [180] based on conserved histidine motifs typical of membrane-bound non-haem iron alkane hydroxylases (AlkB family). The primers were designed aligning the *P. oleovorans* GPo1 and the *Acinetobacter* sp. ADP1 alkane hydroxylase homologues, named AlkB and AlkM, respectively (Fig. 4.2).

```
A

alkB    400  5' ctcaatacaggacacgaactcggtcacaagaaggagact 3'  438
AlkB    134       .L..N..T..G..H..E..L..G..H..K..K..E..T.      146

alkM    436  5' gtgaataccgcgcatgaattgagccataaagcagatcga 3'  474
AlkM    146       .V..N..T..A..H..E..L..S..H..K..A..D..R.      158

TS2S         5' ...aayagagctcaygarytxggtcayaag......... 3'

B

alkB    925  5' cttcagcggcactcggatcaccacgcgcatccaacacgt 3' 963
AlkB    309       .L..Q..R..H..S..D..H..H..A..M..P..T..R.     321

alkM    961  5' ttacaacgacattcagatcatcacgcttatccgacgcgt 3' 999
AlkM    321       .L..Q..R..H..S..D..H..H..A..Y..P..T..R.     333

deg1RE       3' .........gtragictrgtrgtrcgcttaaggtg.... 5'
```

Fig. 4.2 Alignment performed by Smits [180] showing the two conserved regions in the primary sequence of AlkB that allowed the designing of the primers TS2S and deg1RE.

Work by Smits *et al.* [180] described these primers being able to amplify 550-bp PCR fragments encoding peptides with high level of protein sequence identity to the corresponding region of the *P. oleovorans* AlkB and *Acinetobacter* sp. AlkM proteins. By using these primers, *alkB* gene homologues both in Gram-negative and Gram-positive bacterial strains were identified showing the ability to grow on *n*-alkanes. By contrast, the specific PCR product was not detected in bacterial strains that were not able to grow on *n*-alkanes [334].

After isolating the BCP1 DNA genomic region containing *alkB* gene, the aim of our study was to identify the products of the *orfs* included in the *alkB* flanking regions by comparative analysis with the homologues in the database. Since only few reports focused on the molecular nature of *alkB* genes in *Rhodococcus* strains (Chapter 1 § 1.4.1) and new *Rhodococcus* genomes have just become available (Chapter 1 § 1.4), we also considered the possibility to compare the BCP1 *alkB* gene cluster and flanking regions products with the homologues found in other *Rhodoccocus* strains in order to reveal similarities and differences in the amino acid sequences and in the organization of their coding genes.

93

4.2 Materials and Methods

4.2.1 Bacterial strains and growth conditions

Rhodococcus sp. BCP1 and *E. coli* DH5α strains harbouring pUC18 and pMC plamids series were used in this study (see Chapter 2, § 2.1 for relevant genotype features and plasmid characteristics). Bacterial strains were grown on LB medium. The composition of the media and growth conditions are described in the General Materials and Methods, Chapter 2.

4.2.2 Amplification of *alkB* gene fragment from *Rhodococcus* sp. BCP1 genome

Rhodococcus sp. BCP1 genomic DNA was extracted as described in the General materials and methods, Chapter 2. TS2S2 and Deg1RE [180] primers were used to amplify by PCR a sequence of approximately 550 bp from *Rhodococcus* sp. BCP1 genomic DNA. TS2S2 and Deg1RE primers sequences were based on the *Pseudomonas putida* GPo1 AlkB and *Acinetobater* AlkM sequences in correspondence of two histidine conserved motifs (Hist1 and Hist2) [180]. Reaction mixtures (50 μl) contained 5 μl of 10x PCR buffer containing $Mg^{2+,}$ 0.3 pmol of each primer, 0.2 mM of each dNTP, 1 U Taq DNA polymerase (Roche) and 50 ng of template BCP1 genomic DNA. Amplification was performed in a Biometra-T gradient thermalcycler after a hot start at 95 °C for 4 minutes followed by 30 cycles consisting of 95°C for 45 sec, 40ºC for 1 min, and 72°C for 1 min and a final extension of 8 minutes at 72°C. PCR products were separated by electrophoresis on 1% agarose gels and fragments of the expected size (550 bp) were purified using the QIAquick gel extraction kit (QIAGEN). PCR purified fragments were cloned in the pCR 2.1-TOPO plasmid using the TOPO TA cloning® kit (Invitrogen) and sent for sequencing to the BMR-genomics service of the University of Padova (Padova, Italy).

4.2.3 Screening of BCP1 genomic DNA library and shotgun cloning strategy for the isolation of the 10.5 kb genomic fragment containing the *alkB* full-length gene sequence and the flanking regions

Approximately 750 cosmid clones of the BCP1 genomic library, prepared as described in the General materials and methods (Chapter 2), were screened by colony blot hybridization using the 550bp-length *alkB* probe resulting from the amplification with TS2S and Deg1RE primers. The *alkB* probe was labeled with [^{32}P] dCTP as described in the General materials and methods chapter. Bacterial colony blots were prepared on nylon membranes as described by Sambrook *et al.* [320]. Cosmid DNA was extracted from two positive clones, pAlk1 and pAlk3, with the Midi-prep kit (QIAGEN) and subjected to restriction analysis with *KpnI*, *EcoRI* and *BglII* restriction enzymes. Digested cosmid DNA was transferred to a nylon membrane and analysed by Southern blot. Restriction fragments positive to the hybridization with the *alkB* probe were detected in both the positive clones pAlk1 and pAlk3. A 10.5 kb- and a 1.7 kb-fragments from *KpnI*-digested pAlk1 cosmid were cloned in pUC18 and transformed in *E. coli* DH5α competent cells. The plasmids containing the 10.5 kb insert and the 1.7 kb insert were named pMC1 and pMC0, respectively, and they were further subjected to enzymatic digestions in order to obtain smaller fragments that were subcloned in pUC18 (pMC plasmids series, Fig. 4.5) for sequencing. Primers were then designed based on the sequences of the subcloned fragments and walking priming was performed on pMC1 (pUC18 containing the whole 10.5 kb *alkB* fragment) in order to cover the gaps in the nucleotide sequence. The *alkB* full-length sequence and the flanking regions included in the 10.5 kb genomic DNA fragment were thus isolated (pMC plasmids series) and completely sequenced.

4.2.4 Homology searches and phylogenetic analysis

Geneious Pro 4.7.6 software [315] was used to process the nucleotide and amino acid sequences of pMC plasmid series and homology searches were performed with pBLAST with the following parameters: Low complexity filter; Matrix, BLOSUM62; Gap cost, 11 open, 1

extend and Max E-Value 10. The amino acid alignment program Clustal W (http://www.ebi.ac.uk/clustalw/) was used for the amino acid comparative studies and putative conserved domains have been detected by Conserved Domain Database (CDD) (http://www.ncbi.nlm.nih.gov/Structure/cdd/cdd.shtml) [335]. The CLUSTALW parameters were the following: Cost matrix, BLOSUM; Gap open cost, 10; and Gap extend cost, 0.1. After the alignment of BCP1 AlkB with amino acid sequences of homologues proteins, a phylogenetic tree was created using Geneiuos Tree Builder with the following parameters: genetic distance model, Juke-Cantor; tree build method, Neighbor-Joining; *Pseudomonas putida* GPo1 *AlkB* as outgroup.

4.3 Results

4.3.1 Strategy for both detection and cloning of *alkB* gene from *Rhodococcus* sp. BCP1

The PCR amplification conducted using BCP1 genomic DNA with the degenerate primers (TS2S and Deg1RE) from [180] resulted in one 550-bp PCR product (Fig. 4.3). The nucleotide sequence of this PCR product revealed a high degree of similarity to other alkane hydroxylase sequences of Gram-positive bacteria available in database. The product was cloned and the insert was used to screen the *Rhodococcus* sp. BCP1 genomic library. The colony blot revealed two positive clones, pAlk1 and pAlk3 (Fig. 4.3). Single sharp hybridization bands were obtained from the hybridization of *alkB probe* with the electrophoretically separated cosmidic restrictions digested with *EcoRI* (both 1,7 kb) and *KpnI* (pAlk1, 10 kb and pAlk3, 8 kb) (Fig. 4.4). The pAlk1 cosmidic DNA was therefore cut with *EcoRI* and *KpnI* and separated in agarose gel. The fragments of approximately 1.7 kb and 10.5 kb, respectively, were recovered and ligated into pUC18 cloning vector. They were named pMC0 and pMC1 respectively (Fig. 4.5).
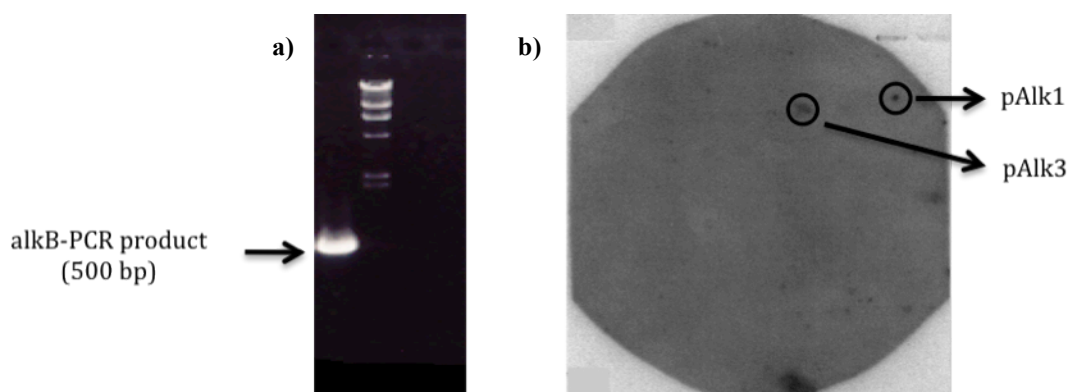
Fig. 4.3 The 550-bp PCR amplified from genomic DNA using degenerate oligonucleotide primers TS2S/Deg1RE is shown (a) The 550-bp PCR product was used as probe. In colony blot assay two clones positive to the hybridization with the *alkB* probe were detected (b).
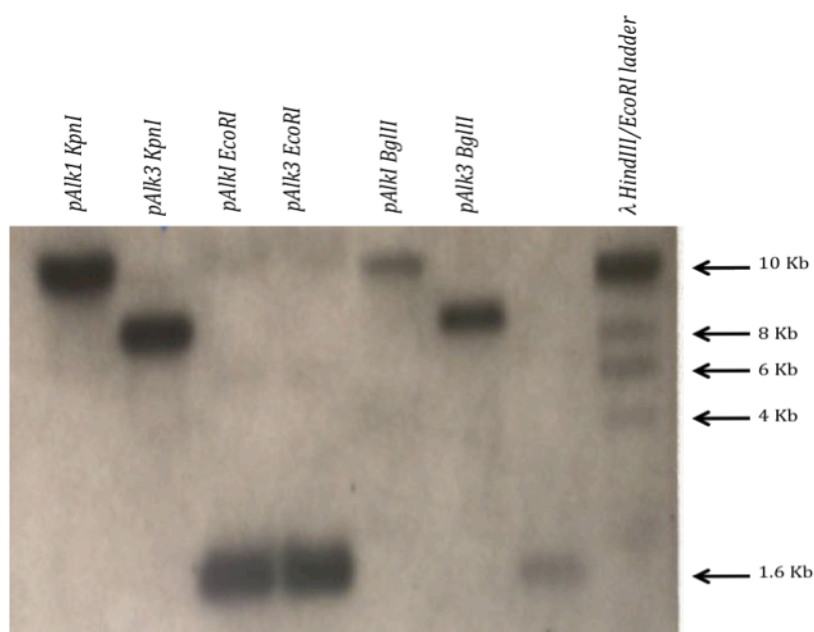
Fig. 4.4 Southern blot hybridization using *alkB* probe and cosmidic DNA from pAlk1 and pAlk3 (positive hybridization colonies on colony blot) digested with *KpnI*, *EcoRI* and *BglII*

Because of the size of the insert (10.5 kb), pMC1 was assumed to include the complete *alkB* gene with the flanking regions and it was decided to be further analyzed. The restriction map of the 10.5 kb fragment was then described and the discrete restriction fragments were inserted into pUC18 cloning vectors and introduced into *E.coli* DH5α. The nucleotide sequences of the sub-clones were determined and they were ordered on the physical map (Fig. 4.5). Furthermore, primer walking was performed in order to cover the DNA sequence gaps between

the clones sequences. As a result the whole 10.5 kb fragment was sequenced and the sequence

data of the *KpnI* fragment covered each strand with a minimum of twofold redundancy.
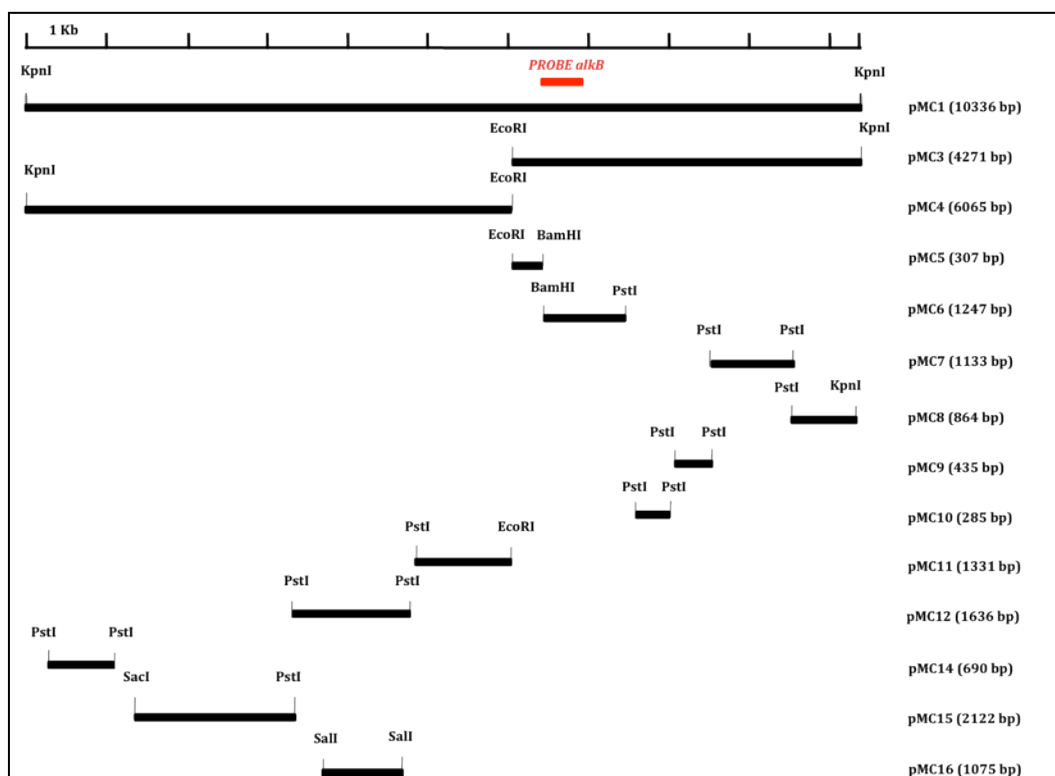
Fig. 4.5 Subclones originating from the 10.5 kb *KpnI* DNA fragment by single or double restriction digestions. Sixteen subclones were created each containing pUC18 with a fragment of the 10.5 kb region as insert. The names of these clones based on pUC18 cloning vector are defined with cardinal numbers after 'pMC'. The 550-bp *alkB* probe is reported on the map with its position inside the DNA region.

4.3.2 Characterization of *the alkB* gene cluster and the flanking orfs included in the 10.5 kb-DNA region from *Rhodococcus* sp. BCP1

The mol % G + C of the entire fragment was 70.7%, which is consistent with the genomic

nucleotide composition of the *Rhodococcus* strains whose complete genomes are available in the

database (67.5%, 62.3% and 67.9% for *Rhodococcus jostii* RHA1, *Rh. erythropolis* PR4 and *Rh.*

opacus B4, respectively) [257, 291-293].

Eleven putative open reading frames (ORFs) were assigned by taking into account the

higher G+C contents in their codon regions and also by analyzing BLAST similarity of the

amino acid and nucleotide sequences of each ORF. The downstream region revealed four

consecutive Orfs homologues to the *alkB* gene cluster components: *alkB* (alkane

98

monooxygenase), *rubA* (rubredoxin), *rubB* (rubredoxin), *rubR* (rubredoxin reductase) (Fig. 4.1, at the end of the Chapter 4), covering a region of 2893 bp. A gene coding for a TetR-related regulatory protein was located downstream of the *alkB* gene cluster.

The eleven putative Orfs were analysed by pBLAST and sequence similarity of each Orf with the homologues in the database was calculated by ClustalW program. Table 4.1 (at the end of the Chapter 4) summarizes the information about the resulting identity values associated with each Orf comprised in the 11 kb-fragment and about the conserved domains identified in the amino acid sequences. In the further paragraphs the *alkB* gene cluster is analysed along with the other Orfs.

4.3.3 The *alkB* gene cluster in *Rhodococcus* sp. BCP1

The only putative Shine-Dalgarno-like ribosome-binding site in the *alkB* region was found 8 bases upstream of the *alkB* start site (GGAGG). The genes *alkB/rubA* and *rubB/rubC* have 3'-end/5'-end overlaps which suggests their translational coupling. The occurring overlap is TGATG for *alkB/rubA* and ATGA for *rubB/rubC*. By contrast, 1 nucleotide divided the stop codon of *rubA* and the start codon of *rubB*. The triplet GTG was found to be the *alkB* gene start codon (instead of the orthodox prokaryotic start codon ATG) that is not unusual in *Rhodococcus* strains genetic codon usage.

BCP1 AlkB amino acid sequence displayed high homology (70% to 83%) with Gram-positive alkane hydroxylases and slightly less homology with Gram-negative alkane hydroxylases. The greatest sequence identity was shown with the two alkane 1-monooxygenases of *Rhodococcus* opacus B4 (84% and 81%) and with the alkane monooxygenase of *Rhodococcus jostii* RHA1 (82%). Regarding the AlkB systems present in the literature, the amino acid similarity of BCP1 AlkB to *Rh. erythropolis* NRRL B-16531 and sp. Q15 alkane-1-monooxygenases [195] was 79% and 76%, respectively, to *Gordonia* sp. TF6 alkane-1-

monooxygenase [336] was 76% and to *Mycobacterium austroafricanum* alkane 1-monooxygenase [67] was 59%. The similarity to the *Geobacillus* sp. MH1 AlkB system [337] was 78%. Less than 50% was the sequence identity with other Gram-negative alkane hydroxylases, as the homology with the putative alkane 1-monooxygenase of *Pseudomans fluorescens* and with the alkane 1-monooxygenase *Pseudomonas mendocina* was 51% and 44%. The homology with *Pseudomonas putida* GPo1 AlkB hydroxylase was 41%. Figure 4.6. shows a dendrogram comparing *Rhodococcus* sp. BCP1 AlkB sequence with the amino acid sequences of other alkane hydroxylases.
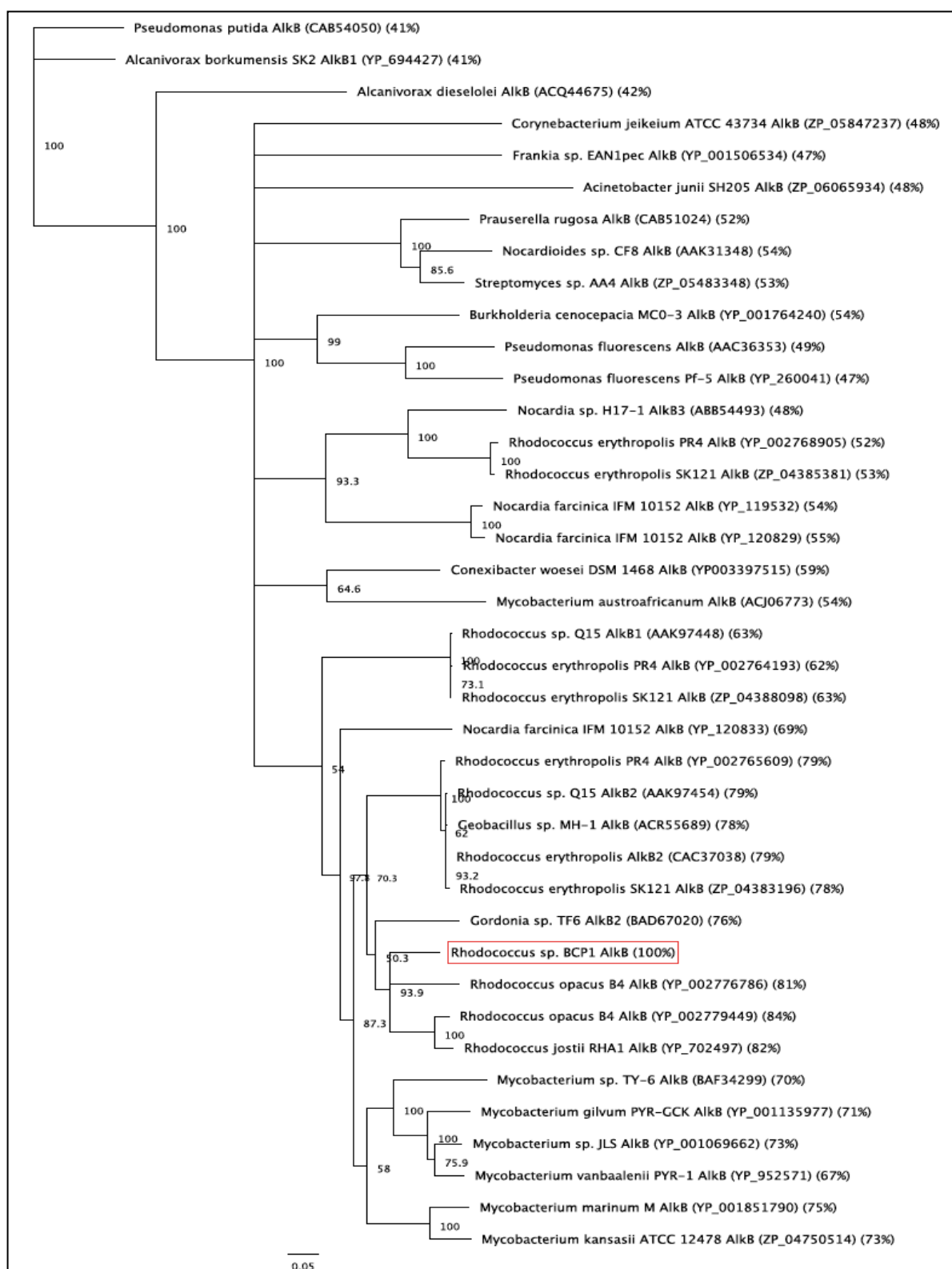
Fig. 4.6 Phylogenetic analysis of *Rhodococcus* sp. BCP1 AlkB. Dendrogram results from the alignment of the amino acid sequence of *Rhodococcus* sp. BCP1 AlkB (marked in red) with representative alkane hydroxylases in the database from Gram-negative and Gram-positive bacteria. The protein IDs are indicated within brackets. Alignment was done with the CLUSTALW program and the tree constructed with Jukes-Cantor genetic model and neighbour-joining algorithm in Geneious platform [315]. *Pseudomonas putida* GPo1 AlkB sequence was used as an outgroup sequence. Bootstrap values based on 1000 replications are listed at the branch nodes. The homology values with BCP1 AlkB are indicated between brackets.

In addition to the high full length homology, the AlkB of *Rhodococcus* sp. BCP1 protein contained the three conserved histidines boxes (Hist1, HELXHK; Hist2, EHXXGHH; and Hist3, LQRHSDHHA) (in red, Fig. 4.7) typical of proteins belonging to the non-hemic iron integral membrane alkane hydroxylase family. The amino acid sequence shows also the additional HYG motif (NYXEHYGL) (in blue, Fig. 4.7) that is a signature motif specific for bacterial alkane monooxygenases [195].


```
GPo1    ---MLEKHRVLDSAPEYVDKKKYLWILSTLWPATPMIG---IWLANETGWG----IFYGL
BCP1    MTTSDIGRYAQAPVEQWRDRKRYLWLMGLIPPTAIFLATALVWGFNQLGWTAVSPMWWWI
            :  .  .. :: *:*:***::.  :  *:: ::.   :*   *:  **      ::: :

GPo1    VLLVWYGALPLLDAMFGEDFNNPPEEVVPKLEKERYYRVLTYLTVPMHYAALIVSAWWVG
BCP1    GPLLVYVLLPILDRFFGPDGQNPPDEVMEMLENDKYYRYCTYAYIPFQLASLVFACYLWS
            *: *   **:** :** *  :***:**:   **::***   **   :*:: *:*:.:.:   .

GPo1    TQPMSWLEIG---------ALALSLGIVNGLALNTGHELGHKKETFDRWMAKIVLAVVGY
BCP1    TGNLSWLGIDGGLGLISKIGLAFSVGVMGGVGINTAHELGHKKDDLERWLSKITLAQTFY
            *  :*** *.       .**:*:*::.*:.:**.******: ::**::**.** . *

GPo1    GHFFIEHNKGHHRDVATPMDPATSRMGESIYKFSIREIPGAFIRAWGLEEQRLSRRGQSV
BCP1    GHFYIEHNRGHHVRVSTPEDPASARFGESFWTFLPRSVWGSLKSSWELEKTRLQRLGKSP
            ***:*****:*** *:** ***::*:***::.*   *.: *::   :* **: **.* *:*

GPo1    WSFDNEILQPMIITVILYAVLLALFGPKMLVFLPIQMAFGWWQLTSANYIEHYGLLRQKM
BCP1    WTLRNDVLNAWAMSVVLFGVLVAVFGPVIIPFLILQAVYGFSLLETVNYLEHYGLLRQKT
            *:: *::*:.   ::*:*:.**:*:*** :: ** :* .:*:  *  :**:*****:***

GPo1    EDGRYEHQKPHHSWNSNHIVSNLVLFHLQRHSDHHAHPTRSYQSLRDFPGLPALPTGYPG
BCP1    ATGRYERCTPAHSWNSDHIVTNIFLYHLQRHSDHHANPTRRYQTLRSMDGAPNLPSGYAS
            ****: .* *****:***:*:.*:********** *:*** **:**.:  *  *  **:**..

GPo1    AFLMAMIPQWFRSVMDPKVVDWAGGDLNKIQIDDSMRETYLKKFGTSSAGHSSSTSAVAS
BCP1    MIGLAYIPPLWRKVMDHRVVEHYDGDITRANIQPSKRGKVLAEFGAQ--------------
            : :* ** :*.*** :**:  .**:.: :*: * * . * :**:.
```

Fig. 4.7 Alignment of BCP1 AlkB with the model *Pseudomonas putida* GPo1 AlkB. The conserved amino acids are indicated by stars below the sequences. The amino acids forming the Hist motifs are boxed in red. The HYG motif is boxed in blue.

Hydrophobic analysis and secondary structure prediction of the deduced amino acid sequence of AlkB suggested the presence of at least 5 transmembrane α-helics; each one is predicted to contain 22 aminoacids. A sixth α-helic is likely to be present although the probability is low (Fig. 4.8).

```
# Sequence POSSIBLE N-term signal sequence
Sequence    TMHMM2.0    inside      1    23
Sequence    TMHMM2.0    TMhelix     24   46
Sequence    TMHMM2.0    outside     47   55
Sequence    TMHMM2.0    TMhelix     56   78
Sequence    TMHMM2.0    inside      79   98
Sequence    TMHMM2.0    TMhelix     99   121
Sequence    TMHMM2.0    outside     122  130
Sequence    TMHMM2.0    TMhelix     131  153
Sequence    TMHMM2.0    inside      154  251
Sequence    TMHMM2.0    TMhelix     252  274
Sequence    TMHMM2.0    outside     275  407
```

Fig. 4.8 Prediction of transmembrane helices in BCP1 AlkB sequence by using TMHMM2.0 [338] (http://www.cbs.dtu.dk/services/TMHMM-2.0/)

Immediately downstream the *alkB* gene, two consecutive rubredoxin genes (*rubA* and *rubB*) showed both the non-heme iron binding domain containing a [Fe(SCys)$_4$] center. The 53-amino acid RubA protein showed the highest sequence identity with the rubredoxin of *Rhodococcus* erythropolis PR4 (70%), the putative rubredoxin of *Nocardia farcinica* IFM 10152 (75%) and the alkene monooxygenase rubredoxin of *Rhodococcus* sp. RHA1 (76%). RubB protein is composed of 61 amino acids and showed the highest amino acid sequence identities with *Mycobacterium ulcerans* Agy99 rubredoxin RubB_1 (86%).

The next large ORF in the *alkB* cluster, *rubR*, encodes a large protein exhibiting significant full-length sequence identity to Gram-positive rubredoxin reductases including two *Rhodococcus opacus* B4 rubredoxin reductases (54% and 57%), *Rhodococcus* sp. RHA1 alkene monooxygenase rubredoxin reductase (56%) and *Rhodococcus* sp. Q15 rubredoxin reductase (47%). A Rossmann-fold NAD(P)H/NAD(P)(+) binding (NADB) domain is detectable in the amino acid sequence of BCP1 RubR (Table 4.1), that is found in numerous redox enzymes of

different metabolic pathways.

The incomplete ORF following the *alkB* cluster, encodes a protein with the highest amino acid sequence identity to a transcriptional regulator of *Rhodococcus* sp. RHA1 (80%) belonging to the TetR-like transcriptional regulator family. Because of this homology, the *orf* immediately downstream of *alkB* gene cluster was named *tetR*. A helix-turn-helix motif (PROSITE signature PS50977) involved in DNA binding was predicted in the N-terminal region of BCP1 TetR amino acid sequence (Fig. 4.9), which is typical of members of this family. Transcriptional regulators belonging to TetR family have been described mapping near by *alkB* gene clusters in other actinobacteria [195].
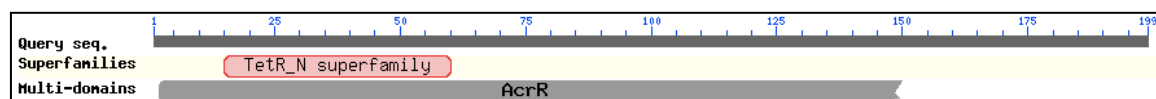
Fig. 4.9 Putative conserved domain identified in the amino acid sequence of TetR. Putative conserved domains have been detected by Conserved Domain Database (CDD). The upper bar indicates the entire protein of TetR. The red bar suggests a TetR N domain (pfam00440) from 15 to 60 amino acid residues. The grey bar suggests the presence of a AcrR multi-domain (COG1309) from 2 to 150 amino acid residues.

4.3.3.1 Open question: how many *alkB* gene copies are present in *Rhodococcus* sp. BCP1 genome?

An interesting question at this point of our research work was referred to whether or not BCP1 contained additional *alkB* homologues. The hybridization of 8 kb-long fragment in the Southern blot corresponding to the *KpnI*-digestion of pAlk3 cosmid diverged in dimension from the hybridization band detected in the *KpnI*-digestion of the pAlk1 cosmid (10.5 kb). This consideration prompted us to attempt to investigate on the presence of at least another *alkB* gene. Thus, an additional Southern blot was carried out hybridizing the 550-bp *alkB probe* with the BCP1 genomic DNA enzimatically restricted by the following rare-cutter enzymes, *EcoRI*, *PstI*, *BamHI*, *SacI* and *KpnI*.

104
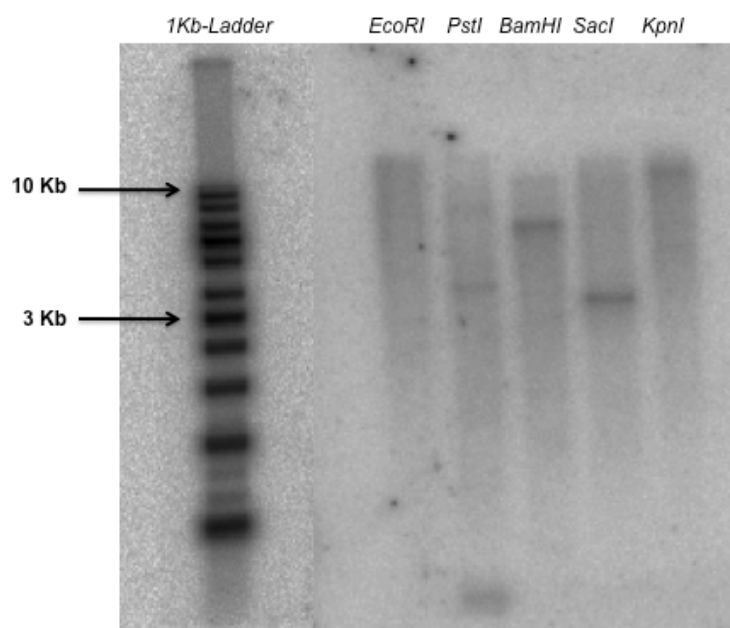
Fig. 4.10 Southern blot on the BCP1 genomic DNA digested with the enzymed indicated above each line.

As shown in Fig. 4.10, the dimensions of the *alkB* probe hybridizing bands obtained by digesting the BCP1 genomic DNA with *SacI* and *KpnI* corresponded to the dimensions of the restriction fragments expected for the BCP1 *alkB* gene that we had already isolated (hereafter named as BCP1 *alkB*). By contrast, the positive bands detected in the *BamHI* and *PstI* digestions of the BCP1 genomic DNA did not match with the dimensions of the fragments expected from the same restriction of BCP1 *alkB*. This result can be due to an inefficient digestion of the BCP1 genomic DNA performed by these two enzymes. The partially ineffective restriction activity would explain the detection of positive bands in *BamHI* and *PstI* digestions with dimensions higher than those expected. In particular the *BamHI* positive band (around 7 kb) seems to correspond to the genomic DNA *BamHI*-fragment including BCP1 *alkB* gene that was not cut in correspondence of one *BamHI* site inside the sequence.

4.3.4 Characterization of *alkB* gene flanking regions from Rhodococcus sp. BCP1

Further BLAST analysis focused on the *alkB* upstream flanking regions included in the 10.5 kb DNA fragment of *Rhodococcus* sp. BCP1 cloned in pMC1. Based on its comparison with the sequences in the database, the direction of transcription and the product of each *orf* was

predicted (Fig. 4.11, Table 4.1). *orfA* product showed the highest homology with the *Rhodococcus jostii* RHA1 hypothetical protein_ro05201 (YP_705140). The BCP1 OrfA amino acid sequence comprised the putative peptidoglycan binding domain (pfam12229) and part of the VanW like protein conserved domain (pfam 04294). Both pfam12229 and pfam04294 constitute the COG2720 conserved domain typical of uncharacterized vancomycin resistance proteins, supposedly involved in defense mechanisms.
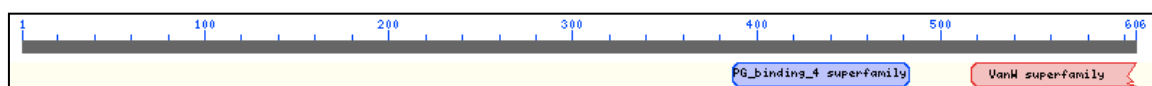
Fig. 4.12 Putative conserved domains identified in the aminoacid sequence of OrfA.

orfB and *orfC* code for an acetyl-CoA acyltransferase and for a 3-oxoacyl-[acyl-carrier-protein] reductase, respectively, while OrfD was predicted to be a MaoC-like dehydratase.

Fig. 4.13 Putative conserved domains identified in the amino acid sequence of OrfB.
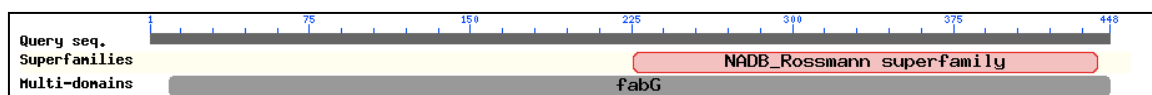
Fig. 4.14 Putative conserved domains identified in the amino acid sequence of OrfC.
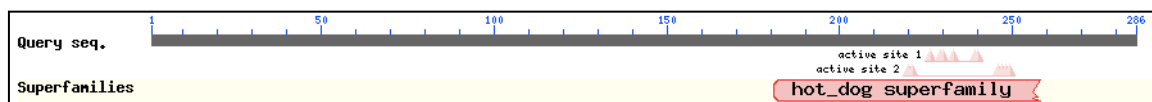
Fig. 4.15 Putative conserved domains identified in the amino acid sequence of OrfD.

Immediately upstream of the *alkB* region, two consecutive ORFs were designed *orfE* and *orfF*. OrfF shows the highest homology to the transcriptional regulator SCO5758 of *Streptomyces coelicor* A3 (67%). The predicted amino acid sequence of OrfF displays the ArsR-type HTH domain (PROSITE signature PS50987) that is a DNA-binding, winged helix-turn-

106

helix (wHTH) domain present in prokaryotic metal-sensing transcription repressors, involved in stress-response to heavy metal ions (Fig. 4.17). OrfE showed the highest homology to the hypothetical protein SvirD4_31611 of *Streptomyces viridochromogenes* DSM 40736 (ZP_05534994) and displays the pfam05146 domain that is a conserved domain typical of polyketide cylcase/dehydrase superfamily of proteins, these enzymes being involved in the biosynthesis of secondary metabolites and/or fatty acid transportation (Fig. 4.16). Interestingly, OrfE amino acid sequence showed also high homology to the hypothetical protein SCO5759 of *Streptomyces coelicolor* A3(2) (72%) that is located, in the genome of *Streptomyces*, consecutively to the transcriptional regulator SCO5758, previously described for being the homologues to the BCP1 OrfF protein. The conservation of the relative positions of *orfE* and *orfF* in BCP1 with the two homologues (SCO5759 and SCO5758, respectively) found in *Streptomyces* suggests a joint function of the two genes products.
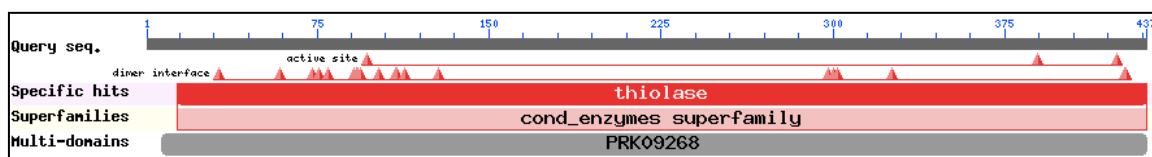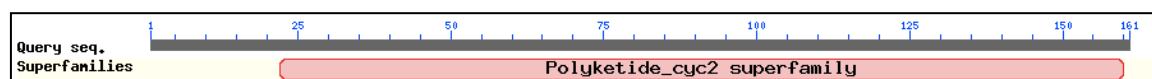

Fig. 4.16 Putative conserved domains identified in the amino acid sequence of OrfE
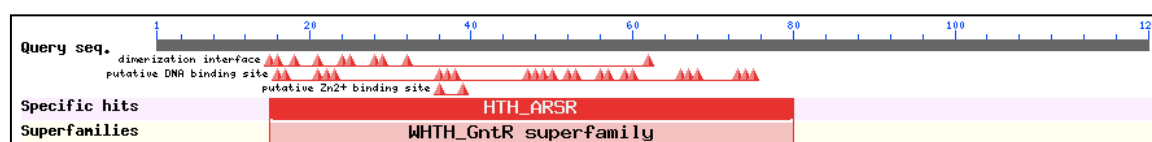
Fig. 4.17 Putative conserved domains identified in the amino acid sequence of OrfF.

4.4 Discussion

In this study a gene coding for an alkane monooxygenase has been isolated from *Rhodococcus* sp. BCP1 using the *alkB* primer set described by Smith *et al.* [180]. A 550 bp PCR fragment was amplified and it was used as a probe to isolate and clone the 10.5 kb genomic region of BCP1 including the *alkB* gene cluster and the flanking regions.

The *alkB* genes have been genetically described in a relative little number of *Rhodococcus* strains including *Rhodococcus opacus* B4 [311] and *Rhodococcus* strains NRRL B-16531 and Q15 [195] whereas the complete *alkB* operons of *Rhodococcus erythropolis* PR4, *Rhodococcus jostii* RHA1 [257], *Rhodococcus erythropolis* strain T7-2 [339] and *Rhodococcus erythropolis* SK121 [294] are available in the database but they have not been further described.

A molecular study aimed to characterize the *alkB* gene product was carried out. The results from the AlkB homology studies with homologues in the database, the identification of typical conserved histidine motifs in the AlkB amino acid sequence and the prediction of a six α-helics secondary structure folding indicated that the BCP1 *alkB* gene codes for an alkane monooxygenase belonging to the integral-membrane non-heme di-iron monooxygenase family. The *alkB* gene resulted to be adjacent to genes encoding two rubredoxins and a rubredoxin reductase that are required in the catalytic process as electron-transfer proteins (for a detailed description of AlkB monoxygenase family, Chapter 1 § 1.3.4.3).
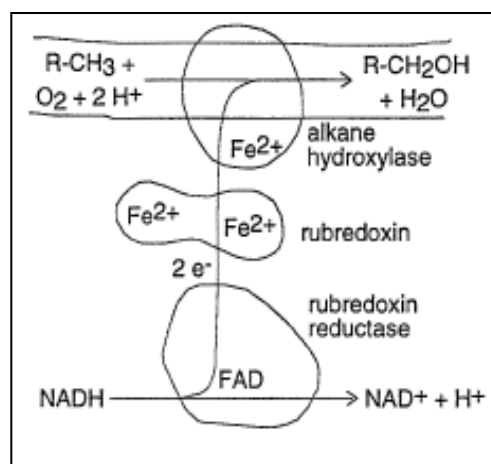
Fig. 4.18 Membrane localization of the AlkB monooxygenase in *Pseudomans putida* GPo1 with the indication of the three components that consitute the AlkB system (§ 1.3.4.3 Introduction).

The phylogenetic analysis of BCP1 AlkB showed the highest similarity with the corresponding members of *Rhodococcus jostii* RHA1 and with the two *alkB* genes described in *Rhodococcus opacus* B4. The head-to-tail genetic organization of *alkB* cluster displayed the phenomenon of overlapping of stop-codons with start-codons that suggests translational coupling

[297] and that is a characteristic of other *alkB* gene cluster in actynomyceta genera. Similarly, the organization in a operon-like structure of the genes coding for the components of AlkB is mostly maintained amongst the *Rhodococcus* strains (red boxes in Fig. 4.19). Only in *Rhodococcus erythropolis* PR4 the final *orf* of the cluster (rubredoxin reductase coding region) was not following the other three *orfs* (*alkB* and the two rubredoxins) (green box in Fig. 4.19).

Rhodococcus sp. BCP1
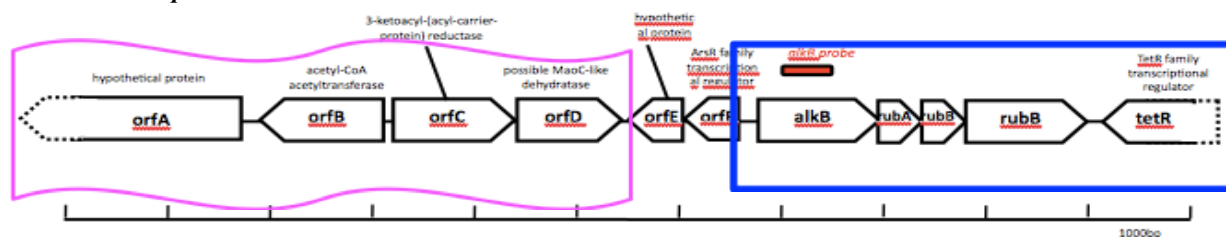
Rhodococcus opacus B4 - *alkB1* (genomic DNA) (ROP_22480, ROP_22490, ROP_22500, ROP_22510, ROP_22520, ROP_22530, ROP_22540, ROP_22550, ROP_22560, **ROP_22570**, ROP_22580, ROP_22590, ROP_22600, ROP_22610)
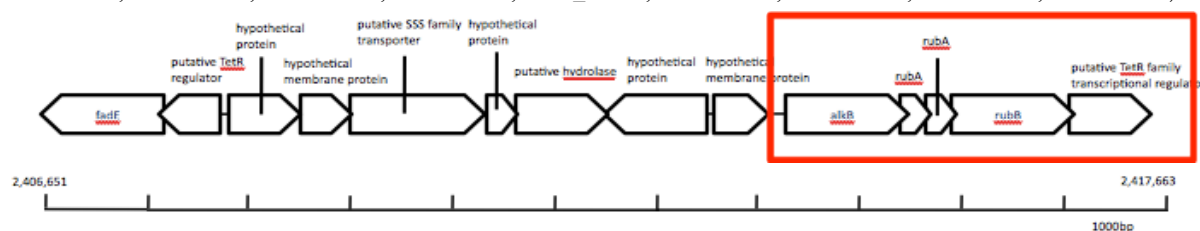
Rhodococcus opacus B4 - *alkB2* (pROB01 endogenous plasmid) (ROP_pROB01_04260, ROP_pROB01_04270, ROP_pROB01_04280, ROP_pROB01_04290, ROP_pROB01_04300, ROP_pROB01_04310, ROP_pROB01_04320, ROP_pROB01_04330, ROP_pROB01_04340, **ROP_pROB01_04350**, ROP_pROB01_04360, ROP_pROB01_04370, ROP_pROB01_04380, ROP_pROB01_04390)
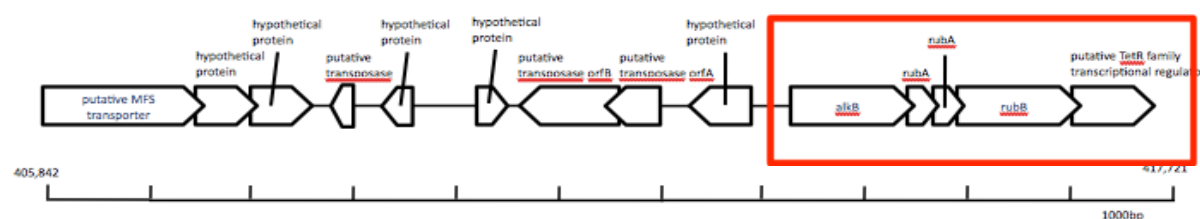
Rhodococcus jostii RHA1 (RHA1_ro02523, RHA1_ro02524, RHA1_ro02525, RHA1_ro02526, RHA1_ro02527, RHA1_ro02528, RHA1_ro02529, RHA1_ro02530, RHA1_ro02531, RHA1_ro02532, RHA1_ro02533, **RHA1_ro02534**, RHA1_ro02535, RHA1_ro02536, RHA1_ro02537, RHA1_ro02538)
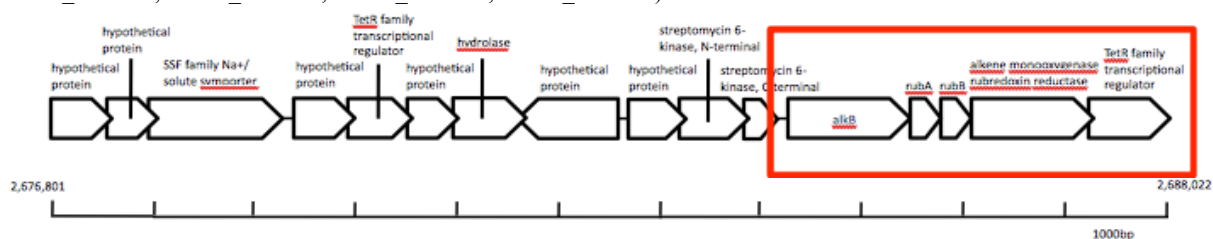
Rhodococcus erythropolis PR4 (RER_21540, RER_21550, RER_21560, RER_21570, RER_21580, RER_21590, RER_21600, RER_21610, **RER_21620**, RER_21630, RER_21640, RER_21650)
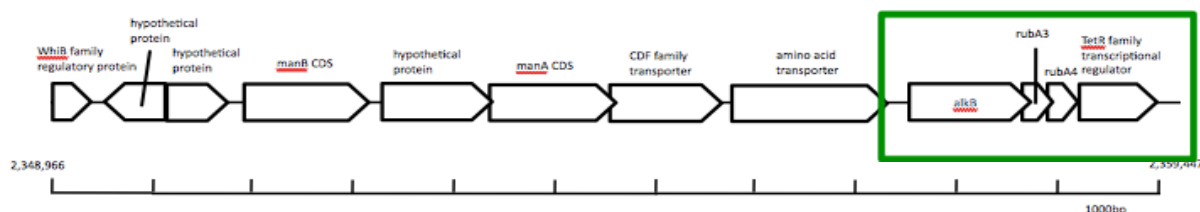
Fig. 4.19 Analysis of 10.5 kb long genomic regions containing the *alkB* gene in related *Rhodococcus* strains. Rectangular boxes with the same colour indicate identical genetic organization of *alkB* gene cluster, also including *tetR* gene. The pink wavy box indicates the *orfA-orfD* region under investigation in BCP1. The locus tags of the orfs included in each *Rhodococcus* 10.5 kb fragment are reported in order between brackets but the BCP1 *orfs* that have not been deposited in database yet.

The presence of other *alkB* homologues in *Rh.* BCP1 genome is still unclear, since the data from colony and southern blot on BCP1 genome were not clear. On the other hand, it is also known that multiple copies of this gene are present amongst *Rhodococcus* strains. Indeed, *Rhodococcus opacus* express two *alkB* genes [311], one mapping in the genome and the other locates on an endogenous plasmid, *Rhodococcus* sp. NRRL B-16531 and sp. Q15 have at least four *alkB* genes [195] while *Rhodococcus* TMP2 has five *alkB* homologues [312]. The only example of *Rhodococcus* strain containing a single *alkB* gene copy is *Rh. jostii* RHA1 [257].

The analysis of the *alkB* gene flanking regions revealed the presence of two putative transcriptional regulators adjacent to *alkB*. A putative Tet-R type transcriptional regulator gene has been found immediately downstream of the *alkB* gene similarly to genetic organization of *alkB* clusters of other *Rhodococcus* strains as well as other actinomycetes (Fig. 4.19). The conservation of the relative position of a Tet-R like protein in proximity of *alkB* gene cluster has already been hypothesized having a role in the alkane-inducing response [297] even though the actual function of this TetR-like transcriptional regulator on *alkB* gene expression has not been characterized yet. Interestingly, in the BCP1 related *Rhodococcus* strains the TetR transcriptional regulator is transcribed in the same direction as the *alkB* gene cluster; by contrast, the BCP1 transcriptional regulator seems to be transcribed divergently from the *alkB* gene (Fig. 4.19, blue box). The *orfF* upstream of BCP1 *alkB* gene also encodes a transcriptional regulator belonging to the ArsR-type transcriptional regulator family that displays the helix-turn-helix motif as DNA binding domain (ArsR HTH domain), that, for instance, has been found in the amino acid sequence of prokaryotic metal-sensing transcription repressors, involved in stress-response to heavy metal ions. *orfF* gene is consecutive to *orfE* whose product amino acid sequence revealed a polyketide_cyc2 region that is a domain conserved amongst enzymes involved in the polyketide synthesis and in lipid transport. Polyketide are secondary metabolites that are biosynthetized through condensation steps similar to those described in fatty acid synthesis. The

consecutive organization of *orfE* and *orfF* was shown to be conserved in other bacteria like *Streptomyces coelicor* A3(2), *Conexibacter woesei*, *Rhodococcus jostii* RHA1, *Mycobacteria* strains and *Arthrobacter* strains, suggesting a functional coupling in regulating target genes transcription.

The 5'-region of the *KpnI*-fragment harbours *orfA*, *orfB*, *orfC* and *orfD* genes that encode a hypothetical protein, a MaoC-like dehydratase, a 3-oxoacyl-[acyl-carrier-protein] reductase, a probable thiolase and an acetyl-CoA acetyltransferase, respectively. Although OrfA sequence is not complete, a peptidoglican binding protein domain and a VanW domain were found in the primary sequence and both together constitute the COG2720 conserved domain present in uncharacterized vancomycin resistance protein, supposedly involved in defense mechanisms. The other proteins are oxidoreductases putatively involved in the fatty acid biosynthesis. Interestingly, although the *orfA*, *orfB*, *orfC* and *orfD* location in proximity to *alkB* has been reported only in *Rh.* BCP1, their homologues resulted being consecutive in all the related *Rhodococcus* strains and also in *Nocardia farcinica* IFM 10152 that is another actinobacterium whose genome has been completely sequenced. The maintenance of their relative position suggests an association in the function of the protein expressed by these genes. The *orfA-D* cluster homologues in the BCP1 related *Rhodococcus* strains are followed by a gene encoding a TetR transcriptional regulator. By contrast, in BCP1, the *orfA-D* cluster is followed by an ArsR transcriptional regulator (OrfF). Since the transcriptional regulator component (OrfF) has helix-turn-helix DNA binding site and the hypothetical protein OrfE contains the polyketide_cyc2 that is a binding region for fatty acid like molecules, it can be speculated that they could jointly act for a fatty acid-dependent response. Thus, it can be proposed that these two components (OrfE and OrfF) replaced in BCP1 the function that TetR family transcriptional regulator may have on the *orfA-orfD* cluster homologues in the other *Rhodococcus* strains. Another possibility would assign a role in *orfA-orfD* regulation to the TetR transcriptional regulator that is transcribed

downstream of the *alkB* gene cluster. However, it is important to notice that TetR-like transcriptional regulators are the most common transcriptional regulators in *Rhodococcus* strains. Indeed, in *Rhodococcus jostii* RHA1 178 regulators belonging to this group have been identified. Owing to this, it would be difficult to assign a regulatory function to TetR-like regulators of a certain gene cluster simply because of the proximity of their coding genes.

Furthermore, it is believed that the growth on *n*-alkanes promotes the perturbation of the bacterial membrane structure in response to the contact with the alkane solvent molecule and in response to the accumulation of AlkB alkane hydroxylase protein in the inner membrane [340]. Regarding to this, Chen *et al.* [221] observed an increase in the production of unsaturated fatty acids lipids during the growth of *Pseudomonas putida* GPo1 on *n*-alkanes. The up-regulation of enzymes involved in the synthesis of unsaturated fatty acids was therefore associated with the need to maintain the membrane fluidity and integrity and to compensate the perturbation caused by the growth on *n*-alkanes in *Ps*. GPo1. Moreover, a recent study of Sabirova *et al* [75] showed the alkane-induced expression of enzymes involved in fatty acid biosynthesis also in *Alcanivorax borkumensis*. Since the *orfA-D* genes seem to code for enzymes involved in the unsaturated fatty acids biosynthesis, the BCP1 genomic region that maps for *orfA-D* and *alkB* gene cluster might be involved in the bacterial adaptation to growth on *n*-alkanes.

4.5 Summary

In this study a new *alkB* gene cluster has been identified in *Rhodococcus* sp. BCP1. Homologies and differences in sequence and organization have also been described by comparing the BCP1 alkane monooxygenase with other AlkB described in related *Rhodococcus* strains. As a result, the peculiar presence in BCP1 of two transcriptional regulators divergently transcribed from *alkB* gene cluster was analyzed. Orfs located in the 5' region of the 10 kb fragment including the *alkB* gene cluster were also characterized and the results of homology

studies in sequence and genetic organization suggested a role of the entire 10.5 kb long genomic

region in the metabolism associated with the growth on *n*-alkanes in *Rhodococcus* sp. BCP1.
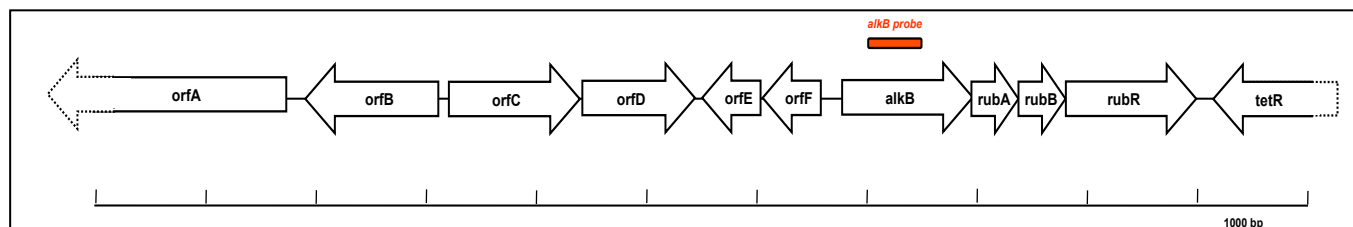
orfA: Hypothetical protein (PG_binding_4, VanW superfamily)

orfB: Acetyl-CoA acetyltransferase

orfC: 3-ketoacyl-(acyl-carrier-protein) reductase

orfD: MaoC-like dehydratase

orfE: Hypothetical protein (Polyketide_cyc2 superfamily)

orfF: ArsR family transcriptional regulator

alkB: Alkane 1-monooxygenase

rubA: Rubredoxin A

rubB: Rubredoxin B

rubR: Rubredoxin reductase

tetR: TetR family transcriptional regulator

Fig. 4.1 Genetic organization and restriction map of the *Rhodococcus* sp. BCP1 10.5 kb region including the *alkB* gene cluster and the flanking regions. Shaded in red is the *alkB probe*. *orfs* with predicted function based on the sequence similarities with protein sequences in the database are indicated. The conserved domains in the amino acid sequences of the hypothetical proteins are reported between brackets. See Table 2.1 for details.

Table 4.1 Summary of the Orfs identified in 10.5 kb long genomic region containing *alkB* gene in *Rhodococcus* sp. BCP1. The following are provided for each Orf sequence: a) conserved domains and motifs; b) most representative protein homologues in database; c) corresponding identity percentages calculated by Clustal W algorithm.

ORF name	Direction of transcription[a)]	Start codon	AA	Significant Conserved domains	Probable function	Representative homologues	Identity (%)	Protein ID	Ref.
OrfA	reverse	GTG	606	pfam12229 (370-483)	**Hypothetical protein**	hypothetical protein _ro05201 *Rhodococcus jostii* RHA1	43%	YP_705140	[258]
				pfam 04294 (517-606)		hypothetical protein ROP_52510 *Rhodococcus opacus* B4	43%	YP_00278244	[293, 339]
						VanW like protein *Rhodococcus erythropolis* SK121	40%	ZP_04388121	[295]
						hypothetical protein RER_11220 *Rhodococcus erythropolis* PR4	38%	YP_002764569	[293, 294]
OrfB	reverse	GTG	437	cd00751 (14-437)	**Acetyl-CoA acyltransferase**	acetyl-CoA acyltransferase *Rhodococcus opacus* B4	84%	YP_002782442	[293, 339]
				pfam02803 (289-437)		acetyl-CoA acyltransferase *Rhodococcus jostii* RHA1	84%	YP_705139	[258]
						3-ketoacyl-CoA thiolase *Rhodococcus erythropolis* SK121	82%	ZP_04387911	[295]
						acetyl-CoA acyltransferase *Rhodococcus erythropolis* PR4	82%	YP_002764568	[293, 294]
						acetyl-CoA acetyltransferase *Nocardia farcinica* IFM 10152	78%	YP_121676	[340]
OrfC	forward	GTG	448	pfam00106 (209-373)	**3-oxoacyl-[acyl-carrier-protein] reductase**	3-oxoacyl-[acyl-carrier-protein] reductase *Rhodococcus erythropolis* PR4	80%	YP_002764567	[293, 294]
						putative 3-oxoacyl-[acyl-carrier-protein] reductase *Rhodococcus opacus* B4	79%	YP_002782441	[293, 339]
						3-ketoacyl-(acyl-carrier-protein) reductase *Rhodococcus jostii* RHA1	79%	YP_705138	[258]
						3-ketoacyl-(acyl-carrier-protein) reductase *Nocardia farcinica* IFM 10153	75%	YP_121677	[340]
						short-chain dehydrogenase/reductase SDR *Gordonia bronchialis* DSM 43247	70%	YP_003275480	[341]

Table 2.1 *Continues*

OrfD	forward	GTG	286	pfam01575 (181-262)	**MaoC-like dehydratase**	MaoC-like dehydratase *Rhodococcus jostii* RHA1	75%	YP_705137	[258]
						putative enoyl-CoA hydratase *Rhodococcus opacus* B4	75%	YP_002782440	[293, 339]
						MaoC like domain protein *Rhodococcus erythropolis* SK121	72%	ZP_04388128	[295]
						hypothetical protein RER_11190 *Rhodococcus erythropolis* PR4	72%	YP_002764566	[293, 294]
						putative dehydratase *Nocardia farcinica* IFM 10154	63%	YP_121678	[340]
OrfE	reverse	ATG	161	pfam08327 (22-160)	**Hypothetical protein**	uncharacterized conserved protein *Stackebrandtia nassauensis* DSM44728	74%	ZP_04486811	[342]
						hypothetical protein SvirD4_31611 *Streptomyces viridochromogenes* DSM 40736	73%	ZP_05534994	[343]
						hypothetical protein SCO5759 *Streptomyces coelicolor* A3(2)	73%	NP_629884	[344]
						hypothetical protein SghaA1_08328 *Streptomyces ghanaensis* ATCC 14672	72%	ZP_04685171	[345]
						Activator of Hsp90 ATPase 1 family protein *Conexibacter woesei* DSM 14684	61%	YP_003392294	[346]
OrfF	reverse	ATG	162	cd00090 (15-80)	**Transcriptional regulator**	transcriptional regulator *Streptomyces coelicolor* A3(2)	67%	NP_629883	[344]
				smart00418 (25-90)		transcriptional regulator *Streptomyces viridochromogenes* DSM 40736	65%	ZP_05534993	[343]
						putative transcriptional regulator, ArsR family *Conexibacter woesei* DSM 14684	65%	YP_003392295	[346]
						transcriptional regulator *Streptomyces ghanaensis* ATCC 14672]	63%	ZP_04685172	[345]
AlkB	forward	GTG	407	cd03512 (57-379)	**Alkane-1-monooxygenase**	alkane-1-monooxygenase *Rhodococcus opacus* B4	84%	YP_002779449	[293, 339]

Table 2.1 *Continues*

				pfam00487 (133-346)			alkane-1-monooxygenase *Rhodococcus jostii* RHA1	82%	YP_702497	[258]
							alkane-1-monooxygenase *Rhodococcus opacus* B4	81%	YP_002776786	[293, 339]
							alkane-1-monooxygenase *Rhodococcus erythropolis* PR4	79%	YP_002765609	[293, 294]
RubA	forward	ATG	53	cd00730 (4-51)	**Rubredoxin A**	alkene monooxygenase rubredoxin *Rhodococcus jostii* RHA1	76%	YP_702498	[258]
				pfam00301 (4-45)		rubredoxin *Rhodococcus opacus* B4	76%	YP_002779450	[293, 339]
						putative rubredoxin *Nocardia farcinica* IFM 10152	75%	YP_120832	[340]
						rubredoxin *Rhodococcus erythropolis* PR4	70%	YP_002765610	[293, 294]
RubB	forward	ATG	61	cd00730 (8-56)	**Rubredoxin B**	rubredoxin RubB_1 *Mycobacterium ulcerans* Agy99	86%	YP_906527	[347]
				pfam00301 (8-53)		rubredoxin *Rhodococcus opacus* B4	85%	YP_002779451	[293, 339]
						rubredoxin RubB *Mycobacterium tuberculosis* H37Rv	85%	NP_217767	[192, 348]
						alkene monooxygenase rubredoxin *Rhodococcus jostii* RHA	81%	YP_702499	[258]
RubR	forward	ATG	413	pfam00070 (144-224)	**Rubredoxin reductase**	rubredoxin reductase *Rhodococcus opacus* B4	57%	YP_002779452	[293, 339]
				pfam07992 (20-280)		alkene monooxygenase rubredoxin reductase *Rhodococcus jostii* RHA1	56%	YP_702500	[258]
						rubredoxin reductase *Rhodococcus opacus* B4	54%	YP_002776789	[293, 339]
						rubredoxin reductase *Rhodococcus* sp. Q15	47%	AAK97451	[195]
TetR	reverse	N/D[b]	414	pfam00440 (15-60)	**Transcriptional regulator**	transcriptional regulator *Rhodococcus jostii* RHA1	80%	YP_705136	[258]

122

Table 2.1 *Continues*

	putative transcriptional regulator *Nocardia farcinica* IFM 10152	67%	YP_121680	[340]
	TetR family transcriptional regulator *Mycobacterium gilvum* PYR-GCK	58%	YP_001131696	[349]

a) respect to the direction of transcription of *alkB* gene
b) N/D= notdetermined

CHAPTER 5. Analysis of the *alkB* gene expression

5.1 Introduction

The mechanisms that regulate the expression of the genes involved in the initial oxidation of alkanes have been described mostly in *Pseudomonas*, *Alcanivorax* and *Burkholderia*. Regulators such as LuxR/MalT, AraC/XylS and GntR were found to be involved in alkane-degrading gene induction which depends on the presence of the appropriate alkanes or/and according to the environmental or physiological conditions (Chapter 1, § 1.3.4.6)

Although several *Rhodococcus* strains have been isolated from oil-contaminated sites and Rhodococci are thought to play a major role in hydrocarbon biodegradation processes, little is known about the mechanisms that regulate the expression of the genes coding for hydroxylases involved in *n*-alkanes degradation pathways in *Rhodococcus* strains. The work by Sameshima *et al.* [311] analysed the *Rhodococcus opacus* B4 *alkB* expression induced by *n*-alkanes in organic solvents. *Rhodococcus opacus* was shown to express two *alkB* genes, namely: *alkB1,* located on genomic DNA and *alkB2* located on one of the three endogenous plasmids, named pROB1. It was demonstrated that only *alkB1* expression was induced by the presence of *n*-alkanes even in organic solvents. By contrast, *alkB2* expression did not seem to be alkane-dependent. Takei *et al* [312] focused their attention on five *alkB* gene homologues of *Rhodococcus* sp. strain TMP2. Through the use of RT-PCR it was shown that only the expression of *alkB1* and *alkB2* was induced by the presence of *n*-alkanes while *alkB3–5* genes were constitutively expressed. However, neither of these studies focused on the molecular characterization of the *alkB* promoter, on the detection of operon-like structure of the *alkB* gene cluster nor on the possible regulatory functions played by *n*-alkane metabolic pathway intermediates on the first oxidation.

In Chapter 4, the detection of *alkB* gene in BCP1 genomic DNA has been described. Indeed, *alkB* gene regulation study is required to determine the role that the AlkB hydroxylase plays in *Rhodococcus* sp. BCP1 physiology during growth on *n*-alkanes. This present Thesis work aims to provide a detailed analysis of the BCP1 *alkB* gene promoter by primer extension assay and by homology study with homologues regions in related *Rhodococcus* strains. Moreover, the co-transcription of the genes composing the *alkB* gene cluster and the *alkB* promoter activity in response to the presence of *n*-alkanes, has been reported. Possible *alkB* promoter regulatory mechanisms have also been investigated by examining the *alkB* promoter activity in the presence of either alternative carbon sources or putative *n*-alkane metabolism intermediates.

5.2 Materials and Methods

5.2.1 Primer Extension

Primer extension studies were basically performed as described by Roncarati *et al* [341]. Transcription from the *alkB* promoter was assayed by primer extension analysis using two 19-mer oligonucleotides named PrEx2 (5'-AGCCCCATGAGCCACAGAT-3') and PrEx8 (5'-ATCAGCCCCATGAGCCACA-3'). An oligonucleotide (5 pmol) was 5' end labelled in the presence of $[\gamma\text{-}^{32}P]$ATP (5,000 Ci/mmol; Amersham) and T4 polynucleotide kinase. The labelled oligonucleotide (0.1 pmol) was co-precipitated with 15 μg of *Rh.* BCP1 total RNA and resuspended in 7.5 μl of H_2O, 3.5 μl of 2 mM deoxynucleoside triphosphates, and 3 μl of 5x reverse transcription buffer (Promega). The reaction mixtures were incubated for 3 min at 95°C and for 1 min at 42°C, and then 1 μl of avian myeloblastosis virus reverse transcriptase (10 U/μl; Promega) was added to each sample and reverse transcription was carried out by incubating the samples at 42°C for 45 min. Samples were then incubated for 10 min at room temperature with 1 μl of RNase A (1 mg/ml), extracted with phenol-chloroform

(1:1), ethanol precipitated, and resuspended in 10 μl of sequencing loading buffer. After denaturation at 95°C for 2 min, samples were subjected to 6% urea–polyacrylamide gel electrophoresis and autoradiographed. To map the *alkB* promoter, T7 sequencing kit (USB) was used to sequence plasmid pMC6 (1.6 kb DNA fragment including BCP1 *alkB* gene and corresponding upstream region inserted in pUC18, Fig. 4.5) in parallel with the same oligonucleotide as the Primer Extension (PrEx2 or PrEx8). The primer extension assays were performed on RNA isolated from grown BCP1 cells grow till early stationary phase that after that they were exposed for four hours to butane, *n*-hexane, *n*-dodecane and succinate as described in Chapter 2 (§ 2.3.1).

5.2.2 Nucleotide alignment of the BCP1 *alkB* promoter region with the *alkB* promoter region of other *Rhodococcus* strains.

The nucleotide sequence of the 210-bp *alkB* promoter region of *Rh*. BCP1 was aligned with the homologues regions of other related *Rhodococcus alkB* genes. The related *Rhodococcus* strains that have been used in the comparison study are: *Rhodococcus erythropolis* PR4 [292, 293], *Rhodococcus opacus* B4 [292, 342], *Rhodococcus jostii* RHA1 [257] and *Rhodococcus erythropolis* SK121 [294] The program Clustal W (http://www.ebi.ac.uk/clustalw/) was used for the nucleotide sequences alignment with the following parameters: Cost matrix, BLOSUM; Gap open cost, 10; and Gap extend cost, 0.1.

5.2.3 RT-PCR

To establish whether the genes coding for the AlkB components are transcribed in operon-like structure, total RNA was extracted from BCP1 cells that were grown till early stationary phase in MMenr medium after that they were exposed to *n*-hexane for four hours as described in General Materials and Methods chapter (Chapter 2 § 2.3). For cDNA synthesis, total RNA was incubated for 60 min at 37°C with Omniscript reverse transcriptase (QIAGEN) (RT step). Control reactions to assess the level of DNA contamination in the RNA samples

were carried out omitting only the reverse transcriptase. Primers RT1 and RT2 were used for the RT reaction, and pairs of primers, F1-R1 and F1-R2, were used for successive PCR amplification (PCR step). The thermal cycling conditions were as follows: 1 min at 94°C, followed by 25 cycles of 30 s at 98°C and 10 min at 72°C with Taq polymerase (La Roche). The sequences of the primers used in this study are reported in Table 5.1.

Table 5.1 Primers used in the *alkB* gene cluster co-transcription analysis

Primers	Oligonucleotide Sequence	Reference
RT1	5'-CGGACGTGTCGTGCTGATC-3'	This work
RT2	5'-GATCACCACGCGAACCCGA-3'	This work
F1	5'-TACATCGAGCACAACCGCGGC-3'	This work
R1	5'- ACGTCGTTACGCAGGGTCCAC -3'	This work
R2	5'-TGACGATGTGGTCGGAGTT -3'	This work

5.2.4 Construction of the *alkB* promoter (*PalkB*) probe vector with *E. coli lacZ* as reporter gene

The *lacZ* gene of *E.coli* W1130 genome was amplified by PCR with primers PLacF (5'-ATCATCGCGACCACCATGATTACGGATTCACTGG-3') and PLacR (5'-ATCAGCATGCTTATTTTTGACACCAGACCAACTG-3') containing *NruI* and *SphI* restriction sites (underlined in the corresponding oligonucleotides), respectively. In order to obtain a translational fusion product with *E. coli lacZ* gene downstream of *PalkB*, the amplicon was digested by *NruI* and *SphI* and cloned into the pMC3 vector replacing the 2111-bp *NruI-SphI* fragment that included the *alkB* gene (from nt 155), *rubA*, *rubB* and part of the rubredoxin reductase coding gene. The resulting vector was designed pMC3::LacZ. The PLacF primer included 2 more nucleotides (in red in the oligonucleotide) before the restriction site in order to keep the *lacZ* gene in frame with the *alkB* start codon (GTG). pMC3::LacZ was used as template in PCR with the primers PalkLF (5'-

ACT<u>TGTACA</u>GTCGTTCCTTCCTGACGA-3') and PalkLR (5'-ACT<u>AGATCT</u>TGCGCTGTTCCAGTTCTCCGT-3') containing *BsrGI* and *BglII* restriction sites (underlined in the oligonucleotide sequences), respectively. The *BsrGI-BglII* digested amplicon was cloned into pTipQT2 (Chapter 2, Table 2.1) causing the elimination of both pTipA promoter and multi cloning site. The resulting plasmid was named pTP$_{alkB}$LacZ. Competent *E. coli* DH5α cells were transformed with the ligation product and recombinant clones were selected on LB agar plates containing ampicillin (50 μg/mL). Recombinant plasmid was purified and introduced in *Rhodococcus* sp. BCP1 by electroporation using the protocol described in Chapter 2 (§ 2.8). The cells were, then, recovered in TSB for 5-6 hours and spread out onto TSB agar plates supplemented with tetracycline (10 μg/mL). BCP1 cells transformed with pTP$_{alkB}$lacZ plasmid appeared on plates after 4 to 5 days of incubation at 30 ºC.

5.2.5 *alkB* promoter (*PalkB*) activity analysis by β-galactosidase assay

5.2.5.1 Exposition to the substrates

1 mL of 2 days LB pre-cultured pTP$_{alkB}$LacZ BCP1 cells was used to inoculate four 500 mL-flasks containing 100 mL of LB each supplemented with tretracycline (5μg/mL) (ratio inoculum/media volume: 1/50). The cultures were incubated at 30 ºC for 50 hours at 200 rpm until the pre-stationary phase of growth was reached. The pTP$_{alkB}$LacZ cells were washed with 100 mL of 25 mM phosphate buffer (pH 7.2) and resuspended in 400 mL of minimal medium (MM) supplemented by tetracycline (5μg/mL). Sixteen 150 mL-bottles were filled with 25 mL of cell suspension each and after the substrate was added to each bottle, the cultures were sealed with butyl rubber stoppers and aluminium crimps and they were incubated at 30 ºC in a rotary shaker at 200 rpm. After different incubation times (10, 18 and 24 hours), 1 mL-aliquots from each bottles were collected in microfuge tubes and were harvested. The pellets were then washed with 25 mM phosphate buffer (pH 7.2) and they

were stored at -20ºC for later use after resuspension in 100 μL of breaking buffer (Tris/HCl 100 mM pH 7.5, glycerol 20%).

5.2.5.2 β-galactosidase assay

The pTP$_{alkB}$LacZ cells to be assayed were thawed on ice and then 400 μL of buffer Z (40mM Na$_2$HPO$_4$•7H$_2$O, 60mM NaH$_2$PO$_4$•H$_2$O, 10mM KCl, 1mM MgSO$_4$•7H$_2$O, 50mM 2-Mercaptoethanol, pH 7.0) was added to each aliquot. At first, the β-galactosidase assay described by Miller [343] that measures a promoter activity in Miller units, was shown not to work for *Rhodococcus* sp. BCP1. Considering the resistance opposed by *Rh*. sp. BCP1 to enzymatic and chemical treatment of lyses and to electroporation procedures that had challenged the manipulation of this microorganism in all the experiments, it was hypothesised that the limiting step in the Miller protocol was the permeabilization of the cells by addition of SDS and chloroform. Thus, the β-gal assays were performed by using the crude extraction method mostly used in yeasts as described by Rose and Botstein [344]. According to this method, the β-galactosidase activity was calculated as specific activity (nmoles/minutes/mg protein). The protocol that follows was optimized for measuring β-gal activity in pTP$_{alkB}$LacZ BCP1 cells. The resulting 500 μL of cell suspension (100 μL of cell+400 μL of buffer Z) was transferred into 2 mL tubes with approximately 0.25 mL of nitric acid pre-washed quartz beads (0.2-0.8 mm-diameter, MERCK KGaA, Germany). The cells were subjected to lyses by bead beater grinding treatment as follows: 5 cycles, 30 seconds each cycle at 6000 m/s (Precellys®24 *bead beater, Bertin* Technologies). The cells were kept on ice for 2 minutes after each cycle to inhibit over warming of the samples. After the lyses, the tubes were centrifuged and the surnatants were collected in 1.5 mL microtubes. 20 μL of each cell extract was added to 980 μL buffer Z and the mix was equilibrated at 30 ºC for 5 minutes before the reaction was initiated by the addition of the 200 μL of (ortho) 2-Nitrophenyl-β-D-

130

galactopyranoside (ONPG) solution (4 mg/mL in buffer Z). The solutions were incubated at

30 ºC for 15 minutes and the reactions were terminated by the addition of 500 µL of Na_2CO_3

(1M in H_2O) to the tubes. In parallel to the samples, a blank sample was prepared in which

buffer Z and ONPG were added to a final volume of 1.2 mL and no biomass was supplied.

The hydrolization of the ONPG into galactose and ortho-nitrophenol catalyzed by the β-

galactosidase activity was detected by colorimetric assay. Indeed, the ortho-nitrophenol has a

yellow color whose intensity can be quantified by measuring the optical density at 420 nm

wavelength. The sample without the biomass was used as the blank in the spectrophotometry

measures. The specific activities of the cell extracts obtained in each condition was calculated

by using the following formula:

$$Activity = \frac{OD_{420} \times 1.4}{0.0045 \times [protein] \times extractvolume \times time \times 2}$$

> *Legend*:
> 1.4 = volume correction factor (total reaction volume is 1.4 mL)
> [protein] = mg/mL, from BCA assay below.
> extract volume = volume of protein assayed in mL
> time = time in minutes.
> 2 = volume correction factor (the cell pellet obtained from harvesting 1 mL of culture was resuspended in 500 µL of buffer Z before the assay)
> 0.0045= the optical density of 1 nmole/mL solution of o-nitrophenol

The specific activity is expressed as nmols/minute/mg protein. The proteins contained

in 50 µL of each cell extract were quantified by BCA protein assay (ThermoScientific). This

protein quantification method combines the reduction of Cu^{2+} to Cu^{1+} by protein in an

alkaline medium with the colorimetric detection of the cuprous cation (Cu^{1+}) by bicinchoninic

acid at OD 562 nm wavelenght. The calibration curve was prepared using bovine serum

albumine (BSA) as a standard. Each experiment was performed at least in triplicate.

5.3 Results

5.3.1 On the promoter of *alkB* gene

The transcriptional start site of the *alkB* gene was determined by Primer Extension analysis. Primer extension is a technique that is used to determine the starting site of RNA transcription for a known gene. This technique requires a radio-labelled primer (usually 20-50 bp in length) which is complementary to a region near the 5'-end of the gene. The primer is allowed to anneal to the RNA and the reverse transcriptase is used to synthesize complementary cDNA to the RNA until it reaches the 5'-end of the RNA. The run of retro-transcription product along with the DNA sequencing reaction of the same gene using the same labelled primer on a polyacrylamide gel allows to determine the size of the extended products. The length of the cDNA represents the number of bases between the labelled nucleotide of the primer and 5′-end of the RNA i.e. the transcriptional starting site. Moreover, the quantity of cDNA product is proportional to the amount of input target RNA so that the intensity of the band detected on the gel allows to quantify the amount of transcript and to compare the gene expression level under different conditions of growth.

In our experiment, two different radioactively labelled oligonucleotides annealing at different positions in the 5' region of *alkB* gene were used. They were named PrExt2 and PrExt8 (§ 5.2.1) and they mapped 70 and 86 nucleotides, respectively, downstream of the GTG codon of *alkB* gene.

Initially, the Primer Extension assay was performed on the mRNA extracted from BCP1 cells exposed to *n*-hexane for 4 hours and the transcription start point was determined with PrEx2 to be a guanine 63 bp upstream of the *alkB* initiation codon (GTG) (Fig 5.1).
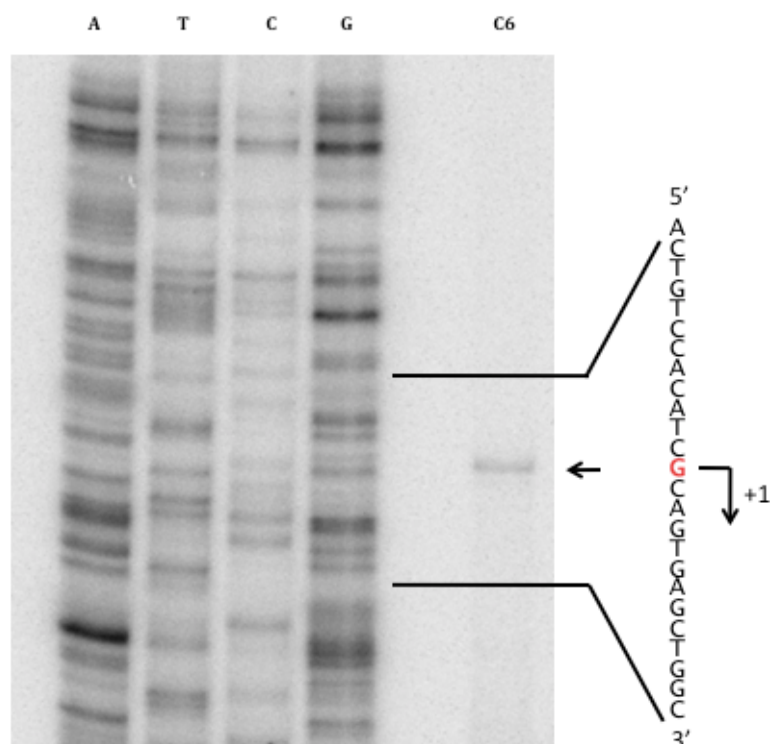
Fig. 5.1 Polyacrilamide gel showing the primer extension product obtained from the total RNA isolated from BCP1 cells exposed to *n*-hexane. Lanes A, T, C and G show the products of the sequencing reactions obtained with PrEx6 as the primer. Lane C6 shows the primer extension signal with the same primer. The deduced transcriptional start site is bolded in red and the direction of transcription is indicated by an arrow onto the sequence indicated in the right.

Subsequently, the primer extension analysis was extended by examining the primer extension products obtained from mRNAs extracted from BCP1 cells that were incubated with succinate, butane, *n*-hexane and *n*-dodecane. PrExt8 was used as oligonucleotide for the retro-transcription in order to validate the result obtained with PrEx2. The transcription starting point was confirmed to be the guanine previously described for the *n*-hexane-grown cells. Furthermore, the primer extension product was detected only by using the total RNAs of *n*-hexane- and *n*-dodecane-grown cells suggesting a regulation on the *alkB* gene induction dependent on the length of *n*-alkanes used as substrate. Indeed, butane did not appear to be *alkB* gene inducer while *n*-dodecane was a better inducer than *n*-hexane (Fig 5.2). Specifically, the analysis of the relative band intensity using Kodak 1D image software (Kodak 1D v.3.6.5 image analysis software, Eastman Kodak Co., Rochester, NY 14650.)

suggested that the transcriptional level of *alkB* was 5-fold higher with *n*-dodecane than in the presence of *n*-hexane.
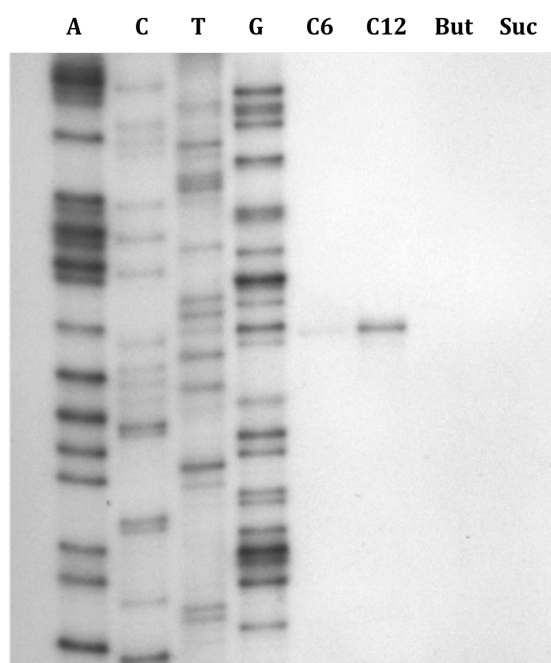
Fig. 5.2 Comparison of *alkB* gene primer extension products induced by a 4 hours-incubation of BCP1 cells with *n*-hexane, *n*-dodecane, *n*-butane and succinate.

By analyzing the region upstream of the *alkB* transcriptional starting site, putative -35 (TTGTCT) and -10 (TACTGT) regions were detected and they were shown to be spaced by 22 bp (Fig. 5.3). In correspondence of the BCP1 putative -35 nucleotide box, two overlapping inverted-repeat sequences were identified (*invrepA*: CGTTTTacAAAttACG and *invrepB*:ACAAAtTAcgaTAtTTTGT, where capital letters indicate the annealing part of the inverted repeated nucleotides strings) sharing a central motif ACAAATTACG that seem to be able to anneal alternatively one of the two sequences mapping at both sides (Fig. 5.3). For this reason these two inverted repeat sequences could be significant as regulatory protein binding regions.

134
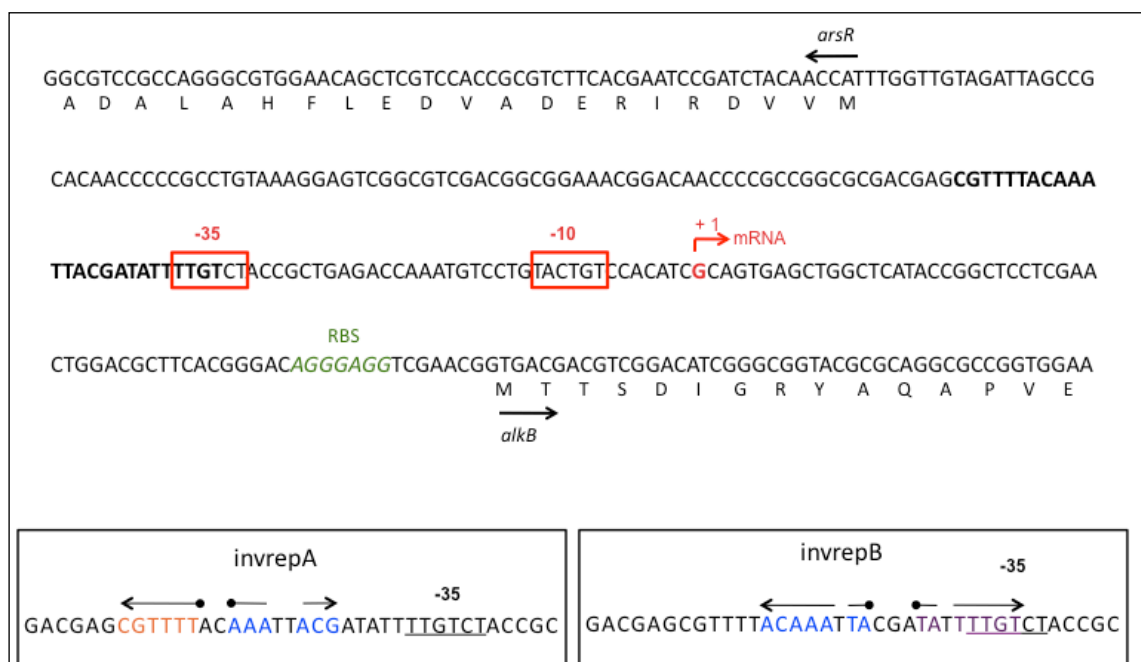
Fig. 5.3 The deduced transcriptional starting site is bolded in red and the direction of transcription is indicated by an arrow. The putative ribosome binding site (RBS) of *alkB* is in italics and the first part of the amino acid sequences of AlkB and ArsR regulator are reported below the nucleotide sequences. The deduced putative -10 and -35 promoter regions are also shown (boxed in sense strand). The region, including the two putative inverted repeated sequences that partially overlaps the -35, is bolded in black. Two enlargements of the region indicating the *invrepA* and the *invrepB* are reported in the bottom where the nucleotide forming the inverted repeats are coloured. The central sequence that seems to be able to anneal with one of the two flanking sequences is blue coloured in both the inverted repeat sequences.

Subsequently, the *Rh.* sp. BCP1 *alkB* upstream region (BCP1 *PalkB*) was aligned with the corresponding 210 bp-long regions in related *Rhodococcus* strains, whose genomes are sequenced and available in the database. For *Rhodococcus erythropolis* PR4 and SK121 strains, which both express more than one *alkB* gene, I considered only the upstream region associated with the *alkB* genes showing the higher homology to the *Rh.* sp. BCP1 *alkB*.
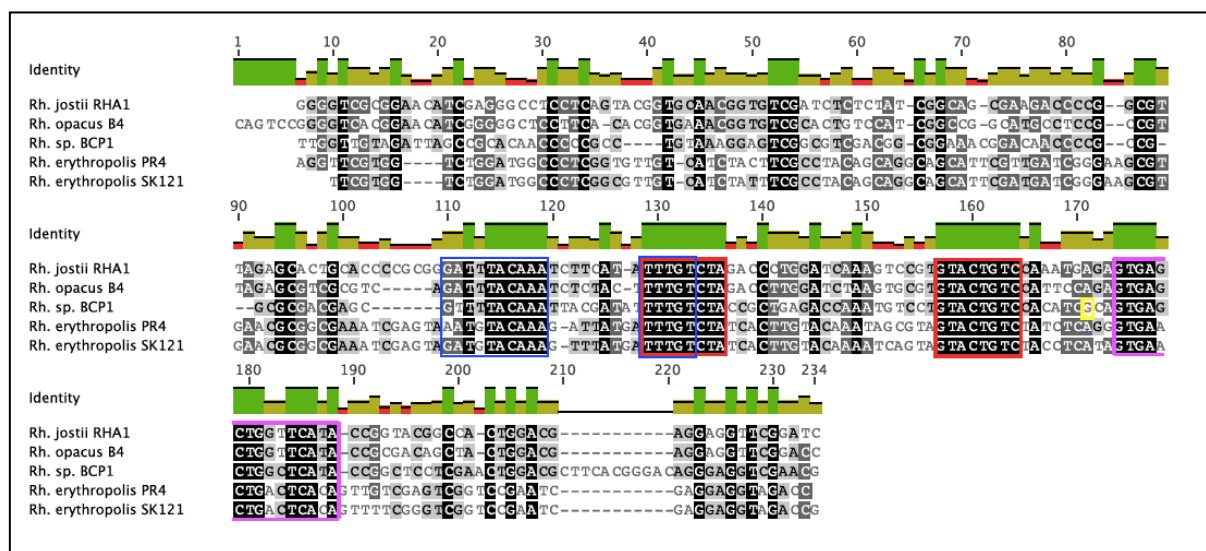
Fig. 5.4 Alignment of rhodococcal *alkB* genes upstream regions. The locus tags of the *alkB* genes taken in consideration are the following: ro02534 (*Rhodococcus jostii* RHA1), RER 21620 (*Rh. erythropolis* PR4), ROP 22570 (*Rh. opacus* B4) and ZP_04383196 for (*Rh. erythropolis* SK121).

The alignment of the *alkB* upstream regions identified the presence of nucleotide sequences conserved amongst the rhodococcal *alkB* promoters. These nucleotide sequences locate around the regions suggested as putative -35 and -10 boxes in BCP1 *PalkB* (red boxes, Fig. 5.4). Interestingly, both the suggested inverted-repeat sequences (*invrepA* and *invrepB*) are conserved (blue boxes, Fig. 5.4). Another region that shows a certain degree of conservation is identified downstream of the guanine (yellow marked in Fig. 5.4) mapping the *alkB* transcriptional start site in *Rh.* BCP1 (pink box, Fig. 5.4).

Subsequently, the research was focused on the promoter regions of the two *alkB* genes of *Rh.* B4 that are the only *alkB* genes, amongst the rhodococal *alkB* genes considered in the previous alignment, that have been analysed so far for their expression in the presence to *n*-alkanes. *Rh.* B4 *alkB1* has been reported to be induced by the presence of *n*-alkanes; conversely, *Rh.* B4 *alkB2* expression did not seem to be affected by these compounds [311]. Both B4 AlkB1 and AlkB2 amino acid sequences showed high homology with BCP1 AlkB (AlkB1 84% and AlkB2 81%); thus, it was hypothesized that the comparison of these *alkB* upstream regions with the BCP1 *PalkB* could allow to distinguish between the conserved sequences involved in the *alkB* gene induction promoted by the presence of *n*-alkanes (regions conserved between BCP1

136

alkBup and B4 *alkB1up*) and the conserved sequences useful for the rhodococcal transcriptional apparatus which is not dependent on *n*-alkanes (regions conserved between BCP1 *alkBup* and B4 *alkB2up*).
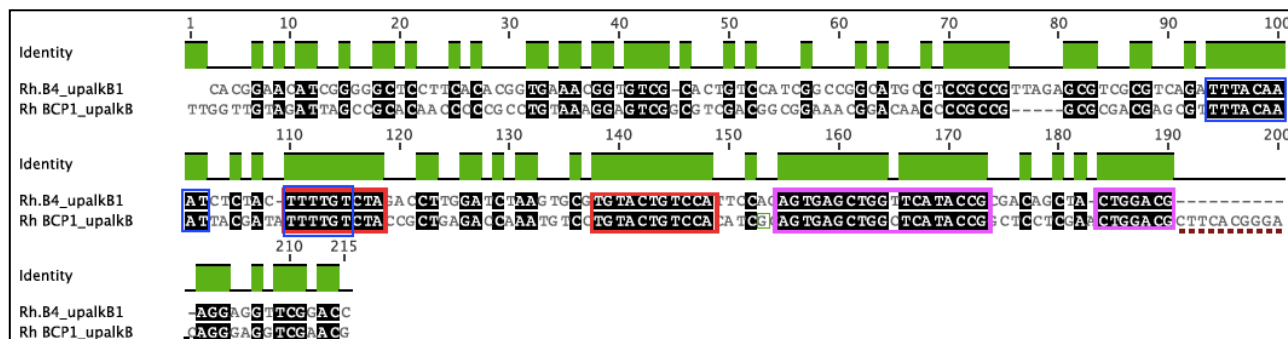
Fig. 5.5 Alignment of BCP1 *PalkB* and B4 *PalkB1*
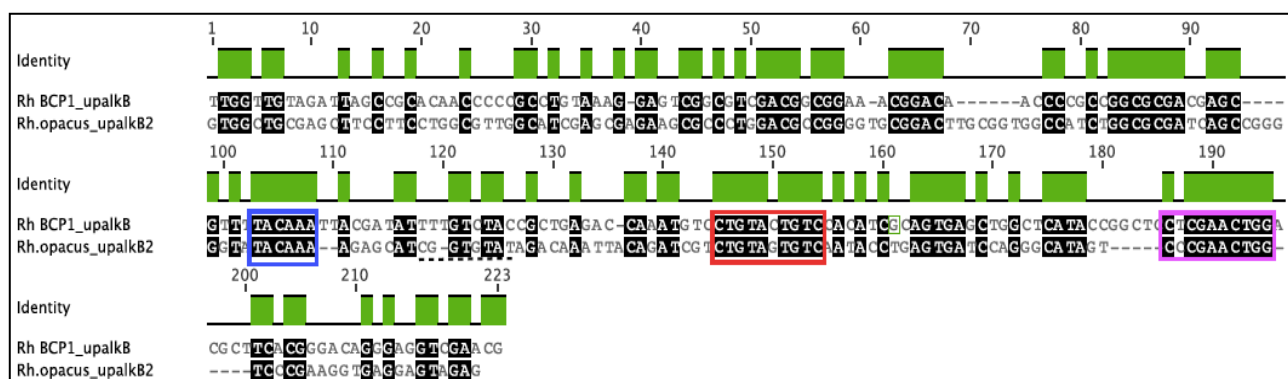
Fig. 5.6 Alignment of BCP1 *PalkB* and B4 *PalkB2*

B4 *PalkB1* showed nucleotide regions conserved having BCP1 *PalkB* in correspondence of -10 and -35 sequences (red boxes, Fig. 5.5) more extended in length than those revealed by the alignments of the four available *Rhodococcus* strains *PalkBs*. The inverted-repeat sequences were conserved (blue box, Fig. 5.5) and two DNA regions seemed to be conserved downstream of the *alkB* transcriptional start point (pink boxes, Fig. 5.5). Nevertheless, 11-bp immediately upstream of the *alkB* gene start codon (underlined in Fig. 5.5) were only present in BCP1 *PalkB* and the guanine that maps at the transcriptional starting point, was not conserved between the two *Rhodococcus* strains.

The alignment between BCP1 *PalkB* and B4 *PalkB2* showed the presence of conserved regions in correspondence to the putative -10 element (red box, Fig. 5.6), one part of the

137

inverted-repeat (*invrepA*) sequence not including the -35 region (blue box, Fig. 5.6) and a sequence after the BCP1 *alkB* transcriptional start site (pink box, Fig. 5.6). Notably, not only the inverted repeat sequence overlapping the -35 region (*invrepB*) was not present in *alkB2up* but also the entire -35 region was not conserved.

5.3.2 *alkB* gene cluster is transcribed as a single operon

To establish whether adjacent genes in the *alkB* gene cluster were co-transcribed, RT-PCR with RNA prepared from *Rh*. BCP1 grown in the minimum medium (MM) with *n*-hexane as a sole carbon source (§ 5.2.3), was performed. The primers used are reported in Table 5.1 and their annealing location is indicated in Fig. 5.7.

When the RT1 primer that hybridizes to the 5'-end of *rubR* and PCR primer pairs F1/R1 and F1/R2 were used, PCR products of 250 bp and 500 bp, respectively, were obtained. The successful amplification by PCR of primers mapping on the *alkB* gene using as template the cDNA produced in retro-transcription by a RT primer that maps on the rubredoxin reductase gene, indicated that the cDNA produced in RT included the four genes comprised in the cluster (*alkB*, *rubA*, *rubB* and *rubR*) (Fig. 5.7). In the positive control experiments, the RT2 primer (annealing the 3' of *alkB* gene) was used in the reverse transcription step and the same primers pairs (F1/R1 and F1/R2) were used in PCR. No amplification product was obtained when reverse transcriptase was omitted from the reaction mixture (lines 2 and 4 in Fig. 5.7). These results demonstrate that *alkB* is co-transcribed with the rubredoxin reductase and, therefore, that *alkB*, *rubA*, *rubB* and *rubR* genes are transcribed as a polycistronic transcriptional unit.
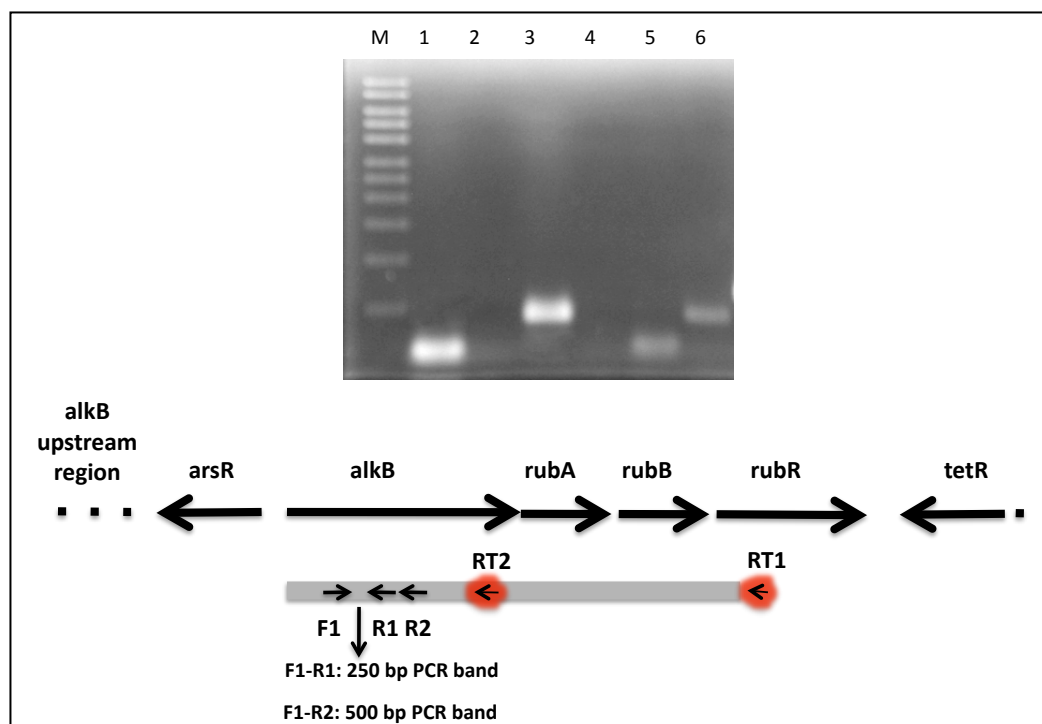
Fig. 5.7 Analysis of *alkB* gene cluster transcription by RT-PCR. Lane 1, amplification with RT2, F1, and R1 (250 bp); lane 3, amplification with RT2, F1, and R2 (500 bp); lane 5, amplification with RT1, F1, and R1 (250 bp); lane 4, amplification with RT1, F1, and R2 (500 bp); lane M, molecular mass markers. Lines 2 and 4 represent the negative controls.

5.3.3 *alkB* gene promoter activity

5.3.3.1 Construction of an alkB promoter probe vector

In order to analyse the transcriptional regulation of the *alkB* gene cluster, the intergenic (*arsR-alkB*) DNA fragment (415 bp) also covering the 5'-end of the divergently oriented coding regions (200 bp and 117 bp, in *arsR* and *alkB*, respectively), was cloned in the expression vector pTipQT2 fused with a promoter-less *lacZ* gene. This promoter probe vector (pTP$_{alkB}$LacZ) was transformed in *Rhodococcus* sp. BCP1 cells and the expression level of the promoter *PalkB* in response to the presence of different substrates was measured by β-galactosidase activity assay.

PTP$_{alkB}$LacZ is based on the expression vector pTipQT2 that has been described in literature for its use in the production of recombinant proteins [274]. This vector is a shuttle vector *E.coli-Rhodocccus* containing the replication origins for both bacteria, *E.coli* (colE1) and *Rhodococcus* (repA and repB). RepA and RepB coding genes originate from the

139

endogenous circular plasmid pRE2895 isolated from *Rh. erythropolis* strain JCM2895 and they are homologues to *repA* and *repB* genes of the pAL5000 plasmid from *Mycobacterium fortuitum* [345] that were shown to be sufficient for the stable maintenance of the plasmid in the host cell [345]. pTipQT2 contains two different antibiotic resistance cassettes: ampicillin resistance box is expressed in *E.coli* strains while the tetracycline resistance box is expressed in *Rhodococcus* strains. The tetracycline-resistant gene, only transcribed in *Rhodococcus* strains, originates from pACYC184 [346]. Furthermore, because of the initial purpose of the vector, pTipQT2 includes a thiostrepton-inducible promoter (*PTipA*) derived from *Streptomyces coelicolor* that is able to regulate the production of recombinant proteins inserted in the multi cloning site (MCS) [274]. Briefly, the thiostrepton-inducible expression system involves the transcriptional regulator TipAL that reacts with the thiostrepton so that the resulting product TipAL-thiostrepton increases the affinity of RNA polymerase for *PTipA* and, thereby, it activates the expression of the gene located in the MCS, downstream *PTipA*. Since we did not intend to express the recombinant protein regulated by *PTipA*, the promoter was excided by digestion with *BsrGI* and *BglII* and the *PalkB-lacZ* fusion product, digested with the same restriction enzymes, was inserted (Fig 5.8).
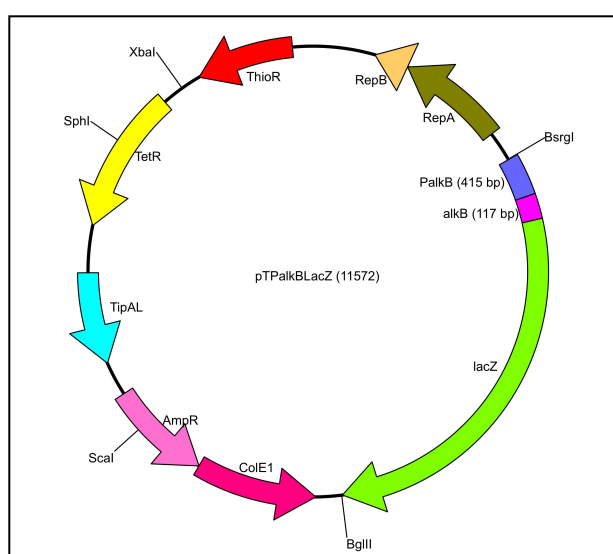
Fig. 5.8 Promoter probe vector PTP$_{alkB}$LacZ map with the indication of the *orfs* and of some enzyme restriction sites

5.3.3.2 alkB promoter activity in the presence of n-alkanes

To measure the *alkB* promoter activity in the presence of different *n*-alkanes, the promoter probe vector was introduced into *Rhodococcus* sp. BCP1 by electroporation as described in Chapter 2. pTP$_{alkB}$LacZ cells were grown on LB supplemented with tetracycline (5μg/mL) until their early stationary phase. Cells were then harvested, washed and suspended in minimal medium (MM) with different *n*-alkanes that were supplied at a concentration suitable to grow BCP1 cells with such a unique carbon source.

Initially, the *alkB* promoter activities after 10-, 18- and 24-hours exposition to hexane (C$_6$) (0.1% v/v), dodecane (C$_{12}$) (0.05% v/v), hexadecane (C$_{16}$) (0.05% v/v) and eicosane (C$_{20}$) (0.1% w/v) *n*-alkanes, were examined. The *alkB* promoter activities, induced by exposure to *n*-alkanes, were compared with that stimulated by succinate (0.1% w/v).
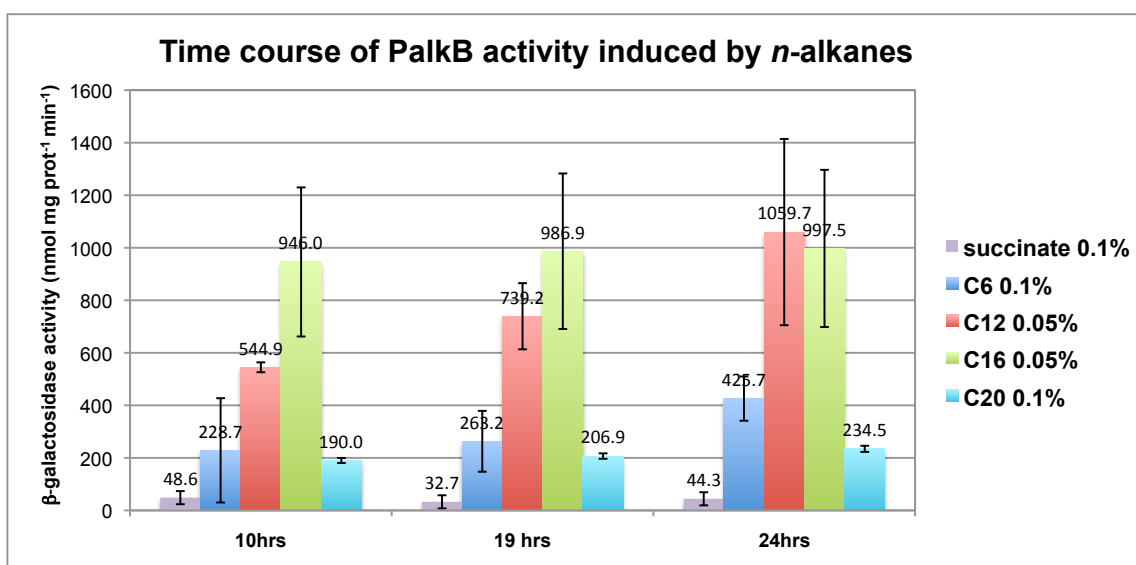
Fig. 5.9 *PalkB* activity induced by 10, 19 and 24 hours exposure to hexane, dodecane, hexadecane, eicosane *n*-alkanes and on succinate

Increasing *PalkB* promoter activities, measured through the use of the β-galactosidase assay, were shown over the three times of exposition to hexane, dodecane, hexadecane and eicosane *n*-alkanes, even though the induction exerted by the latter alkane was less dramatic. The succinate-exposed cells did not show any increase in *PalkB* activity over the whole cultivation period which remained constant around 44 nmol mg prot^{-1}min^{-1}. For this reason,

succinate-grown cells were considered as negative control in all the following experiments representing the basic level of *PalkB* activity.

Subsequently, it was decided to examine and compare the *PalkB* activity on different *n*-alkanes after 24-hours of incubation since it seemed to be the most suitable period of incubation to distinguish between the inducing and non-inducing substrates.
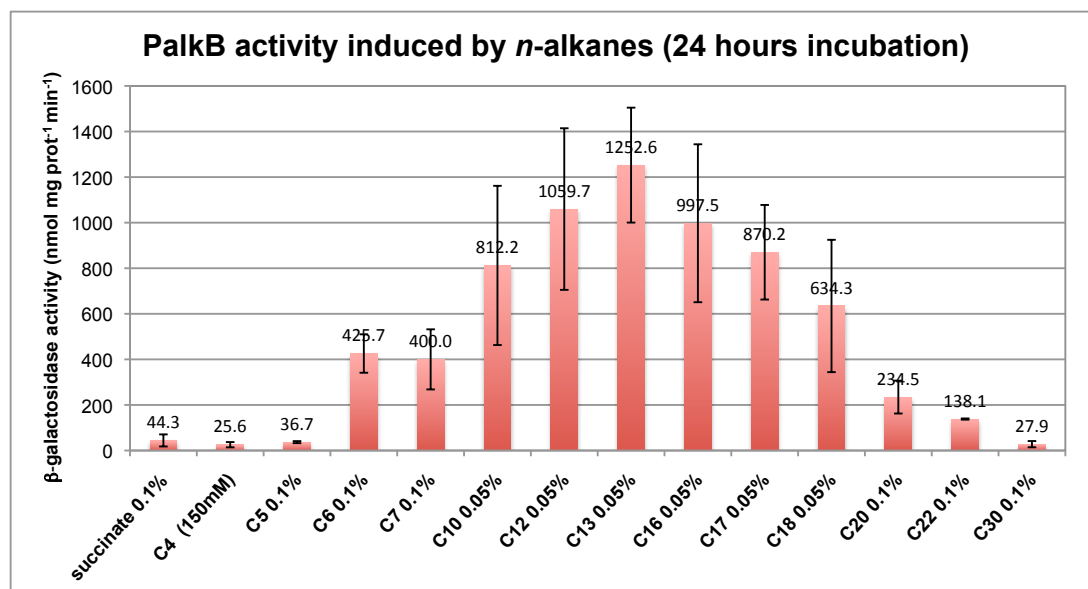
Fig. 5.10 *PalkB* activity induced by 24 h of incubation to different *n*-alkanes (the corresponding concentrations are indicated; in the case of liquid alkanes, % is expressed as v/v while for the solid alkanes % is expressed as w/v)

The activity of *PalkB* was markedly induced by incubation with *n*-alkanes in the range of C_6-C_{20}; no induction was seen on both pentane (C_5) and the only gaseous *n*-alkane tested, butane (C_4) (Fig 5.10). The activity of *PalkB* was also weakly induced (3-fold compared to the succinate) by C_{22} while C_{30} was not a *PalkB* inducer. Interestingly, the set of inducing alkanes also included *n*-decane that, as shown in Chapter 3 (§ 3.3.2), cannot be utilized as carbon source by *Rh*. sp. BCP1. The inducing capacity of the *n*-alkanes can be distinguished at four different levels, namely: a) the highest inducing capacity was seen with C_{10}-C_{18} *n*-alkanes (600-1300 nmol mg prot^{-1}min^{-1}); b) a prompt decrease in *PalkB* induction resulted in switching from C_{10}-C_{18} *n*-alkanes to C_6/C_7 *n*-alkanes (around 400 nmol mg prot^{-1}min^{-1}); c) the third inducing level was associated with C_{20}/C_{22} *n*-alkanes (100-250 nmol mg prot^{-1}min^{-1}) and

(d) the forth level corresponded to the basal expression activity as seen after incubation with *n*-butane, *n*-pentane and *n*-tricontane (C_{30}) which was comparable to the basal expression level of succinate (20-40 nmol mg prot^{-1}min^{-1}).

5.3.3.3 Further parameters affecting alkB promoter activity

A) The inducing substrate: concentration effect

Since the set of *n*-alkanes C_{10}-C_{18} could not be tested at high concentration due to their toxic effect on the BCP1 biomass, we tested the induction of *PalkB* activity under three different concentrations of *n*-hexane at variable incubation times.
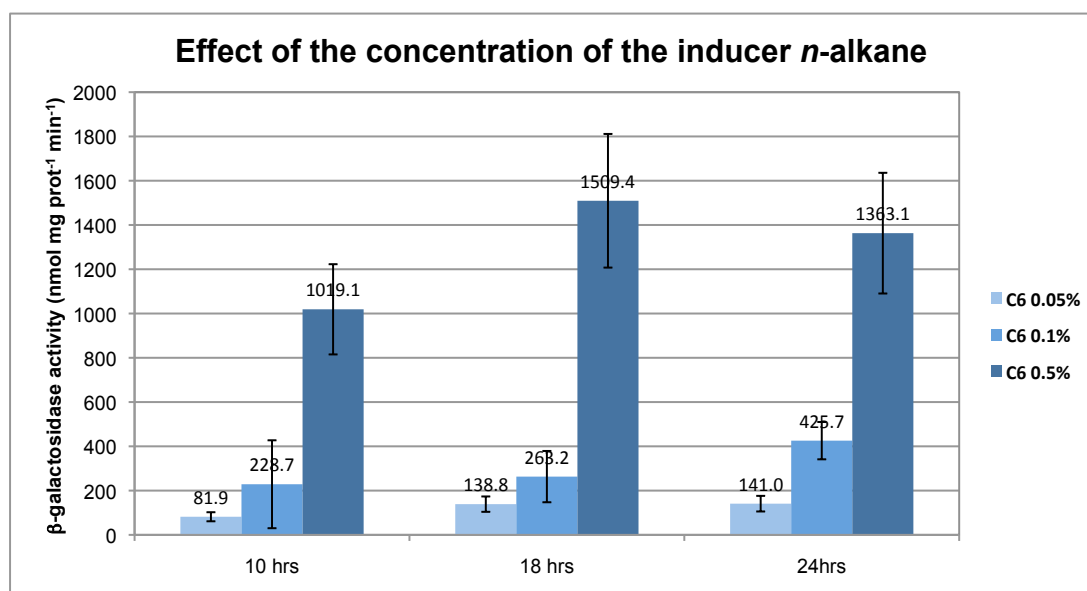
Fig. 5.11 Effect of different concentrations of inducing *n*-alkane on *PalkB* activity

Figure 5.11 shows that a concentration of 0.05% (v/v) *n*-hexane was unable to induce a *PalkB* activity higher than 141 nmol mg prot^{-1}min^{-1} a value that is almost ¼ of that obtained with *n*-hexane 0.1% (v/v). By contrast, a concentration of *n*-hexane of 0.5% (v/v) induced a *PalkB* activity near to 1000 nmol prot^{-1}min^{-1} after only 10 hours of incubation.

These results suggest that the *PalkB* induction level partially depends on the concentration of the *n*-hexane added to the medium during the incubation period, even though the difference between the induction values does not seem to reflect the corresponding

concentrations of the substrate added.

B) Effect of alternative carbon sources on PalkB activity

To investigate on the possibility that a catabolite repression mechanism could affect *PalkB* promoter activity, we examined the effect of carbon sources alternative to *n*-alkanes.

Initially, β-galactosidase activities at three consecutive times of exposure of pTP$_{alkB}$LacZ BCP1 to succinate (0.1% w/v), glucose (0.1% w/v) and LB, were determined. These activities values were considered the levels of basal expression of *PalkB* on the basis of which the induction performed by the addition of the *n*-alkanes could be evaluated.
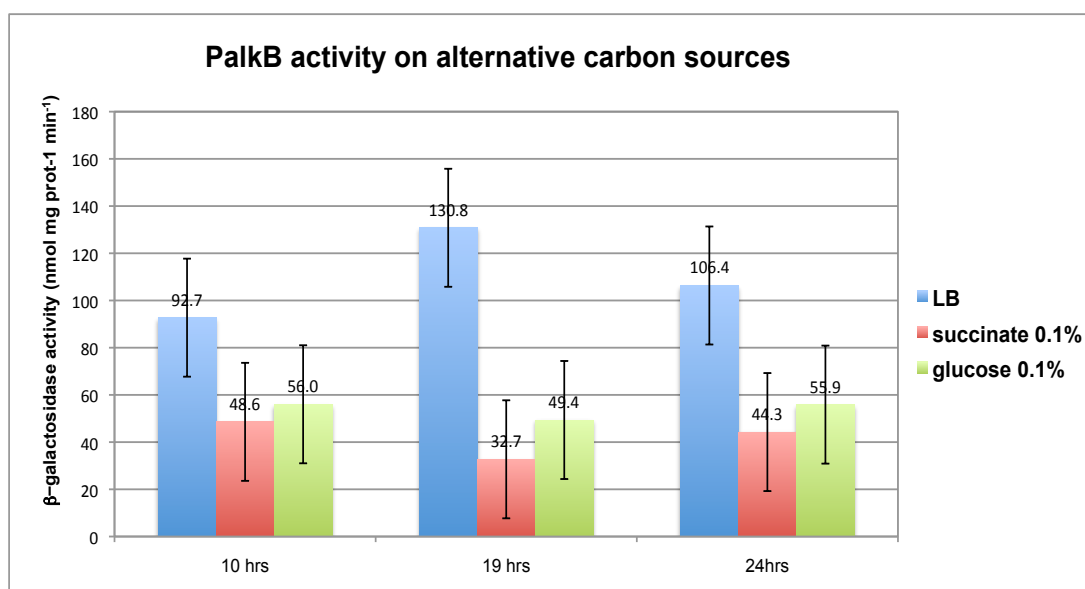
Fig. 5.12 *PalkB* activity induced by growth on LB, MM plus succinate (0.1% w/v) and MM plus glucose (0.1% w/v)

As shown in Fig 5.12, despite the LB-induction values were twice as much those seen in the presence of succinate and glucose, they were still very low being in the range 90-130 nmol mg prot^{-1}min^{-1}; these latter values were clearly different from those obtained with *n*-alkanes C_6-C_{18} (400- 1300 mg prot^{-1}min^{-1}). Additionally, the *PalkB* activities on all the three alternative carbon sources did not change over the three times included in the 24 hours; conversely, the inducing *n*-alkanes were able to stimulate a constant increase in the *PalkB* activity over the 24 hours (Fig. 5.9). Thus, the induction on *PalkB* by alternative carbon

144

sources was considered negligible so that *n*-hexane and *n*-dodecane were added to the BCP1 cultures suspended in MM with alternative carbon sources. *PalkB* induction, over 24 hours, was determined through the use of the β-galactosidase activity after 10-, 18- and 24-hours of exposure to either LB, succinate or glucose each combined with *n*-hexane (0.1% v/v) or *n*-dodecane (0.05% v/v).
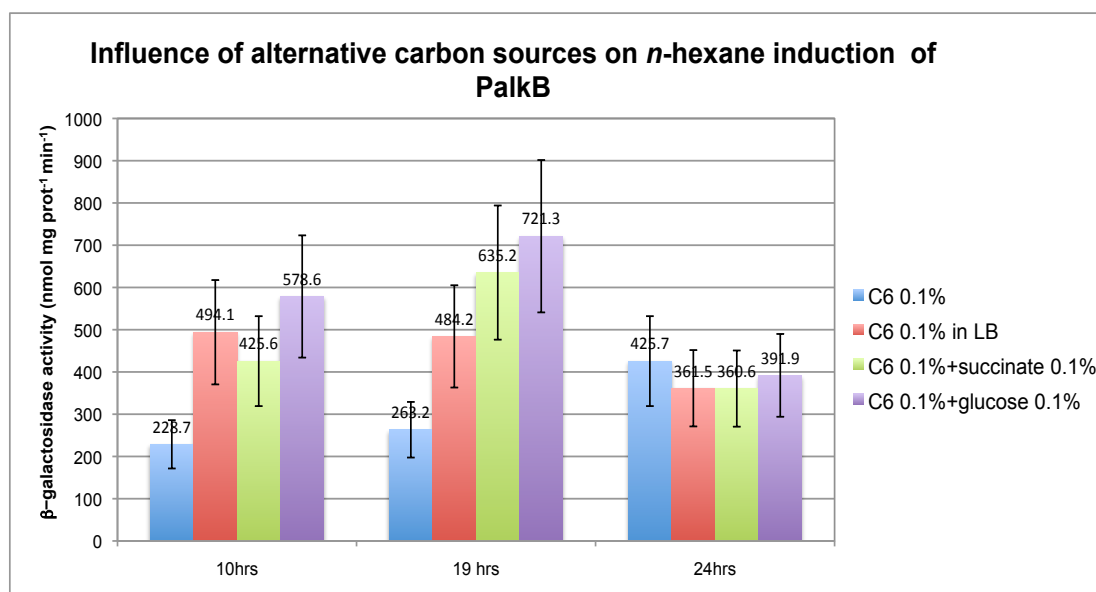
Fig. 5.13 Effect of the presence of alternative carbon sources on the *PalkB* activity induced by the *n*-hexane
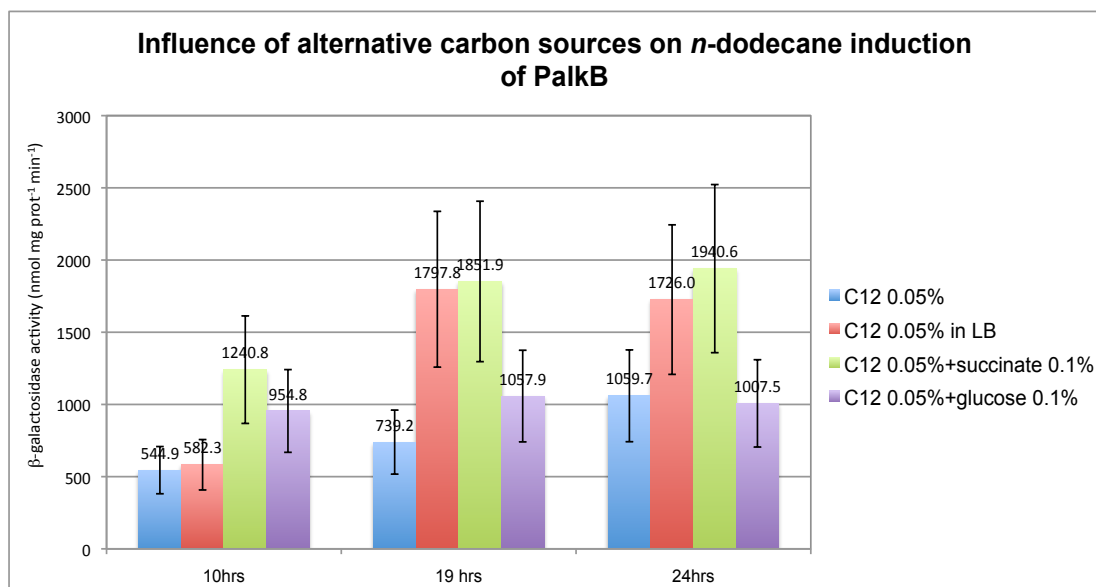
Fig. 5.14 Effect of the presence of alternative carbon sources on the *PalkB* activity induced by the *n*-dodecane

As shown in Fig.s 5.13 and 5.14, the presence of alternative carbon sources did not

seem to repress the *PalkB* induction promoted by *n*-alkanes. By contrast, the presence of an alternative carbon source increased the inducing ability exerted by *n*-hexane after 10 and 18 hours of incubation and by *n*-dodecane all over the 24 hours. This effect was not so evident in the case of *n*-hexane after 24 hours of incubation.

C) Effect on PalkB activity by putative metabolic intermediates of n-hexane metabolism

Finally, we examined the *PalkB* activity in the presence of hypothetical intermediates of the hydroxylation pathways of *n*-hexane (see Fig. 5.15).
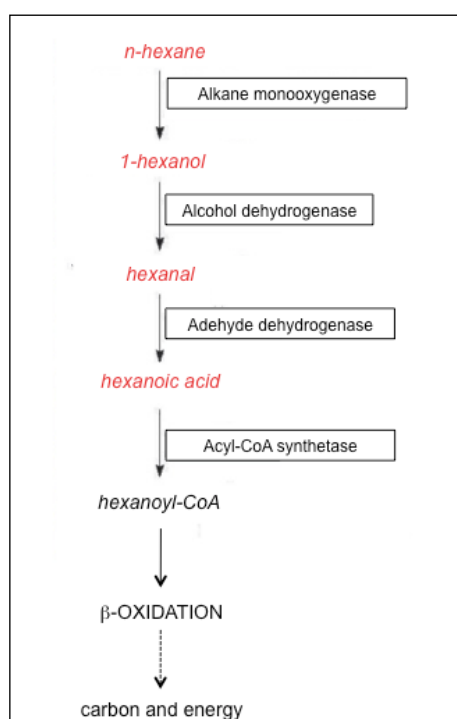
Fig. 5.15 Putative *n*-hexane metabolic pathway. The *n*-hexane metabolism intermediates that were tested in the β-gal assay experiments are indicated in red

The aim of the experiments described hereafter, was to examine the possible repression mechanisms exerted by the putative metabolic products resulting from the transformations catalysed by dehydrogenases acting in series after the alkane monooxygenase. Each intermediate was supplied at the concentration of 0.1% v/v.
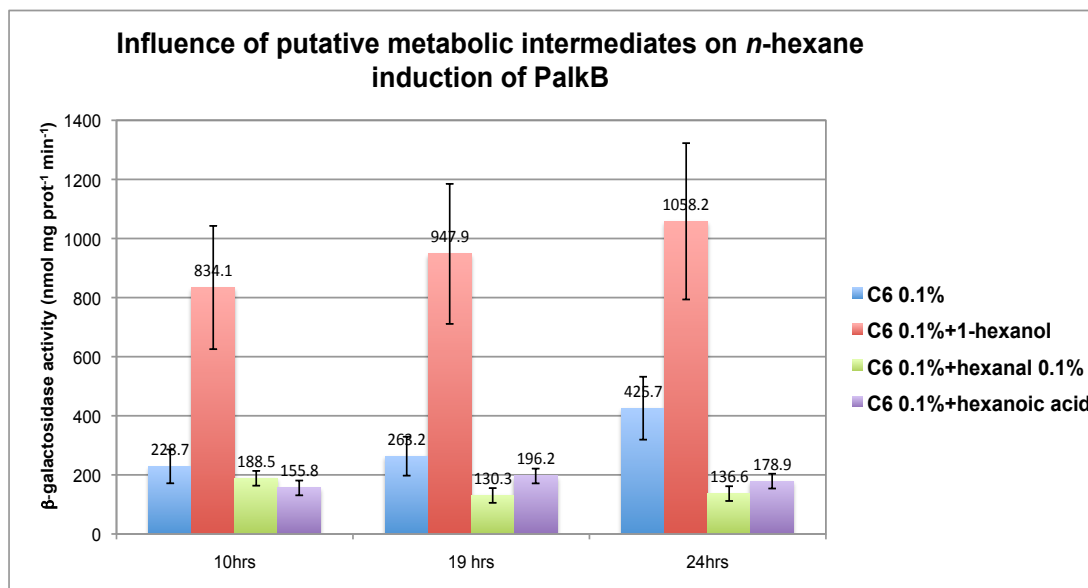
Fig. 5.16 Effect of the putative *n*-hexane metabolism intermediates on the *PalkB* activity induced by *n*-hexane

Histograms in Fig. 5.16, which represent the *PalkB* activity after 10, 19 and 24 hours of exposure to *n*-hexane in the presence of the hypothetical metabolic products, show that the presence of the hexanal (the putative aldehyde produced by alcohol dehydrogenase) and the hexanoic acid (produced by the aldehyde dehydrogenase) affects the *PalkB* activity promoted by *n*-hexane by almost 4-times. By contrast the presence of the alcohol generated by the terminal oxidation of *n*-hexane enhanced the *PalkB* activity by at least two-times.

The effects on *PalkB* activity by *n*-hexane metabolic products was then investigated. Hexene has the same chain length of *n*-hexane but a double bond between two carbons of the aliphatic chain along with a higher hydrophobicity as compared to *n*-hexane.
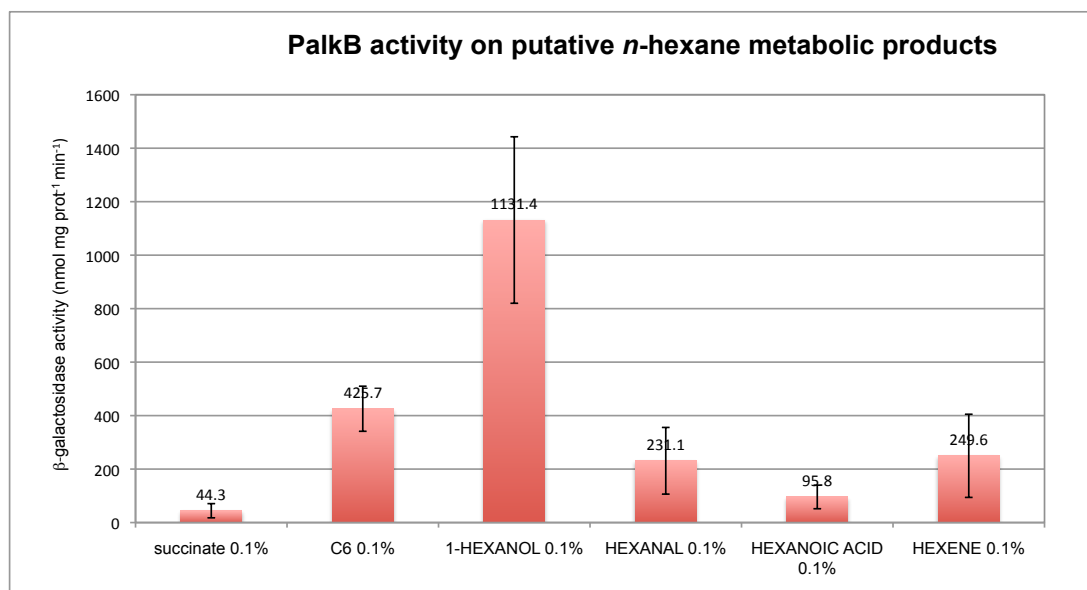
Fig. 5.17 Effect of the putative n-hexane metabolism intermediates on *PalkB* activity

As shown in the Fig. 5.17, both aldehyde and the alkene were able to increase the *alkB* gene expression by a factor of 5-7-times while no effect was seen with hexanoic acid. The inducing capacity of the 1-hexanol was even 3-times higher than the one obtained in the presence of *n*-hexane.

To understand whether the property of 1-hexanol to induce *PalkB* was due to its chemical nature, the *PalkB* activity induced by other unsaturated aliphatic alcohols such 1- and 2-butanol and 1-octanol, was investigated.
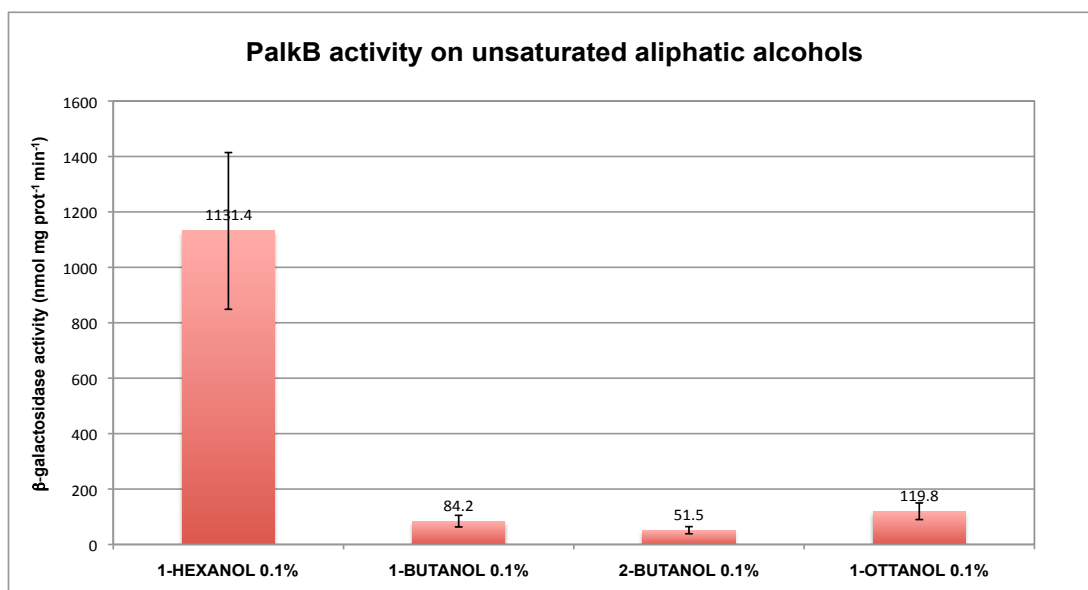
Fig. 5.18 Effect of unsaturated aliphatic alcohols on *PalkB* activity

Since these alcohols did not promote the *PalkB* induction as 1-hexanol, we tentatively speculated that this phenomenon did not depend on the presence of -OH groups.

5.4 Discussion

In this present study, we focused our attention on the correlation between the expression of the *alkB* gene in *Rhodococcus* sp. BCP1 and its ability to grow on *n*-alkanes. To this end we analysed the following aspects: a) characterization of the *alkB* gene promoter; b) investigation on the operon-like structure of genes coding for the alkane monooxygenase components; c) analysis of the induction of the *alkB* promoter activity by *n*-alkanes along with the effects of alternative carbon sources and *n*-alkane metabolic products.

By Primer Extension analysis, the transcriptional starting site of *alkB* gene was identified and preliminary estimations of the *alkB* transcripts induced by *n*-butane (C_4, gaseous), *n*-hexane (C_6, liquid), *n*-dodecane (C_{12}, liquid) and succinate (alternative carbon source) were obtained. As a result, both hexane and dodecane showed primer extension product bands with the same size while no product band was detected with succinate and

butane. Interestingly, the intensity of the primer extension product seen by using the RNA of BCP1 incubated with *n*-dodecane showed an intensity that was 5-times higher than that obtained with hexane. The data showed that the induction of *alkB* gene expression by *n*-alkanes does not include the gaseous alkanes. Moreover, the different intensity associated with the *n*-hexane and the *n*-dodecane primer extension products suggested a differential *alkB* expression level induced by the two *n*-alkanes.

The *alkB* transcriptional site was shown to map 63 nucleotides upstream of the start codon (GTG). Putative -10 and -35 regions were identified spaced by 22 bp. The presence of two inverted repeat sequences (*invrepA*, 16 bp, and *invrepB*, 19 bp) was also hypothesized. The two inverted repeat sequences showed a common part represented by 10 bp sequence that apparently can alternatively anneal with one of the two inverted sequences located at both sides. Interestingly, *invrepB* partially overlaps the -35 region.
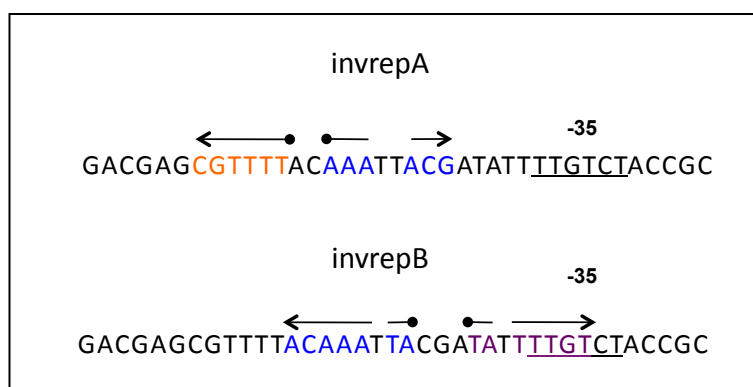
Fig. 5.19 The putative two inverted repeat sequences *invrepA* and *invrepB*

The comparative analysis of *alkB* promoters in *Rhodococcus* sp. BCP1 and in other related *Rhodococcus* strains, indicated the presence of conserved nucleotide sequences that might be involved in *Rhodococcus*- specific regulation mechanism of *alkB* gene expression. By focusing the analysis on the comparison of BCP1 *alkB* promoter (BCP1 *PalkB*) with those of the two *alkB* genes of *Rhodococcus opacus* B4 (B4 *PalkB1* and *PalkB2*), we thought to get insights into the putative regulatory elements involved in the *alkB* expression induced by *n*-

alkanes. Since in a work by Sameshima *et al*. [311] it was shown that the expression of B4 *alkB1* was regulated by *n*-alkanes, whereas *alkB2* was not controlled by alkane-dependent mechanisms, we considered the promoters of *alkB1* (*PalkB1*) and *alkB2* (*PalkB2*) as examples of alkane-inducible promoter and non-alkane dependent promoter, respectively. Indeed, the distinction between the BCP1 *PalkB* nucleotide sequences conserved in B4 *PalkB1* and the BCP1 *PalkB* nucleotide sequences conserved in B4 *PalkB2* would possibly suggest the regulatory elements involved in the *n*-alkane-dependent response in BCP1. Accordingly, the sequences maintained between BCP1 *PalkB* and B4 *PalkB2* would only represent regulatory elements generally involved in the function of rhodococcal transcriptional apparatus. The results of this comparative studies indicated that the only conserved region that may be significant in the *n*-alkanes-dependent response is part of the *invrepB* (in bold red in Fig. 5.20).
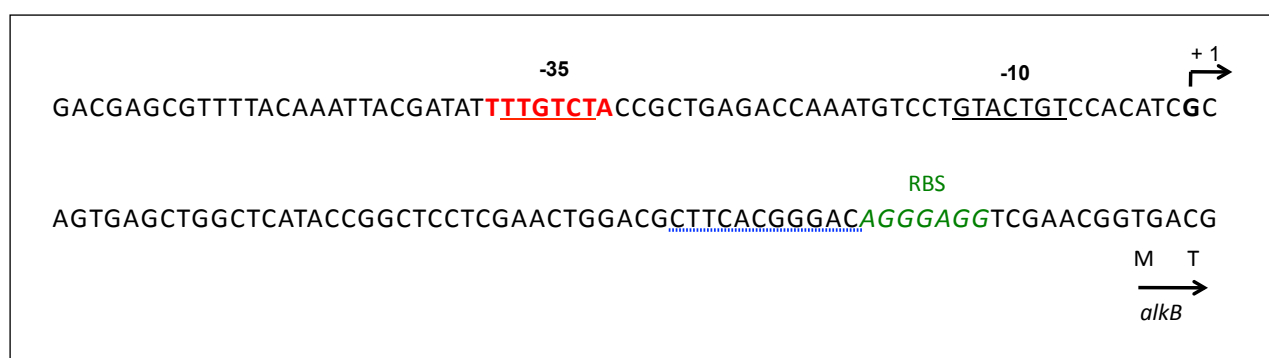
Fig. 5.20 The *alkB* promoter region with the putative sequence (in red) involved in the *n*-alkane dependent response and (in blue) the sequence that is present only in BCP1 *PalkB*

According to this result, neither the -10 region nor the region around the transcriptional start sites are important in the *n*-alkane inducing process. Interestingly, *invrepA*, the putative inverted repeat sequence that does not overlap the -35 region, does not seem to be involved in the alkane-dependent regulation. In Fig. 5.20, the 11 bp sequence underlined in blue does not seem to have correspondence in any other rhodococcal *PalkB* regions.

Our present interpretation of the regulatory elements in the *alkB* gene promoter is

different from that of Sameshima *et al*. [311] about *Rhodococcus alkB* promoter regions as these authors tempted to identify the putative regulatory elements of the promoters region upstream of *alkB1* and *alkB2* in *Rhodococcus opacus* B4. They based their identification of -10 and -35 regions on the existing homology between B4 *PalkB1* and B4 *PalkB2*. Sameshima and co-workers, in line with our present conclusions, also identified the inverted repeat sequence upstream of the -35 region which is named here as *invrepA* (Fig. 5.19, indicated by arrows in Fig. 5.21). Conversely, Sameshima *et al*. did not mention at all the inverted repeat sequence which is named here as *invrepB* (Fig. 5.19 box red in Fig. 5.21).
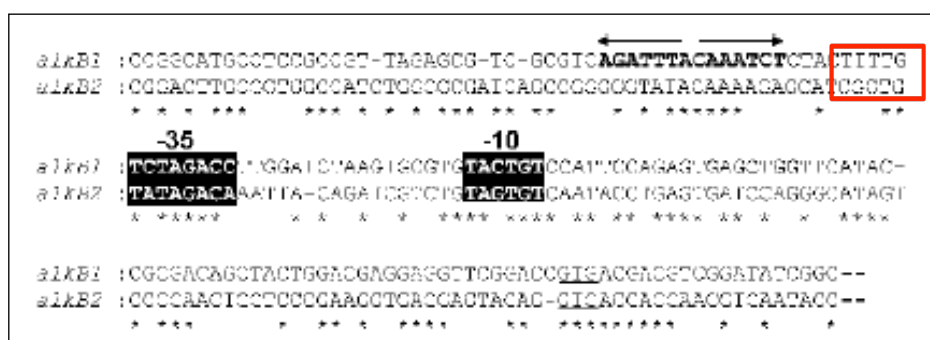
Fig. 5.21 Analysis of the *alkB1* and *alkB2* promoter regions by Sameshima *et al*. [311].

Sameshima *et al*. [311] indicated the *invrepA* as the inverted repeat sequence that can act as a binding domain for AlkS-like regulator in B4. AlkS is a positive transcriptional regulator that activates *PalkB* promoter in the presence of alkanes in *Ps*. *putida GPo1* (see Chapter 1, § 1.3.4.6). In this respect, the results by Canosa et al. [217] and van Beilen [213] on the *alkB* promoters in *Pseudomonas putida* GPo1 and *Alkanivorax borkumensis* AP1, respectively, indicated as binding domain for AlkS the inverted repeat sequence that overlaps the respective *PalkB* -35 regions.
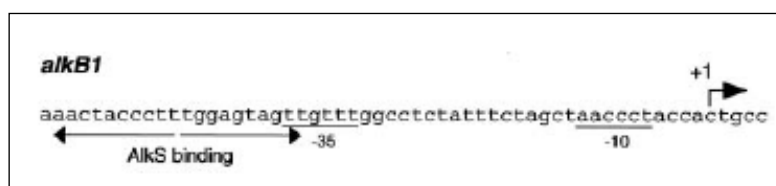
Fig 5.20 *A* .*borkumensis* AP1 *alkB* upstream region with the characterized regulatory elements [213]

152
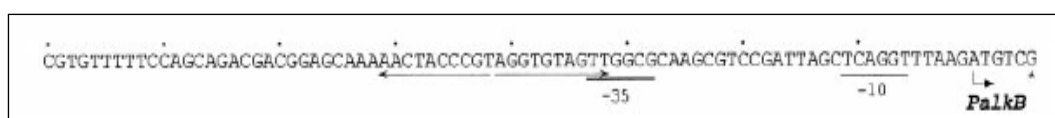
Fig 5.21 *Ps. putida* GPo1 *alkB* promoter region with the characterized regulatory regions [217]

Because of the similarities between the inverted repeat sequences and *invrepB* in BCP1, in contrast to Sameshima *et al.* [311], we are tempted to propose the involvement of *invrepB* in the AlkS-like regulator binding. Further, the presence of two repeated sequences that can alternatively anneal could also possibly indicate a mechanism of regulation. However, mutational analysis experiments are required to investigate on the putative functions associated with the regulatory elements in BCP1 *PalkB*. Moreover, the 11-bp sequence that seems to be unique in BCP1 also requires further investigation.

By RT-PCR experiment the transcriptional clustering of the genes coding for the alkane monooxygenase components was revealed. The consecutive genes *alkB*, *rubA*, *rubB* and *rubR*, that in Chapter 4 were described to have overlapping start and stop codons, have been verified being co-transcribed as a single operon. This characteristic is quite widespread amongst genes that encode components of oxygenases [347]. *Ps putida* GPo1 *alkBFGHJKL* cluster is co-transcribed as a single operon, even though the rubredoxin reductase is not included in the cluster. Whyte *et al.* [297] molecularly described the consecutivity of the *alkB* genes in both *Rhodococcus* sp. NRRL B-16531 and sp. Q15 and reported the occurring overlapping of start and end codons but did not further demonstrate the co-transcription of the genes.

To gain further insights into the expression of BCP1 *alkB*, transcriptional fusion of promoter *PalkB* to the *lacZ* reporter gene was constructed based on the expression vector pTipQT2 described by Nakashima & Tamura [274]. The DNA fragment cloned upstream of the *E. coli lacZ* gene included 415 bp of the *alkB* promoter region and 117 bp of the first part

of *alkB* gene. The transformants containing the *PalkB*::*lacZ* fusion in pTipQT2 were named BCP1 PTP$_{alkB}$LacZ. Early stationary phase grown PTP$_{alkB}$LacZ cells were exposed to either different *n*-alkanes, alternative carbon sources or *n*-alkane metabolic products in minimal medium (MM). The β-galactosidase activity was measured at several points of the incubation as nmoles of o-nitrophenol produced per mg of protein per minute. It was not possible to calculate the activity as Miller units since the step leading to the cells permeabilization by means of SDS/chloroform, described in the Miller protocol [343], was not effective in *Rhodococcus* sp. BCP1 cells. The highest induction level was observed for *n*-alkanes C$_6$-C$_{22}$ while *n*-butane, *n*-pentane and *n*-tricosane (C$_{30}$) did not work as inducers. Alkanes were grouped into four groups, according to their *PalkB*-inducing abilities as revealed by β-gal assay, such as: I) C$_{10}$-C$_{18}$ *n*-alkanes (900-1300 mg prot^{-1}min^{-1}), II) C$_6$ and C$_7$ *n*-alkanes (400 mg prot^{-1}min^{-1}), III) C$_{20}$ and C$_{22}$ (150-250 mg prot^{-1}min^{-1}) *n*-alkanes, IV) C$_4$, C$_5$ and C$_{30}$ *n*-alkanes. This latter group induced *PalkB* at a basal level (40-45 mg prot^{-1}min^{-1}) as seen with succinate. Therefore, a great variability in terms of *PalkB* activity values was observed and the capacity of *n*-alkanes to induce *PalkB* was possibly related to the aliphatic chain-length, as suggested by the drastic change seen between *n*-hexane (inducer) and *n*-pentane (non-inducer). By contrast, in the set of long-chain alkanes, the big difference between the strong inducer C$_{18}$ and the less efficient inducer C$_{20}$ could be due to the change in their physical state, i.e. liquid (C$_{18}$) and solid (C$_{20}$). Indeed, the dispersion of solid alkanes in the aqueous medium is very low and the bio-availability of these alkanes is likely to be the limiting step in their *PalkB* inducing properties.

The difference in *alkB* gene expression level in the presence of *n*-alkanes of C$_{10}$-C$_{18}$ and those of C$_6$-C$_7$ becomes more evident if we consider their relative concentrations in the assay. C$_{10}$-C$_{18}$ *n*-alkanes were added at a final concentration of 0.05% (v/v) while C$_6$, C$_7$ and C$_{20}$ *n*-alkanes were added at a concentration of 0.1% (v/v or w/v). Nevertheless, the induction

values of this latter group were 2-3 times smaller than the former of the two. Interestingly, similar levels of *PalkB* induction were reached when *n*-hexane was supplied at a concentration of 0.5% (v/v) so to suggest an alkane-dependent dose-response effect on the *alkB* gene expression.

The set group of inducing alkanes included the *n*-decane C_{10} which is not utilized as growing carbon source by *Rh*. BCP1 (Chapter 3, § 3.3.2). The property to induce *PalkB* supported the concept that the inability of BCP1 to grow on *n*-decane is more correlated to the toxic effect by this alkane or by the metabolic products than to the absence of catabolic functions for this substrate. By contrast, Grund *et al*. [348] reported that the *n*-alkanes that did not support *Ps*. *putida* GPo1 growth were also unable to induce *alkB* gene expression.

As far as concern the effect of alternative carbon sources together with *alkB* inducing alkanes, we have observed that no catabolite repression mechanism is acting on the *alkB* gene regulation as the presence of alternative carbon sources increases the inducing effect of *n*-alkanes. This effect was evident over three different incubation time periods with *n*-dodecane. The effect on the *n*-hexane induction was evident after 10 and 18 hours of incubation and it was less visible after 24 hours. This phenomenon might reflect not only a solvent effect that initially causes the partial lysis of the biomass but also the induction of undefined metabolic pathways allowing the cells to counteract the hydrophobic environment. The contemporary presence of an alternative carbon source seemed to hinder the solvent effect of the *n*-alkane during all the time course of the assay. Thereby, the presence of alternative carbon sources could introduce a protective effect that may enhance the bacterial adaptation to new conditions of growth, e.g. *n*-alkanes as carbon sources. Moreover, the presence of alternative carbon sources along with *n*-dodecane caused the cells to aggregate in flogs (not shown) that were much less present with succinate, glucose or LB.

In the literature, strong differences are shown to characterize the catabolite repression

mechanisms acting on *alkB* gene expression in bacteria. The expression of both *Ps. putida* GPo1 and *Burkholderia cenopacia alkB* is subjected to catabolite repression [220] indicating that *n*-alkanes are not the preferred growth substrates of these strains. By contrast, *Acinetobacter* sp. ADP1 did not show *PalkB* repression when cultures were resuspended in LB and the alkanes were added [181]. As far as concern *Rhodococcus* genus, the general capacity of *Rhodococcus* strains to degrade pollutants even in the presence of more easily degradable carbon sources [39, 349] is in line with the results obtained for *PalkB* activity in BCP1 (Chapter 1, § 1.4.1).

Finally, the effect of *n*-hexane oxidation products (Fig. 5.15) on the *PalkB* activity was examined. Both hexanal (aldehyde) and hexanoic acid (carbossilic acid) were shown to exert a repression on the *PalkB* activity induced by *n*-hexane. Addition of hexanal to the medium, only, poorly induced *PalkB* activity while hexanoic acid did not induce it at all. 1-Hexanol was shown to be an inducer when added to the medium alone or in the presence of *n*-hexane (the *PalkB* activity was 2-3-fold higher than with the alkane, only) (summarized in Fig. 5.22). Hexene, i.e. an alkene with the same carbon chain length of hexane but having a double bond plus a higher hydrophobicity, poorly induced *PalkB*.

In the literature it has been shown that the property of several alkane-oxidation products to induce the expression of alkane hydroxylases can vary greatly as in *P. putida* GPo1, alkanes and alkanols are good inducers, while alkanals and fatty acids are poor and bad inducers, respectively [348]. In *Burkholderia cepacia* RR10, the alkane hydroxylase is induced by both alkanes and their oxidation products [214]; conversely, in both *Acinetobacter* sp. strain ADP1 and *Ps. aeruginosa*, only alkanes could act as inducers [214, 350]. Further, in *Acinetobacter* sp. strain ADP1 alkens showed good inducing properties [348].
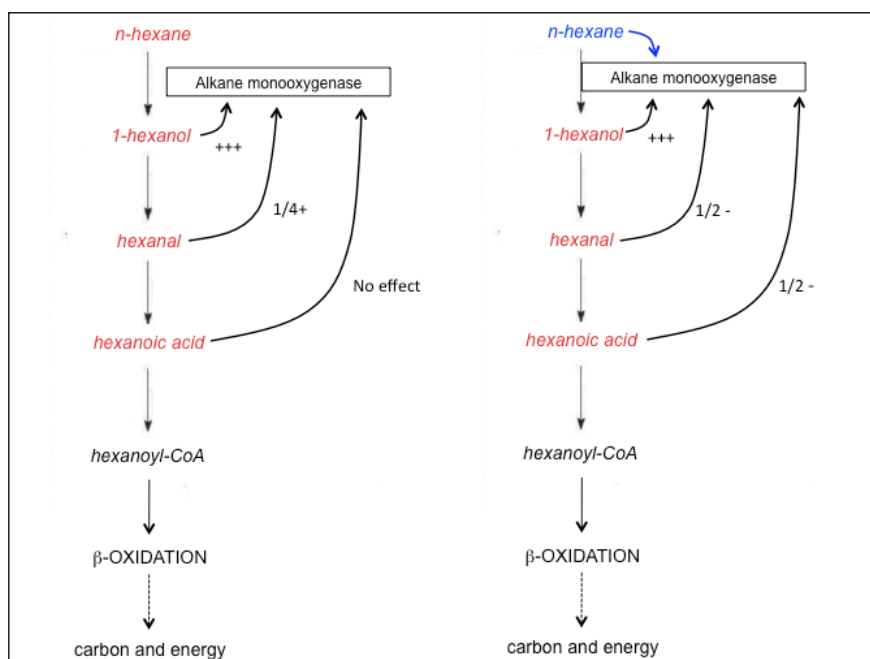
Fig 5.22 Summary of the effect of *n*-hexane metabolic products on the *PalkB* activity when added alone (left) or when added together with the *n*-alkane (- or + refers to the *PalkB* activity value induced by hexane, i.e. +++ means that the inducing effect is three times higher than the hexane inducing value; ½ - means that the value is 1/2 less than the hexane value; ¼+ means that the value is 1/4 less the hexane inducing value).

5.5 Summary

In conclusion, this study aimed to determine a physiological role for the AlkB-like monooxygenase in *Rhodococcus* sp. BCP1 grown on *n*-alkanes by examining different aspects of the *alkB* gene expression. Among the *n*-alkanes used by BCP1 as carbon sources, *alkB* gene expression was not induced by alkanes <C5. Thus, we concluded that this AlkB hydroxylase is not the main monooxygenase involved in the short-chain alkanes metabolism but it can be considered the major enzyme involved in the first metabolic step of alkanes C_{12} - C_{18}. Since the mechanisms regulating the expression of catabolic genes for contaminants are necessary to know the metabolic responses to environmental changes, the evaluation of optimal conditions to induce promoters of genes for degradation of xenobiotics could help to provide suitable conditions promoting bioremediation procedures.

CHAPTER 6. Proteomic analysis of *n*-alkanes growth of *Rhodococcus* sp. BCP1

6.1 Introduction

Aerobic biodegradation of *n*-alkanes molecules is initiated by monooxygenases that usually catalyse the oxidation of a terminal methyl group to render a primary alcohol that is further oxidized to the corresponding aldehyde, and finally converted into fatty acid. Fatty acids are conjugated to CoA and further processed by β-oxidation to generate acetyl-CoA, which can enter the TCA cycle to yield carbon dioxide and energy (Chapter 1 § 1.3.4, Fig. 1.1).

Characterization of *n*-alkane degradation pathways has been carried out predominantly in Gram-negative bacteria, especially in the genus *Pseudomonas*, where information has been obtained generally by techniques that include mutagenesis, gene cloning and sequencing, biochemical characterization and purification of enzymes, and chemical identification of metabolites (Chapter 1, § 1.3.4.3.2).

During the last decade, proteomic techniques turned out to be a powerful tool to provide insights into the physiological response of microorganisms to environmental changes. The development of functional proteomics represents new valuable throughput approach to study the microbial biodegradation pathways useful for potential bioremediation applications [351]. The work by Sabirova *et al*. [75] analyzed the implications that this approach could have in the study of *n*-alkane biodegradation in the hydrocarbonoclastic *Alcanivorax borkumensis* (Chapter 1, § 1.3.4). The protein pattern expressed by *A. borkumensis* grown on *n*-hexadecane (C_{16}) as sole carbon source was examined. The study identified the proteins involved in the metabolic adaptations of *A. borkumensis* to grow on *n*-alkanes and suggested the nature of the alkane oxidation systems involved in the degradation pathway.

Recently, proteomic approaches have become a potent tool for investigating the various

aspects associated with the *Rhodococcus* strains broad metabolic diversity and for bypassing the limits imposed by the rhodococcal strains being refractory to genetic manipulation and mutational analysis. Proteomic studies have been conducted to analyze catabolic pathways for both mono- and polyaromatic compounds in *Rhodococcus* sp. strain TFB [352] and to investigate the apparent redundancy of degradation pathways for mono-aromatic compounds in *Rhodococcus jostii* RHA1 [282]. A few other studies combined proteome analysis with molecular biology techniques to identify new enzymes involved in xenobiotic degradation pathways in *Rhodococcus* strains [353-355].

The previous chapters concentrated on the study of the monooxygenase involved in the first oxidative step of the *n*-alkanes metabolism in *Rhodococcus* sp. BCP1. In this study we adopt a proteomic approach for the investigation of the degradation of *n*-alkanes in BCP1 in order to evaluate its global cellular response to these compounds. In this work we compared the protein patterns expressed by BCP1 growing on *n*-butane, *n*-hexane, *n*-hexadecane or *n*-eicosane with the protein pattern expressed by BCP1 growing on succinate. The results revealed the accumulation of enzymes not only directly involved in the *n*-alkane oxidation steps but also acting in metabolic pathways for microbial adaptation to these hydrophobic and energy-rich substrates. The proteomic analysis of *Rhodococcus* sp. BCP1 was limited by the fact that its complete genome is still unknown; thus, the results obtained in this study only partially provide answers to the initial questions. However, the importance of this work is represented by the demonstration of the feasibility of the proteomic approach for the investigation of the peculiar metabolic characteristics of *Rhodococcus* sp. BCP1 that would be otherwise limited by its recalcitrance to genetic manipulation techniques.

6.2 Materials and Methods

6.2.1 Inducing of *n*-alkanes metabolism in *Rhodococcus* sp. BCP1

Rhodococcus sp. BCP1 was grown on minimal medium (MM) in the presence of succinate (0.1% w/v), *n*-hexane (0.1% v/v), *n*-hexadecane (0.05% v/v) or *n*-eicosane (0.1% w/v) as only carbon source. Four 500-mL flasks with 100 mL of MM were prepared for each condition and they were incubated for 48 hours at 30 ºC on a rotary shaker at 200 rpm. The biomasses grown on succinate and *n*-hexane were harvested by centrifugation (7000 rpm for 5 min at 4 °C) and washed twice with ice-cold buffer phosphate 10 mM (pH 7.2), while *n*-hexadecane- and *n*-eicosane-grown cells were collected by filtration through 0.22-μm membrane filters (Millipore) and the washing steps were conducted directly on the filters. The pellets and the filters were stored at -80ºC for later use.

6.2.2 Preparation of cell extracts of *Rhodococcus* sp. BCP1

For two-dimensional gel electrophoresis the cells were disrupted by bead-beating. The biomass grown on each substrate was resuspended in 5 mL lysis sample solution buffer (8 M urea, 4% CHAPS, 2% IPG buffer in 10 mM Tris, pH 8.5, in the presence of 1mM PMSF). The suspension was aliquoted in five 2 mL-tubes (provided with o-ring on the lid to prevent liquid spillage) containing 0.5 mL of nitric acid pre-washed quartz beads (0.2-0.8 mm-diameter, MERCK KGaA, Germany). The cells were beaten using a Precellys®24 *(Bertin* Technologies) bead beater for five cycles of 30 seconds, speed 6000 m/s. Between each cycle, the tubes were cooled on ice. Unbroken cells and cell debris were removed by low speed centrifugation at 14000 rpm for 10 minutes at 4 °C and the supernatants were cleared by ultracentrifugation (32500 rpm, 1.5 h, 4 °C). Finally, the cell-free protein extracts were either stored at -80°C or used immediately for proteomic studies.

6.2.3 Purification of the cell extract and two-dimensional gel electrophoresis (2-DE)

The sample to be used for two-dimensional gel electrophoresis (2-DE) was concentrated, desalted and separated from low-molecular weight inhibitors by filtration through a 10-kDa filter (millipore centrifugal filters with 10kDa cut off, Millipore). The filtration process will result in a liquid remaining (retentate) in the reservoir that is composed primarily of molecules larger than the cut-off and a liquid in the bottom tube that is composed by molecules below the molecular cut-off that did pass through the filter. The filtration was performed in more passages. The tubes were fractioned alternating 4 °C-centrifuges (15 min each) and 20°C-centrifuges (10 min each) in order to facilitate the filtration of the urea through the filters (that at 4 °C is not as efficient as at higher temperatures). After four centrifuge passages, 0.1 mg/ml (final concentration) of RNase and DNase I were added to the solution remained at the top of the filter (around 100 μL) and the tubes were incubated 30 minutes on ice. The tubes were then subjected to two additional filtration steps so that the nucleic acids fragments, resulting form the nucleases digestions, could pass through the filters and separate from the retentate (liquid remaining). In the end, around 50 μL of purified cell extract was transferred to a new tube and the amount of total soluble protein content was estimated by the Bradford assay [356] that did show compatibility with the small concentration of urea still present in the sample.

A volume of sample corresponding to 300 μg of extracted protein was solubilised in urea rehydration solution (8 M urea, 2% CHAPS, 2% IPG Buffer, 0.002% bromophenol blue, 25 mM DTT) for 30 minutes at room temperature and then was applied to Immobiline DryStrip (13 cm, nonlinear pH 4 to 7) (GE Healthcare) for isoelectric focusing (IEF). Isoelectric focusing in the IPG strips was carried out for a total of 29.3 kVh at 20°C under mineral oil using ETTAN IPGphor (Amersham Biosciences). After IEF, the strips were equilibrated for 30 minutes at room temperature in equilibration solution (40 % glycerol, 50

mM Tris pH 8.8, 8 M urea, 2 % SDS) containing 2 % DTT and then in equilibration solution containing 2.5 % iodoacetamide. Proteins were separated by 12 % sodium dodecyl sulfate-polyacrylamide gel electrophoresis (SDS-PAGE) in the second dimension using a PROTEAN II xi 2-D Cell electrophoresis system (gel size 16 x 20 cm) (BioRad). For protein spots visualization, 2D gels were stained with Coomassie brilliant blue staining.

6.2.4 MALDI-TOF and LC/MS/MS analyses

Protein spots were excised from Coomassie brilliant blue-stained 2D gels and washed for 15 minutes first with water, then acetonitrile (ACN) and finally 50 mM NH_4HCO_3 (aq). The gel fragments were washed in 50:50 25 mM NH_4HCO_3/ACN for 1-2 hours to remove the dye and then the wash with ACN followed by 50 mM NH_4HCO_3 (aq) was repeated. Washed gel pieces were dehydrated with ACN, dried down and then rehydrated with 10 ml of 25 mg/ml modified trypsin (Roche) in 20 mM NH_4CO_3 on ice for 30 min. Excess trypsin was removed and the gel pieces covered with 10 mL of 20 mM NH_4CO_3 and incubated at 37 ℃ overnight. Peptides were extracted by three sequential extractions (70 % ACN for 1 hour, water for 30 minutes, 70 % ACN for 30 minutes), which were pooled together [357] and dried down in a Speed vac concentrator.

MALDI-TOF spectra were obtained on a Voyager DE-STR (Applied Biosystems, Foster City, CA, USA) in the reflectron mode at the Southern Alberta Mass Spectrometry Centre (Calgary, Canada). Dried down peptides were dissolved in 50% ACN:water (vol/vol) 0.3% TFA (vol/vol) and analyzed with a standard dried droplet method using 0.01% α-cyano-4-hydroxycinnamic acid. Peptides were spotted with calibrants (angiotensin I 1296.685(M+H), ACTH clip 1-14 1680.795(M+H), and ACTH clip 18-39 2465.199 (M+H)) for high mass accuracy.

Tandem mass spectra (LC/MS/MS) were obtained on an Agilent 1100 Series LC/MSD

ion Trap XCT Plus at the SAMS facility. Samples were loaded in 3% ACN/0.05% formic acid and separated on a C18 column over a gradient of 0.05% formic acid (buffer A) and ACN/0.05% formic acid (buffer B) at a flow rate of 0.3 µl/min. The gradient was 3% B for 0 to 5 min, 3% to 15% B for 3 min, 15% to 45% B for 42 min and 45% to 90% B for 5 min. Database searches were done with Mascot using the NCBI non-redundant database for Eubacteria. A fixed carbamidomethyl modification at cysteine, peptide tolerance of 100 ppm, MS/MS tolerance of 0.6 Da, 2+ and 3+ charged states and one missed cleavage site were selected for peptide fingerprinting searches.

6.3 Results

6.3.1 2-D gel analysis of proteins produced in *Rhodococcus* sp. BCP1 cells grown on *n*-alkanes

A proteomic approach was used to provide insights into the metabolic pathways for *n*-alkanes catabolism in *Rhodococcus* sp. BCP1. Soluble protein extracts from cells grown with *n*-butane (gaseous alkanes), *n*-hexane (short-chain liquid alkane), *n*-hexadecane (long-chain liquid alkane), and *n*-eicosane (solid alkane), as sole carbon sources, were compared by 2-D gel analysis using the soluble protein extract of succinate as a reference.

Since initial 2-D gel using IPG strips from pH 3 to 10 revealed that most of the cytoplasmic proteins focused in correspondence of pH values below 7 (data not shown), IPG strips from pH 4 to 7 were subsequently used. 2D-gels were independently repeated three times to confirm the consistency of protein patterns obtained in each growth condition. Representative examples of 2D-gels are shown in Figure 4.1.
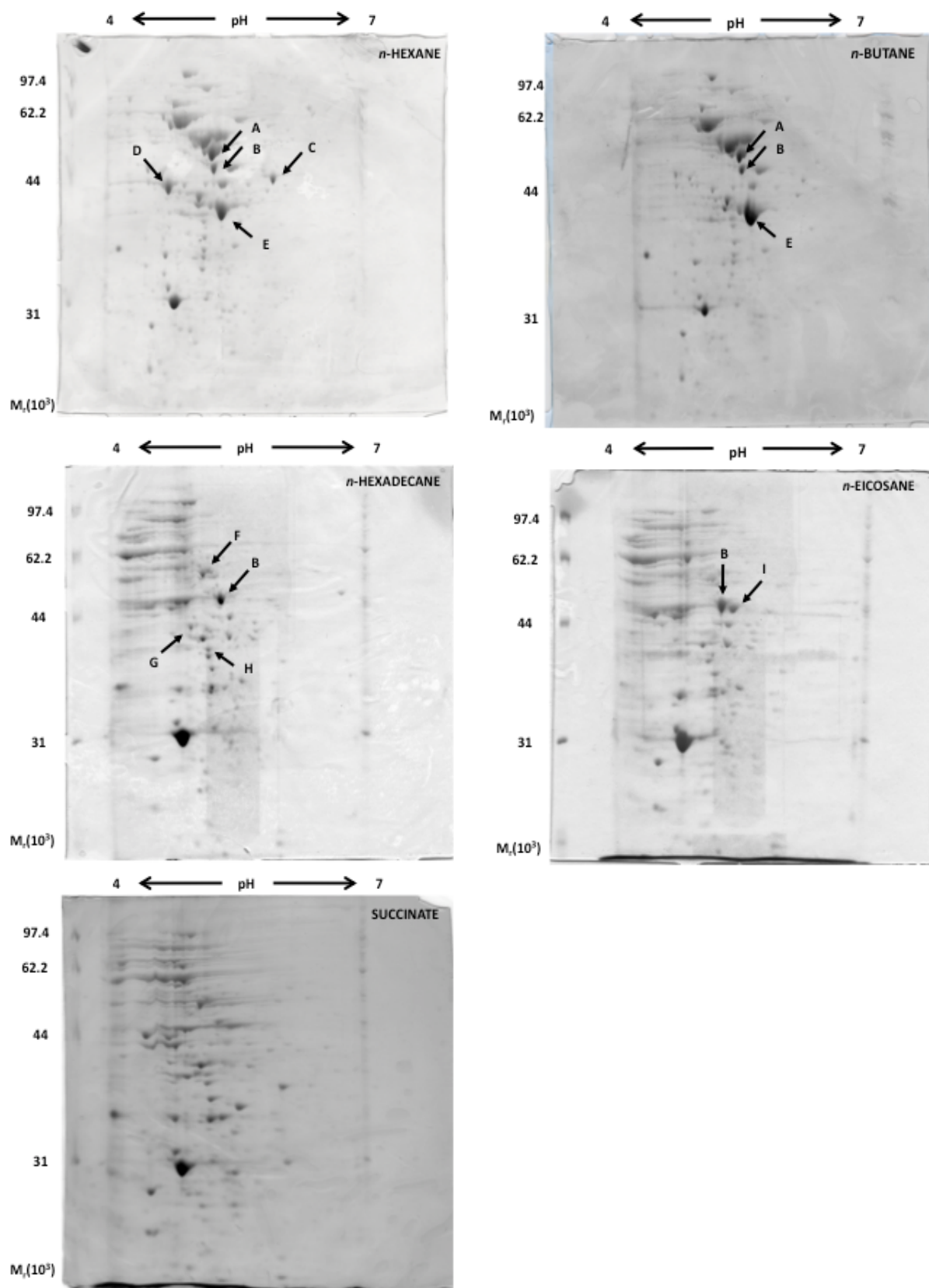
Fig. 6.1 Coomassie blue-stained 2-D gels representing the cytoplasmic fractions of BCP1 cells grown on different *n*-alkanes and on succinate. Arrows indicate spots specifically induced in each *n*-alkane growth condition but not in succinate. Each spot is named with an alphabetic letter. Common spots are named with the same alphabetic letters.

When compared to the control (succinate-grown cell extract), specific proteins were found with increased accumulation in *n*-butane, *n*-hexane, *n*-hexadecane and *n*-eicosane-grown cell extracts. Most of these were clustered towards the upper part of the gel. Proteins consistently expressed in each *n*-alkane but not in succinate are indicated and named by alphabetical letters in Fig. 6.1. Common spots were named with the same letters.

The protein patterns produced in *n*-butane and *n*-hexane-grown cells were very similar to each other and different to that obtained with *n*-hexadecane and *n*-eicosane-grown cells. This suggested that the catabolic pathway for *n*-butane metabolism shared enzymes with that for *n*-hexane degradation. By contrast, these two latter pathways are likely to be quite distinct from those involved in *n*-hexadecane and *n*-eicosane growth.

Although the 2D-gel upper parts, corresponding to high molecular weight protein range, were only partially resolved, yet some spots could be resolved. The spots named A, B and E resulted to be common between the 2D-gels representing the protein patterns produced in *n*-butane- and *n*-hexane-grown cells. Only the protein named B was specifically induced in each *n*-alkane growth condition and not on succinate. The spots C and D were detected only in the *n*-hexane-growing cells.

6.3.2 2-D gel analysis of *n*-hexane-versus glucose-grown BCP1 cells and identification of differentially accumulating proteins

The MALDI-TOF mass spectrometry analysis was initially applied for identifying the spots representing the proteins expressed during the growth on *n*-alkanes. The protein spots that are indicated by arrows in Fig. 6.1 (A÷I) were excised from the gel and subjected to trypsin digestion before being analysed by MALDI-TOF mass spectrometer. This instrument reveals the masses of proteolytic peptides obtained from each digested spot. As result, a peptide mass fingerprint (PMF) is associated with each spot under investigation. A PMF database search is usually employed following MALDI-TOF mass analysis. Identification is

accomplished by matching the observed peptide masses to the theoretical masses derived from a sequence database. Unfortunately, the peptide mass fingerprinting information did not allow unequivocal identification of the protein spots differentially expressed in *Rhodococcus* sp. BCP1. This lack of results originates from the lack of homologous sequences that could provide statistically significant hits in the NCBI database. Mascot [358] is one of the most commonly used protein database that matches the mass of the proteolytic peptides to all candidate peptides of *in silico* protein digests and ranks the candidates based on the matching of theoretical and experimental fragmentation spectra [359]. Mascot score is the identity associated to each of these matches. The matches with Mascot score higher than a certain threshold value (statistically calculated by the program) can be considered significant. An example of chromatogram collected from the spot named B with MALDI-TOF and the correspondent Mascot search result are reported in Fig. 6.2-A.
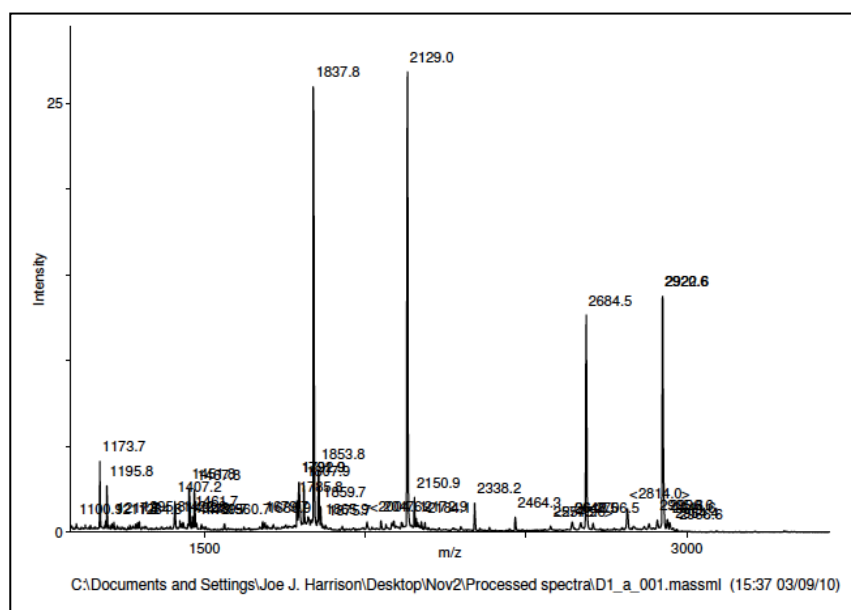
Fig. 6.2-A MALDI-TOF chromatogram of the peptide mixture prepared from tryptic digested spot B.

Concise Protein Summary Report

```
Format As    Concise Protein Summary  ⬍        Help

        Significance threshold p< 0.05    Max. number of hits AUTO

Re-Search All    Search Unmatched

1.    gi|281416940    Mass: 8182    Score: 63    Expect: 3.2  Queries matched: 5
      conserved hypothetical protein [Clostridium thermocellum JW20]
```
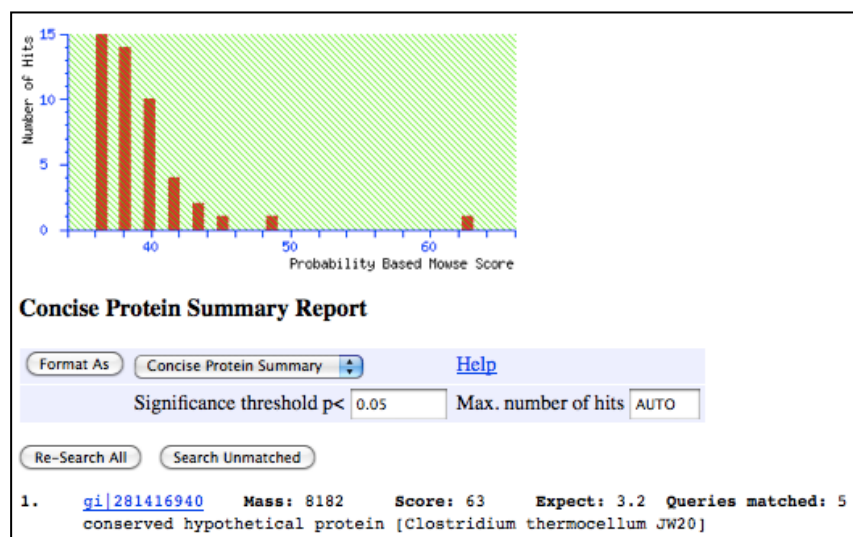
Fig. 6.2-B Mascot window resulting from the database search of the spot B data (since all the matches are in the green area, they result not to be significant).

As shown in Fig. 6.2-B, the Mascot score associated to the MALDI-TOF data of the spot B was not significantly high to allow the identification of the protein (the threshold score was indicated to be 76 and the B spot Mascot score was 63). Likewise, data were evaluated in a similar fashion for all the MALDI-TOF data from all spots considered.

Therefore, it was necessary to subject the samples to the tandem mass spectrometry (LC/MS/MS). The tandem mass spectrometry provides partial sequence information of the peptides associated with the proteolytic digestion increasing the probability to identify the protein under investigation.

We concentrated on the five spots that showed to be significantly changed in *n*-hexane growing condition compared with succinate (Fig. 6.1). They were named 6A, 6B, 6C, 6D and 6E (Fig.6.3).
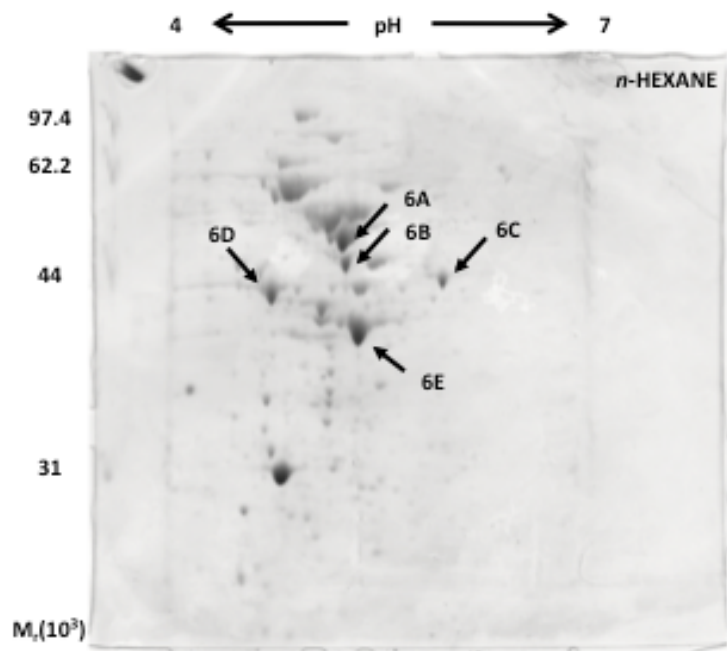
Fig. 6.3 Enlargement of the 2D-gel from *n*-hexane growing cells in Fig.4.1. The spots that were analyzed by LC/MS/MS are indicated by arrows.
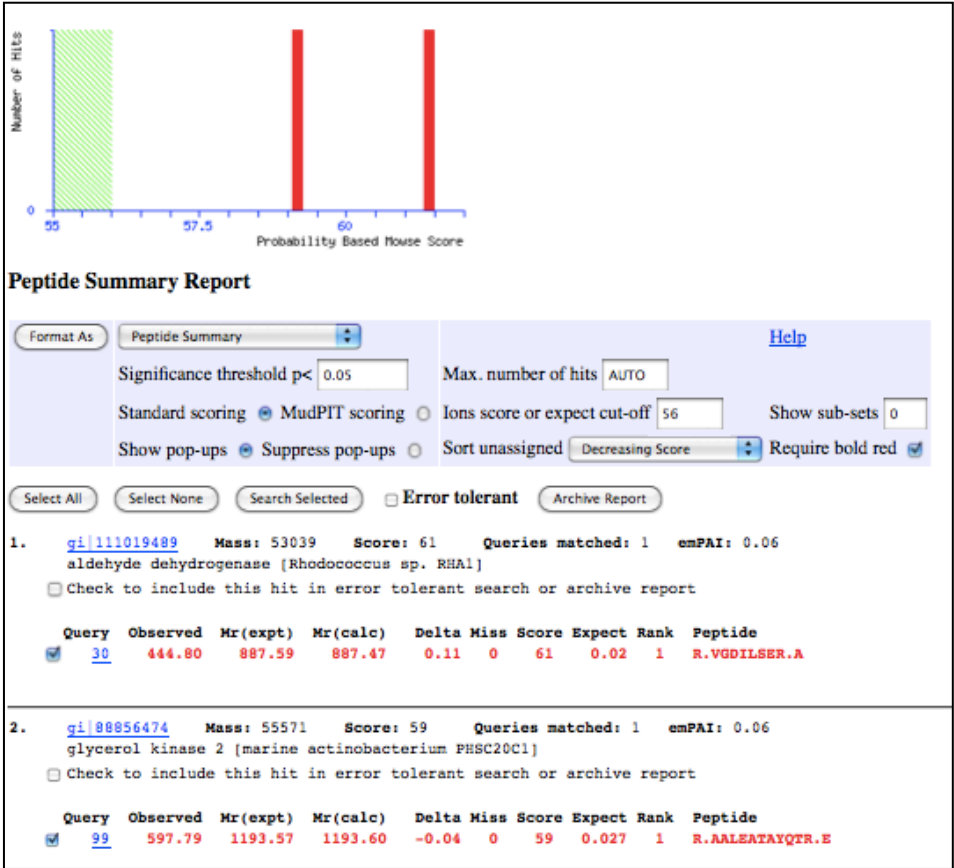
Fig. 6.4 Mascot window showing the database search results relative to the spot 6B data collected from LC/MS/MS analysis. Both the hits are in red and visibly above the significance level threshold. (Compare with Fig. 4.2)

The data collected by LC/MS/MS analyses were used for database searches in NCBI non-redundant database. Mascot was used as protein database search tool. Fig 6.4 shows Mascot analysis results obtained from the LC/MS/MS data collected from the spot 6B. As indicated by the graph (the hits are indicated by red bars) and the Mascot scores (above the threshold of 56), the association of both the proteins to this spot was shown to be statistically significant, therefore the spot protein content was considered identified. Thus, by LC/MS/MS we obtained the identification of the proteins contained in all the five spots under investigation. In Table 6.1 the proteins that were assigned to each spot are reported.

Table 6.1. Identification of *n*-hexane induced *Rhodococcus* sp. BCP1 proteins

Spot ID	MAS-COT score[b]	Accession code	Gene product name	Organism	M_r[a]	pI[a]	Peptide sequences
6A	61	gi|111019489	aldehyde dehydrogenase	*Rhodococcus* sp. RHA1	53039	4.75	R.VGDILSER.A
	59	gi|88856474	glycerol kinase 2	*marine actinobacterium* PHSC20C1	55571	4.85	R.AALEATAYQTR.E
6B	734	gi|15822684	isocitrate lyase	*Rhodococcus equi*	46817	5.04	R.TAEGFYGVK.N K.LQGTVVEEATLAR.R R.EGMTAFVDLQER.E R.TAEEIQKDWDTNPR.W R.TDAEAATLLTSDVDER.D K.AMIAAGVAGSHWEDQLASEK.K K.AMIAAGVAGSHWEDQLASEKK.C K.AYAPYSDLIWMETGVPDLEVAK K.F
6C	500	gi|111023020	probable 1,3-propanediol dehydrogenase	*Rhodococcus* sp. RHA1	43465	5.39	M.GVGAHDIIGVEAK.N K.DVGIPDNFGQVR.T K.IEYQGVEVVLYDK.V R.NLTTVQAADAAVEAAIR.L K.DYNVMEAAALYQKEK.C K.IEYQGVEVVLYDKVESNPK.D
	358	gi|15822684	isocitrate lyase	*Rhodococcus equi*	46817	5.04	K.LQGTVVEEATLAR.R R.LAADVADVPTVVIAR.T R.TDAEAATLLTSDVDER.D K.AMIAAGVAGSHWEDQLASEK.K K.AYAPYSDLIWMETGVPDLEVAK K.F
6D	270	gi|111022963	malate dehydrogenase (oxaloacetate decarboxylating)	*Rhodococcus* sp. RHA1	41230	4.82	R.AIAADETLADR.Y R.VAPAVAEAVAAAAR.A R.LRPSFGAVNLEDISAPR.C K.LAAAEAILSVVGDELAVDK.I
	144	gi|120405820	succinyl-CoA synthetase subunit beta	*Mycobacterium vanbaalenii* PYR-1	40947	4.72	R.TPDDQILALDGK.V K.ALEILGDEANKPLVVR.L
6E	237	gi|29893040	nicotinoprotein alcohol dehydrogenase	*Rhodococcus ruber*	38892	5.13	R.ATISQHSVVK.V K.GGTVVITGLANPEK.L K.GSLFGSANPQYDIVR.L R.YSLEEVNQGYQDLR.D

a) Mr and pI were calculated from the predicted protein sequences.
b) Mascot score is given as S=-10*Log10 (P), where P is the probability that the observed match is a random event. A Mascot Score >56 indicate identity or extensive identity.

The analysis revealed that three of the five spots under investigation contained more than one protein. The spot 6A was identified with a score of 61 and 1% sequence coverage with the aldehyde dehydrogenase of *Rhodococcus* sp. RHA1 (accession number YP_702461) and with a score of 59 and 2% sequence coverage with the glycerol kinase 2 of *Marine actinobacterium* PHSC20C1 (accession number ZP_01131132). The spot B was identified with a score of 734 and a coverage of 20% with the isocytrate lyase of *Rhodococcus equi* (accession number ZP_01131132). The spot C was identified with a score of 500 and a

coverage of 19% with the probable 1,3-propanediol dehydrogenase of *Rhodococcus* sp. RHA1 (accession number YP_705992) and with a score of 358 and a coverage of 12% with the isocytrate lyase of *Rhodococcus equi* (accession number ZP_01131132). The spot D was identified with a score of 270 and a coverage of 15% with the malate dehydrogenase of *Rhodococcus* sp. RHA1 (accession number YP_705935) and with a score of 144 and a coverage of 7% with the succinyl-CoA synthetase subunit beta of *Mycobacterium vanbaalenii* PYR-1 (accession number YP_955649). Spot E was identified with a score of 237 and a coverage of 14% with the nicotinoprotein alcohol dehydrogenase of *Rhodococcus ruber* (accession number AAP02982). The mass values of the query proteins resulting from the Mascot analysis were concordant with the mass of the corresponding spots that could be estimated from the 2D-gels.

6.4 Discussion

In this study using proteomic approaches we obtained consistent data about the metabolic pathways used by *Rhodococcus* sp. BCP1 in the degradation of *n*-alkanes. The number of proteomic studies on *Rhodococcus* strains is very limited, mostly because of the restricted amount of *Rhodococcus* genome information available. To date, the *Rhodococcus* strains that have been completely sequenced are *Rhodococcus jostii* RHA1 [257], *Rhodococcus opacus* B4 [292, 342] and *Rhodococcus erythropolis* PR4 [292, 293]. Indeed, the literature about rhodococcal functional proteomic studies focused mainly on the study of the metabolic pathways associated with mono- and polyaromatic catabolism in *Rhodococcus jostii* RHA1 [282, 352]. Additionally, most of these studies considered only the soluble protein fraction, because of the limitations imposed by the association of low solubility and high hydrophobicity of membrane proteins with the peculiar recalcitrant characteristics of the *Rhodococcus* genus members.

The present chapter described the application of proteomic techniques as a useful approach to study the *n*-alkanes metabolic pathway in *Rhodococcus* sp. BCP1 bypassing the refractory nature of this strain to genetic manipulation. In a first part of the study, 2D gels data from cells growing with *n*-butane (gaseous), *n*-hexane (short-chain liquid), *n*-hexadecane (long-chain liquid) and *n*-eicosane (solid) as sole carbon sources were compared with the data from cells growing on succinate. This analysis provided the global view of the microbial response influenced by the growth on each *n*-alkane with different aliphatic chain-length. By only examining 2D gel images we concluded that the degradation pathways of *n*-hexane and *n*-butane shared some common enzymes while *n*-hexadecane and *n*-eicosane metabolisms seemed to express a distinct pattern of proteins.

In the study here, a broad number of spots that showed differentially accumulating proteins by cells growing on all the *n*-alkanes under investigation were analyzed by MALDI-TOF. Most probably because of the lack of *Rhodococcus* sp. BCP1 genome information, the results obtained by matching the MALDI mass peptide fingerprints with the database sequences were not consistent. Therefore, we decided to subject the protein spots to LC/MS/MS analysis. Due to financial limitations, we focused on the analysis of *n*-hexane-induced protein pattern, since no proteomic analysis has been described so far regarding the degradation pathway of this *n*-alkane. Five spots were consistently expressed in *n*-hexane inducing conditions but not during succinate growth. Three of the five protein spots were shared with butane inducing condition, while only one was common amongst all the *n*-alkanes inducing conditions.

All the five spots were identified and some of them containing more than one protein suggesting an incomplete separation of the protein sample on the 2D gel. This is most probably caused by only partial efficiency of the protein solubilization treatment. Yet their pI's and molecular weights were similar. In spite of this, seven proteins were identified,

namely: a) two proteins are involved in the terminal oxidation of the alkanes: alcohol dehydrogenase (EC 1.1.1.1), aldehyde dehydrogenase (EC 1.2.1.3); b) two proteins are involved in the fatty acid metabolism: glycerol kinase, 1,3-propandiol dehydrogenase (EC 1.1.1.202); and c) three proteins are involved in the TCA cycle: succinyl-CoA synthetase subunit beta, malate dehydrogenase and isocytrate lyase.

Terminal oxidation of the alkanes.

Aerobic metabolism of alkanes generally proceeds through sequential oxidation of a terminal carbon, initiated by monooxygenases, which produce the alcohols that, in turn, are oxidized to the corresponding aldehydes. Aldehydes are further oxidized to the corresponding terminal acyl-CoA derivatives and enter into β-oxidation cycle of fatty acids to generate carbon dioxide and energy (Chapter 1, § 1.3.4).

No monooxygenases were identified in the five spots under investigation (Table 6.1). As demonstrated in Chapter 5 of this dissertation, the growth on *n*-hexane induces the expression of a monooxygenase belonging to the AlkB family. Since AlkB is a transmembrane protein it was expected to be undetectable in the soluble fraction of the BCP1 cell extract. In order to investigate on the induction of the soluble propane monooxygenase coded by the *prm* gene that we identified in *Rhodococcus* sp. BCP1 genome (see Appendix), we aimed to analyze spots representing proteins with size around 63 kDa (mass of the *Rhodococcus jostii* RHA propane monooxygenase homolog to BCP1 Prm). Unfortunately, in this area of the gel, the spots were not resolved enough to be excized from the gel.

Nevertheless, the two oxidoreductases involved in the two steps following the monooxygenase hydroxylation were identified (Fig. 6.5).
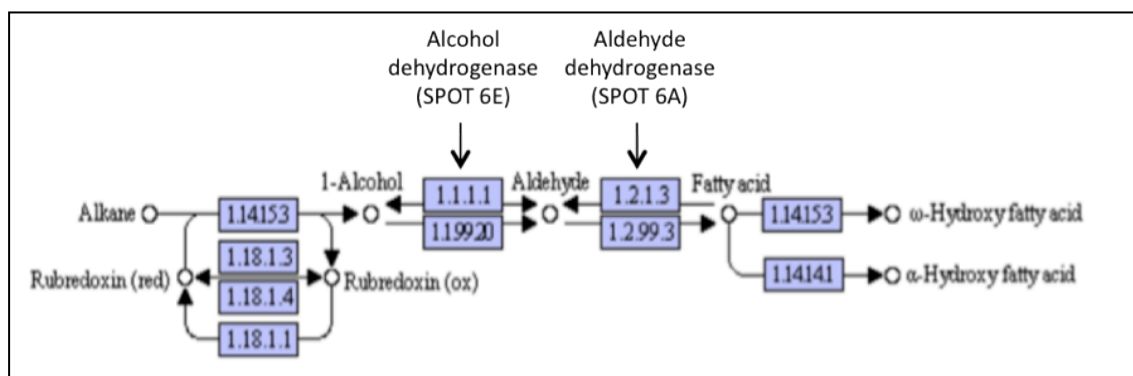
Fig. 6.5 Terminal oxidation of the *n*-alkanes (KEGG Pathway Database; http://www.genome.jp/kegg/pathway.html). The two proteins identified in *Rh*. BCP1 are indicated with the corresponding spots.

Interestingly, the genes encoding the BCP1 alcohol and aldehyde dehydrogenase homologues are consecutive expressed in both *Rhodococcus jostii* RHA1 and *Rhodococcus ruber* P4 genomes (Fig 6.6). Moreover, the stop codon of the aldehyde dehydrogenase gene overlaps with the start codon of the alcohol dehydrogenase gene in both the *Rhodococcus* strains genomes. This genetic structure generally suggests a coupled regulation. Thereby, we can hypothesize the same genetic structure for these two genes in BCP1, because of the increased accumulation identification for both of these proteins in *n*-hexane inducing condition.

Rhodococcus jostii RHA1

RHA1_ro02497: alcohol dehydrogenase (EC 1.1.1.1)

RHA1_ro02498: aldehyde dehydrogenase (EC 1.2.1.3)

Rhodococcus opacus B4
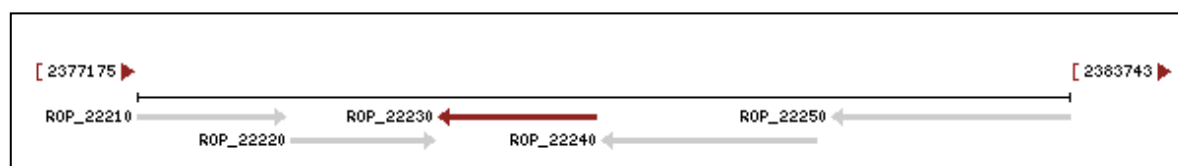
ROP_22230: putative zinc-containing alcohol dehydrogenase (EC 1.1.1.-)

ROP_22240: aldehyde dehydrogenase (EC 1.2.1.3)

Fig. 6.6 *Rhodococcus jostii* RHA1 and *Rhodococcus opacus* B4 genomic regions mapping the two *Rh*. BCP1 oxidoreductases homologues.

175

Fatty acid metabolism.

Fatty acids produced during growth on *n*-alkanes are transformed into CoA-activated fatty acids, which are further degraded via β-oxidation. Most probably because of the limited number of spots under investigation and the limitations of this approach applied to an organism without sequence information, we did not identify any protein associated with this part of the *n*-alkanes metabolism. However, we detected two proteins involved in the fatty acid biosynthesis pathway instead. Glycerol kinase (Spot 6A) catalyzes the transfer of a phosphate from ATP to glycerol thus forming glycerol phosphate. This compound is an initial metabolite in the biosynthesis of phosphoglycerides and triacylglycerols that constitute the phospholipids molecules. 1,3-Propanediol dehydrogenase (Spot 6C) is involved in glycerol synthesis so that it can be considered providing substrate to the glycerol kinase. The induction of enzymes involved in fatty acid biosynthesis by the growth on *n*-alkanes has been already reported in Gram-negative bacteria. The work by Chen *et al* [221] did show the association of the growth on *n*-alkanes by *Pseudomonas putida* GPo1 with an increase in the production of unsaturated fatty acids lipids, while the work by Sabirova *et al* [75] described the induction of enzymes involved in the lipid biosynthetic pathway in *Alcanivorax borkumensis* grown on hexadecane as sole carbon source. Indeed, it has been reported that the growth on *n*-alkanes by *Ps. putida* GPo1 promotes the perturbation of the bacterial membrane structure in response to the accumulation of AlkB alkane hydroxylase protein in the inner membrane [340]. Therefore, on this bacterium, the up-regulation of enzymes involved in the synthesis of unsaturated fatty acids was associated with the need to maintain the membrane fluidity and integrity and to compensate the perturbation caused by the growth on *n*-alkanes [221].

In this present work, we report the association of the growth on *n*-alkanes by *Rhodococcus* sp. BCP1 with the induction of enzymes involved in the unsaturated fatty acids biosynthesis. Similarly to *Pseudomononas putida* GPo1, this result suggests the necessity of

BCP1 to modulate the membrane composition during the growth on *n*-alkanes. It can be due to the perturbation induced by the accumulation in the membrane of the monooxygenase, as it was described for *Ps*. GPo1, or it can be associated with the production of both the long aliphatic chains of mycolic acids and biosurfactants. Mycolic acids constitute the cell wall of bacteria belonging to *Actinobacteria* order and facilitate the uptake of hydrophobic substrates into the cells. Biosurfactants are surface-active substances that can facilitate the adhesion of cells to hydrophobic phases (Chapter 1, § 1.3.1). Since unsaturated fatty acid molecules are biosynthetic precursor of both mycolic acids and biosurfactants, we can hypothesize that the induction of glycerol kinase and 1,3-propandiol dehydrogenase is associated with the mechanisms that allow *Rhodococcus* to contact the *n*-alkanes and, therefore, internalize the hydrophobic carbon source. In general, changes in the fatty acid composition of the membrane lipids of *Actinobacteria* are linked with the ability of these bacteria to alter the fluidity of the cell envelope and the adaptability of membrane composition that are described as efficient ways to resist to toxic compounds (Chapter 1, § 1.3.1).

TCA cycle and glyoxylate bypass.

During growth on alkanes as the sole carbon source, the main intermediate formed during *n*-alkane degradation via β-oxidation of fatty acids is acetyl-CoA. One mechanism to generate all cellular precursor metabolites from this compound is the short-circuiting of the citric acid cycle, through activation of the glyoxylate bypass [75]. Because the standard citric acid cycle involves the addition of two carbons in every cycle, followed by production of two CO_2 molecules, there is no net incorporation of carbons from acetyl-CoA into oxaloacetate. Consequently, during this cycle, acetyl-CoA cannot be converted into glucose (via oxaloacetate of glucoeneogenesis). The glyoxylate cycle is a variant of the standard citric acid cycle which directs acetyl-CoA to the key 3-carbon metabolite phosphoenolpyruvate, via isocitrate, glyoxylate, and malate, by means of isocitrate lyase and malate synthase, thereby

avoiding the CO_2-releasing steps of the cycle as shown in Fig. 6.7.
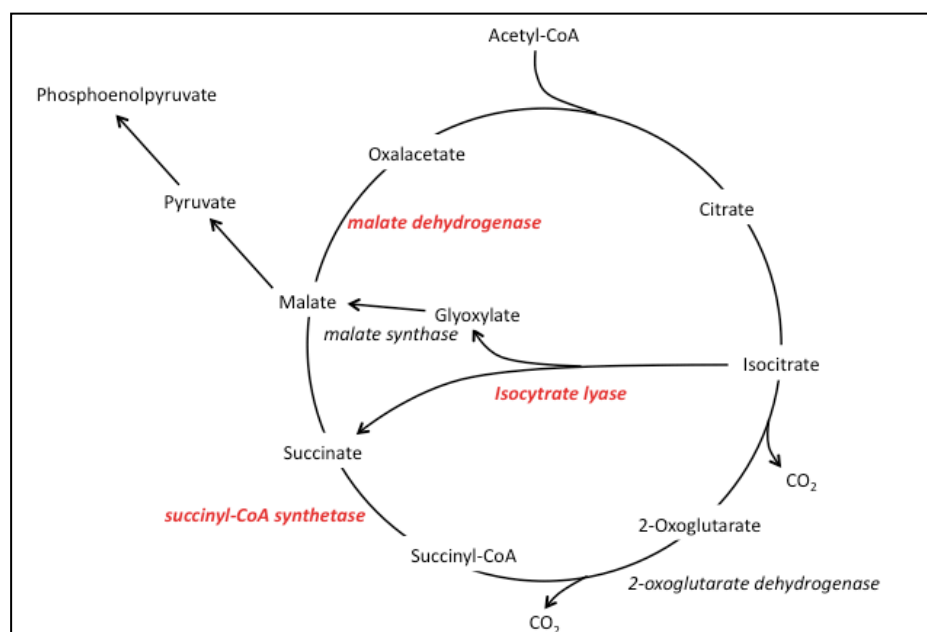
Fig. 6.7 TCA cycle and glyoxylate bypass. Proteins correlated with these cycles and identified in *Rhodococcus* sp. BCP1 cells grown on *n*-hexane are indicated in bold red.

The work by Sabirova *et al* [75] described the up-regulation of isocytrate lyase and malate synthase and a down-regulation of the two CO_2-releasing steps of the TCA cycle in *n*-hexadecane growing *Alcanivorax borkumensis*. Considering that also enzymes involved in gluconeogenesis were up-regulated, they hypothesized that all the biosynthetic precursors in *n*-alkane-grown cells come from acetyl-CoA and that the key metabolic intermediate in *n*-alkane-grown cells is malate, formed through the channeling of acetyl-CoA into the glyoxylate bypass [75].

We identified three enzymes involved in TCA cycle in *Rhodococcus* sp. BCP1 cells grown on *n*-hexane as sole carbon source. Proteins specifically produced in *n*-hexane grown cells but not in succinate grown cells were an isocytrate lyase (spots B and C), a malate dehydrogenase (6D) and the subunit beta of a succinyl CoA synthetase (6D). The two different pI of isocytrate lyase are most likely caused by post-translation modifications of the protein [360]. The over-expression of the isocytrate lyase and malate dehydrogenase would

178

suggest the key role of glyoxylate cycle in *n*-hexane-grown BCP1 cells as it was described in *A. borkumensis,* since the isocytrate lyase is the central enzyme of the cycle and malate dehydrogense has a role in restoring the isocitrate used in the cycle. However, the over-expression of the succinyl CoA synthetase is divergent from this hypothesis because of its role in the complete TCA cycle. Therefore, the utilization of the acetyl-CoA by central metabolic pathways in BCP1 would seem different from that described in *A. borkumensis.* More studies are needed to interpret the role of glyoxylate bypass in context to growth on *n*-alkanes by *Rhodococcus* sp. BCP1.

6.5 Summary

As described above, amongst the five spots excided and analyzed from the 2D gels from *n*-hexane growing cells, three protein spots were shared with butane (6A, 6B, 6E) and one protein (6B) was expressed in all the *n*-alkanes conditions of growth. Thus, the *n*-butane and *n*-hexane-inducing conditions shared the over-expression of alcohol dehydrogenase (6E) and all the *n*-alkanes-inducing conditions shared the over-expression of the isocytrate lyase (6B). The spot 6A was shared by *n*-butane and *n*-hexane growing condition but since it resulted to contain more than one protein, aldehyde dehydrogenase and glycerol kinase, it was not possible to confidently associate the protein content found by mass spectrometry in 6A with the corresponding spot in the 2D gel profile of *n*-butane-growing cells. However, the genetic association in *Rhodococcus jostii* RHA1 of the genes coding for the alcohol and aldehyde dehydrogenases (represented by the spot 6A and 6E) and, therefore, a putative common regulation of the two dehydrogenases, suggested the spot A, in butane-induced map, containing the aldehyde dehydrogenase, while nothing can be said about the other protein present in the spot 6A that is the glycerol kinase.

In conclusion, the results obtained from the proteomic analysis on the growth on *n*-

alkanes by *Rhodococcus* sp. BCP1 suggested that the metabolic pathways involved in the degradation of *n*-butane and *n*-hexane shares the activity of the two oxidoreductases (alcohol and aldehyde dehydrogenase) catalyzing the two steps following the initial alkane oxidation. This indicates that the short chain alkanes metabolism in *Rh*. sp. BCP1 channels *n*-hexane and *n*-butane through the series of oxidation steps described by Fig. 6.5. By contrast, spots corresponding to these oxidoreductases were not detected in *n*-hexadecane and *n*-eicosane-growing BCP1. This suggests the involvement of alternative alcohol and aldehyde dehydrogenases, possibly characterized by specificity for longer carbon chain compounds. The metabolic pathways involved in the degradation of the short chain alkanes (*n*-butane and *n*-hexane) share with those involved in the degradation of long chain alkanes only the isocytrate lyase suggesting the key role of this enzyme in the *Rh*. BCP1 utilization of metabolic products resulting from degradation pathways of all the *n*-alkanes under investigation. In these preliminary studies protein accumulation profiles induced by the growth on C_{16} and C_{20} were distinct from those induced by the growth on short-chain alkanes; however, further studies are needed to identify the spots differentially expressed in C_{16} and C_{20}. Additionally, further improving of the protein sample treatment is required in order to increase the separation of the proteins and thereby the resolution of the 2D-gels and to avoid multiple-proteins spots.

Overall, this study using 2-DE analysis has led to insights into the metabolic pathways involved in the *n*-alkanes degradation in *Rhodococcus* sp. BCP1. We thought to have demonstrated that the combination of this technique with a molecular biology approach is a successful strategy to increase our knowledge about all of the aspects involved in *n*-alkanes degradation and in bacterial adaptation.

Chapter 7 - Conclusions

Nothing is created, nothing is destroyed, everything is transformed. Lavoisier was the first to formally formulate this maxim to express the Law of Conservation of Mass in chemistry. Basically, this statement can also be considered housing the central principle of the *bioremediation* that implies the use of living organisms, primarily microorganisms, to convert environmental contaminants into less toxic forms. When the microorganisms benefit from the use of the contaminant compound as growth substrate, the bioremediation results to be a powerful technology to decontaminate vast polluted areas efficiently and within unprohibiting contained costs.

In the bioremediation science, significant research efforts are focusing on developing and applying molecular techniques to the petroleum microbiology area. The impact of the consequences of hydrocarbon release in the environment maintain a high research interest in the study of microbial metabolisms associated with the biodegradation of aromatic and aliphatic hydrocarbons but also in the analysis of microbial enzymes that can convert petroleum substrates to value-added products [26].

The studies described in this Thesis fall within the research field that directs the efforts into identifying gene/proteins involved in the catabolism of *n*-alkanes and into studying the regulatory mechanisms leading to their oxidation. In particular the studies were aimed at investigating the molecular aspects of the ability of *Rhodococcus* sp. BCP1 to grow on aliphatic hydrocarbons as sole carbon and energy sources.

The data generated in this present Thesis study have led to the following conclusions:

- *Correlation of a monooxygenase activity with the growth on n-alkanes*

The ability of *Rhodococcus* sp. BCP1 to degrade the *n*-alkanes molecules is biochemically correlated with the presence of one or more monooxygenases. In Chapter 3, we observed that

the activation of short-chain alkane molecules, to be entered in the microbial metabolism, is mainly associated with the production of corresponding terminal oxidized alcohols. We also observed that these oxidation activities in *Rh*. BCP1 cells were exclusively induced by the growth on *n*-alkanes. In Chapter 6, two putative oxidoreductases have been detected in the proteome of BCP1 cells grown on short-chain alkanes, but not on succinate. These two oxidoreductases catalyse the degradative steps that follow the first conversion from *n*-alkane to alcohol. The detection of these metabolic activities suggests the *n*-alkane degradation initiates by a monooxygenase followed by another two oxidative steps that convert the alcohol to an aldehyde and then to fatty acid. These results outline the similarities in the initial steps of *n*-alkanes degradation pathway in *Rhodococcus* sp. BCP1 with those described in *Pseudomonas putida* GPo1 (Chapter 1, § 1.3.4.3.2).

- *Detection of a gene encoding a monooxygenase belonging to AlkB family that is induced by liquid and solid n-alkanes*

The growth on liquid and solid *n*-alkanes induces the expression of *alkB* gene that encodes an alkane monooxygenase belonging to the transmembrane monooxygenase family AlkB. The detection and the molecular characterization of the *alkB* gene cluster are described in Chapter 4. In Chapter 5 the transcription of the genes coding for the AlkB components as a single operon was demonstrated and the *n*-alkanes induction of the *alkB* gene expression was examined. A broad range of *n*-alkanes, not including gasses, was shown to induce the *alkB* gene expression. Further analysis of the *alkB* gene expression identified the transcriptional starting site and the putative regulatory elements of the promoter. Furthermore, the effects on *alkB* expression by the presence of alternative carbon sources and putative products of *n*-alkane metabolism were evaluated.

The involvement of an alternative monooxygenase in the gaseous *n*-alkane metabolism was suggested by the detection of a *prmA* gene fragment by PCR-based methodology as described

in Appendix. BCP1 *prmA* gene is homologous to genes encoding soluble di-iron monooxygenases. Some of them have been described in literature to catalyze the first oxidative step on gaseous *n*-alkanes (Chapter 1, § 1.3.4.2).

These studies suggest that the *Rhodococcus* sp. BCP1 AlkB monooxygenase has a role in the first metabolic step of *n*-alkanes in the range from *n*-hexane (C_6) to *n*-eicosane (C_{20}). The analysis of the *alkB* expression also suggest a mechanism of regulation that is in some aspects similar to the *alkB* regulation mechanism described in *Ps*. *putida* GPo1 and *Alkanivorax borkumensis* (Chapter 1, §. 1.3.4.6) (the involvement of AlkS-like transcriptional regulator in BCP1 *alkB* expression). However, some interesting divergences from these known regulatory systems have been also detected (BCP1 *alkB* is not controlled by catabolite repression mechanism).

- *Association of the activation of fatty acid biosynthesis with the growth on n-alkane in Rhodococcus sp. BCP1*

The putative involvement of enzymes for fatty acid biosynthetic pathways in the growth on *n*-alkanes was suggested by the proximity of *alkB* gene to genes encoding enzymes associated with this anabolic pathway (Chapter 4). These hypotheses were verified by the proteomic study reported in Chapter 6 that showed the expression of a glycerol kinase and a 1,3-propandiol dehydrogenase in BCP1 cells grown on *n*-hexane but not on succinate. These two enzymes are involved in the triacylglycerol fatty acids biosynthesis.

In this regard, an up-regulation of enzymes for fatty acid biosynthesis was reported in the proteomic analysis of *Alkanivorax borkumensis* cells grown on *n*-hexadecane [75]. Physiological studies also indicated an increase in the unsaturated fatty acid content in the membrane of *Ps*. *putida* GPo1 cells growing on *n*-alkanes as sole carbon source. This was correlated with the necessity of the cells to increase the fluidity of the membrane structure due to the perturbation associated with the accumulation of AlkB monooxygenases in the inner

membrane [221, 340].

The proteomic studies here on *Rhodococcus* sp. BCP1 confirm the alteration of the fatty acid metabolism in response to the growth on *n*-alkanes. The correlation with the studies on *Ps. putida* GPo1 suggests that the activation of fatty acid biosynthetic pathway in BCP1 is likely a physiological response to the perturbations induced by the growth on *n*-alkanes.

7.1 Future directions

Collectively, these studies have added considerably to the general understanding in the metabolic and adaptive ability of *Rhodococcus* genus to grow on *n*-alkanes and have provided insight into some interesting aspects concerning the expression of *alkB* gene in this genus. Nevertheless, the construction of *alkB* gene knockout mutant is required in order to confirm the role of AlkB in the degradation of the *n*-alkanes in *Rhodococcus* sp. BCP1. Additionally, the construction of random-mutagenesis libraries would provide a high throughput approach to study the genetic system of this strain correlated with the broad range of metabolic activities, including the role still unknown of two new monooxygenases detected in the genome of *Rh.* sp. BCP1 (Appendix).

The versatility in utilizing hydrocarbons and the discovery of new remarkable metabolic activities outline the potential applications of this microorganism in environmental and industrial biotechnologies.

Preamble to Appendix

In addition to the main project of my Thesis concerning the AlkB monooxygenase, other works have been conducted in parallel to evaluate the presence of alternative monooxygenases in *Rhodococcus* sp. BCP1 that could be involved in the BCP1 metabolism of gaseous *n*-alkanes. Although the results obtained are only preliminary, they are reported in this Appendix for the sake of completeness. Since the experiments are still under progress, the data collected to date are described without providing an exhaustive discussion. However, I considered appropriate to report them here since they can help to complete the discussion about the role of AlkB in the BCP1 metabolism of *n*-alkanes (that does not include gaseous *n*-alkanes).

APPENDIX - Detection of other monooxygenases in *Rhodococcus* sp. BCP1 genome

The gene expression results obtained in Chapter 5 suggested that the transmembrane monooxygenase AlkB is not involved in the metabolism of gaseous *n*-alkanes in *Rhodococcus* sp. BCP1. Therefore, the presence of genes encoding other monooxygenases that could have a role in this metabolism was hypothesized.

In this study, preliminary work has been carried out in order to identify genes coding for monooxygenases belonging to the soluble di-iron monooxygenase (SDIMO) and cytochrome P450 families (Chapter 1, § 1.3.4.2 and § 1.3.4.4, respectively). By using a PCR-based method with degenerate primers for each family, two BCP1 genome fragments were amplified and were cloned. The two genes were identified and comparative analysis of their sequences confirmed their association to these monooxygenase families.

Further analyses are necessary in order to obtain the full sequence of these two genes. Expression and metabolic analysis will finally evaluate their role in the *n*-alkanes metabolism in *Rhodococcus* sp. BCP1

A.1 Amplification of *prmA* gene fragment from *Rhodococcus* sp. BCP1 and hybridization results of the *prmA probe* with *Rhodococcus* sp. BCP1 genome

Rhodococcus sp. BCP1 genomic DNA was extracted as described in the General materials and methods chapter. The degenerate primers NVC57, NVC58, NVC65 and NVC66 described by Coleman *et al*. [121] were used to PCR-amplify a region of the SDIMO alpha subunit gene from the BCP1 genome. The primers were designed to target the conserved regions resulting from the alignment of alkene and alkane monooxygenases belonging to the SDIMO groups 3, 4 and 5 (Chapter 1, § 1.3.4.2). The coding region of the two iron-binding motifs E…E/DX$_2$H, that are highly conserved across the SDIMO family [120], were used as the target for the two forward primers (NVC57, NVC58). The positions of the four primers on

186

the sequences and the sizes of the expected PCR products are indicated in Fig. A.1.
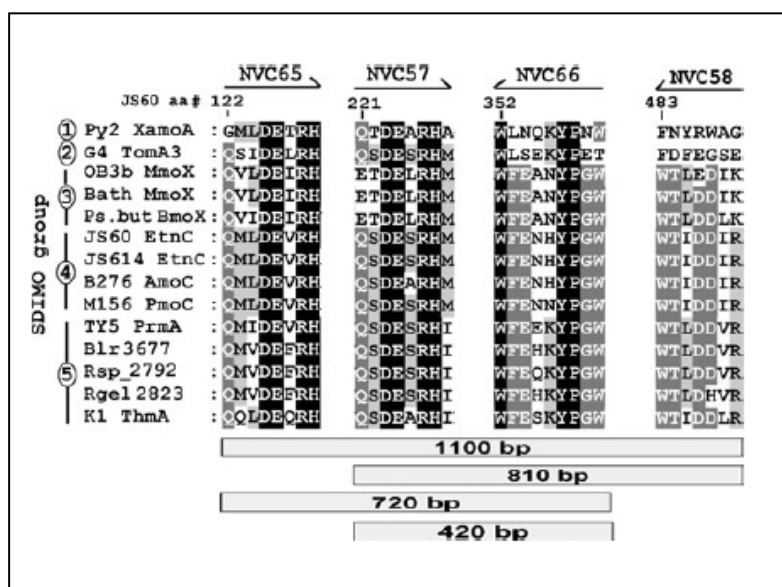
Fig A.1. Amino acid alignment showing conserved regions of SDIMO alpha subunits targeted for primer design by Coleman *et al* [121].

The *Rhodococcus* sp. BCP1 DNA genome was extracted as described in General materials and methods (Chapter 2, § 2.2) and was used as template for the PCR reactions described by Coleman *et al*. [121]. The products obtained by the four different conventional PCRs (using two-primer combinations) and by one nested PCR (using a four-primer combination) were examined (Fig. A.1). The nested PCR was performed using 1 μl of a NVC65-NVC58 PCR mixture as the template for secondary amplification with NVC57-NVC66. The PCR amplification parameters used are described by Coleman *et al* [121]. For each PCR reaction a single product band was detected of the expected size. Each band was purified from the 1.5 % agarose gel, and then cloned in the pCR 2.1-TOPO plasmid using the TOPO TA cloning kit (Invitrogen). Finally, each clone was sent for sequencing to the BMR-genomics service of the University of Padova (Padova, Italy).
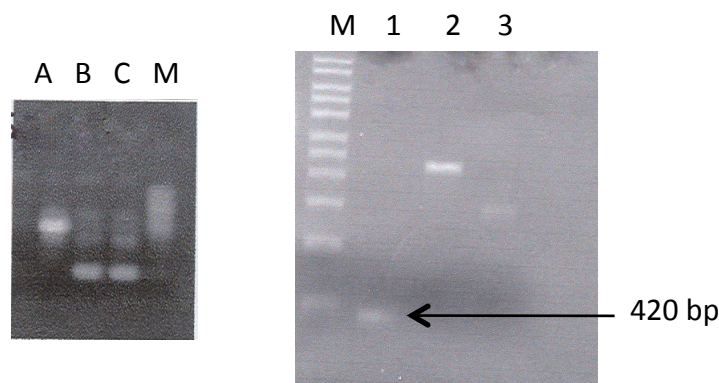
Fig. A.2 The gel on the left shows the PCR products resulting from the two primer combinations (Lines A, B) and from the nested PCR (4 primers combination) (Line C) (M represents the 1kb ladder). The gel on the right represents the PCR bands after purification. The 420 bp product is indicated by an arrow. The other two PCR products (Lines 2 and 3) resulted to be nonspecific products.

As result, several PCR products with and without expected sizes were amplified from BCP1 genome. Finally, only the nested-PCR product (420 bp) showed homology in nucleotide and translated amino acid sequence to members of the soluble di-iron monooxygenase family present in database (Line 1 in Fig. A.2). The other two PCR products resulted to be PCR non-specific products (Lines 2 and 3 in Fig. A.2).
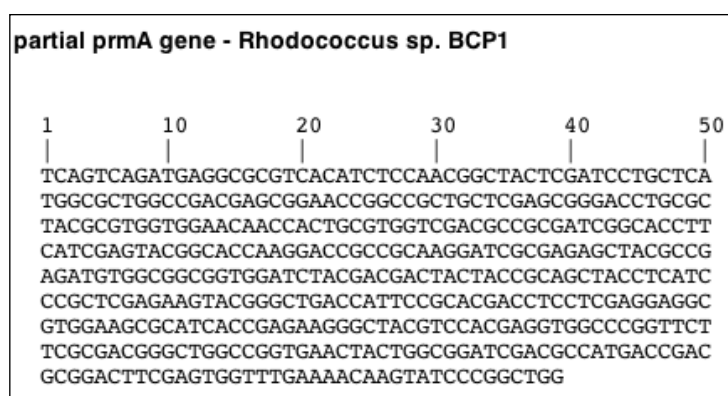
Fig. A.3 Nucleotide sequence of the fragment *prmA* amplified by using nested-PCR methodology with degenerate primers described by Coleman *et al.* [121]

The amino acid sequence of this new BCP1 gene revealed to be part of the ferritin-like di-iron-binding domain (cd01057) that is typically found in the sequence of alpha subunits in aromatic and alkene monooxygenase hydroxylases. The BCP1 SDIMO fragment showed the highest homology in database with the alpha subunits of the propane monooxygenase hydroxylases of three *Rhodococcus* strains (sp. SMV105, sp. SMV106 and sp. SMV156), and

with the large subunit of the propane monooxygenase hydroxylase of *Rhodococcus jostii* RHA1. The work by Rodriguez, F. *et al.* [361] described the three *Rhodococcus* strains to be involved in light hydrocarbon oxidation, while Prm hydroxylase in RHA1 was shown to be up-regulated in this microorganism during the growth on *n*-propane. It was also described to be involved in the propane-induced co-metabolism for the removal of the contaminant N-nitrosodimethylamine (NMDA) [65]. The BCP1 SDIMO amino acid sequence was then aligned with other SDIMO members available in database.
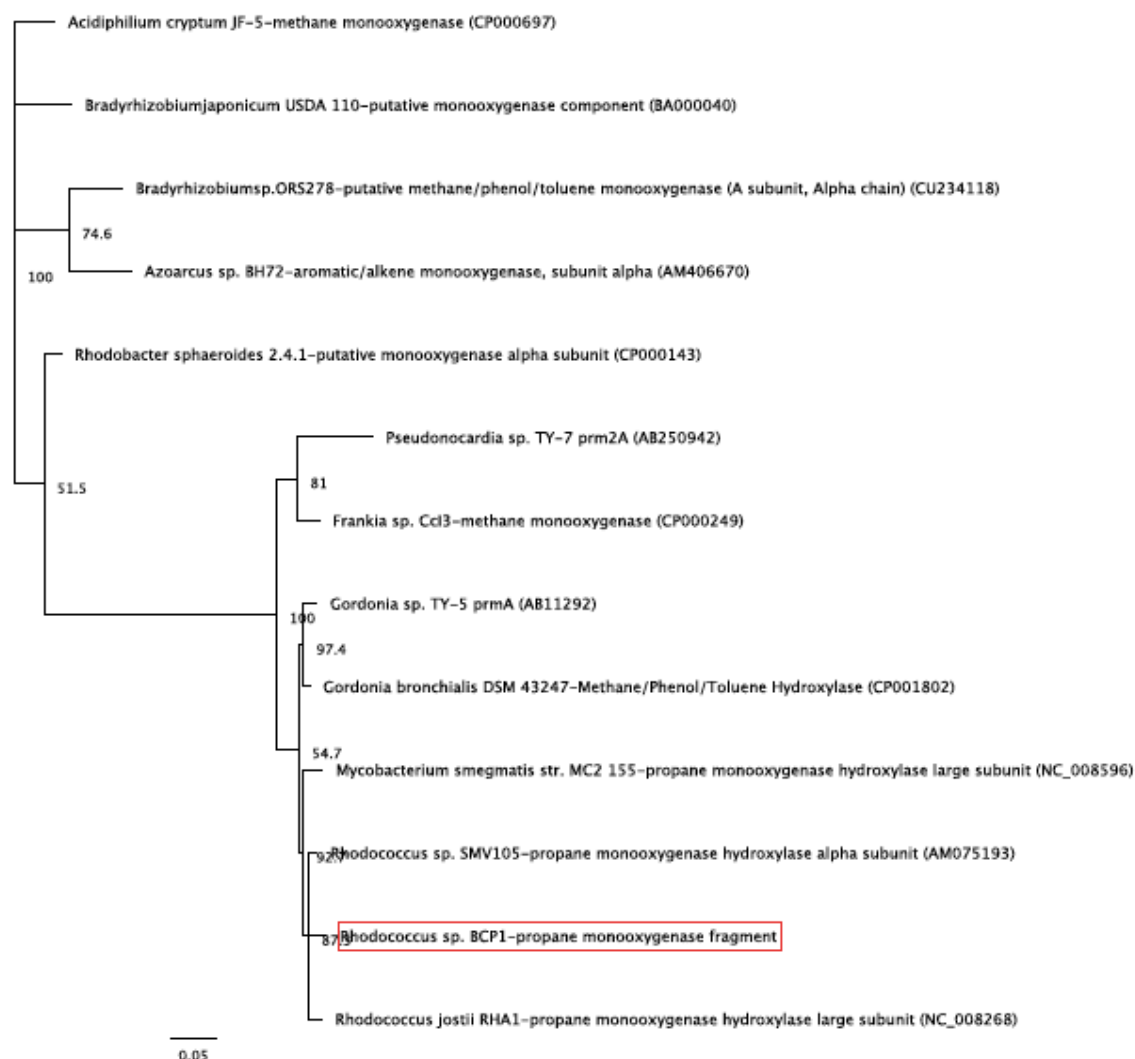
Fig. A.4. Phylogenetic analysis of *Rhodococcus* sp. BCP1 *prmA* fragment. Dendrogram results from the alignment of *Rhodococcus* sp. BCP1 Prm amino acid sequence (marked in red) with representative SDIMO members of Gram-negative and Gram-positive bacteria. The protein IDs are indicated within brackets. Alignment was done with the CLUSTALW program and the tree was constructed with Jukes-Cantor genetic model and neighbour-joining algorithm in Geneious platform [315]. The *Acidiphilium cryptum* JF-5-methane monooxygenase sequence (CP000697) was used as outgroup sequence. Bootstrap values based on 1000 replications are listed at the branch nodes.

The phylogenetic analysis in Fig. A.4 suggested the association of BCP1 SDIMO gene product with the group of SDIMO including the propane monooxygenases (Prm) of related *Rhodococcus*, *Mycobacterium*, and *Gordonia* strains. According with this phylogenetical analysis, the new gene was designed *Rhodococcus* sp. BCP1 *prmA*.

Subsequently, the *prmA* fragment of BCP1 was used as a probe (*prmA probe*) in order to isolate and clone the *prm* full-length gene sequence. The 420 bp fragment, amplified by nested PCR with the four NVC primers, was labeled with [^{32}P]dCTP as described in the

190

General materials and methods chapter (Chapter 2, § 2.5) and used for Southern blot analysis of BCP1 genomic DNA digested with *EcoRI, BamHI, Kpn*I, *Pst*I, and *Sac*I restriction enzymes (Fig. A.5).
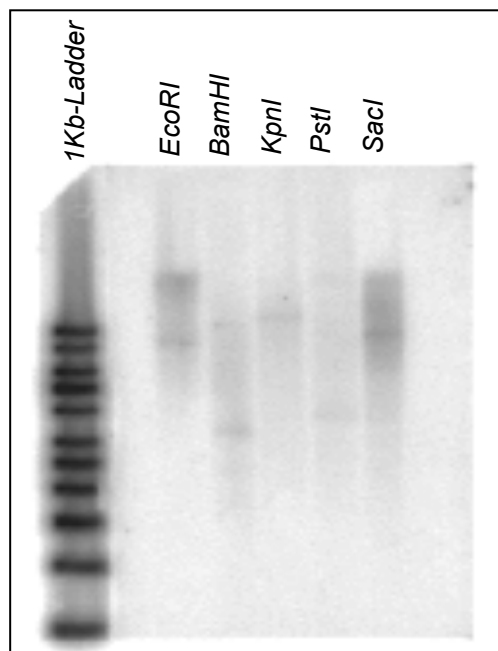
Fig. A.5 Southern blot analysis of the *Rhodococcus* sp. BCP1 genome hybridized with the *prmA probe*

The fragment of ~ 4.2 Kb hybridizing with BCP1 genomic DNA digested with *BamHI* was subsequently cloned in pUC18 cloning vector and transformed in *E. coli* DH5α competent cells. Positive clones were transferred by tooth-picking on LB plates containing ampicillin (50 μg/ml) to form ordered grids and bacterial colony blots were prepared from LB agar plates on nylon membranes as described by Sambrook *et al* [320].

Hybridization analysis was performed as described in the General materials and methods chapter (Chapter 2, § 2.5) with the 420 bp *prm* radioactive-labeled probe. Plasmid DNA was isolated from positive clones using the PureLink™ Quick Plasmid Miniprep but unfortunately only 'false positive' clones were identified. Further attempts are in progress to isolate clones from colony blot that contains *prm* full gene. The high background problem signal that affected the Colony blot results may be associated to the short size of the *prm* probe.

A.2 Amplification of cytochrome P450 coding gene fragment from *Rhodococcus* sp. BCP1

A gene coding for a cytochrome P450 monooxygenase was identified in *Rhodococcus* sp. BCP1 by using degenerate primers for this protein family. Different degenerate primer pairs have been described in literature to be able to amplify conserved regions of different classes of P450 cytochromes. Indeed, the P450 cytochromes are a large and diverse group of enzyme that catalyzes the oxidation of a big variety of organic compounds [205]. We decided to use the oligonucleotides described in literature that seemed to have the most suitable characteristics for our purpose that included either targeting a *n*-alkane degradation system or being specific for *Rhodococcus* genus peculiar codon usage.

1) P450fw1 (5'-GTSGGCGGCAACGACACSAC-3'), and P450rv3 (5'-GCASCGGTGGATGCCGAAGCCRAA-3') were designed by van Beilen *et al* [334]. They were designed on the conserved regions detected by the alignment between the hexane hydroxylase sequence of *A. calcoaceticus* EB104 and two homologues in *Caulobacter crescentus* and *Bradyrhizobium japonicum* genomes. The two conserved sequences corresponded to the oxygen-binding stretch (GGNDTTRN) in the I-helix and the sequence ending with the heme-binding cysteine (HLSFGFGIHRC). The hexane hydroxylase of *Acinetobacter calcoaceticus* EB014 is the first described member of the CYP153 monooxygenase family. To date, CYP153 monooxygenases represent the only group of the P450 superfamily that has been described to have a role in microbial *n*-alkanes oxidation [205, 334]

2) CypF1 (5'-CTACTGGGTSGTCACSCGSTACGA-3'), CypR1 (5'-GCAYTCCTCGAYGGCSTTGGGGAT-3') were designed by Liu L. *et al.* [362]. These primers were used to identify a new member of class IV of cytochrome P450 monooxygenases in *Rhodococcus ruber* strain DSM 44319. This new P450

monooxygenase was described to have hydroxylation activity towards a broad range of aromatic compounds.

3)   The oligonucleotides, named OBM (5'-TSCTSCTSATCGCSGGSCACGAGAC-3') and HLP (5'-GCSAGGTTCTGSCCSAGGCACTGGTG-3'), were designed by Roberts *et al* [363]. Similarly to the first primer pair here described, their sequences are based on the oxygen- and heme-binding motifs of the cytochrome P450 hydroxylases but they were specifically designed to accommodate the highly biased codon usage pattern typical of *Rhodococcus* strains. By using these primers the authors amplified PCR products by using DNA genomes of different *Rhodococcus* spp. that resulted to code for a new self-sufficient P450 cytochrome called P450RhF, which consisted of a cytochrome P450 fused to a dioxygenase reductase-like activity.

Amongst these three primers pairs, CypF1/CypR1 (2) and OBM/HLP (3) gave PCR products with expected sizes (Fig. A.6).
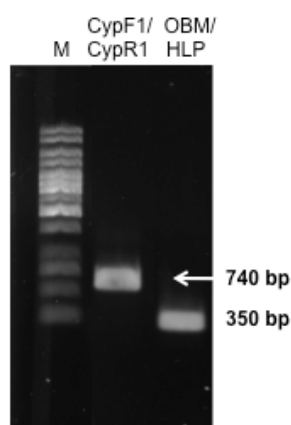
Fig. A.6 PCR amplification products using BCP1 genome as template in two PCR reactions with the degenerate primer pairs CypF1/CypR1 and OBM/HLP. The corresponding sizes of the PCR products are indicated by arrows.

The 740 bp PCR-product translated amino acid sequence showed high similarity with *Rhodococcus opacus* B4 cytochrome P450 (YP_002779008) and *Rhodococcus jostii* RHA1 cytochrome P450 CYP254 (YP_700147). The other PCR product sequence (350 bp) is still under investigation.

```
partial gene coding for cytochrome P450- Rh. sp. BCP1


 1        10        20        30        40        50
 |         |         |         |         |         |
TCTACTGGGTCGTCACCCGCTACGAGGAGCTCCACGAGGTCCTCCGCGAC
CCGGAAACCTTCTCGAGTTACCCGAACAACCTCGTCAATGCCGGGGACGG
CAAGTTTCTGCCGCTCGAGCTCGACCCGCCGGAGCACACCGGATATCGGG
TGGCCCTGCAGCCGCTGTTCTCCCCGAACCGGATGAAGGCGCTGTCCGAG
CAGATCCGGGGCGTGGTCAACGAACTGATCGACAGTTTCGCGGGCAAGGG
TGAGGCGGAGTTCATCGCCGACTTCGCGCACGAGCTGCCCACCCGCGTCT
TCCTCGCGTTGATGGACTGGCCACTCGAGGACGCCCCGATACTCACCGAG
GCCACCGACACCGCCCTGATGGGCAAGCCCGGCGCCAGCGAGGACGAGTC
GGCGAAGGCACGCGCCGAGGCAGCCCAGCAGATGTTCGCCTACTTCCAGA
AGATCGTCGACGAGCGTCGCGCGAACCCCGGTGAGGATGTCACCTCCGCA
CTCATCCGCACCGAGGTCGACCTCGAGGACGGCAAGCGACTGCTCACCGA
CGAAGAGCTGACCCGCATGTTCTTCCTCCTGCTCATCGCAGGTCTGCACA
CCGTTCAGGGATCGCTGGCCTGGGCCGTGATCCACCTGGTGAACAATCCT
CGTCAGCGCGCCGCGCTCATCGAGGACGACTCGCTGATCCCCAACGCCAT
CGAGGAGTGCA
```

Fig. A.7 Nucleotide sequence of the 740 bp-fragment of the *Rhododoccus sp.* BCP1 cytochrome P450 CYP254

The gene coding for the cytochrome P450 homologue in *Rh.* RHA1 was reported by Gonçalves *et al* [280] to be involved in the degradation of mono- or bi-aromatic compounds. Furthermore, KEGG pathway collection (Kyoto Encyclopedia of Genes and Genomes, http://www.genome.jp/kegg/) reports the involvement of this P450 monooxygenase in the RHA1 metabolic pathways of naphthalene, anthracene, limonene, pinene and γ-hexachlorocyclohexane.

A.3 Summary and future directions

PCR-based methodologies are proven to be useful tools to clone genes encoding monooxygenases in *Rhodococcus* sp. BCP1.

The primers designed by Coleman *et al.* [121] detected a gene for a propane monooxygenase in *Rhodococcus* sp. BCP1. This hydroxylase belongs to the family of the soluble di-iron monooxygenase (SDIMO) that includes also the soluble methane monooxygenases and aromatic (toluene) monooxygenases. Since members of this family have been described to be involved in the metabolism of gaseous *n*-alkanes, we can hypothesize a role of this new Prm monooxygenase in butane and *n*-propane metabolism in *Rhodococcus* sp.

BCP1.

With regard to the P450 identification study, the established diversity that exists across members of the cytochrome P450 family motivated the attempts to identify a P450 monooxygenase from BCP1 by using different primer pairs. In the literature other degenerate primer pairs for P450 cytochromes subfamilies have been described and it seems that each of these is able to amplify only a subset of cytochrome P450 genes. This aspect limits the efficacy of PCR-base methods in the identification of monooxygenases belonging to this family.

Further investigations about *Rhodococcus* sp. BCP1 *prm* gene in short-chain alkanes metabolism will include RT-PCR studies and the analysis in heterologous expression systems. Indeed, by transforming *E. coli* cells with a shuttle vector able to express BCP1 Prm in this microbial system, the function of the monooxygenase in gaseous *n*-alkane oxidations could be verified. Its over-expression and purification from the heterologous system could also provide enough amount of protein in order to obtain biochemical information about the hydroxylating reaction performed. With regard to the *Rhodococcus* sp. BCP1 cytochrome P450 CYP254, it does not seem to have homologues monooxygenase previously described to be active on *n*-alkanes, thus, it can have a role in still unknown metabolic pathway in *Rhodococcus* sp. BCP1. Phenotype analysis of a deletion mutant for the gene encoding this P450 will identify its role amongst the *Rhodococcus* sp. BCP1 degradation abilities.

Bibliography

1. Vidali, M., *Bioremediation. An overview*. Pure Appl. Chem., 2001. **73**(7): p. 1163-1172.

2. Allard ann-Sophie, N.A.H., *Bioremediation of organic waste sites: a critical review of microbiological aspects*. International Biodeterioration and Biodegradation, 1997. **39**(4): p. 253-285.

3. Leung, M., *Bioremediation: Techniques for Cleaning up a mess*. BioTeach J, 2004. **2**: p. 18-22.

4. Chaudhry, G.R. and S. Chapalamadugu, *Biodegradation of halogenated organic compounds*. Microbiol Rev, 1991. **55**(1): p. 59-79.

5. Alexander, M., *Biodegradation of chemicals of environmental concern*. Science, 1981. **211**(4478): p. 132-8.

6. Robles-Gonzalez, I.V., F. Fava, and H.M. Poggi-Varaldo, *A review on slurry bioreactors for bioremediation of soils and sediments*. Microb Cell Fact, 2008. **7**: p. 5.

7. Atlas, R.M., *Microbial degradation of petroleum hydrocarbons: an environmental perspective*. Microbiol Rev, 1981. **45**(1): p. 180-209.

8. Field, J. and R. Sierra-Alvarez, *Biodegradability of chlorinated solvents and related chlorinated aliphatic compounds*. Reviews in Environmental Science & Bio/Technology, 2004. **3**: p. 185-254.

9. Tiedje, J., *Bioremediation from an ecological perspec- tive. In: In Situ Bioremediation: When Does it Work?* 1993, Washington, DC: National Academy Press.

10. McCarty, P.L., *Breathing with chlorinated solvents*. Science, 1997. **276**(5318): p. 1521-2.

11. Wackett, L., *Bacterial co-metabolism of halogenated organic compounds*, in *Microbial Transformation and Degradation of Toxic Organic Chemicals*, Y.L.C. C, Editor. 1995, John Wiley & Sons New York. p. 217-241.

12. Horvath, R.S., *Microbial co-metabolism and the degradation of organic compounds in nature*. Bacteriol Rev, 1972. **36**(2): p. 146-55.

13. Alvarez-Cohen, L. and G.E. Speitel, Jr., *Kinetics of aerobic cometabolism of chlorinated solvents*. Biodegradation, 2001. **12**(2): p. 105-26.

14. Kuhn, T.K., et al., *The occurrence of short chain n-alkanes with an even over odd predominance in higher plants and soils*. ORGANIC GEOCHEMISTRY, 2009: p. 1-8.

15. Alexander, L. and D. Grierson, *Ethylene biosynthesis and action in tomato: a model for climacteric fruit ripening*. J Exp Bot, 2002. **53**(377): p. 2039-55.

16. Dennis, M. and P.E. Kolattukudy, *A cobalt-porphyrin enzyme converts a fatty aldehyde to a hydrocarbon and CO*. Proc Natl Acad Sci U S A, 1992. **89**(12): p. 5306-10.

17. Deppenmeier, U., *The unique biochemistry of methanogenesis*. Prog Nucleic Acid Res Mol Biol, 2002. **71**: p. 223-83.

18. Boehm, P.D., J.M. Neff, and D.S. Page, *Assessment of polycyclic aromatic hydrocarbon exposure in the waters of Prince William Sound after the Exxon Valdez oil spill: 1989-2005*. Mar Pollut Bull, 2007. **54**(3): p. 339-56.

19. Peterson, C.H., et al., *Long-term ecosystem response to the Exxon Valdez oil spill*. Science, 2003. **302**(5653): p. 2082-6.

20. Rosenberg E., E.Z.R., *Bioremediation of petroleum contamination*, in *Bioremediation: principles and*
applications, R.L.C.a.D.L. Crawford, Editor. 1996, Cambridge university press: Cambridge.

21. Van Hamme, J.D. and O.P. Ward, *Physical and metabolic interactions of Pseudomonas sp. strain JA5-B45 and Rhodococcus sp. strain F9-D79 during growth on crude oil and effect of a chemical surfactant on them.* Appl Environ Microbiol, 2001. **67**(10): p. 4874-9.

22. Smits, T.H.M., *Cloning and functional analysis of bacterial genes involved in alkane oxidation*, in *Istitute of Biotechnology.* 2001, SWISS FEDERAL INSTITUTE OF TECHNOLOGY ZU¨RICH: Zurich. p. 181.

23. Walker, G., *Climate Change 2007: a world melting from the top down.* Nature, 2007. **446**(7137): p. 718-221.

24. Mehlman, M.A., *Dangerous and cancer-causing properties of products and chemicals in the oil-refining and petrochemical industry--Part XXII: Health hazards from exposure to gasoline containing methyl tertiary butyl ether: study of New Jersey residents.* Toxicol Ind Health, 1996. **12**(5): p. 613-27.

25. Doughty, D.M., *Control of Alkane Monooxygenase Activity and Expression in Pseudomonas butanovora.* 2007, Oregon State University. p. 105.

26. Van Hamme, J.D., A. Singh, and O.P. Ward, *Recent advances in petroleum microbiology.* Microbiol Mol Biol Rev, 2003. **67**(4): p. 503-49.

27. Owsianiak, M., et al., *Biodegradation and surfactant-mediated biodegradation of diesel fuel by 218 microbial consortia are not correlated to cell surface hydrophobicity.* Appl Microbiol Biotechnol, 2009. **84**(3): p. 545-53.

28. van Beilen, J.B., M.G. Wubbolts, and B. Witholt, *Genetics of alkane oxidation by Pseudomonas oleovorans.* Biodegradation, 1994. **5**(3-4): p. 161-74.

29. Beilen, J.B.v., *Alkane oxidation by Pseudomonas oleovorans: genes and proteins.* 1994, University of Groningen: Groningen. p. 127.

30. J.B. van Beilen, Z.L.W.A.D.T.H.M.S. and B. Witholt, *Diversity of alkane hydroxylase systems in the environment.* Oil & Gas Science and Technology 2003: p. 1-14.

31. Watkinson, R.J. and P. Morgan, *Physiology of aliphatic hydrocarbon-degrading microorganisms.* Biodegradation, 1990. **1**(2-3): p. 79-92.

32. Pfaender FK, E.B., *Effects of petroleum on microbial communities.*, in *Petroleum Microbiology*, A. RM, Editor. 1984, Macmillan: New York. p. 507-536.

33. Wentzel, A., et al., *Bacterial metabolism of long-chain n-alkanes.* Appl Microbiol Biotechnol, 2007. **76**(6): p. 1209-21.

34. Boulton CA, R.C., *The physiology of hydrocarbon-utilizing microorganisms*, in *Enzyme and fermentation biotechnology.*, W. A, Editor. 1984, Halstead Press, Wiley: New York. p. 11-77.

35. Singer ME, F.W., *Microbial metabolism of straight- chain and branched alkanes.*, in *Microbial metabolism of straight-chain and branched alkanes*, A. RM, Editor. 1984, Macmillan Publishing Company: New York. p. 1-60.

36. Haferburg D, H.R., Claus R, Kleber HP, *Extracellular microbial lipids as biosurfactants.* Adv Biochem Eng Biotechnol 1986. **33**: p. 53-93.

37. Bouchez-Naitali, M., et al., *Diversity of bacterial strains degrading hexadecane in relation to the mode of substrate uptake.* J Appl Microbiol, 1999. **86**(3): p. 421-8.

38. Finnerty, W.R., *The biology and genetics of the genus Rhodococcus.* Annu Rev Microbiol, 1992. **46**: p. 193-218.

39. Bell, K.S., et al., *The genus Rhodococcus.* J Appl Microbiol, 1998. **85**(2): p. 195-210.

40. de Carvalho, C.C.C.R. and M.M.R. da Fonseca, *The remarkable Rhodococcus erythropolis.* Appl Microbiol Biotechnol, 2005. **67**(6): p. 715-26.

41. Martínková, L., et al., *Biodegradation potential of the genus Rhodococcus.* Environment International, 2009. **35**(1): p. 162-177.

42. T Köhler, L.K.C., F Barja, C van Delden, J C Pechère, *Swarming of Pseudomonas aeruginosa is dependent on cell-to-cell signaling and requires flagella and pili*. J Bacteriology, 2000. **182**(21): p. 5990-6.

43. Caiazza, N.C., R.M. Shanks, and G.A. O'Toole, *Rhamnolipids modulate swarming motility patterns of Pseudomonas aeruginosa*. J Bacteriol, 2005. **187**(21): p. 7351-61.

44. Neu, T.R., *Significance of bacterial surface-active compounds in interaction of bacteria with interfaces*. Microbiol Rev, 1996. **60**(1): p. 151-66.

45. Boles, B.R., M. Thoendel, and P.K. Singh, *Rhamnolipids mediate detachment of Pseudomonas aeruginosa from biofilms*. Mol Microbiol, 2005. **57**(5): p. 1210-23.

46. Montes-Matiʹas, M.C., *Identification and characterization of a novel monooxygenase from burkholderia xenovorans LB400*, in *The Graduate School of Biomedical Sciences*. 2008, University of Medicine and Dentistry of New Jersey: New Jersey. p. 128.

47. Widdel, F. and R. Rabus, *Anaerobic biodegradation of saturated and aromatic hydrocarbons*. Curr Opin Biotechnol, 2001. **12**(3): p. 259-76.

48. Heider, J., Spormann, A. M., Beller, H. R. & Widdel, F., *Review: anaerobic bacterial metabolism of hydrocarbons*. FEMS Microbiol Lett, 1999. **22**: p. 459-473.

49. Rojo, F., *Degradation of alkanes by bacteria*. Environ Microbiol, 2009. **11**(10): p. 2477-90.

50. Kniemeyer, O., et al., *Anaerobic oxidation of short-chain hydrocarbons by marine sulphate-reducing bacteria*. Nature, 2007. **449**(7164): p. 898-901.

51. Rabus, R., et al., *Anaerobic initial reaction of n-alkanes in a denitrifying bacterium: evidence for (1-methylpentyl)succinate as initial product and for involvement of an organic radical in n-hexane metabolism*. J Bacteriol, 2001. **183**(5): p. 1707-15.

52. Murrell, J.C., B. Gilbert, and I.R. McDonald, *Molecular biology and regulation of methane monooxygenase*. Arch Microbiol, 2000. **173**(5-6): p. 325-32.

53. Lieberman, R.L. and A.C. Rosenzweig, *Biological methane oxidation: regulation, biochemistry, and active site structure of particulate methane monooxygenase*. Crit Rev Biochem Mol Biol, 2004. **39**(3): p. 147-64.

54. Black, P.N. and C.C. DiRusso, *Molecular and biochemical analyses of fatty acid transport, metabolism, and gene regulation in Escherichia coli*. Biochim Biophys Acta, 1994. **1210**(2): p. 123-45.

55. Ashraf, W., A. Mihdhir, and J.C. Murrell, *Bacterial oxidation of propane*. FEMS Microbiol Lett, 1994. **122**(1-2): p. 1-6.

56. SMITS, T.H.M., *Cloning and functional analysis of bacterial genes involved in alkane oxidation-PhD thesis*. 2001: p. 1-181.

57. Coon, M.J., *Omega oxygenases: nonheme-iron enzymes and P450 cytochromes*. Biochem Biophys Res Commun, 2005. **338**(1): p. 378-85.

58. Whyte, L.G., et al., *Biodegradation of variable-chain-length alkanes at low temperatures by a psychrotrophic Rhodococcus sp*. Applied and Environmental Microbiology, 1998. **64**(7): p. 2578-84.

59. Kotani, T., et al., *Gene structure and regulation of alkane monooxygenases in propane-utilizing Mycobacterium sp. TY-6 and Pseudonocardia sp. TY-7*. J Biosci Bioeng, 2006. **102**(3): p. 184-92.

60. Kotani, T., et al., *Novel acetone metabolism in a propane-utilizing bacterium, Gordonia sp. strain TY-5*. Journal of Bacteriology, 2007. **189**(3): p. 886-93.

61. Doumenq, P., et al., *Changes in fatty acids of Pseudomonas nautica, a marine denitrifying bacterium, in response to n-eicosane as carbon source and various culture conditions*. FEMS Microbiology Ecology, 1999. **28**: p. 151-161.

62.   Hamamura, N., et al., *Diversity in butane monooxygenases among butane-grown bacteria*. Appl Environ Microbiol, 1999. **65**(10): p. 4586-93.

63.   Dubbels, B.L., L.A. Sayavedra-Soto, and D.J. Arp, *Butane monooxygenase of 'Pseudomonas butanovora': purification and biochemical characterization of a terminal-alkane hydroxylating diiron monooxygenase*. Microbiology (Reading, Engl), 2007. **153**(Pt 6): p. 1808-16.

64.   van Beilen, J.B. and E.G. Funhoff, *Alkane hydroxylases involved in microbial alkane degradation*. Appl Microbiol Biotechnol, 2007. **74**(1): p. 13-21.

65.   Sharp, J.O., et al., *An inducible propane monooxygenase is responsible for N-nitrosodimethylamine degradation by Rhodococcus sp. strain RHA1*. Applied and Environmental Microbiology, 2007. **73**(21): p. 6930-8.

66.   Hamamura, N., C.M. Yeager, and D.J. Arp, *Two distinct monooxygenases for alkane oxidation in Nocardioides sp. strain CF8*. Applied and Environmental Microbiology, 2001. **67**(11): p. 4992-8.

67.   Lopes Ferreira, N., et al., *n-Alkane assimilation and tert-butyl alcohol (TBA) oxidation capacity in Mycobacterium austroafricanum strains*. Appl Microbiol Biotechnol, 2007. **75**(4): p. 909-19.

68.   Margesin, R., et al., *Characterization of hydrocarbon-degrading microbial populations in contaminated and pristine Alpine soils*. Appl Environ Microbiol, 2003. **69**(6): p. 3085-92.

69.   Harayama, S., Y. Kasai, and A. Hara, *Microbial communities in oil-contaminated seawater*. Curr Opin Biotechnol, 2004. **15**(3): p. 205-14.

70.   Schneiker, S., et al., *Genome sequence of the ubiquitous hydrocarbon-degrading marine bacterium Alcanivorax borkumensis*. Nat Biotechnol, 2006. **24**(8): p. 997-1004.

71.   Yakimov, M.M., et al., *Thalassolituus oleivorans gen. nov., sp. nov., a novel marine bacterium that obligately utilizes hydrocarbons*. Int J Syst Evol Microbiol, 2004. **54**(Pt 1): p. 141-8.

72.   Golyshin, P.N., et al., *Oleiphilaceae fam. nov., to include Oleiphilus messinensis gen. nov., sp. nov., a novel marine bacterium that obligately utilizes hydrocarbons*. Int J Syst Evol Microbiol, 2002. **52**(Pt 3): p. 901-11.

73.   Yakimov, M.M., et al., *Oleispira antarctica gen. nov., sp. nov., a novel hydrocarbonoclastic marine bacterium isolated from Antarctic coastal sea water*. Int J Syst Evol Microbiol, 2003. **53**(Pt 3): p. 779-85.

74.   Yakimov, M.M., K.N. Timmis, and P.N. Golyshin, *Obligate oil-degrading marine bacteria*. Curr Opin Biotechnol, 2007. **18**(3): p. 257-66.

75.   Sabirova, J.S., et al., *Proteomic insights into metabolic adaptations in Alcanivorax borkumensis induced by alkane utilization*. Journal of Bacteriology, 2006. **188**(11): p. 3763-73.

76.   Chistoserdova, L., J.A. Vorholt, and M.E. Lidstrom, *A genomic view of methane oxidation by aerobic bacteria and anaerobic archaea*. Genome Biol, 2005. **6**(2): p. 208.

77.   Trotsenko, Y.A. and V.N. Khmelenina, *Biology of extremophilic and extremotolerant methanotrophs*. Arch Microbiol, 2002. **177**(2): p. 123-31.

78.   Dalton, H., *The Leeuwenhoek Lecture 2000 the natural and unnatural history of methane-oxidizing bacteria*. Philos Trans R Soc Lond B Biol Sci, 2005. **360**(1458): p. 1207-22.

79.   Anthony, C., *The Biochemistry of Methylotrophs*. . 1982, London: Academic Press.

80.   Dumont, M.G. and J.C. Murrell, *Community-level analysis: key genes of aerobic methane oxidation*. Meth Enzymol, 2005. **397**: p. 413-27.

81.   Csaki, R., et al., *Genes involved in the copper-dependent regulation of soluble methane monooxygenase of Methylococcus capsulatus (Bath): cloning, sequencing and mutational analysis*. Microbiology-Sgm, 2003. **149**: p. 1785-1795.

82.   Stafford, G.P., et al., *rpoN, mmoR and mmoG, genes involved in regulating the expression of soluble methane monooxygenase in Methylosinus trichosporium OB3b*. Microbiology-Sgm, 2003. **149**: p. 1771-1784.

83.   Lieberman, R.L. and A.C. Rosenzweig, *Crystal structure of a membrane-bound metalloenzyme that catalyses the biological oxidation of methane*. Nature, 2005. **434**(7030): p. 177-182.

84.   Hakemian, A.S. and A.C. Rosenzweig, *The biochemistry of methane oxidation*. Annu Rev Biochem, 2007. **76**: p. 223-41.

85.   Prior, S.D. and H. Dalton, *The Effect of Copper Ions on Membrane Content and Methane Monooxygenase Activity in Methanol-Grown Cells of Methylococcus-Capsulatus (Bath)*. Journal of General Microbiology, 1985. **131**(Jan): p. 155-163.

86.   Murrell, J.C., I.R. McDonald, and B. Gilbert, *Regulation of expression of methane monooxygenases by copper ions*. Trends Microbiol, 2000. **8**(5): p. 221-5.

87.   Stanley, S., S. Prior, and D.L.a.H. Dalton, *Copper stress underlies the fundamental change in intracellular location of methane mono-oxygenase in methane-oxidizing organisms: Studies in batch and continuous cultures* Biotechnology Letters, 1983. **5**(7): p. 487-492.

88.   Sazinsky, M.H., et al., *X-ray structure of a hydroxylase-regulatory protein complex from a hydrocarbon-oxidizing multicomponent monooxygenase, Pseudomonas sp OX1 phenol hydroxylase*. Biochemistry, 2006. **45**(51): p. 15392-15404.

89.   Merkx, M., et al., *Dioxygen activation and methane hydroxylation by soluble methane monooxygenase: A tale of two irons and three proteins*. Angewandte Chemie-International Edition, 2001. **40**(15): p. 2782-2807.

90.   Colby, J., D.I. Stirling, and H. Dalton, *Soluble Methane Mono-Oxygenase of Methylococcus-Capsulatus-(Bath) - Ability to Oxygenate Normal-Alkanes, Normal-Alkenes, Ethers, and Alicyclic, Aromatic and Heterocyclic-Compounds*. Biochemical Journal, 1977. **165**(2): p. 395-402.

91.   Burrows, K.J., A. Cornish, D. Scott, and I. J. Higgins., *Substrate specificities of the soluble and particulate methane mono-oxygenases of Methylosinus trichosporium OB3b.* . J. Gen. Microbiol., 1984. **130**: p. 3327-3333.

92.   Lipscomb, J.D., *Biochemistry of the soluble methane monooxygenase*. Annu Rev Microbiol, 1994. **48**: p. 371-99.

93.   Liu, K.E., and Lippard, S.J., *Studies of the soluble methane monooxygenase protein system: structure, component interactions, and hydroxylation mechanism.* . Adv Inorg Chem 1995. **42**: p. 263–289.

94.   Wallar, B.J. and J.D. Lipscomb, *Dioxygen Activation by Enzymes Containing Binuclear Non-Heme Iron Clusters*. Chem Rev, 1996. **96**(7): p. 2625-2658.

95.   Rosenzweig, A.C., and Lippard, S.J. , *Structure and biochemistry of methane monooxygenase enzyme systems. In Iron and re- lated transition metals in microbial metabolism*, ed. G. Winkelmann and C.J. Carrano. 1997, Amsterdam, The Netherlands: Harwood Academic Publishers.

96.   Baik, M.H., et al., *Mechanistic studies on the hydroxylation of methane by methane monooxygenase*. Chem Rev, 2003. **103**(6): p. 2385-419.

97.   Whittington, D.A., Valentine, A.M., and Lippard, S.J. , *Substrate binding and C H bond activation in the soluble methane monooxy- genase hydroxylase.* . J Biol Inorg Chem, 1998. . **3**: p. 307–313.

98.   Fox, B.G., et al., *Methane monooxygenase from Methylosinus trichosporium OB3b. Purification and properties of a three-component system with high specific activity from a type II methanotroph.* J Biol Chem, 1989. **264**(17): p. 10023-33.

99.   Sullivan, J.P., D. Dickinson, and H.A. Chase, *Methanotrophs, Methylosinus trichosporium OB3b, sMMO, and their application to bioremediation.* Crit Rev Microbiol, 1998. **24**(4): p. 335-73.

100.   Rosenzweig, A.C., et al., *Crystal structure of a bacterial non-haem iron hydroxylase that catalyses the biological oxidation of methane.* Nature, 1993. **366**(6455): p. 537-43.

101.   Woodland, M.P. and H. Dalton, *Purification and characterization of component A of the methane monooxygenase from Methylococcus capsulatus (Bath).* J Biol Chem, 1984. **259**(1): p. 53-9.

102.   Fox, B.G., et al., *Evidence for a mu-oxo-bridged binuclear iron cluster in the hydroxylase component of methane monooxygenase. Mossbauer and EPR studies.* J Biol Chem, 1988. **263**(22): p. 10553-6.

103.   Dewitt, J.G., Bentsen, J. G., Rosenzweig, A. C. & 7 other authors, *X-ray absorption, Mossbauer, and EPR studies of the dinuclear iron center in the hydroxylase component of methane monooxygenase.* J Am Chem Soc 1991. **113**: p. 9219–9235.

104.   Beauvais, L.G. and S.J. Lippard, *Reactions of the diiron(IV) intermediate Q in soluble methane monooxygenase with fluoromethanes.* Biochem Biophys Res Commun, 2005. **338**(1): p. 262-6.

105.   Balasubramanian, R. and A.C. Rosenzweig, *Structural and mechanistic insights into methane oxidation by particulate methane monooxygenase.* Acc Chem Res, 2007. **40**(7): p. 573-80.

106.   Stainthorpe, A.C., et al., *The methane monooxygenase gene cluster of Methylococcus capsulatus (Bath).* Gene, 1990. **91**(1): p. 27-34.

107.   Stainthorpe, A.C., et al., *Molecular analysis of methane monooxygenase from Methylococcus capsulatus (Bath).* Arch Microbiol, 1989. **152**(2): p. 154-9.

108.   Merkx, M. and S.J. Lippard, *Why OrfY? Characterization of MMOD, a long overlooked component of the soluble methane monooxygenase from Methylococcus capsulatus (Bath).* J Biol Chem, 2002. **277**(8): p. 5858-65.

109.   Murrell, J.C., *Genetics and molecular biology of methanotrophs.* FEMSMicrobiologyReview, 1992. **88**: p. 233-248.

110.   Nielsen, A.K., et al., *Regulation of bacterial methane oxidation: transcription of the soluble methane mono-oxygenase operon of Methylococcus capsulatus (Bath) is repressed by copper ions.* Microbiology, 1996. **142 (Pt 5)**: p. 1289-96.

111.   McDonald, I.R., et al., *The soluble methane monooxygenase gene cluster of the trichloroethylene-degrading methanotroph Methylocystis sp. strain M.* Appl Environ Microbiol, 1997. **63**(5): p. 1898-904.

112.   Nielsen, A.K., K. Gerdes, and J.C. Murrell, *Copper-dependent reciprocal transcriptional regulation of methane monooxygenase genes in Methylococcus capsulatus and Methylosinus trichosporium.* Mol Microbiol, 1997. **25**(2): p. 399-409.

113.   Phelps, P.A., et al., *Methylosinus trichosporium OB3b Mutants Having Constitutive Expression of Soluble Methane Monooxygenase in the Presence of High Levels of Copper.* Appl Environ Microbiol, 1992. **58**(11): p. 3701-3708.

114.   Zahn, J.A. and A.A. DiSpirito, *Membrane-associated methane monooxygenase from Methylococcus capsulatus (Bath).* J Bacteriol, 1996. **178**(4): p. 1018-29.

115.   Chan, S.I., et al., *Toward delineating the structure and function of the particulate methane monooxygenase from methanotrophic bacteria.* Biochemistry, 2004. **43**(15): p. 4421-30.

116.   Semrau, J.D., et al., *Particulate methane monooxygenase genes in methanotrophs*. J Bacteriol, 1995. **177**(11): p. 3071-9.

117.   Stolyar, S., et al., *Role of multiple gene copies in particulate methane monooxygenase activity in the methane-oxidizing bacterium Methylococcus capsulatus Bath*. Microbiology (Reading, Engl), 1999. **145 (Pt 5)**: p. 1235-44.

118.   Seila, R.L., et al., *Atmospheric volatile organic compound measurements during the 1996 Paso del Norte Ozone Study*. Sci Total Environ, 2001. **276**(1-3): p. 153-69.

119.   Kotani, T., et al., *Propane monooxygenase and NAD+-dependent secondary alcohol dehydrogenase in propane metabolism by Gordonia sp. strain TY-5*. Journal of Bacteriology, 2003. **185**(24): p. 7120-8.

120.   Leahy, J.G., P.J. Batchelor, and S.M. Morcomb, *Evolution of the soluble diiron monooxygenases*. FEMS Microbiology Reviews, 2003. **27**(4): p. 449-479.

121.   Coleman, N.V., N.B. Bui, and A.J. Holmes, *Soluble di-iron monooxygenase gene diversity in soils, sediments and ethene enrichments*. Environmental Microbiology, 2006. **8**(7): p. 1228-39.

122.   Zhang, J., et al., *Methane monooxygenase hydroxylase and B component interactions*. Biochemistry, 2006. **45**(9): p. 2913-26.

123.   Zhang, Y., et al., *Structural studies on 3-hydroxyanthranilate-3,4-dioxygenase: the catalytic mechanism of a complex oxidation involved in NAD biosynthesis*. Biochemistry, 2005. **44**(21): p. 7632-43.

124.   Elsen, N.L., et al., *Redox and functional analysis of the Rieske ferredoxin component of the toluene 4-monooxygenase*. Biochemistry, 2007. **46**(4): p. 976-86.

125.   Moe, L.A., et al., *Structure of T4moC, the Rieske-type ferredoxin component of toluene 4-monooxygenase*. Acta Crystallogr D Biol Crystallogr, 2006. **62**(Pt 5): p. 476-82.

126.   Moe, L.A., L.A. McMartin, and B.G. Fox, *Component interactions and implications for complex formation in the multicomponent toluene 4-monooxygenase*. Biochemistry, 2006. **45**(17): p. 5478-85.

127.   Small, F.J. and S.A. Ensign, *Alkene monooxygenase from Xanthobacter strain Py2. Purification and characterization of a four-component system central to the bacterial metabolism of aliphatic alkenes*. J Biol Chem, 1997. **272**(40): p. 24913-20.

128.   Arp, D.J., *Butane metabolism by butane-grown 'Pseudomonas butanovora'*. Microbiology (Reading, Engl), 1999. **145 (Pt 5)**: p. 1173-80.

129.   Takahashi, J., *Production of intracellular protein from n-butane by Pseudomonas butanovora sp. nov.*. Adv. Appl. Microbiol., 1980. **26**: p. 117–127.

130.   Mclee, A.G., M. Wayman, and A.C. Kormendy, *Isolation and Characterization of Butane-Utilizing Microorganisms*. Canadian Journal of Microbiology, 1972. **18**(8): p. 1191-&.

131.   Sluis, M.K., L.A. Sayavedra-Soto, and D.J. Arp, *Molecular analysis of the soluble butane monooxygenase from 'Pseudomonas butanovora'*. Microbiology (Reading, Engl), 2002. **148**(Pt 11): p. 3617-29.

132.   Halsey, K.H., et al., *Site-directed amino acid substitutions in the hydroxylase alpha subunit of butane monooxygenase from Pseudomonas butanovora: Implications for substrates knocking at the gate*. Journal of Bacteriology, 2006. **188**(13): p. 4962-9.

133.   Vangnai, A.S., D.J. Arp, and L.A. Sayavedra-Soto, *Two distinct alcohol dehydrogenases participate in butane metabolism by Pseudomonas butanovora*. Journal of Bacteriology, 2002. **184**(7): p. 1916-24.

134.   Vangnai, A.S., L.A. Sayavedra-Soto, and D.J. Arp, *Roles for the two 1-butanol dehydrogenases of Pseudomonas butanovora in butane and 1-butanol metabolism*. Journal of Bacteriology, 2002. **184**(16): p. 4343-50.

135. Whittington, D.A. and S.J. Lippard, *Crystal structures of the soluble methane monooxygenase hydroxylase from Methylococcus capsulatus (Bath) demonstrating geometrical variability at the dinuclear iron active site*. Journal of the American Chemical Society, 2001. **123**(5): p. 827-838.

136. Coufal, D.E., et al., *Sequencing and analysis of the Methylococcus capsulatus (Bath) soluble methane monooxygenase genes*. European Journal of Biochemistry, 2000. **267**(8): p. 2174-2185.

137. Doughty, D.M., et al., *Product repression of alkane monooxygenase expression in Pseudomonas butanovora*. Journal of Bacteriology, 2006. **188**(7): p. 2586-92.

138. Sayavedra-Soto, L.A., C.M. Byrd, and D.J. Arp, *Induction of butane consumption in Pseudomonas butanovora*. Arch Microbiol, 2001. **176**(1-2): p. 114-20.

139. Kurth, E.G., et al., *Involvement of BmoR and BmoG in n-alkane metabolism in 'Pseudomonas butanovora'*. Microbiology (Reading, Engl), 2008. **154**(Pt 1): p. 139-47.

140. Doughty, D.M., et al., *Effects of dichloroethene isomers on the induction and activity of butane monooxygenase in the alkane-oxidizing bacterium "Pseudomonas butanovora"*. Applied and Environmental Microbiology, 2005. **71**(10): p. 6054-9.

141. Sayavedra-Soto, L.A., et al., *Product and product-independent induction of butane oxidation in Pseudomonas butanovora*. FEMS Microbiol Lett, 2005. **250**(1): p. 111-6.

142. Shennan, J.L., *Utilisation of C2-C4 gaseous hydrocarbons and isoprene by microorganisms*. J. Chem. Technol. Biotechnol., 2006. **81**(3): p. 237-256.

143. LeBlanc, J.C., E.R. Gonçalves, and W.W. Mohn, *Global response to desiccation stress in the soil actinomycete Rhodococcus jostii RHA1*. Applied and Environmental Microbiology, 2008. **74**(9): p. 2627-36.

144. Hamamura, M., et al., *Differential decreases in c-fos and aldolase C mRNA expression in the rat cerebellum after repeated administration of methamphetamine*. Brain Res Mol Brain Res, 1999. **64**(1): p. 119-31.

145. Hamamura, N. and D.J. Arp, *Isolation and characterization of alkane-utilizing Nocardioides sp strain CF8*. FEMS Microbiology Letters, 2000. **186**(1): p. 21-26.

146. Lees, H., *Biochemistry of autotrophic bacteria*. 1955, London: Butterworths Scientific Publs.

147. Padda, R.S., et al., *A novel gene encoding a 54 kDa polypeptide is essential for butane utilization by Pseudomonas sp. IMT37*. Microbiology (Reading, Engl), 2001. **147**(Pt 9): p. 2479-91.

148. Green, J. and H. Dalton, *Substrate specificity of soluble methane monooxygenase. Mechanistic implications*. J Biol Chem, 1989. **264**(30): p. 17698-703.

149. Ensign, S.A., *Microbial metabolism of aliphatic alkenes*. Biochemistry, 2001. **40**(20): p. 5845-53.

150. Fox, B.G., et al., *Methane monooxygenase from Methylosinus trichosporium OB3b*. Methods Enzymol, 1990. **188**: p. 191-202.

151. Ensign, S.A., M.R. Hyman, and D.J. Arp, *Cometabolic degradation of chlorinated alkenes by alkene monooxygenase in a propylene-grown Xanthobacter strain*. Appl Environ Microbiol, 1992. **58**(9): p. 3038-46.

152. Saeki, H., et al., *Degradation of trichloroethene by a linear-plasmid-encoded alkene monooxygenase in Rhodococcus corallinus (Nocardia corallina) B-276*. Microbiology, 1999. **145 (Pt 7)**: p. 1721-30.

153. Rui, L., et al., *Metabolic pathway engineering to enhance aerobic degradation of chlorinated ethenes and to reduce their toxicity by cloning a novel glutathione S-transferase, an evolved toluene o-monooxygenase, and gamma-glutamylcysteine synthetase*. Environ Microbiol, 2004. **6**(5): p. 491-500.

154.   van Beilen, J.B. and E.G. Funhoff, *Expanding the alkane oxygenase toolbox: new enzymes and applications*. Curr Opin Biotechnol, 2005. **16**(3): p. 308-14.

155.   Shanklin, J. and E. Whittle, *Evidence linking the Pseudomonas oleovorans alkane omega-hydroxylase, an integral membrane diiron enzyme, and the fatty acid desaturase family*. FEBS Lett, 2003. **545**(2-3): p. 188-92.

156.   Schmid, A., A. Kollmer, and B. Witholt. , *Effects of biosurfactant and emulsificationontwo liquid phase Pseudomonas oleovorans cultures and cell-free emulsions containing n-decane*. . Enzyme Microb. Technol., 1998. **22**: p. 487-493.

157.   Kusunose, M., et al., *Requirement of three proteins for hydrocarbon oxidation*. J Biochem, 1967. **61**(5): p. 665-7.

158.   Geissdorfer, W., et al., *Two genes encoding proteins with similarities to rubredoxin and rubredoxin reductase are required for conversion of dodecane to lauric acid in Acinetobacter calcoaceticus ADP1*. Microbiology, 1995. **141 (Pt 6)**: p. 1425-32.

159.   Eaton, R.W., *p-Cymene catabolic pathway in Pseudomonas putida F1: cloning and characterization of DNA encoding conversion of p-cymene to p-cumate*. J Bacteriol, 1997. **179**(10): p. 3171-80.

160.   James, K.D. and P.A. Williams, *ntn genes determining the early steps in the divergent catabolism of 4-nitrotoluene and toluene in Pseudomonas sp. strain TW3*. J Bacteriol, 1998. **180**(8): p. 2043-9.

161.   Suzuki, M., et al., *Primary structure of xylene monooxygenase: similarities to and differences from the alkane hydroxylation system*. J Bacteriol, 1991. **173**(5): p. 1690-5.

162.   Shanklin, J., E. Whittle, and B.G. Fox, *Eight histidine residues are catalytically essential in a membrane-associated iron enzyme, stearoyl-CoA desaturase, and are conserved in alkane hydroxylase and xylene monooxygenase*. Biochemistry, 1994. **33**(43): p. 12787-94.

163.   van Beilen, J.B., Veenhoff, L., and Witholt, B. (1998), *Alkane Hydroxylase Systems in Pseudomonas aeruginosa Strains Able to Grow on n-Octane.* , in *New Frontiers in Screening for Microbial Biocatalysts Kieslich,* , v.d.B. K., C.P., de Bont, J.A.M., and van den Tweel, W.J.J. (Ed.), Editor. 1998, Elsevier Science B.V.: Amsterdam.

164.   Shanklin, J., et al., *Mössbauer studies of alkane omega-hydroxylase: evidence for a diiron cluster in an integral-membrane enzyme*. Proc Natl Acad Sci USA, 1997. **94**(7): p. 2981-6.

165.   Johnson, E.L. and M.R. Hyman, *Propane and n-butane oxidation by Pseudomonas putida GPo1*. Applied and Environmental Microbiology, 2006. **72**(1): p. 950-2.

166.   Kok, M., et al., *The Pseudomonas oleovorans alkane hydroxylase gene. Sequence and expression*. J Biol Chem, 1989. **264**(10): p. 5435-41.

167.   van Beilen, J.B., et al., *Analysis of Pseudomonas putida alkane-degradation gene clusters and flanking insertion sequences: evolution and regulation of the alk genes*. Microbiology, 2001. **147**(Pt 6): p. 1621-30.

168.   Witholt, B., et al., *Bioconversions of aliphatic compounds by Pseudomonas oleovorans in multiphase bioreactors: background and economic potential*. Trends Biotechnol, 1990. **8**(2): p. 46-52.

169.   van Beilen, J.B., et al., *Rubredoxins involved in alkane oxidation*. J Bacteriol, 2002. **184**(6): p. 1722-32.

170.   Baptist, J.N., R.K. Gholson, and M.J. Coon, *Hydrocarbon oxidation by a bacterial enzyme system. I. Products of octane oxidation*. Biochim Biophys Acta, 1963. **69**: p. 40-7.

171.   Katopodis, A.G., K. Wimalasena, J. Lee, and S. W. May., *Mechanistic studies on non-heme iron monooxygenase catalysis: epoxidation, aldehyde formation, and*

demethylation by the ᴡ-hydroxylation system of Pseudomonas oleovorans. . J. Am. Chem. Soc., 1984. **106**: p. 7928–7935.

172. May, S.W. and B.J. Abbott, *Enzymatic Epoxidation .1. Alkene Epoxidation by Omega-Hydroxylation System of Pseudomonas Oleovorans.* Biochemical and Biophysical Research Communications, 1972. **48**(5): p. 1230-&.

173. May, S.W. and A.G. Katopodis, *Oxygenation of Alcohol and Sulfide Substrates by a Prototypical Nonheme Iron Monooxygenase - Catalysis and Biotechnological Potential.* Enzyme and Microbial Technology, 1986. **8**(1): p. 17-21.

174. van Beilen, J.B., et al., *Identification of an amino acid position that determines the substrate range of integral membrane alkane hydroxylases.* J Bacteriol, 2005. **187**(1): p. 85-91.

175. van Beilen, J.B., D. Penninga, and B. Witholt, *Topology of the membrane-bound alkane hydroxylase of Pseudomonas oleovorans.* J Biol Chem, 1992. **267**(13): p. 9194-201.

176. Bertrand, E., et al., *Reaction mechanisms of non-heme diiron hydroxylases characterized in whole cells.* J Inorg Biochem, 2005. **99**(10): p. 1998-2006.

177. van Beilen, J.B., et al., *Practical issues in the application of oxygenases.* Trends Biotechnol, 2003. **21**(4): p. 170-7.

178. van Beilen, J.B., et al., *Identification of an amino acid position that determines the substrate range of integral membrane alkane hydroxylases.* Journal of Bacteriology, 2005. **187**(1): p. 85-91.

179. Smits, T.H.M., et al., *Functional analysis of alkane hydroxylases from gram-negative and gram-positive bacteria.* Journal of Bacteriology, 2002. **184**(6): p. 1733-42.

180. Smits, T.H., et al., *Molecular screening for alkane hydroxylase genes in Gram-negative and Gram-positive strains.* Environ Microbiol, 1999. **1**(4): p. 307-17.

181. Ratajczak, A., W. Geissdörfer, and W. Hillen, *Expression of alkane hydroxylase from Acinetobacter sp. Strain ADP1 is induced by a broad range of n-alkanes and requires the transcriptional activator AlkR.* Journal of Bacteriology, 1998. **180**(22): p. 5822-7.

182. Marín, M.M., et al., *The alkane hydroxylase gene of Burkholderia cepacia RR10 is under catabolite repression control.* Journal of Bacteriology, 2001. **183**(14): p. 4202-9.

183. Tani, A., et al., *Gene structures and regulation of the alkane hydroxylase complex in Acinetobacter sp. strain M-1.* Journal of Bacteriology, 2001. **183**(5): p. 1819-23.

184. Smits, T.H., et al., *Functional analysis of alkane hydroxylases from gram-negative and gram-positive bacteria.* J Bacteriol, 2002. **184**(6): p. 1733-42.

185. Smits, T.H., B. Witholt, and J.B. van Beilen, *Functional characterization of genes involved in alkane oxidation by Pseudomonas aeruginosa.* Antonie Van Leeuwenhoek, 2003. **84**(3): p. 193-200.

186. van Beilen, J.B., et al., *Characterization of two alkane hydroxylase genes from the marine hydrocarbonoclastic bacterium Alcanivorax borkumensis.* Environmental Microbiology, 2004. **6**(3): p. 264-73.

187. Kuhn, E., G.S. Bellicanta, and V.H. Pellizari, *New alk genes detected in Antarctic marine sediments.* Environmental Microbiology, 2009. **11**(3): p. 669-73.

188. Mckenna, E.J. and M.J. Coon, *Enzymatic Omega-Oxidation .4. Purification and Properties of Omega-Hydroxylase of Pseudomonas-Oleovorans.* Journal of Biological Chemistry, 1970. **245**(15): p. 3882-&.

189. Smits, T.H.M., B. Witholt, and J.B. van Beilen, *Functional characterization of genes involved in alkane oxidation by Pseudomonas aeruginosa.* Antonie Van Leeuwenhoek, 2003. **84**(3): p. 193-200.

190. Cardini, G. and P. Jurtshuk, *Enzymatic Hydroxylation of Normal-Octane by Corynebacterium Sp Strain 7e1c*. Journal of Biological Chemistry, 1970. **245**(11): p. 2789-&.

191. Jenkins, P.G., F. Moran, and D. Raboin, *Mutants of Mycobacterium Rhodochrous with Modified Patterns of Paraffin Utilization*. Journal of General Microbiology, 1972. **72**(Sep): p. 395-&.

192. Cole, S.T., et al., *Deciphering the biology of Mycobacterium tuberculosis from the complete genome sequence (vol 393, pg 537, 1998)*. Nature, 1998. **396**(6707): p. 190-198.

193. Andreoni, V., et al., *Detection of genes for alkane and naphthalene catabolism in Rhodococcus sp. strain 1BN*. Environ Microbiol, 2000. **2**(5): p. 572-7.

194. van Beilen, J.B., et al., *Alkane hydroxylase homologues in Gram-positive strains*. Environ Microbiol, 2002. **4**(11): p. 676-82.

195. Whyte, L.G., et al., *Gene cloning and characterization of multiple alkane hydroxylase systems in Rhodococcus strains Q15 and NRRL B-16531*. Applied and Environmental Microbiology, 2002. **68**(12): p. 5933-42.

196. Chakrabarty, A.M., G. Chou, and I.C. Gunsalus, *Genetic regulation of octane dissimilation plasmid in Pseudomonas*. Proc Natl Acad Sci U S A, 1973. **70**(4): p. 1137-40.

197. Rojo, F., *Degradation of alkanes by bacteria*. Environmental Microbiology, 2009. **11**(10): p. 2477-90.

198. Munro, A.W. and J.G. Lindsay, *Bacterial cytochromes P-450*. Molecular Microbiology, 1996. **20**(6): p. 1115-1125.

199. Karlson, U., et al., *2 Independently Regulated Cytochromes-P-450 in a Rhodococcus-Rhodochrous Strain That Degrades 2-Ethoxyphenol and 4-Methoxybenzoate*. Journal of Bacteriology, 1993. **175**(5): p. 1467-1474.

200. Funhoff, E.G., et al., *CYP153A6, a soluble P450 oxygenase catalyzing terminal-alkane hydroxylation*. Journal of Bacteriology, 2006. **188**(14): p. 5220-7.

201. Ohkuma, M., et al., *Evidence That the Expression of the Gene for Nadph-Cytochrome P-450 Reductase Is N-Alkane-Inducible in Candida-Maltosa*. Bioscience Biotechnology and Biochemistry, 1995. **59**(7): p. 1328-1330.

202. Sanglard, D., C. Chen, and J.C. Loper, *Isolation of the Alkane Inducible Cytochrome-P450 (P450alk) Gene from the Yeast Candida-Tropicalis*. Biochemical and Biophysical Research Communications, 1987. **144**(1): p. 251-257.

203. Skinner, K.M., *Characterization of the Molecular Foundations and Biochemistry of Alkane and Ether Oxidation in a Filamentous Fungus, a Graphium Species*. 2007, Oregon State University. p. 1-152.

204. Schmitz, C., et al., *Competition between n-alkane-assimilating yeasts and bacteria during colonization of sandy soil microcosms*. Appl Microbiol Biotechnol, 2000. **54**(1): p. 126-32.

205. Maier, T., et al., *Molecular characterization of the 56-kDa CYP153 from Acinetobacter sp. EB104*. Biochem Biophys Res Commun, 2001. **286**(3): p. 652-8.

206. Eremina, S.S., O. Asperger, and H.P. Kleber, *[Cytochrome P-450 and the respiratory activity of Acinetobacter calcoaceticus growing on n-nonane]*. Mikrobiologiia, 1987. **56**(5): p. 764-9.

207. Asperger, O., E. Flechsig, and H.P. Kleber, *Detection and Enrichment of Bacterial Cytochromes P-450*. Biological Chemistry Hoppe-Seyler, 1991. **372**(9): p. 627-628.

208. van Beilen, J.B., et al., *Cytochrome P450 alkane hydroxylases of the CYP153 family are common in alkane-degrading eubacteria lacking integral membrane alkane hydroxylases*. Applied and Environmental Microbiology, 2006. **72**(1): p. 59-65.

209. Maeng, J.H., et al., *Isolation and characterization of a novel oxygenase that catalyzes the first step of n-alkane oxidation in Acinetobacter sp. strain M-1*. J Bacteriol, 1996. **178**(13): p. 3695-700.

210. Throne-Holst, M., et al., *Identification of novel genes involved in long-chain n-alkane degradation by Acinetobacter sp. strain DSM 17874*. Applied and Environmental Microbiology, 2007. **73**(10): p. 3327-32.

211. Feng, L., et al., *Genome and proteome of long-chain alkane degrading Geobacillus thermodenitrificans NG80-2 isolated from a deep-subsurface oil reservoir*. Proc Natl Acad Sci USA, 2007. **104**(13): p. 5602-7.

212. Li, L., et al., *Crystal structure of long-chain alkane monooxygenase (LadA) in complex with coenzyme FMN: unveiling the long-chain alkane hydroxylase*. J Mol Biol, 2008. **376**(2): p. 453-65.

213. van Beilen, J.B., et al., *Characterization of two alkane hydroxylase genes from the marine hydrocarbonoclastic bacterium Alcanivorax borkumensis*. Environ Microbiol, 2004. **6**(3): p. 264-73.

214. Marín, M.M., L. Yuste, and F. Rojo, *Differential expression of the components of the two alkane hydroxylases from Pseudomonas aeruginosa*. Journal of Bacteriology, 2003. **185**(10): p. 3232-7.

215. Hara, A., et al., *Cloning and functional analysis of alkB genes in Alcanivorax borkumensis SK2*. Environmental Microbiology, 2004. **6**(3): p. 191-7.

216. Canosa, I., L. Yuste, and F. Rojo, *Role of the alternative sigma factor sigmaS in expression of the AlkS regulator of the Pseudomonas oleovorans alkane degradation pathway*. Journal of Bacteriology, 1999. **181**(6): p. 1748-54.

217. Canosa, I., et al., *A positive feedback mechanism controls expression of AlkS, the transcriptional regulator of the Pseudomonas oleovorans alkane degradation pathway*. Mol Microbiol, 2000. **35**(4): p. 791-9.

218. Yuste, L. and F. Rojo, *Role of the crc gene in catabolic repression of the Pseudomonas putida GPo1 alkane degradation pathway*. J Bacteriol, 2001. **183**(21): p. 6197-206.

219. Doughty, D.M., et al., *Propionate inactivation of butane monooxygenase activity in 'Pseudomonas butanovora': biochemical and physiological implications*. Microbiology (Reading, Engl), 2007. **153**(Pt 11): p. 3722-9.

220. Marin, M.M., et al., *The alkane hydroxylase gene of Burkholderia cepacia RR10 is under catabolite repression control*. J Bacteriol, 2001. **183**(14): p. 4202-9.

221. Chen, Q., D.B. Janssen, and B. Witholt, *Growth on octane alters the membrane lipid fatty acids of Pseudomonas oleovorans due to the induction of alkB and synthesis of octanol*. J Bacteriol, 1995. **177**(23): p. 6894-901.

222. Chen, Q., D.B. Janssen, and B. Witholt, *Physiological changes and alk gene instability in Pseudomonas oleovorans during induction and expression of alk genes*. J Bacteriol, 1996. **178**(18): p. 5508-12.

223. Panke, S., et al., *An alkane-responsive expression system for the production of fine chemicals*. Appl Environ Microbiol, 1999. **65**(6): p. 2324-32.

224. Sticher, P., et al., *Development and characterization of a whole-cell bioluminescent sensor for bioavailable middle-chain alkanes in contaminated groundwater samples*. Appl Environ Microbiol, 1997. **63**(10): p. 4053-60.

225. Yuste, L., I. Canosa, and F. Rojo, *Carbon-source-dependent expression of the PalkB promoter from the Pseudomonas oleovorans alkane degradation pathway*. Journal of Bacteriology, 1998. **180**(19): p. 5218-26.

226.   Staijen, I.E., R. Marcionelli, and B. Witholt, *The PalkBFGHJKL promoter is under carbon catabolite repression control in Pseudomonas oleovorans but not in Escherichia coli alk+ recombinants*. Journal of Bacteriology, 1999. **181**(5): p. 1610-6.

227.   Dinamarca, M.A., et al., *Expression of the Pseudomonas putida OCT plasmid alkane degradation pathway is modulated by two different global control signals: evidence from continuous cultures*. J Bacteriol, 2003. **185**(16): p. 4772-8.

228.   Dinamarca, M.A., A. Ruiz-Manzano, and F. Rojo, *Inactivation of cytochrome o ubiquinol oxidase relieves catabolic repression of the Pseudomonas putida GPo1 alkane degradation pathway*. Journal of Bacteriology, 2002. **184**(14): p. 3785-93.

229.   Moreno, R., et al., *The Pseudomonas putida Crc global regulator is an RNA binding protein that inhibits translation of the AlkS transcriptional regulator*. Mol Microbiol, 2007. **64**(3): p. 665-75.

230.   Moreno, R., et al., *The Crc global regulator binds to an unpaired A-rich motif at the Pseudomonas putida alkS mRNA coding sequence and inhibits translation initiation*. Nucleic Acids Res, 2009. **37**(22): p. 7678-90.

231.   Ruiz-Manzano, A., L. Yuste, and F. Rojo, *Levels and activity of the Pseudomonas putida global regulatory protein Crc vary according to growth conditions*. J Bacteriol, 2005. **187**(11): p. 3678-86.

232.   MacGregor, C.H., et al., *The nucleotide sequence of the Pseudomonas aeruginosa pyrE-crc-rph region and the purification of the crc gene product*. J Bacteriol, 1996. **178**(19): p. 5627-35.

233.   Hester, K.L., K.T. Madhusudhan, and J.R. Sokatch, *Catabolite repression control by crc in 2xYT medium is mediated by posttranscriptional regulation of bkdR expression in Pseudomonas putida*. J Bacteriol, 2000. **182**(4): p. 1150-3.

234.   Hester, K.L., et al., *Crc is involved in catabolite repression control of the bkd operons of Pseudomonas putida and Pseudomonas aeruginosa*. J Bacteriol, 2000. **182**(4): p. 1144-9.

235.   Morales, G., et al., *The Pseudomonas putida Crc global regulator controls the expression of genes from several chromosomal catabolic pathways for aromatic compounds*. J Bacteriol, 2004. **186**(5): p. 1337-44.

236.   Aranda-Olmedo, I., J.L. Ramos, and S. Marques, *Integration of signals through Crc and PtsN in catabolite repression of Pseudomonas putida TOL plasmid pWW0*. Appl Environ Microbiol, 2005. **71**(8): p. 4191-8.

237.   Moreno, R. and F. Rojo, *The target for the Pseudomonas putida Crc global regulator in the benzoate degradation pathway is the BenR transcriptional regulator*. J Bacteriol, 2008. **190**(5): p. 1539-45.

238.   Morales, G., A. Ugidos, and F. Rojo, *Inactivation of the Pseudomonas putida cytochrome o ubiquinol oxidase leads to a significant change in the transcriptome and to increased expression of the CIO and cbb3-1 terminal oxidases*. Environ Microbiol, 2006. **8**(10): p. 1764-74.

239.   Petruschka, L., et al., *The cyo operon of Pseudomonas putida is involved in carbon catabolite repression of phenol degradation*. Mol Genet Genomics, 2001. **266**(2): p. 199-206.

240.   Saier, M.H., Jr., *Regulatory interactions controlling carbon metabolism: an overview*. Res Microbiol, 1996. **147**(6-7): p. 439-47.

241.   Saier, M.H., Jr., *Multiple mechanisms controlling carbon metabolism in bacteria*. Biotechnol Bioeng, 1998. **58**(2-3): p. 170-4.

242.   Staijen, I.E., R. Marcionelli, and B. Witholt, *The PalkBFGHJKL promoter is under carbon catabolite repression control in Pseudomonas oleovorans but not in Escherichia coli alk+ recombinants*. J Bacteriol, 1999. **181**(5): p. 1610-6.

243. Murphy, D.J. and J. Vance, *Mechanisms of lipid body formation*. Trends in Biochemical Sciences, 1999. **24**(3): p. 109-115.

244. Alvarez, H.M. and A. Steinbuchel, *Triacylglycerols in prokaryotic microorganisms*. Applied Microbiology and Biotechnology, 2002. **60**(4): p. 367-376.

245. Waltermann, M., et al., *Mechanism of lipid-body formation in prokaryotes: how bacteria fatten up*. Molecular Microbiology, 2005. **55**(3): p. 750-763.

246. Kalscheuer, R., et al., *Analysis of storage livid accumulation in Alcanivorax borkumensis: Evidence for alternative triacylglycerol biosynthesis routes in bacteria*. Journal of Bacteriology, 2007. **189**(3): p. 918-928.

247. Desmet, M.J., et al., *Characterization of Intracellular Inclusions Formed by Pseudomonas-Oleovorans during Growth on Octane*. Journal of Bacteriology, 1983. **154**(2): p. 870-878.

248. Ishige, T., et al., *Wax ester production from n-alkanes by Acinetobacter sp strain M-1: Ultrastructure of cellular inclusions and role of acyl coenzyme A reductase*. Applied and Environmental Microbiology, 2002. **68**(3): p. 1192-1195.

249. Ishige, T., et al., *Long-chain aldehyde dehydrogenase that participates in n-alkane utilization and wax ester synthesis in Acinetobacter sp strain M-1*. Applied and Environmental Microbiology, 2000. **66**(8): p. 3481-3486.

250. Heald, S.C., et al., *Physiology, biochemistry and taxonomy of deep-sea nitrile metabolising Rhodococcus strains*. Antonie Van Leeuwenhoek International Journal of General and Molecular Microbiology, 2001. **80**(2): p. 169-183.

251. Langdahl, B.R., P. Bisp, and K. Ingvorsen, *Nitrile hydrolysis by Rhodococcus erythropolis BL1, an acetonitrile-tolerant strain isolated from a marine sediment*. Microbiology-Uk, 1996. **142**: p. 145-154.

252. Whyte, L.G., et al., *Prevalence of alkane monooxygenase genes in Arctic and Antarctic hydrocarbon-contaminated and pristine soils*. FEMS Microbiol Ecol, 2002. **41**(2): p. 141-50.

253. de Carvalho, C.C.C.R. and M.M.R. da Fonseca, *Degradation of hydrocarbons and alcohols at different temperatures and salinities by Rhodococcus erythropolis DCL 14*. FEMS Microbiology Ecology, 2005. **51**(3): p. 389-399.

254. Gurtler, V., B.C. Mayall, and R. Seviour, *Can whole genome analysis refine the taxonomy of the genus Rhodococcus?* FEMS Microbiology Reviews, 2004. **28**(3): p. 377-403.

255. Cejkova, A., et al., *Potential of Rhodococcus erythropolis as a bioremediation organism*. World Journal of Microbiology & Biotechnology, 2005. **21**(3): p. 317-321.

256. Larkin, M.J., L.A. Kulakov, and C.C.R. Allen, *Biodegradation and Rhodococcus--masters of catabolic versatility*. Current Opinion in Biotechnology 2005. **16**(3): p. 282-90.

257. McLeod, M.P., et al., *The complete genome of Rhodococcus sp RHA1 provides insights into a catabolic powerhouse*. Proceedings of the National Academy of Sciences of the United States of America, 2006. **103**(42): p. 15582-15587.

258. Wakisaka, Y., et al., *Hygromycin and Epihygromycin from a Bacterium, Corynebacterium-Equi No-2841*. Journal of Antibiotics, 1980. **33**(7): p. 695-704.

259. Yamada, S., et al., *Production of D-Alanine by Corynebacterium-Fascians*. Applied Microbiology, 1973. **25**(4): p. 636-640.

260. Andreoni, V., et al., *Metabolism of Lignin-Related Compounds by Rhodococcus-Rhodochrous - Bioconversion of Anisoin*. Applied Microbiology and Biotechnology, 1991. **36**(3): p. 410-415.

261. Reh, M. and H.G. Schlegel, *Hydrogen Autotrophy as a Transferable Genetic Character of Nocardia-Opaca 1b*. Journal of General Microbiology, 1981. **126**(Oct): p. 327-336.

262. Bicca, F.C., L.C. Fleck, and M.A.Z. Ayub, *Production of biosurfactant by hydrocarbon degrading Rhodococcus ruber and Rhodococcus erythropolis*. Revista De Microbiologia, 1999. **30**(3): p. 231-236.

263. Philp, J.C., et al., *Alkanotrophic Rhodococcus ruber as a biosurfactant producer*. Applied Microbiology and Biotechnology, 2002. **59**(2-3): p. 318-324.

264. van der Geize, R. and L. Dijkhuizen, *Harnessing the catabolic diversity of rhodococci for environmental and biotechnological applications*. Curr Opin Microbiol, 2004. **7**(3): p. 255-61.

265. Shao, Z.Q. and R. Behki, *Cloning of the Genes for Degradation of the Herbicides Eptc (S-Ethyl Dipropylthiocarbamate) and Atrazine from Rhodococcus Sp Strain Te1*. Applied and Environmental Microbiology, 1995. **61**(5): p. 2061-2065.

266. Powell, J.A.C. and J.A.C. Archer, *Molecular characterisation of a Rhodococcus ohp operon*. Antonie Van Leeuwenhoek International Journal of General and Molecular Microbiology, 1998. **74**(1-3): p. 175-188.

267. Williams, T., Sharplegs,. P., Serrano,J . A., Serrano, A. A. & Lacey, J., *The micromorphology and fine structure of nocardioform organisms.*, in *The Biology of the Nocardiae*
, G.H.B.J.A.S. M. Goodfellow, Editor. 1976, London: Academic Press. p. 102-140

268. Locci R., S.G.P., *Micromorphology*, in *The Biology of Actinomycetes*, M.M.W.S.E. Goodfellow M, Editor. 1984, Academic Press, London. p. 165–199.

269. Denome, S.A., E.S. Olson, and K.D. Young, *Identification and Cloning of Genes Involved in Specific Desulfurization of Dibenzothiophene by Rhodococcus sp. Strain IGTS8*. Applied and Environmental Microbiology, 1993. **59**(9): p. 2837-2843.

270. Schäfer, A., et al., *High-frequency conjugal plasmid transfer from gram-negative Escherichia coli to various gram-positive coryneform bacteria*. J Bacteriol, 1990. **172**(3): p. 1663-6.

271. Sallam, K.I., Y. Mitani, and T. Tamura, *Construction of random transposition mutagenesis system in Rhodococcuserythropolis using IS1415*. J Biotechnol, 2006. **121**(1): p. 13-22.

272. Matsui, T., et al., *Analysis of the 7.6-kb cryptic plasmid pNC500 from Rhodococcus rhodochrous B-276 and construction of Rhodococcus-E-coli shuttle vector*. Applied Microbiology and Biotechnology, 2007. **74**(1): p. 169-175.

273. Hirasawa, K., et al., *Improvement of desulfurization activity in Rhodococcus erythropolis KA2-5-1 by genetic engineering*. Bioscience Biotechnology and Biochemistry, 2001. **65**(2): p. 239-246.

274. Nakashima, N. and T. Tamura, *Isolation and characterization of a rolling-circle-type plasmid from Rhodococcus erythropolis and application of the plasmid to multiple-recombinant-protein expression*. Appl Environ Microbiol, 2004. **70**(9): p. 5557-68.

275. Fernandes, P.J., J.A. Powell, and J.A. Archer, *Construction of Rhodococcus random mutagenesis libraries using Tn5 transposition complexes*. Microbiology (Reading, Engl), 2001. **147**(Pt 9): p. 2529-36.

276. Mangan, M.W. and W.G. Meijer, *Random insertion mutagenesis of the intracellular pathogen Rhodococcus equi using transposomes*. FEMS Microbiol Lett, 2001. **205**(2): p. 243-6.

277. Jäger, W., et al., *Isolation of insertion elements from gram-positive Brevibacterium, Corynebacterium and Rhodococcus strains using the Bacillus subtilis sacB gene as a positive selection marker*. FEMS Microbiol Lett, 1995. **126**(1): p. 1-6.

278. Denis-Larose, C., et al., *Characterization of the basic replicon of Rhodococcus plasmid pSOX and development of a Rhodococcus-Escherichia coli shuttle vector.* Applied and Environmental Microbiology, 1998. **64**(11): p. 4363-7.

279. van der Geize, R., et al., *Unmarked gene deletion mutagenesis of kstD, encoding 3-ketosteroid Delta1-dehydrogenase, in Rhodococcus erythropolis SQ1 using sacB as counter-selectable marker.* FEMS Microbiol Lett, 2001. **205**(2): p. 197-202.

280. Goncalves, E.R., et al., *Transcriptomic assessment of isozymes in the biphenyl pathway of Rhodococcus sp strain RHA1.* Applied and Environmental Microbiology, 2006. **72**(9): p. 6183-6193.

281. Hara, H., et al., *Transcriptomic analysis reveals a bifurcated terephthalate degradation pathway in Rhodococcus sp strain RHA1.* Journal of Bacteriology, 2007. **189**(5): p. 1641-1647.

282. Patrauchan, M.A., et al., *Catabolism of benzoate and phthalate in Rhodococcus sp strain RHA1: Redundancies and convergence.* Journal of Bacteriology, 2005. **187**(12): p. 4050-4063.

283. Eulberg, D. and M. Schlomann, *The putative regulator of catechol catabolism in Rhodococcus opacus 1CP - an IclR-type, not a LysR-type transcriptional regulator.* Antonie Van Leeuwenhoek International Journal of General and Molecular Microbiology, 1998. **74**(1-3): p. 71-82.

284. Nga, D.P., J. Altenbuchner, and G.S. Heiss, *NpdR, a repressor involved in 2,4,6-trinitrophenol degradation in Rhodococcus opacus HL PM-1.* Journal of Bacteriology, 2004. **186**(1): p. 98-103.

285. Veselý, M., et al., *Analysis of catRABC operon for catechol degradation from phenol-degrading Rhodococcus erythropolis.* Appl Microbiol Biotechnol, 2007. **76**(1): p. 159-68.

286. Takeda, H., et al., *Biphenyl-inducible promoters in a polychlorinated biphenyl-degrading bacterium, Rhodococcus sp. RHA1.* Biosci Biotechnol Biochem, 2004. **68**(6): p. 1249-58.

287. Knoppová, M., et al., *Plasmid vectors for testing in vivo promoter activities in Corynebacterium glutamicum and Rhodococcus erythropolis.* Curr Microbiol, 2007. **55**(3): p. 234-9.

288. Veselý, M., et al., *Host-vector system for phenol-degrading Rhodococcus erythropolis based on Corynebacterium plasmids.* Appl Microbiol Biotechnol, 2003. **61**(5-6): p. 523-7.

289. Lessard, P.A., et al., *pB264, a small, mobilizable, temperature sensitive plasmid from Rhodococcus.* BMC Microbiol, 2004. **4**: p. 15.

290. Nakashima, N. and T. Tamura, *A novel system for expressing recombinant proteins over a wide temperature range from 4 to 35 degrees C.* Biotechnol Bioeng, 2004. **86**(2): p. 136-48.

291. Na, K.-S., et al., *Development of a genetic transformation system for benzene-tolerant Rhodococcus opacus strains.* J Biosci Bioeng, 2005. **99**(4): p. 408-14.

292. Takarada H., S.M., Hosoyama A., Yamada R., Fujisawa T., Omata S., Shimizu A., Tsukatani N., Tanikawa S., Fujita N., Harayama S., *Comparison of the complete genome sequences of Rhodococcus erythropolis PR4 and Rhodococcus opacus B4.* Unpublished.

293. Sekine, M., et al., *Sequence analysis of three plasmids harboured in Rhodococcus erythropolis strain PR4.* Environmental Microbiology, 2006. **8**(2): p. 334-46.

294. Sebastian, Y., Madupu,R., Durkin,A.S., Torralba,M., Methe,B., Sutton,G.G., Strausberg,R.L. and Nelson,K.E., *Rhodococcus erythropolis SK121, whole genome*

shotgun sequencing project. J. Craig Venter Institute, 9704 Medical Center Drive, Rockville, MD 20850, USA, Submitted (20-APR-2009)

.

295. Warhurst, A.M. and C.A. Fewson, *Biotransformations catalyzed by the genus Rhodococcus*. Crit Rev Biotechnol, 1994. **14**(1): p. 29-73.

296. Larkin, M.J., et al., *Applied aspects of Rhodococcus genetics*. Antonie Van Leeuwenhoek, 1998. **74**(1-3): p. 133-53.

297. Whyte, L.G., et al., *Gene cloning and characterization of multiple alkane hydroxylase systems in Rhodococcus strains Q15 and NRRL B-16531*. Appl Environ Microbiol, 2002. **68**(12): p. 5933-42.

298. Philp, J.C., et al., *Alkanotrophic Rhodococcus ruber as a biosurfactant producer*. Appl Microbiol Biotechnol, 2002. **59**(2-3): p. 318-24.

299. de Carvalho, C.C.C.R., et al., *Adaptation of Rhodococcus erythropolis DCL14 to growth on n-alkanes, alcohols and terpenes*. Appl Microbiol Biotechnol, 2005. **67**(3): p. 383-8.

300. Tapilatu, Y., et al., *Isolation of alkane-degrading bacteria from deep-sea Mediterranean sediments*. Letters in Applied Microbiology, 2010. **50**(2): p. 234-236.

301. Quatrini, P., et al., *Isolation of Gram-positive n-alkane degraders from a hydrocarbon-contaminated Mediterranean shoreline*. Journal of Applied Microbiology, 2008. **104**(1): p. 251-259.

302. Zhukov, D.V., V.P. Murygina, and S.V. Kalyuzhnyi, *Kinetics of the degradation of aliphatic hydrocarbons by the bacteria Rhodococcus ruber and Rhodococcus erythropolis*. Applied Biochemistry and Microbiology, 2007. **43**(6): p. 587-592.

303. Panicker, G., et al., *Detection, expression and quantitation of the biodegradative genes in Antarctic microorganisms using PCR*. Antonie Van Leeuwenhoek International Journal of General and Molecular Microbiology, 2010. **97**(3): p. 275-287.

304. Frascari, D., et al., *Chloroform degradation by butane-grown cells of Rhodococcus aetherovorans BCP1*. Appl Microbiol Biotechnol, 2006. **73**(2): p. 421-8.

305. Aislabie, J., D.J. Saul, and J.M. Foght, *Bioremediation of hydrocarbon-contaminated polar soils*. Extremophiles, 2006. **10**(3): p. 171-179.

306. de Carvalho, C.C.C.R., L.Y. Wick, and H.J. Heipieper, *Cell wall adaptations of planktonic and biofilm Rhodococcus erythropolis cells to growth on C5 to C16 n-alkane hydrocarbons*. Appl Microbiol Biotechnol, 2009. **82**(2): p. 311-20.

307. Bouchez-Naitali, M. and J.P. Vandecasteele, *Biosurfactants, an help in the biodegradation of hexadecane? The case of Rhodococcus and Pseudomonas strains*. World Journal of Microbiology & Biotechnology, 2008. **24**(9): p. 1901-1907.

308. Peng, F., et al., *An oil-degrading bacterium: Rhodococcus erythropolis strain 3C-9 and its biosurfactants*. J Appl Microbiol, 2007. **102**(6): p. 1603-11.

309. Lee, E.H. and K.S. Cho, *Characterization of cyclohexane and hexane degradation by Rhodococcus sp EC1*. Chemosphere, 2008. **71**(9): p. 1738-1744.

310. Kulikova, A.K. and A.M. Bezborodov, *Assimilation of propane and characterization of propane monooxygenase from Rhodococcus erythropolis 3/89*. Applied Biochemistry and Microbiology, 2001. **37**(2): p. 164-167.

311. Sameshima, Y., et al., *Expression of Rhodococcus opacus alkB genes in anhydrous organic solvents*. J Biosci Bioeng, 2008. **106**(2): p. 199-203.

312. Takei, D., K. Washio, and M. Morikawa, *Identification of alkane hydroxylase genes in Rhodococcus sp strain TMP2 that degrades a branched alkane*. Biotechnology Letters, 2008. **30**(8): p. 1447-1452.

212

313. Frascari, D., et al., *Aerobic cometabolism of chloroform by butane-grown microorganisms: long-term monitoring of depletion rates and isolation of a high-performing strain*. Biodegradation, 2005. **16**(2): p. 147-58.

314. Cole, J.R., et al., *The Ribosomal Database Project: improved alignments and new tools for rRNA analysis*. Nucleic Acids Research, 2009. **37**: p. D141-D145.

315. Drummond AJ, A.B., Cheung M, Heled J, Kearse M, Moir R, Stones-Havas S, Thierer T, Wilson A *Geneious v4.8*. 2009.

316. Arp, D.J., C.M. Yeager, and M.R. Hyman, *Molecular and cellular fundamentals of aerobic cometabolism of trichloroethylene*. Biodegradation, 2001. **12**(2): p. 81-103.

317. Chang, H.L. and L. Alvarezcohen, *Model for the Cometabolic Biodegradation of Chlorinated Organics*. Environmental Science & Technology, 1995. **29**(9): p. 2357-2367.

318. Hanahan, D., *Studies on Transformation of Escherichia-Coli with Plasmids*. Journal of Molecular Biology, 1983. **166**(4): p. 557-580.

319. Silhavy TJ., B.M., and Enquist LW. , *Experiments with gene fusions*, ed. C.S. Harbor. 1984, N.Y.: Cold Spring Harbor Laboratory.

320. Sambrook, J.F., E.F. and Maniatis, T., *Molecular Cloning: A Laboratory Manual 2nd edition*., ed. Cold Spring Harbor Laboratory Press. Vol. vol. I. . 1989.

321. Keen, N.T., et al., *Improved broad-host-range plasmids for DNA cloning in gram-negative bacteria*. Gene, 1988. **70**(1): p. 191-7.

322. Nakashima, N. and T. Tamura, *Isolation and characterization of a rolling-circle-type plasmid from Rhodococcus erythropolis and application of the plasmid to multiple-recombinant-protein expression*. Applied and Environmental Microbiology, 2004. **70**(9): p. 5557-68.

323. Treadway, S.L., et al., *Isolation and characterization of indene bioconversion genes from Rhodococcus strain I24*. Appl Microbiol Biotechnol, 1999. **51**(6): p. 786-93.

324. Lowry, O.H., et al., *Protein Measurement with the Folin Phenol Reagent*. Journal of Biological Chemistry, 1951. **193**(1): p. 265-275.

325. Prior, S.D. and H. Dalton, *Acetylene as a Suicide Substrate and Active-Site Probe for Methane Monooxygenase from Methylococcus-Capsulatus (Bath)*. FEMS Microbiology Letters, 1985. **29**(1-2): p. 105-109.

326. Hyman, M.R. and P.M. Wood, *Suicidal Inactivation and Labeling of Ammonia Mono-Oxygenase by Acetylene*. Biochemical Journal, 1985. **227**(3): p. 719-725.

327. Salanitr.Jp and W.S. Wegener, *Growth of Escherichia-Coli on Short-Chain Fatty Acids - Nature of Uptake System*. Journal of Bacteriology, 1971. **108**(2): p. 893-&.

328. Salanitro, J.P. and W.S. Wegener, *Growth of Escherichia coli on short-chain fatty acids: nature of the uptake system*. Journal of Bacteriology, 1971. **108**(2): p. 893-901.

329. Aono, R. and H. Kobayashi, *Cell surface properties of organic solvent-tolerant mutants of Escherichia coli K-12*. Applied and Environmental Microbiology, 1997. **63**(9): p. 3637-3642.

330. Woods, N.R. and J.C. Murrell, *The Metabolism of Propane in Rhodococcus-Rhodochrous Pnkb1*. Journal of General Microbiology, 1989. **135**: p. 2335-2344.

331. Leahy, J.G. and R.R. Colwell, *Microbial-Degradation of Hydrocarbons in the Environment*. Microbiological Reviews, 1990. **54**(3): p. 305-315.

332. Inoue, A. and K. Horikoshi, *A Pseudomonas Thrives in High-Concentrations of Toluene*. Nature, 1989. **338**(6212): p. 264-266.

333. Laane, C., et al., *Rules for Optimization of Biocatalysis in Organic-Solvents*. BIOTECHNOLOGY AND BIOENGINEERING, 1987. **30**(1): p. 81-87.

334. van Beilen, J.B., et al., *Cytochrome P450 alkane hydroxylases of the CYP153 family are common in alkane-degrading eubacteria lacking integral membrane alkane hydroxylases.* Appl Environ Microbiol, 2006. **72**(1): p. 59-65.

335. Marchler-Bauer, A., et al., *CDD: specific functional annotation with the Conserved Domain Database.* Nucleic Acids Research, 2009. **37**: p. D205-D210.

336. Fujii, T., et al., *Biotransformation of various alkanes using the Escherichia coli expressing an alkane hydroxylase system from Gordonia sp. TF6.* Biosci Biotechnol Biochem, 2004. **68**(10): p. 2171-7.

337. Liu, Y.-C., et al., *Molecular characterization of the alkB gene in the thermophilic Geobacillus sp. strain MH-1.* Res Microbiol, 2009. **160**(8): p. 560-6.

338. Sonnhammer, E.L., G. von Heijne, and A. Krogh, *A hidden Markov model for predicting transmembrane helices in protein sequences.* Proc Int Conf Intell Syst Mol Biol, 1998. **6**: p. 175-82.

339. Huang, L., et al., *Optimization of nutrient component for diesel oil degradation by Rhodococcus erythropolis.* Mar Pollut Bull, 2008. **56**(10): p. 1714-8.

340. Eggink, G., et al., *Controlled and Functional Expression of the Pseudomonas-Oleovorans Alkane Utilizing System in Pseudomonas-Putida and Escherichia-Coli.* Journal of Biological Chemistry, 1987. **262**(36): p. 17712-17718.

341. Roncarati, D., et al., *Transcriptional regulation of stress response and motility functions in Helicobacter pylori is mediated by HspR and HrcA.* J Bacteriol, 2007. **189**(20): p. 7234-43.

342. Na, K.S., et al., *Isolation and characterization of benzene-tolerant Rhodococcus opacus strains.* Journal of Bioscience and Bioengineering, 2005. **99**(4): p. 378-382.

343. Miller, J.H., *Experiments in molecular genetics.*, ed. C.S.H. Laboratory. 1972: Cold Spring Harbor, N.Y.

344. Rose M., B.D., *Construction and use of gene fusions to lacZ (beta-galactosidase) that are expressed in yeast.* Methods Enzymol. Vol. 101. 1983 167–180.

345. Stolt, P. and N.G. Stoker, *Functional definition of regions necessary for replication and incompatibility in the Mycobacterium fortuitum plasmid pAL5000.* Microbiology, 1996. **142 (Pt 10)**: p. 2795-802.

346. Rose, R.E., *The nucleotide sequence of pACYC184.* Nucleic Acids Res, 1988. **16**(1): p. 355.

347. Arp, D., *Understanding the diversity of trichloroethene oxidations. .* Vol. 6. 1995: Curr Opin Biotechnol

348. Grund, A., et al., *Regulation of alkane oxidation in Pseudomonas putida.* J Bacteriol, 1975. **123**(2): p. 546-56.

349. Martínková, L., et al., *Biodegradation potential of the genus Rhodococcus.* Environment International, 2009. **35**(1): p. 162-77.

350. Ratajczak, A., W. Geissdörfer, and W. Hillen, *Alkane hydroxylase from Acinetobacter sp. strain ADP1 is encoded by alkM and belongs to a new family of bacterial integral-membrane hydrocarbon hydroxylases.* Applied and Environmental Microbiology, 1998. **64**(4): p. 1175-9.

351. Singh, O.V. and N.S. Nagaraj, *Transcriptomics, proteomics and interactomics: unique approaches to track the insights of bioremediation.* Brief Funct Genomic Proteomic, 2006. **4**(4): p. 355-62.

352. Tomas-Gallardo, L., et al., *Proteomic and transcriptional characterization of aromatic degradation pathways in Rhodoccocus sp. strain TFB.* Proteomics, 2006. **6 Suppl 1**: p. S119-32.

353. Okamoto, S. and L.D. Eltis, *Purification and characterization of a novel nitrile hydratase from Rhodococcus sp. RHA1.* Mol Microbiol, 2007. **65**(3): p. 828-38.

354. Nagy, I., et al., *A single cytochrome P-450 system is involved in degradation of the herbicides EPTC (S-ethyl dipropylthiocarbamate) and atrazine by Rhodococcus sp. strain NI86/21*. Applied and Environmental Microbiology, 1995. **61**(5): p. 2056-60.

355. Iwasaki, T., et al., *Multiple-subunit genes of the aromatic-ring-hydroxylating dioxygenase play an active role in biphenyl and polychlorinated biphenyl degradation in Rhodococcus sp. strain RHA1*. Appl Environ Microbiol, 2006. **72**(8): p. 5396-402.

356. Bradford, M.M., *A rapid and sensitive method for the quantitation of microgram quantities of protein utilizing the principle of protein-dye binding*. Anal Biochem, 1976. **72**: p. 248-54.

357. Lauber, W.M., et al., *Mass spectrometry compatibility of two-dimensional gel protein stains*. Electrophoresis, 2001. **22**(5): p. 906-18.

358. Perkins, D.N., et al., *Probability-based protein identification by searching sequence databases using mass spectrometry data*. Electrophoresis, 1999. **20**(18): p. 3551-67.

359. Carrillo, B., et al., *Increasing peptide identification in tandem mass spectrometry through automatic function switching optimization*. J Am Soc Mass Spectrom, 2005. **16**(11): p. 1818-26.

360. Bedhomme, M., et al., *Regulation by Glutathionylation of Isocitrate Lyase from Chlamydomonas reinhardtii*. Journal of Biological Chemistry, 2009. **284**(52): p. 36282-36291.

361. Rodriguez, F., Franchi, E., Serbolisca, L.P., de Ferra, F., *Monitoring of bacterial species involved in light hydrocarbon oxidation*. Unpublished.

362. Liu, L., R.D. Schmid, and V.B. Urlacher, *Cloning, expression, and characterization of a self-sufficient cytochrome P450 monooxygenase from Rhodococcus ruber DSM 44319*. Appl Microbiol Biotechnol, 2006. **72**(5): p. 876-82.

363. Roberts, G.A., et al., *Identification of a new class of cytochrome P450 from a Rhodococcus sp*. J Bacteriol, 2002. **184**(14): p. 3898-908.